ISSN (1230-0322)
2023, Vol. 73, No. 2

Food

Polish Journal of Food and Nutrition Sciences

formerly Acta Alimentaria Polonica

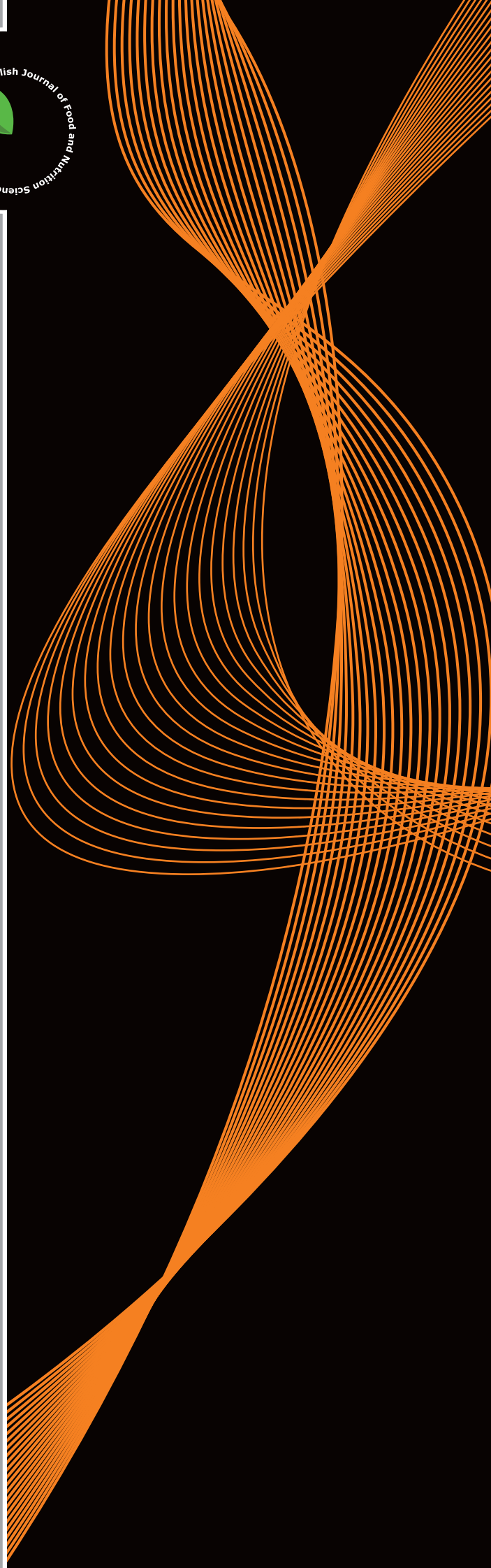

Published

by Institute of Animal Reproduction and Food Research of the Polish Academy of Sciences, Olsztyn

Published since 1957 as
Roczniki Chemii i Technologii Żywności and Acta Alimentaria Polonica (1975–1991)

SCOPE: The Journal covers fundamental and applied research in food area and nutrition sciences with a stress on interdisciplinary studies in the areas of food, nutrition and related subjects.

POLICY: Editors select submitted manuscripts in relation to their relevance to the scope. Reviewers are selected from the Advisory Board and from Polish and international scientific centres. Identity of reviewers is kept confidential.

AUTHORSHIP FORMS referring to Authorship Responsibility, Conflict of Interest and Financial Disclosure, Copyright Transfer and Acknowledgement, and Ethical Approval of Studies are required for all authors.

FREQUENCY: Quarterly – one volume in four issues (March, June, September, December).

COVERED by Web of Science, Current Contents/Agriculture, Biology & Environmental Sciences, Journal Citation Reports and Science Citation Index Expanded, BIOSIS (Biological Abstracts), SCOPUS, FSTA (formerly: Food Science and Technology Abstracts), CAS (Chemical Abstracts), AGRICOLA, AGRO-LIBREX data base, EBSCO, FOODLINE, Leatherhead FOOD RA data base FROSTI, AGRIS and Index Copernicus data bases, Biblioteka Nauki ICM, Biblioteka Narodowa – POLONA, and any www browser; ProQuest: The Summon, Bacteriology Abstracts, Immunology Abstracts.

EDITORIAL AND BUSINESS CORRESPONDENCE: Submit contributions (see Instructions to Authors) and address all communications regarding subscriptions, changes of address, etc. to:

CORRESPONDENCE TO: Ms. Joanna Molga
Polish Journal of Food and Nutrition Sciences
Institute of Animal Reproduction and Food Research
of Polish Academy of Sciences
ul. Tuwima 10, 10-747 Olsztyn, Poland
e-mail: pjfns@pan.olsztyn.pl; http://journal.pan.olsztyn.pl

Polish Journal of Food and Nutrition Sciences

ADVISORY BOARD OF PJFNS 2023–2026

Contents

ORIGINAL PAPERS

covered by CURRENT CONTENTS/AGRICULTURE, BIOLOGY & ENVIRONMENTAL SCIENCES, JOURNAL CITATION REPORTS AND SCIENCE CITATION INDEX EXPANDED, BIOSIS, SCOPUS, IFIS Publishing and CAS abstracts, and AGRO-Librex, FROSTI, PSJC, AGRIS and Index Copernicus data bases

Ministerstwo
Edukacji i Nauki

W latach 2022–2024 kwartalnik naukowy ***Polish Journal of Food and Nutrition Sciences*** realizuje projekt nr RCN/SP/0520/2021/1 finansowany ze środków budżetu państwa – Ministerstwo Edukacji i Nauki w ramach programu „Rozwój czasopism naukowych". Dofinansowanie wynosi 120 000 zł. W ramach projektu podejmowane są działania zmierzające do podniesienia poziomu praktyk wydawniczych i edytorskich, zwiększenia wpływu czasopism na rozwój nauki oraz utrzymania się czasopism w międzynarodowym obiegu naukowym.

Ministry of Education and Science
Republic of Poland

In the years 2022–2024, the scientific quarterly ***Polish Journal of Food and Nutrition Sciences*** accomplishes a project no. RCN/SP/0520/2021/1 financed from the state budged – Ministry of Education and Science Republic of Poland in the framework of a program "Development of scientific journals". The financing amounts to 120,000 PLN. The program aims at improving the level of publishing and editing practices, increasing the impact of scientific journals on science development, and extending the international range of scientific journals.

Subscription
2023 – One volume, four issues per volume. Annual subscription rates are: Poland 150 PLN, all other countries 80 EUR. Prices are subject to exchange rate fluctuation. Subscription payments should be made by direct bank transfer to Bank Gospodarki Żywnościowej, Olsztyn, Poland, account No 17203000451110000000452110 SWIFT code: GOPZPLWOLA with corresponding banks preferably. Subscription and advertising offices at the Institute of Animal Reproduction and Food Research of Polish Academy of Sciences, ul. J. Tuwima 10, 10-747 Olsztyn, Poland, tel./fax (48 89) 5234670, fax (48 89) 5240124, e-mail: pjfns@pan.olsztyn.pl; http://journal.pan.olsztyn.pl

Zamówienia prenumeraty: Joanna Molga (e-mail: pjfns@pan.olsztyn.pl)

Wersja pierwotna (referencyjna) kwartalnika PJFNS: wersja papierowa (ISSN 1230–0322)
Nakład: 70 egz.; Ark. wyd. 16; Ark. druk. 13
Skład i druk: ITEM

ORIGINAL ARTICLE
http://journal.pan.olsztyn.pl

Polish Journal of Food and Nutrition Sciences
2023, Vol. 73, No. 2, 109–119
DOI: 10.31883/pjfns/162504
ISSN 1230-0322, e-ISSN 2083-6007

Comparison of the Quality of Selected Meat Products and Their Plant-Based Analogs

Tomasz Daszkiewicz[1]*, Mariusz Florek[2], Monika Wodzak[1], Dorota Kubiak[1], Ewa Burczyk[1]

[1]Department of Commodity Science and Processing of Animal Raw Materials, Faculty of Animal Bioengineering, University of Warmia and Mazury in Olsztyn, Oczapowskiego 5, 10-719 Olsztyn, Poland
[2]Department of Quality Assessment and Processing of Animal Products, Faculty of Animal Sciences and Bioeconomy, University of Life Sciences in Lublin, Akademicka 13, 20-950 Lublin, Poland

The aim of this study was to compare the quality of selected meat products, *i.e.* frankfurters, Polish *kabanos* sausages, and salami, with their plant-based (vegetarian) analogs. Five items from five different product batches were analyzed in each examined product category. The analyzed items were vacuum-packaged in bags to standardize the parameters of the compared products, and their quality was evaluated before the use-by date declared by the manufacturer. Meat products had higher dry matter and lipid contents. Salami contained more protein, whereas frankfurters and *kabanos* sausages contained less protein than their respective analogs. Moreover, traditional *kabanos* sausages had a higher pH than their vegetarian alternatives. Indicators of the nutritional value of lipids and pH of vegetarian frankfurters and salami were higher than those of their meat counterparts. In turn, lipids of vegetarian *kabanos* sausages had lower ratios of unsaturated to saturated fatty acids, monounsaturated to saturated fatty acids and hypocholesterolemic to hypercholesterolemic fatty acids than traditional *kabanos* sausages. Among the color parameters, redness (a^*), yellowness (b^*) and chroma (C^*) of plant-based meat analogs were higher compared to those of meat products. These results indicate that the names of plant-based analogs, which make a direct reference to the corresponding traditional meat products, can be misleading for consumers who expect products with similar quality attributes.

Key words: meat product, plant-based meat analog, quality

INTRODUCTION

There is no doubt that the inclusion of meat in the human diet played a significant role in the development of the human race [Williams & Hill, 2017]. According to Milton [1999], the incorporation of meat into the diet of early hominid species around 2.6 million years ago was a key event in their evolution. Meat procurement strategies contributed to technical progress, including the construction of tools and weapons, and the organization of hunting expeditions promoted the formation of social bonds and structures [Hladik & Pasquet, 2002]. Over time, meat consumption induced profound biological changes, including a decrease in the size of human teeth and intestines and changes in their morphology, as well as an increase in the size of the human body and brain, which ultimately led to the emergence of modern humans [Magkos, 2022]. The growing demand for animal protein contributed to animal rearing and breeding [Cucchi & Arbuckle, 2021]. In turn, food preservation and storage techniques were developed to prevent meat from spoilage during long-term storage [Knorr & Augustin, 2022].

***Corresponding Author:**
e-mail: tomasz.daszkiewicz@uwm.edu.pl (T. Daszkiewicz)

Submitted: 24 January 2023
Accepted: 22 March 2023
Published on-line: 25 April 2023

At present, meat and meat products continue to play a significant role in the human diet, both in developed and developing countries. In 2018, average global *per capita* consumption of unprocessed red meat reached 51 g/day [Miller *et al.*, 2022]. Meat is popular among consumers because it is a highly versatile food with numerous preparation options, desirable sensory attributes, and a high nutritional value [Dekkers *et al.*, 2018]. Global annual meat consumption, estimated at 34 kg *per capita* in 2019, is expected to increase by 14% in 2030. The projected increase will differ across continents, and it could reach 30% in Africa, 18% in Asia and the Pacific, 12% in Latin America, 9% in North America, and 0.4% in Europe [OECD/FAO, 2021]. The demand for various meat types will also differ. In 2018, meat products had the following market share: ruminant meat – 23%, poultry – 34%, pork – 32%, and meat of other animals – 2% [Smith *et al.*, 2022].

However, despite the positive implications of meat consumption, meat intake is also associated with certain health risks. Research has shown that the consumption of red meat is correlated with the incidence of type 2 diabetes [Sanders *et al.*, 2023], coronary heart disease [Papier *et al.*, 2023], and cancer [Demeyer *et al.*, 2016]. The Working Group of the International Agency for Research on Cancer (IARC) classified red meat as potentially carcinogenic for humans (Group 2A) and processed meat as carcinogenic for humans (Group 1) [Bouvard *et al.*, 2015]. The World Cancer Research Fund International [World Cancer Research Fund International, 2018] recommends that the consumption of red meat is limited to around three servings *per* week, *i.e.* 350–500 g (700–750 g of raw meat). The use of antibiotics in livestock production (including as growth promoters), the presence of antibiotic residues in foods [Van Boeckel *et al.*, 2015], and meat-borne zoonotic diseases [Lee Bouvard *et al.*, 2022] also pose health risks for consumers. It should also be noted that meat production, especially ruminant rearing, exerts a negative impact on the environment by contributing to greenhouse emissions, increasing the demand for pasture and land for the cultivation of forage and fodder crops, increasing the demand for water, and leading to environmental pollution [González *et al.*, 2020].

The health risks associated with meat consumption and the adverse impact of meat production on the environment and the well-being of animals have led to changes in consumer perceptions of meat. Many consumers give up meat or limit their meat intake based on the recommendations made by physicians and dieticians, environmental activists (promotion of sustainable development), and animal rights activists (moral and ethical implications of meat consumption), as well as for financial reasons. These consumers switch to meat analogs containing plant proteins, mycoproteins, algal or edible insect proteins. The production of meat cultured *in vitro* is also possible in the future [Lima *et al.*, 2022a]. It should be noted that the popularity of meat substitutes extends beyond the reach of the vegetarian movement and is increasingly associated with flexitarianism [Dagevos, 2021]. As a result, the sales of meat analogs increased by 38% between 2017 and 2021 [Ishaq *et al.*, 2022]. The value of the meat substitute market is projected to reach USD 2,651 million in 2026, increasing at a compound annual growth rate (CAGR) of 5.1% in 2021–2026 [IndustryARC™, 2023]. According to the IndustryARC™ report [2023], Europe was the dominant player on the meat substitute market with a major share of 42.6% in 2020, but Asia-Pacific is expected to outpace all regions with an estimated CAGR of 6.05% in 2021–2026.

Various types of meat substitutes are being introduced to the market to cater to the growing demand for meat analogs. In general, meat alternatives can be divided into analogs that "mimic" meat in appearance, taste or preparation method, and analogs that do not resemble meat [Bryngelsson *et al.*, 2022]. The names of products that imitate meat often make a direct reference to the substituted meat product. The aim of this marketing trick is to attract the consumers' attention to items that mimic traditional meat products, and to improve the positioning of plant-based analogs in the marketplace [Lacy-Nichols *et al.*, 2021]. The practice of naming meat analogs after their traditional counterparts has stirred a debate among producers and consumers, who have observed this strategy could be misleading and could undermine the foundations of the meat industry [Froggatt & Wellesley, 2019]. The question whether the practice of labeling meat substitutes with the names of the corresponding traditional meat products is justified by similarities in their chemical composition and physicochemical properties could be answered based on the results of research. However, there is a general scarcity of published studies addressing this issue. Therefore, this study was undertaken to verify the research hypothesis postulating that meat products and plant-based meat analogs have similar quality attributes. The research hypothesis was verified by comparing the proximate chemical composition, fatty acid profile, acidity, and color parameters of selected processed meats and their plant-based analogs available in retail.

MATERIALS AND METHODS

Materials

The quality of three processed meat products, *i.e.* frankfurters, Polish *kabanos* sausages, and salami, was compared with the corresponding plant-based analogs. The ingredient lists of meat products and their analogs, declared by manufacturers, are presented in Table 1. The analyzed products were manufactured by the leading Polish suppliers, and they were purchased between October and December 2021 in a hypermarket belonging to a popular international retail chain operating in Europe and Asia. Five items from five different product batches supplied by the same manufacturer were analyzed in each examined product category. The analyzed items were vacuum-packaged in bags to standardize the parameters of the compared products, and their quality was evaluated before the use-by date declared by the manufacturer. The compared products were refrigerated under identical conditions (4°C) until analysis.

Proximate chemical composition analysis

The proximate chemical composition of the products was determined in accordance with the Official Analytical Methods [AOAC, 2005]: moisture content (sample drying at a temperature

Table 1. Ingredient lists of the meat products and their analogs, declared by manufactures.

Frankfurter		*Kabanos*		Salami	
Meat product	**Meat analog**	**Meat product**	**Meat analog**	**Meat product**	**Meat analog**
Pork (71 %), water, salt, soy protein, modified starch, pork collagen protein, glucose, stabilizers (diphosphates, triphosphates), flavor enhancer (monosodium glutamate), spices, spice extracts, antioxidant (sodium ascorbate), preservative (sodium nitrite)	Water, soy protein isolate (10.9%), rapeseed oil, wheat protein (gluten) – 7.3%, modified corn starch, salt, flavorings, thickener (carrageenan), ground red pepper, colorings (iron oxides and hydroxides), liquid hickory smoke	Pork (100 g of product was obtained from 171 g of meat), salt, spices, antioxidant (sodium erythorbate), preservative (sodium nitrite), rapeseed oil	Water, wheat protein, vegetable oil (coconut oil), soy protein, spices, salt, flavorings, spice extracts, colorings (concentrated pepper extract, fenugreek extract, concentrated beetroot juice, iron oxides)	Beef, pork (100 g of product was obtained from 70 g of beef and 56 g of pork), pork fat, salt, spices, glucose, sugar, antioxidant (sodium ascorbate), bacterial starter cultures, preservatives (sodium nitrite, potassium nitrate)	Textured soy protein (7%), rapeseed oil, wheat protein (gluten) - 5%, modified corn starch, flavorings, salt, thickener (carrageenan), spices, vinegar powder, barley malt extract, colorings (iron oxides and hydroxides)

of 105°C to constant weight), total protein content (Kjeldahl method using Kjeltec™ 2200 auto distillation unit, FOSS Analytical, Hilleroed, Denmark), lipid content (Soxhlet extraction with diethyl ether using Soxtec™ 2050 auto fat extraction system, FOSS Analytical), and ash content (sample incineration at a temperature of 550°C to constant weight).

Fatty acid profile determination

Fatty acid profile in the products was analyzed according to the analytical procedure described by Daszkiewicz & Gugołek [2020]. Fatty acids were separated on the VARIAN CP-3800 gas chromatograph (Varian Inc., Palo Alto, CA, USA) with a flame ionization detector (FID) and a capillary column (length – 50 m, inner diameter – 0.25 mm, film thickness – 0.25 µm). Helium was used as a carrier gas (flow rate – 1.2 mL/min). The results were expressed as proportions (%) of individual fatty acids in total fatty acids.

Color parameter determination

The color parameters – lightness (L^*), redness (a^*) and yellowness (b^*) – were measured in the CIE Lab system [International Commission on Illumination, 1978] using the HunterLab MiniScan XE Plus spectrophotometer (Hunter Associates Laboratory, Reston, VA, USA) with illuminant D65, 10° standard observer angle, and 2.54 cm diameter aperture. The measurements were performed at three different points over the surface area of samples (salami slices and ground frankfurters and *kabanos* sausages). Chroma (C^*) values were calculated with the formula (1):

$$C^* = (a^{*2} + b^{*2})^{1/2} \quad (1)$$

Measurement of pH

The pH values of products were measured with the use of a Polilyte Lab electrode (Hamilton Bonaduz AG, Bonaduz, Switzerland) and an inoLab level 2 pH-meter equipped with a TFK 325 temperature sensor (WTW Wissenschaftlich-Technische Werkstatten GmbH, Weilheim, Germany). The samples of products were homogenized in redistilled water (ratio 1:1, *w/v*) before measurement [Daszkiewicz & Gugołek, 2020].

Statistical analysis

The results were processed statistically using STATISTICA software ver. 13.3 (TIBCO Software Inc., Palo Alto, CA, USA). The effect of the experimental factor (product type – meat products *vs.* their plant-based analogs) on the evaluated quality attributes of the products was analyzed by Student's *t*-test. The significance of differences between groups was determined at $p \leq 0.05$.

RESULTS AND DISCUSSION

Proximate chemical composition of meat products and their plant-based analogs

The proximate chemical composition of the compared products is presented in Table 2. Meat products had higher ($p \leq 0.05$) dry matter content than meat substitutes, mostly due to their higher ($p \leq 0.05$) lipid content. Salami and frankfurters had also higher ($p \leq 0.05$) ash content than their plant-based counterparts. Salami contained more ($p \leq 0.05$) protein, whereas frankfurters and *kabanos* sausages contained less ($p \leq 0.05$) protein than their respective analogs.

The differences in the proximate chemical composition of meat products and their vegetarian alternatives resulted from the use of different ingredients and production technologies. Plant-based meat analogs contain a considerably lower amount of lipids, a lot of protein, and different amount of water to achieve the desired textural properties and health benefits appreciated by consumers [Kyriakopoulou *et al.*, 2021]. However, the actual protein content of plant-based products may be difficult to determine. It may vary depending on the value of the nitrogen-to-protein conversion factor (NPCF) in the Kjeldahl method. According to Fujihara *et al.* [2008], the NPCF of 6.25 has been historically applied to all proteins based on the assumptions that all proteins contain 16% nitrogen (100/16 = 6.25) and that all nitrogen is derived from protein. However, research [Krul, 2019] showed that the NPCF of 6.25 overestimates the protein content of many food products due to differences in amino acid profiles and the presence of non-protein nitrogen. This is an important consideration when assessing the actual nutritional and economic value of food products. Koletzko & Shamir [2006] suggested that the use of the NPCF of 6.25 instead of 6.38 for all dairy products would lead

to a loss of approximately EUR 80 million in Europe. Therefore, all food market actors (consumers, producers of food raw materials, food processing companies, sales specialists, and nutritionists) are interested in solving the above problem and establishing NPCF values applicable to different proteins in food products that are already on the market and those that will be introduced in the future. This will apply, in particular, to analogs of traditional meat products whose quality, nutritional value and production costs should be assessed equitably. The absence of standardized methods for determining food-specific NPCF values has resulted in continued use of 6.25 [WHO/FAO, 2019]. The NPCF of 6.25 was also used in this study, but it was confronted with the average values of the ingredient-specific NPCF proposed for soybean protein (5.70) [WHO/FAO, 2020] and wheat protein (5.81) [Fujihara *et al.*, 2008] contained in the analyzed plant-based products. As a result, the protein content of vegetarian frankfurters, *kabanos* sausages and salami, determined by two different methods, differed by 1.84, 3.02 and 1.36 percentage points, respectively (Table 2). The above information may be important for persons who need a balanced diet, including older adults and individuals with special nutritional needs [Reid-McCann *et al.*, 2022], especially that the value of vegetable protein can be decreased due to amino acid composition (insufficient concentration of one or several essential amino acids). According to Hertzler *et al.* [2020], legumes are often deficient in sulfur-containing amino acids (methionine and cysteine), whereas cereals are poor in lysine. The need for accurate protein quantification in plant-based products was also emphasized by Bakaloudi *et al.* [2021] who found that vegan diets were lower in protein than all other diet types. This information and the fact that consumers' knowledge about vegetarian and vegan diets is often insufficient suggest that followers of such diets could have higher risk of developing nutrient deficiencies. Bakaloudi *et al.* [2021] reported that vegans had low intake of vitamins B_2, niacin (B_3), B_{12} and D, as well as iodine, zinc, calcium, potassium, and selenium. The above authors found that daily vitamin B_{12} intake among vegans was considerably lower (0.24–0.49 µg) than the recommended level (2.4 µg), and calcium intake was also below the norm (750 mg/day) in most vegan diet followers. According to Sanne & Bjørke-Monsen [2022], nutritional education should be improved as vegetarian and vegan diets are becoming increasingly popular. The cited study revealed gaps in nutritional knowledge about vegetarian diets even among Norwegian medical students who declared to be vegetarians.

Bryngelsson *et al.* [2022] assessed the nutritional quality of plant-based meat analogs available on the Swedish market based on three nutrition labeling systems. In terms of macronutrient content, most categories of meat analogs were healthier options to meat references, primarily due to their higher fiber content and lower content of lipids with saturated fatty acids. In terms of salt content, many plant-based meat analogs were healthy alternatives to processed meat products, but often less healthy options to unprocessed meat products. Similar analyses performed by Cutroneo *et al.* [2022] for commercial meat analogs available on the Italian market revealed that all analogs had

Table 2. Proximate chemical composition (g/100 g) of the meat products and their plant-based analogs.

Parameter	Product	Product type		SEM	*p*-Value
		Meat product	Meat analog		
Dry matter	Frankfurter	40.57^a	35.66^b	0.90	<0.001
	Kabanos	79.04^a	71.13^b	1.47	<0.001
	Salami	66.15^a	35.85^b	5.10	<0.001
Protein[1]	Frankfurter	13.24^b	16.73^a	0.59	<0.001
	Kabanos	25.16^b	38.50^a	2.38	<0.001
	Salami	22.98^a	17.32^b	0.96	<0.001
Protein[2]	Frankfurter	13.24^b	14.89^a	0.38	<0.001
	Kabanos	25.16^b	35.48^a	1.85	<0.001
	Salami	22.98^a	15.96^b	1.18	<0.001
Lipids	Frankfurter	22.21^a	4.35^b	2.99	<0.001
	Kabanos	47.87^a	12.09^b	6.33	<0.001
	Salami	35.85^a	5.61^b	5.07	<0.001
Ash	Frankfurter	2.92^a	1.94^b	0.17	<0.001
	Kabanos	4.42^a	4.46^a	0.08	0.854
	Salami	4.59^a	3.34^b	0.22	<0.001

[1] Protein content determined based on the fixed nitrogen-to-protein conversion factor (NPCF) of 6.25. [2] Protein content determined based on the average values of the ingredient-specific NPCF of 5.70 and 5.81 in plant-based products containing soybean protein and wheat protein, respectively. SEM, standard error of the mean. Values followed by different letters within the same row are significantly different ($p \leq 0.05$).

higher fiber content, whereas plant-based burgers and meatballs had lower protein content than their meat counterparts. Sliced meat analogs had also lower salt content. All plant-based products had longer lists of ingredients than the corresponding animal meat products. Due to their long lists of ingredients, most of which are highly refined, meat analogs face criticism for being artificial products [Kyriakopoulou *et al.*, 2021]. Modern consumers expect food products to be healthy, nutritious, and as natural as possible (minimally processed and without additives) [Hüppe & Zander, 2021].

Table 3. Saturated fatty acid profile of the meat products and their plant-based analogs (% of individual fatty acids in total fatty acids).

Parameter	Product	Product type		SEM	*p*-Value
		Meat product	Meat analog		
C8:0	Frankfurter	-	-	-	-
	Kabanos	0.00^{b}	5.40^{a}	0.95	<0.001
	Salami	0.00^{a}	0.17^{a}	0.08	0.347
C10:0	Frankfurter	-	-	-	-
	Kabanos	0.00^{b}	5.17^{a}	0.91	<0.001
	Salami	0.00^{a}	0.15^{a}	0.07	0.347
C12:0	Frankfurter	0.20^{a}	0.06^{b}	0.03	<0.001
	Kabanos	0.15^{b}	39.14^{a}	6.91	<0.001
	Salami	0.62^{a}	1.16^{a}	0.52	0.635
C14:0	Frankfurter	2.35^{a}	0.41^{b}	0.32	<0.001
	Kabanos	2.16^{b}	15.38^{a}	2.36	<0.001
	Salami	2.66^{a}	0.69^{b}	0.39	0.002
C15:0	Frankfurter	0.00^{a}	0.09^{a}	0.05	0.347
	Kabanos	-	-	-	-
	Salami	0.17^{a}	0.18^{a}	0.04	0.887
C16:0	Frankfurter	35.99^{a}	8.42^{b}	4.62	<0.001
	Kabanos	32.28^{a}	11.65^{b}	3.77	<0.001
	Salami	36.01^{a}	8.00^{b}	4.72	<0.001
C17:0	Frankfurter	0.34^{a}	0.07^{b}	0.05	<0.001
	Kabanos	0.32^{a}	0.05^{b}	0.05	<0.001
	Salami	0.57^{a}	0.09^{b}	0.08	<0.001
C18:0	Frankfurter	17.80^{a}	3.19^{b}	2.45	<0.001
	Kabanos	16.21^{a}	3.47^{b}	2.28	<0.001
	Salami	19.31^{a}	3.32^{b}	2.69	<0.001
C20:0	Frankfurter	0.24^{b}	0.62^{a}	0.06	<0.001
	Kabanos	0.23^{a}	0.10^{b}	0.02	<0.001
	Salami	0.30^{b}	0.55^{a}	0.05	<0.001
C22:0	Frankfurter	0.00^{b}	0.31^{a}	0.05	<0.001
	Kabanos	0.00^{a}	0.04^{a}	0.02	0.292
	Salami	0.00^{b}	0.28^{a}	0.05	<0.001
SFAs	Frankfurter	56.93^{a}	13.17^{b}	7.33	<0.001
	Kabanos	51.36^{b}	80.39^{a}	5.38	<0.001
	Salami	59.63^{a}	14.59^{b}	7.63	<0.001

SEM, standard error of the mean; SFAs, saturated fatty acids. Values followed by different letters within the same row are significantly different ($p \leq 0.05$).

Fatty acid profile of meat products and their plant-based analogs

The fatty acid profile of the compared products, including saturated fatty acids (SFAs), unsaturated fatty acids (UFAs) and fatty acid ratios, are presented in Tables 3, 4 and 5, respectively. Vegetarian frankfurters and salami were characterized by higher ($p \leq 0.05$), *i.e.* more desirable, values of all analyzed indicators of the nutritional value of lipids than their meat counterparts. Vegetarian *kabanos* sausages had lower ($p \leq 0.05$) ratios of unsaturated to saturated fatty acids (UFAs/SFAs), monounsaturated to saturated fatty acids (MUFAs/SFAs) and ratio of hypocholesterolemic

Table 4. Unsaturated fatty acid profile of the meat products and their plant-based analogs (% of individual fatty acids in total fatty acids).

Parameter	Product	Product type		SEM	*p*-Value
		Meat product	Meat analog		
C14:1	Frankfurter	-	-	-	-
	Kabanos	-	-	-	-
	Salami	0.16[a]	0.00[a]	0.07	0.292
C16:1	Frankfurter	2.56[a]	0.44[b]	0.36	<0.001
	Kabanos	2.51[a]	0.28[b]	0.40	<0.001
	Salami	2.18[a]	0.47[b]	0.29	<0.001
C17:1	Frankfurter	0.16[a]	0.07[b]	0.02	<0.001
	Kabanos	0.21[a]	0.03[b]	0.03	0.001
	Salami	0.27[a]	0.09[b]	0.03	<0.001
C18:1 *cis*-9	Frankfurter	33.09[b]	62.75[a]	4.97	<0.001
	Kabanos	35.98[a]	8.06[b]	5.11	<0.001
	Salami	30.12[b]	60.70[a]	5.17	<0.001
C18:1 *cis*-11	Frankfurter	2.64[a]	2.88[a]	0.07	0.094
	Kabanos	2.79[a]	0.39[b]	0.43	<0.001
	Salami	2.10[b]	2.69[a]	0.10	<0.001
C18:2	Frankfurter	2.81[b]	14.55[a]	2.01	<0.001
	Kabanos	5.25[a]	8.19[a]	0.90	0.108
	Salami	3.48[b]	15.31[a]	2.04	<0.001
C18:3	Frankfurter	0.07[b]	4.15[a]	0.70	<0.001
	Kabanos	0.31[a]	0.46[a]	0.07	0.355
	Salami	0.17[b]	4.57[a]	0.76	<0.001
C20:1	Frankfurter	1.75[a]	1.90[a]	0.10	0.468
	Kabanos	1.40[a]	0.17[b]	0.23	<0.001
	Salami	1.82[a]	1.48[a]	0.09	0.052
C20:2	Frankfurter	0.00[a]	0.06[a]	0.02	0.157
	Kabanos	0.14[a]	0.06[a]	0.05	0.501
	Salami	0.06[a]	0.09[a]	0.04	0.750
C20:3	Frankfurter	-	-	-	-
	Kabanos	0.02[a]	0.02[a]	0.01	0.833
	Salami	-	-	-	-
C20:4	Frankfurter	-	-	-	-
	Kabanos	0.02[a]	0.00[a]	0.01	0.407
	Salami	-	-	-	-

Table 4. Continued.

Parameter	Product	Product type		SEM	*p*-Value
		Meat product	Meat analog		
C22:1	Frankfurter	0.00[a]	0.04[a]	0.01	0.141
	Kabanos	-	-	-	-
	Salami	0.01[a]	0.02[a]	0.01	0.347
MUFAs	Frankfurter	40.19[b]	68.08[a]	4.67	<0.001
	Kabanos	42.90[a]	10.88[b]	5.72	<0.001
	Salami	36.66[b]	65.45[a]	4.88	<0.001
PUFAs	Frankfurter	2.88[b]	18.75[a]	2.72	<0.001
	Kabanos	5.74[a]	8.73[a]	1.02	0.155
	Salami	3.71[b]	19.96[a]	2.79	<0.001

SEM, standard error of the mean; MUFAs, monounsaturated fatty acids; PUFAs, polyunsaturated fatty acids. Values followed by different letters within the same row are significantly different ($p \leq 0.05$).

Table 5. Fatty acid ratios in the meat products and their plant-based analogs.

Parameter	Product	Product type		SEM	*p*-Value
		Meat product	Meat analog		
UFAs/SFAs	Frankfurter	0.76[b]	6.79[a]	1.05	<0.001
	Kabanos	0.97[a]	0.25[b]	0.14	0.001
	Salami	0.68[b]	6.76[a]	1.21	0.003
MUFAs/SFAs	Frankfurter	0.71[b]	5.31[a]	0.79	<0.001
	Kabanos	0.85[a]	0.14[b]	0.13	<0.001
	Salami	0.62[b]	5.17[a]	0.91	0.003
PUFAs/SFAs	Frankfurter	0.05[b]	1.48[a]	0.26	<0.001
	Kabanos	0.12[a]	0.11[a]	0.02	0.809
	Salami	0.06[b]	1.60[a]	0.31	0.003
DFAs/OFAS	Frankfurter	1.56[b]	9.22[a]	1.32	<0.001
	Kabanos	1.89[a]	0.30[b]	0.29	<0.001
	Salami	1.49[b]	9.11[a]	1.54	0.003
EFAs	Frankfurter	2.88[b]	18.69[a]	2.71	<0.001
	Kabanos	5.56[a]	8.65[a]	0.97	0.119
	Salami	3.64[b]	19.87[a]	2.79	<0.001

SEM, standard error of the mean; SFAs, saturated fatty acids; MUFAs, monounsaturated fatty acids; PUFAs, polyunsaturated fatty acids; UFAs, unsaturated fatty acids (MUFAs+PUFAs); DFAs, hypocholesterolemic fatty acids (UFAs+C18:0); OFAs, hypercholesterolemic fatty acids (SFAs–C18:0); EFAs, essential fatty acids (C18:2+C18:3). Values followed by different letters within the same row are significantly different ($p \leq 0.05$).

fatty acids (UFAs+C18:0) to hypercholesterolemic fatty acids (SFAs–C18:0) (DFAs/OFAs).

The differences in the fatty acid profiles of meat products and their plant-based analogs resulted from the different origin of lipids. Long-chain fatty acids, such as palmitic acid (C16:0), stearic acid (C18:0), oleic acid (C18:1), and linoleic acid (C18:2), predominate in lipids of meat and meat products, whereas the contents of polyunsaturated fatty acids (PUFAs) are low [Bohrer, 2019], which was also observed in this study. The proportion of PUFAs is particularly low in meat from ruminants, because they undergo biohydrogenation in the rumen. De Smet *et al.* [2004] reported that the average PUFAs/SFAs ratio in beef, lamb, and pork (steaks and chops) purchased in supermarkets in the United Kingdom was 0.11, 0.15 and 0.58, respectively. The above ratios are even lower in meat products because processing affects PUFAs [Domínguez *et al.*, 2019].

Vegetable oils/fats and animal fats differ in fatty acid composition and the mutual proportions of fatty acid groups. Different

types of edible oils/fats are also characterized by considerable differences in their fatty acid profiles. Orsavova *et al.* [2015] analyzed the fatty acid composition of 14 edible vegetable oils (safflower, grape, *Silybum marianum*, hemp, sunflower, wheat germ, pumpkin seed, sesame, rice bran, almond, rapeseed, peanut, olive, and coconut oil) and found that the contents of the major fatty acids varied widely: C16:0 – from 4.6% to 20.0%, C18:1 – from 6.2% to 71.1%, and C18:2 – from 1.6% to 79%. The proportions of fatty acid groups were determined in the following ranges: SFAs – from 6.3% (rapeseed oil) to 92.1% (coconut oil), MUFAs – from 6.2% (coconut oil) to 72.8% (rapeseed oil), and PUFAs – from 54.3% (pumpkin seed oil) to 79.1% (sunflower oil). Technological processes and refinement techniques (pressing, fractionation, isomerization) can also alter the fatty acid composition of vegetable oils/fats [Bohrer, 2019].

The vast majority of vegetable oils/fat used in the production of meat analogs contain mostly UFAs. In the present study, vegetarian frankfurters and salami were produced with the use of rapeseed oil, which contributed to their desirable fatty acid profiles. Increased contents of UFAs, in particular PUFAs, in lipids of plant-based meat analogs, deliver health benefits to consumers. However, they are also susceptible to oxidation, leading to the formation of multiple chemical compounds that negatively affect the sensory properties (flavor, color) of the products, and exert adverse health effects [Domínguez *et al.*, 2019]. Physical technological treatments that can reduce the oxidation of PUFAs in oils include pre-emulsification of oil with non-meat proteins and microencapsulation [Lima *et al.*, 2022b].

Fatty acids have different melting temperatures, therefore oils used in the production of plant-based meat analogs should be carefully selected because they affect the texture of the final product. In order to impart meat-like consistency and mouthfeel, meat alternatives are produced with the use of solid fats extracted from tropical fruit such as coconuts or, less frequently, cocoa beans [Sha & Xiong, 2020]. The dominant fatty acids in coconut oil are lauric acid (12:0), myristic acid (14:0) and palmitic acid (16:0), which account for 46%, 17% and 9% of total fatty acids, respectively [Boemeke *et al.*, 2015]. In the current study, coconut oil was used in the production of vegetarian *kabanos* sausages, which explains the low values of indicators characterizing the nutritional value of lipids in this product, relative to vegetarian products containing rapeseed oil and meat products. Coconut oil consists mostly of SFAs that account for approximately 90% of its total fatty acids, which has stirred a debate about its potential adverse health effects, by analogy with animal fats. A meta-analysis of clinical trials conducted by Neelakantan *et al.* [2020] revealed that the consumption of coconut oil contributed to a greater increase in low-density lipoprotein (LDL) cholesterol levels than the consumption of non-tropical vegetable oils. However, coconut oil was not significantly associated with the markers of glycemia, inflammation or obesity. According to Hewlings [2020], the health implications of SFAs should be analyzed in both quantitative (total SFAs content) and qualitative (proportions of individual SFAs) terms. A good example is coconut oil which is classified as saturated fat although most of its fatty acids are medium-chain ones. In contrast, beef contains mostly long-chain SFAs. Medium-chain SFAs are absorbed differently than long-chain SFAs; the former have been associated with several health benefits, including improved metabolic and cognitive functions in humans [Roopashree *et al.*, 2021], which may be linked with reduced oxidative stress [Mett & Müller, 2021]. Nevertheless, the dietary intake of UFAs, in particular PUFAs, should be increased [Snetselaar *et al.*, 2021]. Further research is needed to investigate potential relationships between individual SFAs and the risk of developing certain diseases in order to establish objective guidelines for the dietary inclusion or elimination of selected SFAs.

pH and color of meat products and their plant-based analogs

The pH values and color parameters of the compared products are presented in Table 6. The greatest difference ($p \leq 0.05$) in pH was noted between salami and its plant-based analog. The pH of salami was considerably lower because it was manufactured with the use of starter bacterial cultures. According to Bis-Souza *et al.* [2020], salami is a typical dry fermented sausage, and selected starter cultures are used in the process of its fermentation. Bacteria produce lactic acid that acidifies the product, imparts a distinctive taste, and extends its shelf life [Laranjo *et al.*, 2017]. Considerable differences in average pH values ($p \leq 0.05$) were also found between frankfurters and *kabanos* sausages *vs*. their plant-based analogs. Vegetarian frankfurters had a higher pH ($p \leq 0.05$) than their meat counterparts, and traditional *kabanos* sausages had a higher pH ($p \leq 0.05$) than their vegetarian alternatives. Therefore, there is no clear correlation between product type (meat product *vs*. meat analog) and its active acidity.

Color measurements revealed (Table 6) that plant-based meat analog of frankfurter was darker in color (lower L^* value, $p \leq 0.05$) than its traditional counterpart. All vegetarian products were also characterized by higher ($p \leq 0.05$) values of parameters a^* (redness) and b^* (yellowness), and, in consequence, higher ($p \leq 0.05$) chroma (C^*) values.

The color of meat alternatives is affected by the type and amount of coloring agents that are added to mimic the color of traditional meat products. According to the information on the labels of the plant-based products analyzed in the present study, they contained the following colorants: pepper extract, fenugreek extract (*Trigonella foenum-graecum* L.), concentrated beetroot (*Beta vulgaris* L. *subsp. vulgaris*) juice, iron oxides and hydroxides. The effect exerted by colorants on the color of meat substitutes depends not only on their type, but also stability. This applies in particular to natural pigments whose stability and brightness are affected by exposure to light, temperature, and pH [Harsito *et al.*, 2021]. Similar observations were made by Ekielski *et al.* [2013] who analyzed red pepper extract and found that its color was unstable under exposure to intensive light, and that natural pigments were more sensitive to light intensity than to increasing storage temperature. Regardless of the content and transformations of colorants, the color of food products may also be affected

Table 6. Values of pH and color parameters of the meat products and their plant-based analogs.

Parameter	Product	Product type		SEM	*p*-Value
		Meat product	Meat analog		
pH	Frankfurter	6.08^{b}	6.51^{a}	0.08	<0.001
	Kabanos	5.94^{a}	5.42^{b}	0.10	<0.001
	Salami	4.83^{b}	6.22^{a}	0.23	<0.001
*L**	Frankfurter	70.52^{a}	61.42^{b}	1.55	<0.001
	Kabanos	46.34^{a}	46.07^{a}	0.66	0.854
	Salami	46.23^{a}	45.76^{a}	0.72	0.765
*a**	Frankfurter	9.15^{b}	16.49^{a}	1.23	<0.001
	Kabanos	13.79^{b}	19.87^{a}	1.10	<0.001
	Salami	16.08^{b}	23.33^{a}	1.30	<0.001
*b**	Frankfurter	16.56^{b}	26.14^{a}	1.62	<0.001
	Kabanos	16.85^{b}	30.34^{a}	2.41	<0.001
	Salami	12.06^{b}	24.31^{a}	2.10	<0.001
*C**	Frankfurter	18.92^{b}	30.91^{a}	2.02	<0.001
	Kabanos	21.78^{b}	36.26^{a}	2.59	<0.001
	Salami	19.07^{b}	34.49^{a}	2.67	<0.001

SEM, standard error of the mean; *L**, lightness; *a**, redness; *b**, yellowness; *C**, chroma. Values followed by different letters within the same row are significantly different ($p \leq 0.05$).

by other factors. Herlina *et al.* [2021] suggested that the darker color (lower brightness) of plant-based meat analogs may be due to a high content of carbohydrates that participate in Maillard reactions. Lipid autooxidation may also significantly affect the color of plant-based products have high contents of UFAs [Barden & Decker, 2016]. According to Kim *et al.* [2014], moisture can act as a substrate for lipid oxidation. In the current study, plant-based meat analogs contained more carbohydrates (according to the manufacture's declaration), UFAs (except for *kabanos* sausages), and water than traditional meat products, which could be responsible for their darker color.

CONCLUSIONS

Differences in the ingredient composition and production technology had a significant effect on the proximate chemical composition, fatty acid profile, color, and pH of the analyzed meat products (frankfurters, Polish *kabanos* sausages, and salami) and their plant-based analogs. Meat substitutes differed from meat products in chemical composition and physicochemical properties. Therefore, the names, form and packaging of plant-based analogs, which make a direct reference to the corresponding traditional meat products, can be misleading for consumers who expect products with similar quality attributes.

RESEARCH FUNDING

Project financially supported by Minister of Education and Science in the range of the program entitled "Regional Initiative of Excellence" for the years 2019–2023, Project No. 010/RID/2018/19, amount of funding 12.000.000 PLN.

CONFLICT OF INTERESTS

The authors declare that they have no competing interests.

ORCID IDs

E. Burczyk https://orcid.org/0000-0002-8308-8372
T. Daszkiewicz https://orcid.org/0000-0001-5344-5490
M. Florek https://orcid.org/0000-0003-0941-1714
D. Kubiak https://orcid.org/0000-0002-8855-6446
M. Wodzak https://orcid.org/0009-0000-5168-0390

REFERENCES

1. AOAC International (2005). *Official Methods of Analysis*. 18th ed., Association of Official Analytical Chemists, Washington, DC, USA.
2. Bakaloudi, D.R., Halloran, A., Rippin, H.L., Oikonomidou, A.C., Dardavesis T.I., Williams, J., Wickramasinghe, K., Breda, J., Chourdakis, M. (2021). Intake and adequacy of the vegan diet. A systematic review of the evidence. *Clinical Nutrition*, *40*(5), 3503–3521. https://doi.org/10.1016/j.clnu.2020.11.035
3. Barden, L., Decker, E.A. (2016). Lipid oxidation in low-moisture food: A review. *Critical Reviews in Food Science and Nutrition*, *56*(15), 2467–2482. https://doi.org/10.1080/10408398.2013.848833
4. Bis-Souza, C.V., Penna, A.L.B., da Silva Barretto, A.C. (2020). Applicability of potentially probiotic *Lactobacillus casei* in low-fat Italian type salami with added fructooligosaccharides: *in vitro* screening and technological evaluation. *Meat Science*, *168*, art. no. 108186. https://doi.org/10.1016/j.meatsci.2020.108186
5. Boemeke, L., Marcadenti, A., Busnello, F.M., Gottschall, C.B.A. (2015). Effects of coconut oil on human health. *Open Journal of Endocrine and Metabolic Diseases*, *5*(7), 84–87. https://doi.org/10.4236/ojemd.2015.57011
6. Bohrer, B.M. (2019). An investigation of the formulation and nutritional composition of modern meat analogue products. *Food Science and Human Wellness*, *8*(4), 320–329. https://doi.org/10.1016/j.fshw.2019.11.006
7. Bouvard, V., Loomis, D., Guyton, K.Z., Grosse, Y., El Ghissassi, F., Benbrahim-Tallaa, L., Guha, N., Mattock, H., Straif, K., International Agency for Research on Cancer Monograph Working Group (2015). Carcinogenicity of consumption of red and processed meat. *The Lancet Oncology*, *16*(16), 1599–1600. https://doi.org/10.1016/S1470-2045(15)00444-1

8. Bryngelsson, S., Moshtaghian, H., Bianchi, M., Hallström, E. (2022). Nutritional assessment of plant-based meat analogues on the Swedish market. *International Journal of Food Sciences and Nutrition*, *73*(7), 889–901. https://doi.org/10.1080/09637486.2022.2078286
9. Cucchi, T., Arbuckle, B. (2021). Animal domestication: from distant past to current development and issues. *Animal Frontiers*, *11*(3) 6–9. https://doi.org/10.1093/af/vfab013
10. Cutroneo, S., Angelino, D., Tedeschi, T., Pellegrini, N., Martini, D., SINU Young Working Group (2022). Nutritional quality of meat analogues: Results from the Food Labelling of Italian Products (FLIP) Project. *Frontiers in Nutrition*, *9*, art. no. 852831. https://doi.org/10.3389/fnut.2022.852831
11. Dagevos, H. (2021). Finding flexitarians: Current studies on meat eaters and meat reducers. *Trends in Food Science and Technology*, *114*, 530–539. https://doi.org/10.1016/j.tifs.2021.06.021
12. Daszkiewicz, T., Gugołek, A. (2020). A comparison of the quality of meat from female and male Californian and Flemish Giant Gray rabbits. *Animals*, *10*(12), art. no. 2216. https://doi.org/10.3390/ani10122216
13. De Smet, S., Raes K., Demeyer, D. (2004). Meat fatty acid composition as affected by fatness and genetic factors: a review. *Animal Research*, *53*(2), 81–98. https://doi.org/10.1051/animres:2004003
14. Dekkers, B.L., Boom, R.M., van der Goot, A.J. (2018). Structuring processes for meat analogues. *Trends in Food Science and Technology*, *81*, 25–36. https://doi.org/10.1016/j.tifs.2018.08.011
15. Demeyer, D., Mertens, B., De Smet, S., Ulens, M. (2016). Mechanisms linking colorectal cancer to the consumption of (processed) red meat: A review. *Critical Reviews in Food Science and Nutrition*, *56*(16), 2747–2766. https://doi.org/10.1080/10408398.2013.873886
16. Domínguez, R., Pateiro, M., Gagaoua, M., Barba, F.J., Zhang, W., Lorenzo, J.M. (2019). A comprehensive review on lipid oxidation in meat and meat products. *Antioxidants*, *8*(10), art. no. 429. https://doi.org/10.3390/antiox8100429
17. Ekielski, A., Powałka, M., Żelaziński, T. (2013). The accelerated colour stability studies for selected plant pigments. *Nauki Inżynierskie i Technologie*, *4*(11), 9–19 (in Polish, English abstract).
18. Froggatt, A., Wellesley, L. (2019). *Meat Analogues: Considerations for the EU*, The Royal Institute of International Affairs, Chatham House, London, UK, pp. 25–28.
19. Fujihara, S., Sasaki, H., Aoyagi, Y., Sugahara, T. (2008). Nitrogen-to-protein conversion factors for some cereal products in Japan. *Journal of Food Science*, *73*(3), C204–C209. https://doi.org/10.1111/j.1750-3841.2008.00665.x
20. González, N., Marquès, M., Nadal, M., Domingo, J.L. (2020). Meat consumption: Which are the current global risks? A review of recent (2010-2020) evidences. *Food Research International*, *137*, art. no. 109341. https://doi.org/10.1016/j.foodres.2020.109341
21. Harsito, C., Prabowo, A.R., Prasetyo, S.D., Arifin, Z. (2021). Enhancement stability and color fastness of natural dye: A review. *Open Engineering*, *11*(1), 548–555. https://doi.org/10.1515/eng-2021-0055
22. Herlina, H., Aji, S.B., Purnomo, B.H. (2021). Physical, chemical, and sensory characteristics of chicken sausage with analog meat substitution. *Industria: Jurnal Teknologi dan Manajemen Agroindustri*, *10*(1), 67–77. https://doi.org/10.21776/ub.industria.2021.010.01.8
23. Hertzler, S.R., Lieblein-Boff, J.C., Weiler, M., Allgeier, C. (2020). Plant proteins: Assessing their nutritional quality and effects on health and physical function. *Nutrients*, *12*(12), art. no. 3704. https://doi.org/10.3390/nu12123704
24. Hewlings, S. (2020). Coconuts and health: Different chain lengths of saturated fats require different consideration. *Journal of Cardiovascular Development and Disease*, *7*(4), art. no. 59. https://doi.org/10.3390/jcdd7040059
25. Hladik, C.M., Pasquet, P. (2002). The human adaptations to meat eating: a reappraisal. *Human Evolution*, *17*(3–4), 199–206. https://doi.org/10.1007/BF02436371
26. Hüppe, R., Zander, K. (2021). Consumer perspectives on processing technologies for organic food. *Foods*, *10*(6), art. no. 1212. https://doi.org/10.3390/foods10061212
27. IndustryARC™. (2023). Meat Substitutes Market Forecast (2021-2026). Retrieved from: https://www.industryarc.com/Report/7489/meat-substitutes-market.html. Accessed: January 23, 2023.
28. International Commission on Illumination (1978). *Recommendations on Uniform Color Spaces-Color Difference Equations: Psychometric Color Terms. Supplement No. 2 to CIE Publication No. 15 (E-1.3.1.), 1971/(TC-1-3)*. CIE, Paris, France.
29. Ishaq, A., Irfan, S., Sameen, A., Khalid, N. (2022). Plant-based meat analogs: A review with reference to formulation and gastrointestinal fate. *Current Research in Food Science*, *5*, 973–983. https://doi.org/10.1016/j.crfs.2022.06.001
30. Kim, J.Y., Kim, M.-J., Lee, J.H. (2014). Role of moisture on the lipid oxidation determined by D_2O in a linoleic acid model system. *Food Chemistry*, *146*, 134–140. https://doi.org/10.1016/j.foodchem.2013.09.025
31. Knorr, D., Augustin, M.A. (2022). Preserving the food preservation legacy. *Critical Reviews in Food Science and Nutrition*. https://doi.org/10.1080/10408398.2022.2065459
32. Koletzko, B., Shamir, R. (2006). Standards for infant formula milk. *British Medical Journal*, *332*, 621–622. https://doi.org/10.1136/bmj.332.7542.621
33. Krul, E.S. (2019). Calculation of nitrogen-to-protein conversion factors: A review with a focus on soy protein. *Journal of the American Oil Chemists' Society*, *96*(4), 339–364. https://doi.org/10.1002/aocs.12196
34. Kyriakopoulou, K., Keppler, J.K., van der Goot, A.J. (2021). Functionality of ingredients and additives in plant-based meat analogues. *Foods*, *10*(3), art. no. 600. https://doi.org/10.3390/foods10030600
35. Lacy-Nichols, J., Hattersley, L., Scrinis, G. (2021). Nutritional marketing of plant-based meat-analogue products: An exploratory study of front-of-pack and website claims in the USA. *Public Health Nutrition*, *24*(14), 4430–4441. https://doi.org/10.1017/S1368980021002792
36. Laranjo, M., Elias, M., Fraqueza, M.J. (2017). The use of starter cultures in traditional meat products. *Journal of Food Quality*, 2017, art. no. 9546026. https://doi.org/10.1155/2017/9546026
37. Lee, J.-S., Oh, H., Choi, I., Yoon, C.S., Han, J. (2022). Physico-chemical characteristics of rice protein-based novel textured vegetable proteins as meat analogues produced by low-moisture extrusion cooking technology. *LWT – Food Science and Technology*, *157*, art. no. 113056. https://doi.org/10.1016/j.lwt.2021.113056
38. Lima, M., Costa, R., Rodrigues, I., Lameiras, J., Botelho, G. (2022a). A narrative review of alternative protein sources: Highlights on meat, fish, egg and dairy analogues. *Foods*, *11*(14), art. no. 2053. https://doi.org/10.3390/foods11142053
39. Lima, T.L.S., da Costa, G.F., Alves, R.N., de Araújo, C.D.L., da Silva, G.F.G., Ribeiro, N.L., de Figueiredo, C.F.V., de Andrade, R.O. (2022b). Vegetable oils in emulsified meat products: a new strategy to replace animal fat. *Food Science and Technology*, *42*, art. no. e103621. https://doi.org/10.1590/fst.103621
40. Magkos, F. (2022). Meat in the human diet: in transition from evolutionary hallmark to scapegoat. *The American Journal of Clinical Nutrition*, *115*(5), 1263–1265. https://doi.org/10.1093/ajcn/nqac041
41. Mett, J., Müller, U. (2021). The medium-chain fatty acid decanoic acid reduces oxidative stress levels in neuroblastoma cells. *Scientific Reports*, *11*, art. no. 6135. https://doi.org/10.1038/s41598-021-85523-9
42. Miller, V., Reedy, J., Cudhea, F., Zhang, J., Shi, P., Erndt-Marino, J., Coates, J., Micha, R., Webb, P., Mozaffarian, D. (2022). Global, regional, and national consumption of animal-source foods between 1990 and 2018: Findings from the Global Dietary Database. *The Lancet Planetary Health*, *6*(3), e243–e256. https://doi.org/10.1016/S2542-5196(21)00352-1
43. Milton, K. (1999). A hypothesis to explain the role of meat-eating in human evolution. *Evolutionary Anthropology*, *8*(1), 11–21. https://doi.org/10.1002/(SICI)1520-6505(1999)8:1<11::AID-EVAN6>3.0.CO;2-M
44. Neelakantan, N., Seah, J.Y.H., van Dam, R.M. (2020). The effect of coconut oil consumption on cardiovascular risk factors. A systematic review and meta-analysis of clinical trials. *Circulation*, *141*, 803–814. https://doi.org/10.1161/CIRCULATIONAHA.119.043052
45. OECD/FAO (2021). *OECD-FAO Agricultural Outlook 2021-2030*. OECD Publishing, Paris, France. p. 171. https://doi.org/10.1787/19428846-en
46. Orsavova, J., Misurcova, L., Ambrozova, J.V., Vicha, R., Mlcek, J. (2015). Fatty acids composition of vegetable oils and its contribution to dietary energy intake and dependence of cardiovascular mortality on dietary intake of fatty acids. *International Journal of Molecular Sciences*, *16*(6), 12871–12890. https://doi.org/10.3390/ijms160612871
47. Papier, K., Knuppel, A., Syam, N., Jebb, S.A., Key, T.J. (2023). Meat consumption and risk of ischemic heart disease: A systematic review and meta-analysis. *Critical Reviews in Food Science and Nutrition*, *63*(3), 426–437. https://doi.org/10.1080/10408398.2021.1949575
48. Reid-McCann, R.J., Brennan, S.F., McKinley, M.C., McEvoy, C.T. (2022). The effect of animal *versus* plant protein on muscle mass, muscle strength, physical performance and sarcopenia in adults: protocol for a systematic review. *Systematic Reviews*, *11*, art. no. 64. https://doi.org/10.1186/s13643-022-01951-2
49. Roopashree, P.G., Shetty, S.S., Kumari, N.S. (2021). Effect of medium chain fatty acid in human health and disease. *Journal of Functional Foods*, *87*, art. no. 104724. https://doi.org/10.1016/j.jff.2021.104724

50. Sanders, L.M., Wilcox, M.L., Maki, K.C. (2023). Red meat consumption and risk factors for type 2 diabetes: A systematic review and meta-analysis of randomized controlled trials. *European Journal of Clinical Nutrition*, *77*(2), 156–165. https://doi.org/10.1038/s41430-022-01150-1
51. Sanne, I., Bjørke-Monsen, A.-L. (2022). Lack of nutritional knowledge among Norwegian medical students concerning vegetarian diets. *Journal of Public Health: From Theory to Practice*, *30*(2), 495–501. https://doi.org/10.1007/s10389-020-01327-7
52. Sha, L., Xiong, Y.L. (2020). Plant protein-based alternatives of reconstructed meat: Science, technology, and challenges. *Trends in Food Science and Technology*, *102*, 51–61. https://doi.org/10.1016/j.tifs.2020.05.022
53. Smith, N.W., Fletcher, A.J., Hill, J.P., McNabb, W.C. (2022). Modeling the contribution of meat to global nutrient availability. *Frontiers in Nutrition*, 9, art. no. 766796. https://doi.org/10.3389/fnut.2022.766796
54. Snetselaar, L.G., de Jesus, J.M., DeSilva, D.M., Stoody, E.E. (2021). Dietary Guidelines for Americans, 2020-2025: Understanding the scientific process, guidelines, and key recommendations. *Nutrition Today*, *56*(6), 287–295. https://doi.org/10.1097/NT.0000000000000512
55. Van Boeckel, T.P., Brower, C., Gilbert, M., Grenfell, B.T., Levin, S.A., Robinson, T.P., Teillant, A., Laxminarayan, R. (2015). Global trends in antimicrobial use in food animals. *The Proceedings of the National Academy of Sciences*, *112*(18), 5649–5654. https://doi.org/10.1073/pnas.1503141112
56. WHO/FAO (2019). *Nitrogen and protein content measurement and nitrogen to protein conversion factors for dairy and soy protein-based foods: A systematic review and modelling analysis*. World Health Organization and Food and Agriculture Organization of the United Nations, Geneva, Switzerland.
57. WHO/FAO (2020). *The Joint FAO/WHO Expert Meetings on Nutrition (JEMNU): Nitrogen to protein conversion factors for soy-based and milk-based ingredients used in infant formula and follow-up formula. Report of the meeting of the expert panel, Geneva, Switzerland, 16-17 July 2019*. World Health Organization and Food and Agriculture Organization of the United Nations, Geneva, Switzerland.
58. Williams, A.C., Hill, L.J. (2017). Meat and nicotinamide: A causal role in human evolution, history, and demographics. *International Journal of Tryptophan Research*, *10*, 2017. https://doi.org/10.1177/1178646917704661
59. World Cancer Research Fund International (2018). Recommendations and public health and policy implications. Retrieved from: https://www.wcrf.org/sites/default/files/Recommendations.pdf. Accessed January 23, 2023.

ORIGINAL ARTICLE
http://journal.pan.olsztyn.pl

Polish Journal of Food and Nutrition Sciences
2023, Vol. 73, No. 2, 120–129
DOI: 10.31883/pjfns/162710
ISSN 1230-0322, e-ISSN 2083-6007

Kefir Prevents Adipose Tissue Growth Through the Induction of Apoptotic Elements in High-Fructose Corn Syrup-Fed Rats

Esra Aslan[1], Gökhan Sadi[2], Hilal Guzel[3], Cigdem Karaca[1], Omer A. Korkmaz[4], Mine K. Pektas[5], Mehmet Celegen[6], Tugce Aladag[1], Seyma Oncu[7], Mehmet B. Pektas[7]*

[1]Department of Histology and Embryology, Faculty of Medicine, Afyonkarahisar Health Sciences University, 03200, Afyonkarahisar, Turkey
[2]Department of Biology, K.Ö. Science Faculty, Karamanoglu Mehmetbey University, 70100, Karaman, Turkey
[3]Department of Anatomy, Faculty of Medicine, Afyonkarahisar Health Sciences University, 03200, Afyonkarahisar, Turkey
[4]Department of Chemistry, Faculty of Science, Yildiz Technical University, 34220, Istanbul, Turkey
[5]Department of Obstetrics and Gynecology, Faculty of Medicine, Afyonkarahisar Health Sciences University, 03200, Afyonkarahisar, Turkey
[6]Department of Pediatrics, Faculty of Medicine, Afyonkarahisar Health Sciences University, 03200, Afyonkarahisar, Turkey
[7]Department of Medical Pharmacology, Faculty of Medicine, Afyonkarahisar Health Sciences University, 03200, Afyonkarahisar, Turkey

Consumption of high-fructose corn syrup (HFCS) in the diet is a causal factor in the development of abdominal obesity; however, the molecular mechanism behind this association is still up for debate. This study evaluated the metabolic disturbances that are caused by HFCS on adipose tissue as well as the possibility of kefir as a therapy to prevent these metabolic disturbances. Male *Wistar* rats were divided into four groups: control, kefir, HFCS, and HFCS+kefir. HFCS (20%, *w/v*) was given in drinking water and kefir (1 mL/100 g body weight) by gastric gavage daily for 8 weeks. Levels of insulin signaling, inflammation, and apoptosis-associated proteins of adipose tissues were determined with Western blot and immunohistochemical techniques. Gene expressions were evaluated with semi-quantitative real-time polymerase chain reaction (qRT-PCR). The indirect terminal deoxynucleotidyl transferase dUTP nick-end labeling (TUNEL) method was used to assess changes in apoptotic cells, and hematoxylin/eosin staining to determine adipocyte number and diameter. Accordingly, HFCS boosted protein kinase B (Akt) and p-Akt while reducing nuclear factor κB (NF-κB), and tumor necrosis factor alpha (TNFα) levels and kefir treatment restored Akt induction in HFCS-treated rats despite raising NF-κB, and TNFα. Increased expression of *Akt* and B-cell lymphoma-2 gene (*Bcl2*) was contrasted with decreased expression of *Nfkb, Tnfa,* tumor protein 53 gene (*p53*), and caspase-8 gene (*Casp8*). Furthermore, while there was a marked reduction in TUNEL-positive cells in the HFCS group, the number of such cells was greater in the HFCS+kefir group. These results show that HFCS intake suppresses apoptosis in adipose tissues, which may be responsible for tissue development and abdominal obesity and may be reversed with kefir administration due to the activation of apoptosis-associated genes and proteins.

Key words: adipose tissue, fructose, kefir, apoptosis, inflammation

INTRODUCTION

Obesity is a form of chronic disease that is experiencing a rise in incidence and is now being recognized on a worldwide scale as an epidemic [Hill *et al.*, 2022]. Recent research suggests that differences in lifestyle and eating habits are the most significant contributors [Khorshidian *et al.*, 2021], and carbohydrate consumption, especially from refined sources, might lead to the development of chronic diseases including obesity, insulin resistance, metabolic syndrome, and diabetes [Stanhope, 2016]. Research evaluating the negative impacts of various forms of carbohydrates,

***Corresponding Author:**
tel.: +90 532 253 39 40; e-mail: mbpektas@gmail.com (M.B. Pektas)

Submitted: 7 January 2023
Accepted: 27 March 2023
Published on-line: 5 May 2023

including glucose, fructose, and sucrose, has found that fructose in sweetened foods and beverages has the most pronounced effect [Zafar *et al.*, 2021]. Due to the fact that insulin cannot regulate fructose metabolism, it develops abdominal fat deposition that is distinct from overall obesity [Akar *et al.*, 2021]. It is also well-known that a diet high in fructose causes insulin resistance, metabolic syndrome, diabetes, and heart disease, as well as serious damage to the liver, kidneys, vascular smooth muscle, ovaries, and testicles [Sumlu *et al.*, 2022; Yildirim *et al.*, 2019]. However, its impact on cellular signaling pathways may vary depending on the tissue type. For instance, hepatic insulin receptor substrate-1 (IRS-1), endothelial nitric oxide synthase (eNOS), protein kinase B (Akt), and sirtuin-1 (SIRT-1) levels were recently reported to be reduced in rats fed a long-term diet of 10% fructose [Korkmaz *et al.*, 2019; Yildirim *et al.*, 2019], whereas they were elevated in adipose tissues [Pektas *et al.*, 2016]. This abnormality is due to insulin's anabolic nature, which enhances adipose tissue growth. Furthermore, adipose tissue regulates various physiological processes *via* the hormones it secretes, including leptin, adiponectin, resistin, and visfatin [Liu *et al.*, 2021], which may amplify the consequences of feeding--related metabolic disorders.

Insulin and insulin-like growth factor (IGF) signaling have been found to be associated with cell growth and division by promoting cell-cycle activators and inhibiting apoptosis-related pathways, which suggests a relationship between metabolic diseases and cancer development [Harvey *et al.*, 2011]. There have been several postulated links between cancer development and obesity. For instance, increased levels and bioavailability of insulin and insulin-like growth factors, altered adipocytokine levels such as leptin, adiponectin, and visfatin, and oxidative stress have been associated with cancer development in obese people [Berger, 2014]. Epidemiological, clinical, and experimental studies also revealed the effects of weight loss in preventing breast, endometrium, esophagus, adenocarcinomas, pancreatic, colorectal, colon, and kidney cancers [Irigaray *et al.*, 2007]. Recent studies present data revealing the alteration of insulin signaling components and apoptosis-associated parameters in high-fructose-induced obesity animals. For instance, caspase-3 levels were elevated [Savran *et al.*, 2019], phosphorylated insulin receptor substrate (p-IRS-1) and phosphorylated protein kinase B (p-Akt), levels were lowered [Prasatthong *et al.*, 2021], and insulin receptor (IR), IRS-1, IRS-2, and Akt were suppressed in the bladder of rats administered a high-fructose diet [Lee *et al.*, 2021]. Caspase-3, -8, and -9 levels were elevated in the pancreas [Nephan *et al.*, 2018], while tumor necrosis factor α (TNFα), B-cell lymphoma 2 protein (Bcl-2), Bcl-2-associated X protein (Bax), and caspase-3 levels were elevated in the liver [Zaki *et al.*, 2019], and p53 levels were decreased in the colon epithelium of rats fed with high-fructose diets [Narayanankutty *et al.*, 2022]. Similarly, we have previously demonstrated that levels of IR, IRS-1, IRS-2, Akt, phosphoinositide 3-kinase (PI3K), eNOS, and SIRT-1 in adipose tissue were enhanced [Pektas *et al.*, 2016]. Even though these studies attempted to establish the molecular action mechanisms of fructose in various tissues, the effects of fructose on adipose tissue remain understudied.

Probiotics are a mixture of beneficial bacteria and/or yeasts that occur naturally in the human body, and when combined with prebiotics, they have been shown to treat a variety of ailments such as allergies, gastrointestinal problems, and inflammation [Markowiak & Śliżewska, 2017]. Kefir, a fermented milk product classified as source of probiotics, comprises lactic and acetic acid bacteria in a polysaccharide matrix [Rosa *et al.*, 2016] and has been found to have anti-viral [Hamida *et al.*, 2021], anti-inflammatory [Akar *et al.*, 2021; Pektaş *et al.*, 2022], and anti-allergic properties [Barros *et al.*, 2021]. It has also been demonstrated to prevent problems brought on by fructose or high-fructose corn syrup (HFCS) ingestion [Akar *et al.*, 2021; Chen *et al.*, 2016; Ekici *et al.*, 2022a; Rosa *et al.*, 2016]. Also, the major bacteria in kefir, *Lactobacillus kefiri*, reduced the size of adipose tissue and had anti-inflammatory effects in fructose-fed mice [Zubiría *et al.*, 2017]. Similar results were also seen in the adipose tissue of obese mice, where it reduced lipid production and inflammatory cytokines [Choi *et al.*, 2017]. We have previously shown [Ekici *et al.*, 2022a] that kefir protects young rats against the HFCS-induced inflammation of the masseter muscle and gingival tissue, as well as from the altered metabolic parameters that accompany this inflammation. We also showed the preventive effects on HFCS-induced bone loss in the craniofacial region of rat models [Ekici *et al.*, 2022b]. Herein, we aimed to investigate the importance of apoptosis on adipocytes and adipogenesis, and the effects of kefir consumption on high-fructose corn syrup-induced adipogenesis at the molecular level.

MATERIALS AND METHODS

Animals and protocols

Male *Wistar* rats aged four weeks and weighing around 100 g were fed a regular rodent chow diet. Before the experiment, the rats were housed on a 12-h night and day cycle in an environment of 24–26°C and 50–60% humidity. The work was authorized by Afyon Kocatepe University's Ethical Animal Research Committee (AKUHADYEK 49533702-55). The rats were cared in accordance with the National Health and Medical Research Council's Experimental Animal Principles and Guidelines [National Health and Medical Research Council, 2013] and the National Institute of Health's Experimental Animal Care and Use Guidelines (NIH issue no. 85-23, 1985 amended) [National Research Council, 2011]. A total of 48 animals were given a week to adapt to the environment before any practical applications were made, after which they were divided into four groups: control, kefir, HFCS, and HFCS+kefir. Kefir (DanemKefir, Isparta, Turkey) was supplied ready-made commercially available. Kefir was given to the rats as 1 mL/100 g body weight daily *via* gastric gavage. HFCS F55 (56% of fructose, 37% glucose, 2% higher saccharides, Cargill, Wayzata, MN, USA) was applied in drinking water (20%, *w/v*) *ad libitum* throughout 8 weeks. The terminal weights of the animals were 291±5 g (control), 322±3 g (kefir), 365±9 g (HFCS), and 335±2 g (HFCS+kefir). Following the administration of HFCS and kefir, the rats were rendered unconscious with ketamine (100 mg/kg) and xylazine (10 mg/kg), and then their omental white adipose tissues were removed and examined. Before being frozen using

liquid nitrogen and kept at –85°C, the samples were washed with physiological saline solution. Some tissues were also fixed in 10% neutral formalin for the immunohistochemical analysis.

Determination of NF-κB and TNFα levels in the adipose tissues

Adipose tissue samples were homogenized in 0.1 M phosphate buffer (1:10 (*w/v*), pH 7.4) with Ultra-Turrax homogenizer (Ika Works Inc., Wilmington, NC, USA) at 24,000 cycles/min. Then, homogenates were further ultrasonicated at 20,000 cycles/s for 1 min (Dr. Hielscher ultrasonic device, Teltow, Germany). Supernatants were collected after centrifugation at +4°C at 10,000×g for 15 min and stored at –85°C until further use. Nuclear factor κB (NF-κB) and TNFα levels were determined using SEB824Ra and SEA133Ra commercial enzyme-linked immunosorbent assay (ELISA) kits, respectively (Cloud-Clone Corp., Houston, TX, USA) and performing the procedures outlined by the kit's manufacturer.

Determination of protein levels by Western blot

Adipose tissues were homogenized using a Tissue Ruptor™ homogenizer (Qiagen, Venlo, Netherlands) in 2-fold volumes of a homogenization medium (50 mM Tris, 150 mM sodium chloride, 5 mM ethylenediaminetetraacetic acid, 1% (*w/w*) Triton X-100, 0.26% (*w/v*) sodium deoxycholate, 50 mM sodium fluoride). The homogenates were then centrifuged at 1,500×*g* for 10 min at +4°C. Supernatants whose protein concentrations were determined by the Lowry method [Lowry *et al.*, 1951] were collected and processed for Western blot analysis.

One hundred mg of proteins were separated on a polyacrylamide gel electrophoresis (12% separating and 4% stacking gels) and then transferred onto polyvinylidene fluoride membranes using the Trans-Blot Turbo transfer system (Bio-Rad Laboratories, Hercules, CA, USA). After that, the membranes were blocked with 3% bovine serum albumin for 1 h, and primary antibodies were utilized for priming the respective Akt (anti-Akt rabbit IgG, Santa Cruz Biotechnology, Dallas, TX, USA; dilution 1:1,000) and p-Akt (anti-pAkt rabbit IgG, Santa Cruz Biotechnology; dilution 1:500) antibodies overnight at +4°C. As an internal control, anti-GAPDH rabbit IgG (Santa Cruz Biotechnology; dilution 1:4,000) was used to label glyceraldehyde 3-phosphate dehydrogenase (GAPDH) for data normalization. Subsequent to washing, the blots were incubated with secondary antibodies conjugated with horseradish peroxidase (HRP) for 1 h (goat anti-rabbit IgG-HRP conjugate, Santa Cruz Biotechnology; dilution 1:10,000) before being exposed to a Clarity™ Western ECL (Bio-Rad Laboratories) substrate solution for 5 min. A ChemiDoc™ MP chemiluminescence detection device was used to capture the blot pictures (Bio-Rad Laboratories) and ImageLab 4.1 software (Bio-Rad Laboratories) was used to determine the protein's relative level in relation to GAPDH.

Determination of the gene expressions with the real-time polymerase chain reaction

Relative expression levels of genes: *Akt, Nfkb, Tnfa, p53, Casp8,* and *Bcl2*, with respect to *Gapdh* were determined with a semi-quantitative real-time polymerase chain reaction (qRT-PCR). To begin, total RNAs were extracted from adipose tissues using a commercial kit (GeneJET RNA purification kit, Thermo Fisher Scientific, Waltham, MA, USA) and then analyzed by agarose gel electrophoresis and a spectrophotometery at 260/280 nm for quality control. RevertAid™ First Strand cDNA Synthesis Kit was used to reverse transcribe 1 µg of total RNA to cDNA (Thermo Fisher Scientific). Gene expressions were determined by qRT-PCR protocol as we described previously [Ekici *et al.*, 2022a]. The used primer pairs are given in Table 1. The relative expressions of the genes were determined using LightCycler™ 480 SW 1.5.1 software (Roche, Forrenstrasse, Switzerland), with *Gapdh* expression serving as the internal control.

Immunohistochemical analysis

Tissue slices (5 µm) were microwaved in a citrate buffer (0.1 M, pH: 6.0) for an antigen retrieval process after being deparaffinized and rehydrated. Hydrogen peroxide at a concentration of 3% was used to block peroxidase activity. To identify the desired protein, primary antibodies of NF-κB (sc-8008, 1/100), perilipin 1 (PLIN-1; bs-3789R, 1/200), Bax (sc-526, 1/100), caspase-3 (sc-56053, 1/100), and TNFα (ab34674, 1/200) were utilized. A secondary antibody coupled with horseradish peroxidase (HRP) was used to probe primed samples (TP-125-HL, Thermo Fisher Scientific). 3-Amino-9-ethylcarbazole (LabVision AB, Värmdö, Sweden) was applied as a chromogen. All of the slides were counterstained with Mayers hematoxylin and mounted using a water-based mounting solution. Under a bright light microscope (Eclipse E600, Nikon,

Table 1. Primer sequences used in gene expression analysis with quantitative real-time polymerase chain reaction.

Gene name	Forward primer 5′→3′	Reverse primer 5′→3′
Akt	GAAGAAGAGCTCGCCTCCAT	GAAGGAGAAGGCCACAGGTC
Nfkb	GGGTCAGAGGCCAATAGAGA	CCTAGCTTTCTCTGAACTGCAAA
Tnfa	ATGGGCTCCTCTCATCAGT	GCTTGGTTTGCTACGAC
Casp88	GCTGTAACCTGTCGCCG	ACCTCCGGTGTTTTATAGTTCC
Bcl2	TTCCTGCATCTCATGCCAAG	TACCAATAGCACTTCGCGTC
p53	TCCCCTGAAGACTGGATAACT	TTCCTCTGGGCCTTCTAACA
Gapdh	TGATGACATCAAGAAGGTGGTGAAG	TCCTTGGAGGCCATGTGGGCCAT

Tokyo, Japan), the immuno-positive adipocytes were counted in 5 randomly chosen areas for each section to analyze the immunoreactivity of the specimens. Image analysis was carried out using imaging software (NIS Elements) specifically designed for that purpose (Nikon).

Terminal deoxynucleotidyl transferase dUTP nick-end labeling (TUNEL) assay

For the detection of apoptotic cells in adipose tissue, the indirect TUNEL method was used according to the manufacturer's protocol of ApopTag plus Peroxidase *in Situ* Apoptosis Detection Kit (S7101, Merck Millipore, Burlington, MA, USA). TUNEL-positive cells were counted for each section in five different areas. Dark brown stained cells were considered positive.

Histochemical staining

Adipose tissue samples were fixed in 10% neutral formalin and histologically examined. Five micrometer-thick slices of paraffin blocks were cut and stained with hematoxylin and eosin (H&E). Five randomly selected areas from each section were evaluated from tissues of at least six rats. The average was used to compute the number of cells per unit. Furthermore, the diameter of at least 100 cells in each segment was measured, and the mean cell diameter was determined.

Statistical analysis

Throughout the course of the study, all of the data is given as a mean ± standard error of the mean (SEM). The one-way analysis of variance (ANOVA) and the necessary post hoc tests (Tukey) were used to conduct the statistical comparisons. Comparisons with $p<0.05$ were considered statistically significant. The expressions of genes and levels of proteins were standardized relative to the mean of the control group. The data was also normalized with corresponding GAPDH and *Gapdh* within the same groups.

RESULTS AND DISCUSSION

The information on the body and omentum weights of rats, their intake of food, fluids, and calories, as well as various metabolic

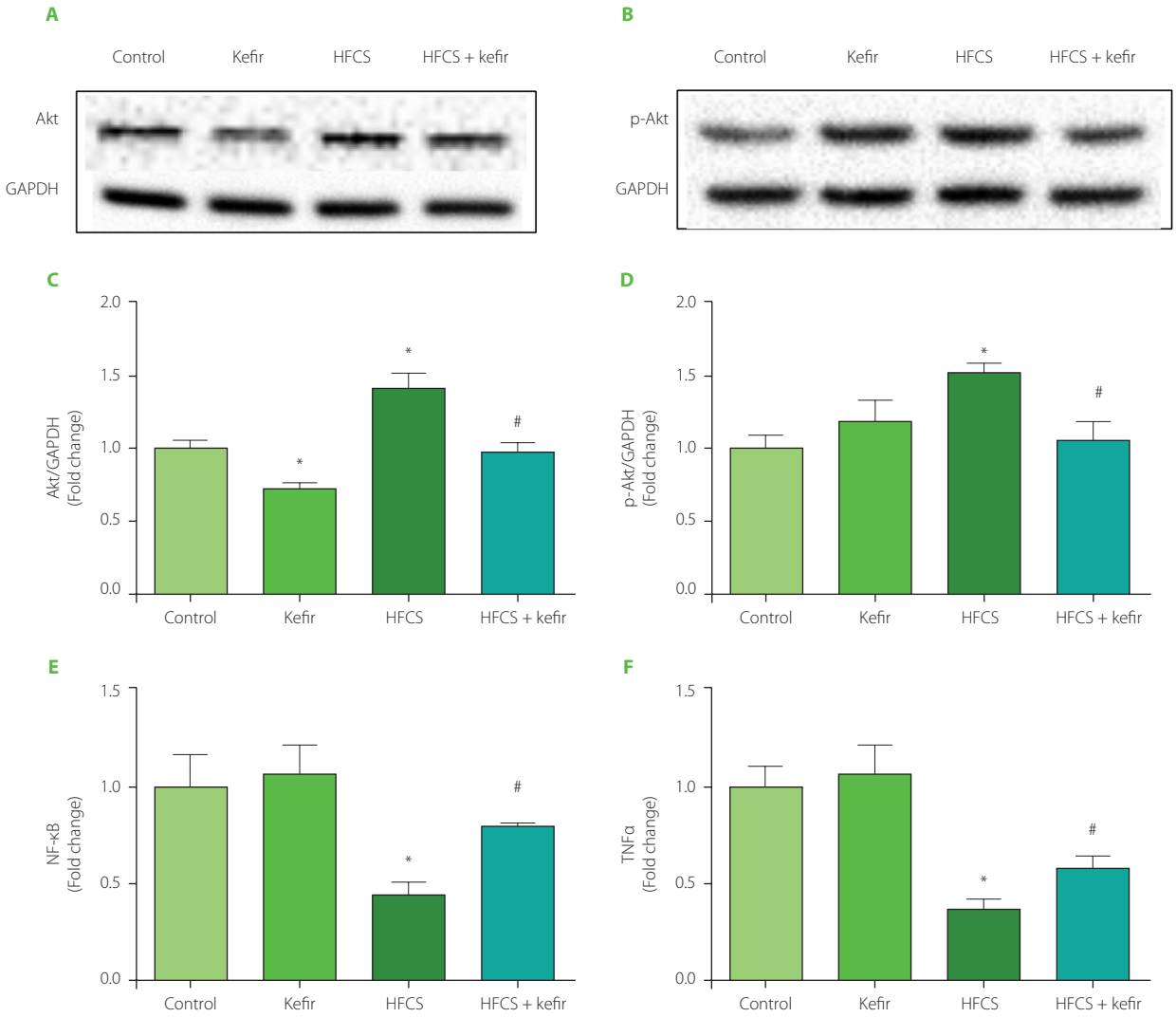

Figure 1. Western blot images for protein kinase B, Akt (**A**) and phosphorylated Akt, p-Akt (**B**), relative levels of Akt (**C**) and p-Akt (**D**) quantified using densitometry and normalized with corresponding glyceraldehyde 3-phosphate dehydrogenase (GAPDH), and levels of nuclear factor κB, NF-κB (**E**) and tumor necrosis factor α, TNFα (**F**) measured by ELISA in adipose tissues of rats from the control, kefir, high-fructose corn syrup (HFCS), and HFCS+kefir groups. Each band presented in a row (**A** and **B**) derived from the same experiment and blots were processed in parallel experiments. Values (**C**–**F**) are expressed as mean ± standard error of the mean. *Significantly different compared to the control group ($p<0.05$). #Significantly different compared to the HFCS group ($p<0.05$).

characteristics, was published in our previous research [Ekici *et al*., 2022a]. Briefly, HFCS treatment significantly increased the body and omental weights of rats and dietary supplementation with kefir reduced the omental weights. HFCS-feeding resulted in an increase in plasma glucose, fructose, insulin, triglycerides, very low-density lipoprotein (VLDL) and total cholesterol, urea and uric acid levels. In turn, kefir administration to rats significantly lowered values of all these parameters.

In the current study, the effects of HFCS and kefir consumption on the Akt, p-Akt NF-κB, and TNFα proteins of the adipose tissue of rats were analyzed first. The results are depicted in Figure 1. Accordingly, HFCS-feeding increased Akt and p-Akt levels in rat adipose tissue while decreasing NF-κB, and TNFα levels ($p<0.05$ compared to control). Kefir administration in rats did not substantially alter Akt phosphorylation or inflammatory marker levels, although it did lower overall Akt levels ($p<0.05$). Kefir, when given to HFCS-treated rats, normalized the induction of total and phosphorylated form of Akt while simultaneously elevating levels of NF-κB, and TNFα in rats' adipose tissues.

The levels of mRNA expression of *Akt*, *Nfkb*, *Tnfa*, *p53*, *Casp8*, and *Bcl2* were determined using the qRT-PCR technique, and the findings are shown in Figure 2. The treatment with kefir had no significant influence on the levels of gene expression for apoptotic or inflammatory markers. In contrast, ingestion of HFCS led to an increase in the expression of the *Akt* and *Bcl2* in the adipose tissues of rats, while at the same time leading to a decrease in the expression of the *Nfkb, Tnfα*, p53, and *Casp8*. In addition, the administration of kefir greatly returned all of the abnormalities that had been caused by HFCS.

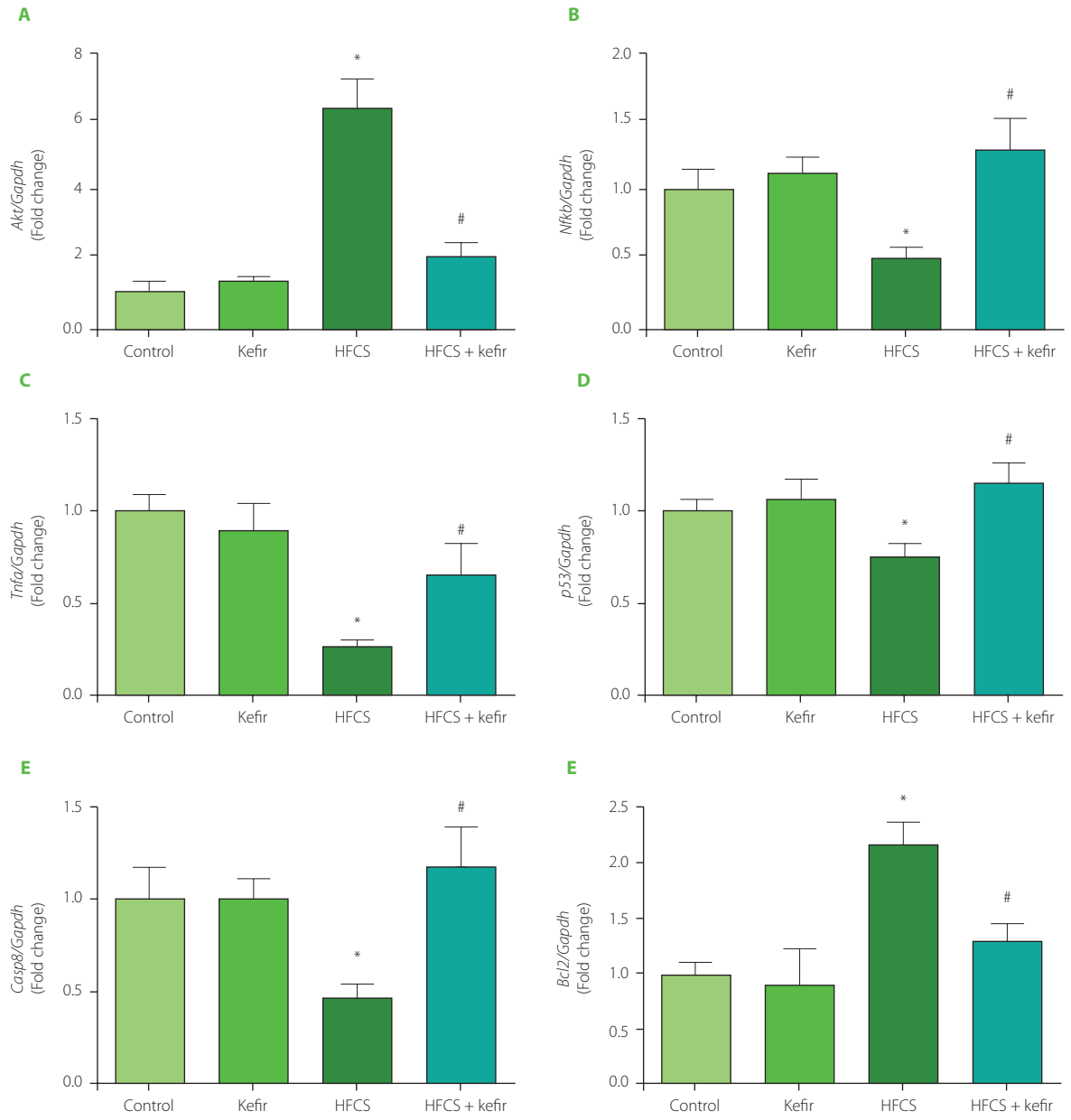

Figure 2. Relative mRNA expression levels of *Akt* (**A**), *Nfkb* (**B**), *Tnfa* (**C**), *p53* (**D**), *Casp8* (**E**), and *Bcl2* (**F**) of the adipose tissues of rats from the control, kefir, high-fructose corn syrup (HFCS), and HFCS+kefir groups. Data were normalized by *Gapdh*. Values are expressed as mean ± standard error of the mean (n=6–12). *Significantly different compared to the control group ($p<0.05$); #Significantly different compared to the HFCS group ($p<0.05$).

The images of adipose tissues of rats treated with HFCS and kefir after histochemical and immunohistochemical staining are given in Figure 3. The quantitative results of immunohistochemical analysis are summarized in Figure 4A–E. In comparison to the control group, the level of PLIN-1 in adipose tissues of rats consuming kefir was lower and the tissues of the group treated with HFCS had the highest PLIN-1 level (Figure 4A). It was also shown that the staining of PLIN-1 was less intense for the group that consumed HFCS+kefir compared to the group that consumed only HFCS. The NF-κB and TNFα levels, on the other hand, were higher

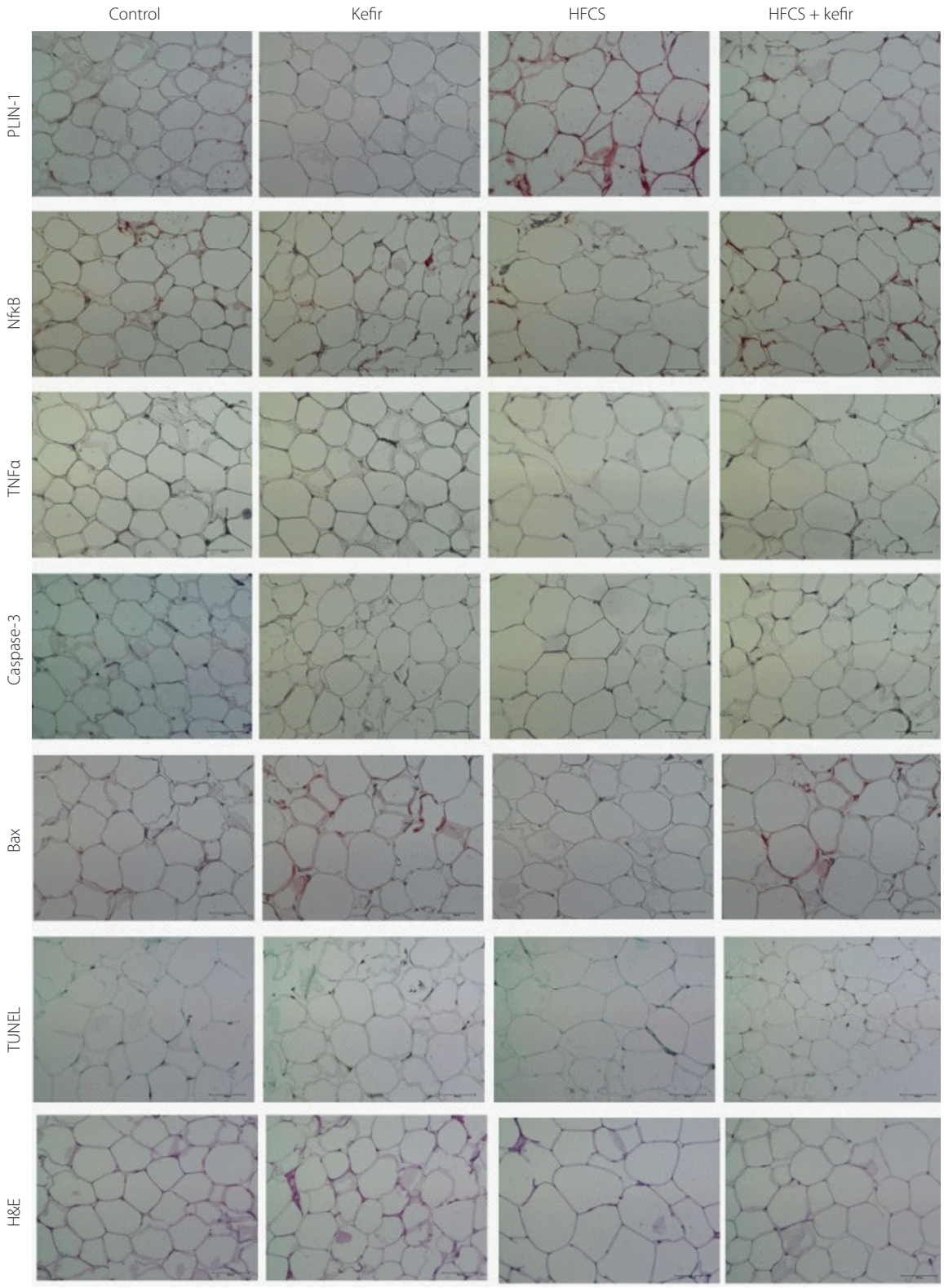

Figure 3. Images of histochemical and immunohistochemical staining of adipose tissues of rats from the control, kefir, high-fructose corn syrup (HFCS), and HFCS+kefir groups. H&E, hematoxylin and eosin staining.

in the adipocytes of kefir group (Figure 4B and 4C, respectively). When compared to the control group, NF-κB and TNFα levels were lower (p<0.05) for the HFCS group; however, the values for HFCS+kefir group were significantly (p<0.05) higher than for the HFCS group.

Figure 4F shows that the number of TUNEL-positive cells decreased significantly (p<0.05) in the HFCS group compared to the control group, and the number of apoptotic cells increased in the kefir group. Additionally, the number of apoptotic cells

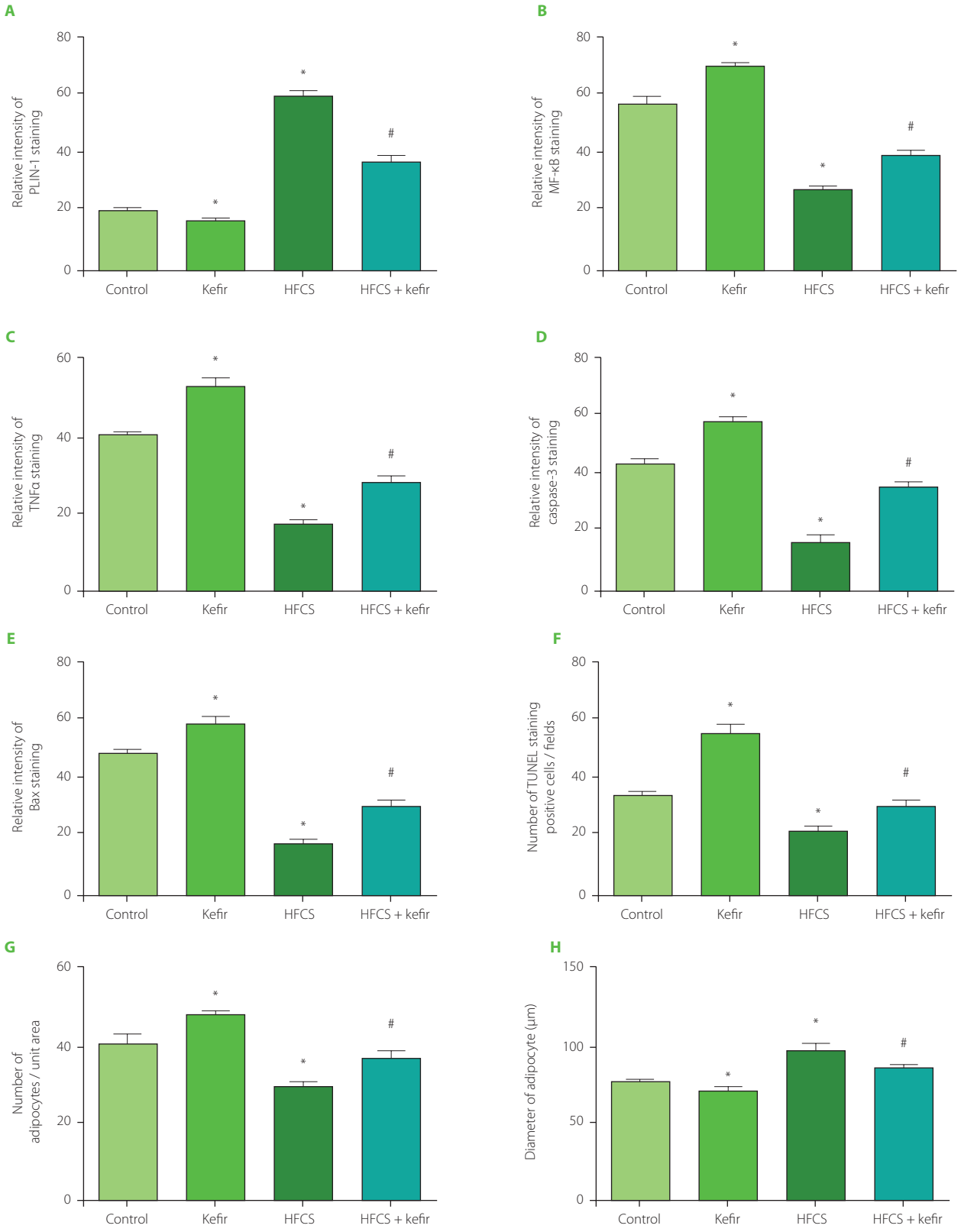

Figure 4. Relative intensity of immunohistochemical staining of PLIN-1 (**A**), NF-κB (**B**), TNFα (**C**), caspase-3 (**D**) and Bax (**E**) of adipocytes, number of TUNEL apoptotic cells (**F**) and number (**G**) and diameter (**H**) of hematoxylin and eosin (H&E) stained adipocytes of rats from the control, kefir, high-fructose corn syrup (HFCS), and HFCS+kefir groups. Values are expressed as mean ± standard error of the mean (n=6–12). *Significantly different compared to the control group (p<0.05); #Significantly different compared to the HFCS group (p<0.05).

was higher in the HFCS+kefir group than in the HFCS group. On the other hand, the distribution of caspase-3 (Figure 4D) and Bax (Figure 4E) levels demonstrated a correlation with the number of TUNEL-positive cells. The levels of both markers were higher in the adipocytes of kefir group when compared to the control group, but they were shown to be lower in the HFCS group. In addition, an increase was found in the HFCS+kefir group in comparison to the HFCS group.

The changes in the number and diameter of adipocytes were evaluated with histological examinations under a light microscope. Results are shown in Figure 4G and H. It was found that the number of cells *per* unit area of tissues decreased while the cell diameter increased in the HFCS group as compared with control group. Besides, kefir administration to rats increased the average number of adipocyte but decreased the cell diameters. When administered to the HFCS-treated rats, kefir normalized the reduced cell number to the value of control group and decreased the cell diameters towards the value of the control group.

It is well known that consumption of processed foods that include fructose, glucose, sucrose, or any combination of these three in particular quantities can have negative consequences on human health [Stanhope, 2016]. Even though the effects of these dietary components on human health have been unequivocally demonstrated, the molecular mechanisms of their action continue to be the subject of debate. It has been demonstrated that an increase in dietary fructose intake lowers insulin sensitivity in liver tissue [Akar *et al.*, 2021], but raises it in adipose tissue [Pektas *et al.*, 2016]. Recent research indicates that feeding experimental animals with HFCS results in the development of omental obesity [DiNunzio *et al.*, 2020; Hattori *et al.*, 2021; Sadowska & Rygielska, 2019]. Despite this, there is still a great deal of confusion about the leading molecular mechanisms. As a result, the causes of possible adipogenesis due to the consumption of HFCS were investigated at the molecular level in this study. Additionally, the effects of milk kefir, which contains many bacterial species collectively referred to as beneficial bacteria, on possible changes were observed and analyzed in an effort to find a treatment.

What sets adipose tissue apart from other organs and tissues is its widespread distribution and its ability to enlarge in response to excess energy in the form of stored lipids. White adipose tissue and subcutaneous brown adipose tissue are the two primary forms of adipose tissue in animals, both of which surround the internal organs. Insulation and the storage of energy are the two primary physiological activities that are performed by adipose tissue, which are intimately related to the metabolic issues that are brought on by obesity, insulin resistance, and diabetes. In obese individuals, the expansion of adipose tissue may be mediated by hypertrophy, hyperplasia, or both processes. It is not yet known, however, how adipose tissue growth is regulated at the molecular level [Choe *et al.*, 2016].

Recently, abdominal obesity due to long-term fructose consumption has been associated with increased insulin sensitivity due to enhanced level of Akt [Pektas *et al.*, 2016], and decreased p-Akt levels in adipose tissues [Li *et al.*, 2021]. However, augmented Akt and p-Akt levels in adipose tissues of mice fed a high-fat and high-fructose corn syrup diet for eight weeks were shown to be independent of plasma insulin levels [Zhang *et al.*, 2020]. The proliferation of adipose tissue in fructose-fed rats was also associated with an increase in insulin sensitivity, in which Akt has an important role in the activation of the insulin signaling pathway [Maines *et al.*, 2021]. Despite conflicting findings in the literature, this study provides evidence for Akt induction owing to HFCS intake at both gene and protein expression/phosphorylation levels. Besides, we also demonstrated the normalization of HFCS-induced Akt levels by kefir treatment. Furuno & Nakanishi [2012] demonstrated the suppression of antigen-induced mast cell activation with kefir through Akt inhibition, and Akt levels in rat kidney tissues were reduced with fructose and raised with the administration of *Lactobacillus plantarum*, which is the main beneficial bacteria in kefir [Korkmaz *et al.*, 2019]. The usefulness of kefir ingestion in Akt regulation was obvious in HFCS-fed animals, even though study results vary depending on the tissue, duration, and dietary modeling.

Studies also indicated the function that TNFα played in the development of obesity-induced insulin resistance [Stephens & Pekala, 1992; Stephens *et al.*, 1997]. Insulin resistance and the insulin signaling pathway have been found to be associated with TNFα and NF-κB. For example, changes in the level of TNFα in adipocytes can modulate the transcription of IRS-1 and Glucose transporter type-4 (Glut-4), both of which are involved in the transport of glucose [Barzilay & Freedland, 2003; Duncan *et al.*, 2003]. A diet containing 10% fructose reduced TNFα and NF-κB protein level in adipose tissue while increasing their levels in the liver and kidney tissues [Qiao *et al.*, 2018; Veličković *et al.*, 2013] and modulated the tissue inflammatory states. Herein, our findings also demonstrated the suppression of TNFα and NF-κB levels by long-term HFCS-feeding while it also reduced the rate of apoptosis as evidenced by decreased apoptotic *Casp8* and increased anti-apoptotic *Bcl2* mRNA expressions in adipose tissues. Although similar studies in the literature have found that a high-fructose diet causes tissue inflammation [Akar *et al.*, 2021; Korkmaz *et al.*, 2019], the long-term use of HFCS appears to prevent apoptosis, leading to an increase in adipocyte survival.

Among the primary lipid droplet-binding proteins, PLIN-1 is abundantly expressed in adipocytes and its decreased expression leads to lower fat mass and insulin sensitivity. A recent study demonstrates that PLIN-1 deficiency promotes inflammatory responses and lipolysis in adipose tissue, resulting in insulin resistance [Sohn *et al.*, 2018]. Increases in adipocyte diameters and sizes, as well as an increase in PLIN-1 level as measured by immunohistochemical technique in this study, are consistent with these investigations. However, results from TUNEL and H&E staining showed a reduction in both the number of viable adipocytes and the overall number of cells *per* unit area. The primary cause for this is the increase in the diameter of adipocytes that occurs in response to an increase in the number of cells that survive. In contrast to previous research [Pektas *et al.*, 2016],

the results of this study showed that omental obesity induced by fructose intake is caused by the suppression of apoptotic pathways in adipocytes. Considering the apoptotic potential of kefir and its constituent bacteria, a few studies have shown that kefir causes apoptosis in animal models of Ehrlich ascites carcinoma [Badr El-Din *et al.*, 2020; Bozkurt *et al.*, 2020; Esener *et al.*, 2018] and enhances the apoptosis pathway [El Golli-Bennour *et al.*, 2019]. Further, kefir was shown to have a modulatory role in initiating apoptosis and avoiding inflammation by lowering TNFα and NF-κB levels, as evidenced by the present study.

CONCLUSIONS

Our study results demonstrate that consumption of HFCS leads to adipogenesis *via* suppressing apoptosis and raising insulin sensitivity in adipocytes, in addition to the previously established link between the two. Although the clinical significance of these findings has yet to be confirmed, we showed that kefir might be a beneficial functional food against HFCS-induced abdominal obesity.

RESEARCH FUNDING

The study did not receive any external funding.

ACKNOWLEDGEMENTS

The authors would like to appreciate Danem-Kefir (Isparta, TURKEY) for providing kefir.

CONFLICT OF INTERESTS

The authors of this manuscript report no conflict of interests. All co-authors have seen and agreed with the contents of the manuscript.

ETHICAL APPROVAL

The Ethical Animal Research Committee of Afyon Kocatepe University (AKUHADYEK 49533702-55) approved the study.

ORCID IDs

T. Aladağ https://orcid.org/0000-0003-3250-6113
E. Aslan https://orcid.org/0000-0002-3191-4978
M. Çeleğen https://orcid.org/0000-0002-6841-3675
H. Güzel https://orcid.org/0000-0001-7692-8890
Ç. Karaca https://orcid.org/0000-0003-2106-2422
Ö.A. Korkmaz https://orcid.org/0000-0001-5670-1314
Ş. Öncü https://orcid.org/0000-0003-2468-2416
M.B. Pektaş https://orcid.org/0000-0003-0055-7688
M.K. Pektaş https://orcid.org/0000-0003-2862-3288
G. Sadi https://orcid.org/0000-0002-6422-1203

REFERENCES

1. Akar, F., Sumlu, E., Alçığır, M.E., Bostancı, A., Sadi, G. (2021). Potential mechanistic pathways underlying intestinal and hepatic effects of kefir in high-fructose-fed rats. *Food Research International*, *143*, art. no. 110287. https://doi.org/10.1016/j.foodres.2021.110287
2. Badr El-Din, N.K., Shabana, S.M., Abdulmajeed, B.A., Ghoneum, M. (2020). A novel kefir product (PFT) inhibits Ehrlich ascites carcinoma in mice *via* induction of apoptosis and immunomodulation. *BMC Complementary Medicine and Therapies*, *20*(1), art. no. 127. https://doi.org/10.1186/s12906-020-02901-y
3. Barros, S.É.L., Rocha, C.S., de Moura, M.S.B., Barcelos, M.P., da Silva, C.H.T.P., Hage-Melim, L.I.S. (2021). Potential beneficial effects of kefir and its postbiotic, kefiran, on child food allergy. *Food and Function*, *12*(9), 3770–3786. https://doi.org/10.1039/D0FO03182H
4. Barzilay, J., Freedland, E. (2003). Inflammation and its association with glucose disorders and cardiovascular disease. *Treatments in Endocrinology*, *2*(2), 85–94. https://doi.org/10.2165/00024677-200302020-00002
5. Berger, N.A. (2014). Obesity and cancer pathogenesis. *Annals of the New York Academy of Sciences*, *1311*(1), 57–76. https://doi.org/10.1111/nyas.12416
6. Bozkurt, E., Atay, E., Pektaş, G., Ertekin, A., Vurmaz, A., Korkmaz, Ö.A., Sadi, G., Aslan, E., Koca, O.H., Pektaş, M.B. (2020). Potential anti-tumor activity of kefir-induced juglone and resveratrol fractions against Ehrlich ascites carcinoma-bearing BALB/c mice. *Iranian Journal of Pharmaceutical Research*, *19*(3), 358–369. https://doi.org/10.22037/ijpr.2020.112993.14060
7. Chen, H.L., Tsai, T.C., Tsai, Y.C., Liao, J.W., Yen, C.C., Chen, C.M. (2016). Kefir peptides prevent high-fructose corn syrup-induced non-alcoholic fatty liver disease in a murine model by modulation of inflammation and the JAK2 signaling pathway. *Nutrition and Diabetes*, *6*, art. no. e237. https://doi.org/10.1038/nutd.2016.49
8. Choe, S.S., Huh, J.Y., Hwang, I.J., Kim, J.I., Kim, J.B. (2016). Adipose tissue remodeling: Its role in energy metabolism and metabolic disorders. *Frontiers in Endocrinology (Lausanne)*, *7*, art. no. 30. https://doi.org/10.3389/fendo.2016.00030
9. Choi, J.-W., Kang, H.W., Lim, W.-C., Kim, M.-K., Lee, I.-Y., Cho, H.-Y. (2017). Kefir prevented excess fat accumulation in diet-induced obese mice. *Bioscience, Biotechnology, and Biochemistry*, *81*(5), 958–965. https://doi.org/10.1080/09168451.2016.1258984
10. DiNunzio, G., Belew, G.D., Torres, A.N., Silva, J.G., Silva, L.P., Barosa, C., Tavares, L., Jones, J.G. (2020). Determining the contribution of a high-fructose corn syrup formulation to hepatic glycogen synthesis during *ad-libitum* feeding in mice. *Scientific Reports*, *10*(1), art. no. 12852. https://doi.org/10.1038/s41598-020-69820-3
11. Duncan, B.B., Schmidt, M.I., Pankow, J.S., Ballantyne, C.M., Couper, D., Vigo, A., Hoogeveen, R., Folsom, A.R., Heiss, G. (2003). Low-grade systemic inflammation and the development of type 2 diabetes: The atherosclerosis risk in communities study. *Diabetes*, *52*(7), 1799–1805. https://doi.org/10.2337/diabetes.52.7.1799
12. Ekici, Ö., Aslan, E., Aladağ, T., Güzel, H., Korkmaz, Ö.A., Bostancı, A., Sadi, G., Pektaş, M.B. (2022a). Masseter muscle and gingival tissue inflammatory response following treatment with high-fructose corn syrup in rats: Anti-inflammatory and antioxidant effects of kefir. *Journal of Food Biochemistry*, *46*(3), art. no. e13732. https://doi.org/10.1111/jfbc.13732
13. Ekici, O., Aslan, E., Guzel, H., Korkmaz, O.A., Sadi, G., Gurol, A.M., Boyaci, M.G., Pektas, M.B. (2022b). Kefir alters craniomandibular bone development in rats fed excess dose of high fructose corn syrup. *Journal of Bone and Mineral Metabolism*, *40*(1), 56–65. https://doi.org/10.1007/s00774-021-01273-8
14. El Golli-Bennour, E., Timoumi, R., Koroit, M., Bacha, H., Abid-Essefi, S. (2019). Protective effects of kefir against zearalenone toxicity mediated by oxidative stress in cultured HCT-116 cells. *Toxicon*, *157*, 25–34. https://doi.org/10.1016/j.toxicon.2018.11.296
15. Esener, O.B.B., Balkan, B.M., Armutak, E.I., Uvez, A., Yildiz, G., Hafizoglu, M., Yilmazer, N., Gurel-Gurevin, E. (2018). Donkey milk kefir induces apoptosis and suppresses proliferation of Ehrlich ascites carcinoma by decreasing iNOS in mice. *Biotechnic and Histochemistry*, *93*(6), 424–431. https://doi.org/10.1080/10520295.2018.1448112
16. Furuno, T., Nakanishi, M. (2012). Kefiran suppresses antigen-induced mast cell activation. *Biological and Pharmaceutical Bulletin*, *35*(2), 178–183. https://doi.org/10.1248/bpb.35.178
17. Hamida, R.S., Shami, A., Ali, M.A., Almohawes, Z.N., Mohammed, A.E., Bin-Meferij, M.M. (2021). Kefir: A protective dietary supplementation against viral infection. *Biomedicine and Pharmacotherapy*, *133*, art. no. 110974. https://doi.org/10.1016/j.biopha.2020.110974
18. Harvey, A.E., Lashinger, L.M., Hursting, S.D. (2011). The growing challenge of obesity and cancer: an inflammatory issue. *Annals of the New York Academy of Sciences*, *1229*(1), 45–52. https://doi.org/10.1111/j.1749-6632.2011.06096.x
19. Hattori, H., Hanai, Y., Oshima, Y., Kataoka, H., Eto, N. (2021). Excessive intake of high-fructose corn syrup drinks induces impaired glucose tolerance. *Biomedicines*, *9*(5), art. no. 541. https://doi.org/10.3390/biomedicines9050541
20. Hill, D., Conner, M., Clancy, F., Moss, R., Wilding, S., Bristow, M., O'Connor, D.B. (2022). Stress and eating behaviours in healthy adults: a systematic review and meta-analysis. *Health Psychology Review*, *16*(2), 280–304. https://doi.org/10.1080/17437199.2021.1923406
21. Irigaray, P., Newby, J.A., Lacomme, S., Belpomme, D. (2007). Overweight/obesity and cancer genesis: More than a biological link. *Biomedicine and Pharmacotherapy*, *61*(10), 665–678. https://doi.org/10.1016/j.biopha.2007.10.008

22. Khorshidian, N., Shadnoush, M., Zabihzadeh Khajavi, M., Sohrabvandi, S., Yousefi, M., Mortazavian, A.M. (2021). Fructose and high fructose corn syrup: are they a two-edged sword? *International Journal of Food Sciences and Nutrition*, *72*(5), 592–614. https://doi.org/10.1080/09637486.2020.1862068
23. Korkmaz, O.A., Sumlu, E., Koca, H.B., Pektas, M.B., Kocabas, A., Sadi, G., Akar, F. (2019). Effects of *Lactobacillus plantarum* and *Lactobacillus helveticus* on renal insulin signaling, inflammatory markers, and glucose transporters in high-fructose-fed rats. *Medicina*, *55*(5), art. no. 207. https://doi.org/10.3390/medicina55050207
24. Lee, W.-C., Leu, S., Wu, K.L.H., Tain, Y.-L., Chuang, Y.-C., Chan, J.Y.H. (2021). Tadalafil ameliorates bladder overactivity by restoring insulin-activated detrusor relaxation *via* the bladder mucosal IRS/PI3K/AKT/eNOS pathway in fructose-fed rats. *Scientific Reports*, *11*(1), art. no. 8202. https://doi.org/10.1038/s41598-021-87505-3
25. Li, K.-P., Yu, Y., Yuan, M., Zhang, C.-M., Rong, X.-L., Turnbull, J.E., Guo, J. (2021). Tian-Huang formula, a traditional Chinese medicinal prescription, improves hepatosteatosis and glucose intolerance targeting AKT-SREBP nexus in diet-induced obese rats. *Evidence-Based Complementary and Alternative Medicine*, *2021*, art. no. 6617586. https://doi.org/10.1155/2021/6617586
26. Liu, Y., Wang, C., Wei, M., Yang, G., Yuan, L. (2021). Multifaceted roles of adipose tissue-derived exosomes in physiological and pathological conditions. *Frontiers in Physiology*, *12*, art. no. 669429. https://doi.org/10.3389/fphys.2021.669429
27. Lowry, O.H., Rosebrough, N.J., Farr, A.L., Randall, R.J. (1951). Protein measurement with the Folin phenol reagent. *Journal of Biological Chemistry*, *193*(1), 265–275. https://doi.org/10.1016/S0021-9258(19)52451-6
28. Maines, E., Franceschi, R., Martinelli, D., Soli, F., Lepri, F.R., Piccoli, G., Soffiati, M. (2021). Hypoglycemia due to PI3K/AKT/mTOR signaling pathway defects: two novel cases and review of the literature. *Hormones*, *20*(4), 623–640. https://doi.org/10.1007/s42000-021-00287-1
29. Markowiak, P., Śliżewska, K. (2017). Effects of probiotics, prebiotics, and synbiotics on human health. *Nutrients*, *9*(9), art. no. 1021. https://doi.org/10.3390/nu9091021
30. National Health and Medical Research Council (2013). Australian Code for the Care and Use of Animals for Scientific Purposes. 8th edition. National Health and Medical Research Council, Canberra, Australia. Available from: http://www.nhmrc.gov.au/guidelines-publications/ea28.
31. National Research Council (US) Committee for the Update of the Guide for the Care and Use of Laboratory Animals (2011). *Guide for the Care and Use of Laboratory Animals*. 8th edition. National Academies Press (US), Washington, DC, USA. Available from: https://www.ncbi.nlm.nih.gov/books/NBK54050/
32. Narayanankutty, A., Kuzhivelil, B.T., Raghavamenon, A.C. (2022). A high-fructose diet formulated with thermally oxidized monounsaturated fat aggravates metabolic dysregulation in colon epithelial tissues of rats. *Journal of the American Nutrition Association*, *41*(1), 38–49. https://doi.org/10.1080/07315724.2020.1846145
33. Nephan, G., Coskun, Z.M., Bolkent, S. (2018). Dipeptidyl peptidase-4 inhibition prevents cell death *via* extrinsic and intrinsic apoptotic pathways in rat pancreas with insulin resistance. *Cell Biochemistry and Function*, *36*(4), 212–220. https://doi.org/10.1002/cbf.3333
34. Pektaş, M.B., Aslan, E., Güzel, H., Korkmaz, Ö.A., Çeleğen, K, Pektaş, A., Bostanci, A., Sadi, G. (2022). Kefir protects the liver against high fructose corn syrup induced phosphodiesterase hyperactivity. *Turkish Journal of Biochemistry*, *47*(3), 351–360. https://doi.org/10.1515/tjb-2021-0180
35. Pektas, M.B., Koca, H.B., Sadi, G., Akar, F. (2016). Dietary fructose activates insulin signaling and inflammation in adipose tissue: Modulatory role of resveratrol. *BioMed Research International*, *2016*, art. no. 8014252. https://doi.org/10.1155/2016/8014252
36. Prasatthong, P., Meephat, S., Rattanakanokchai, S., Bunbupha, S., Prachaney, P., Maneesai, P., Pakdeechote, P. (2021). Hesperidin ameliorates signs of the metabolic syndrome and cardiac dysfunction *via* IRS/Akt/GLUT4 signaling pathway in a rat model of diet-induced metabolic syndrome. *European Journal of Nutrition*, *60*(2), 833–848. https://doi.org/10.1007/s00394-020-02291-4
37. Qiao, Y., Xu, L., Tao, X., Yin, L., Qi, Y., Xu, Y., Han, X., Tang, Z., Ma, X., Liu, K., Peng, J. (2018). Protective effects of dioscin against fructose-induced renal damage *via* adjusting Sirt3-mediated oxidative stress, fibrosis, lipid metabolism and inflammation. *Toxicology Letters*, *284*, 37–45. https://doi.org/10.1016/j.toxlet.2017.11.031
38. Rosa, D.D., Grześkowiak, Ł.M., Ferreira, C.L.L.F., Fonseca, A.C.M., Reis, S.A., Dias, M.M., Siqueira, N.P., Silva, L.L., Neves, C.A., Oliveira, L.L., Machado, A.B.F., Peluzio, M.C.P. (2016). Kefir reduces insulin resistance and inflammatory cytokine expression in an animal model of metabolic syndrome. *Food and Function*, *7*(8), 3390–3401. https://doi.org/10.1039/C6FO00339G
39. Sadowska, J., Rygielska, M. (2019). The effect of high fructose corn syrup on the plasma insulin and leptin concentration, body weight gain and fat accumulation in rat. *Advances in Clinical and Experimental Medicine*, *28*(7), 879–884. https://doi.org/10.17219/acem/94069
40. Savran, M., Asci, H., Ozmen, O., Erzurumlu, Y., Savas, H.B., Sonmez, Y., Sahin, Y. (2019). Melatonin protects the heart and endothelium against high fructose corn syrup consumption-induced cardiovascular toxicity *via* SIRT-1 signaling. *Human and Experimental Toxicology*, *38*(10), 1212–1223. https://doi.org/10.1177/0960327119860188
41. Sohn, J.H., Lee, Y.K., Han, J.S., Jeon, Y.G., Kim, J.I., Choe, S.S., Kim, S.J., Yoo, H.J., Kim, J.B. (2018). Perilipin 1 (Plin1) deficiency promotes inflammatory responses in lean adipose tissue through lipid dysregulation. *Journal of Biological Chemistry*, *293*(36), 13974–13988. https://doi.org/10.1074/jbc.RA118.003541
42. Stanhope, K.L. (2016). Sugar consumption, metabolic disease and obesity: The state of the controversy. *Critical Reviews in Clinical Laboratory Sciences*, *53*(1), 52–67. https://doi.org/10.3109/10408363.2015.1084990
43. Stephens, J.M., Lee, J., Pilch, P.F. (1997). Tumor necrosis factor-α-induced insulin resistance in 3T3-L1 adipocytes is accompanied by a loss of insulin receptor substrate-1 and GLUT4 expression without a loss of insulin receptor-mediated signal transduction. *Journal of Biological Chemistry*, *272*(2), 971–976. https://doi.org/10.1074/jbc.272.2.971
44. Stephens, J.M., Pekala, P.H. (1992). Transcriptional repression of the C/EBP-alpha and GLUT4 genes in 3T3-L1 adipocytes by tumor necrosis factor-alpha. Regulations is coordinate and independent of protein synthesis. *Journal of Biological Chemistry*, *267*(19), 13580–13584. https://doi.org/10.1016/S0021-9258(18)42251-X
45. Sumlu, E., Bostancı, A., Sadi, G., Alçığır, M.E., Akar, F. (2022). *Lactobacillus plantarum* improves lipogenesis and IRS-1/AKT/eNOS signalling pathway in the liver of high-fructose-fed rats. *Archives of Physiology and Biochemistry*, *128*(3), 786–794. https://doi.org/10.1080/13813455.2020.1727527
46. Veličković, N., Djordjevic, A., Vasiljević, A., Bursać, B., Milutinović, D.V., Matić, G. (2013). Tissue-specific regulation of inflammation by macrophage migration inhibitory factor and glucocorticoids in fructose-fed Wistar rats. *British Journal of Nutrition*, *110*(3), 456–465. https://doi.org/10.1017/S0007114512005193
47. Yildirim, O.G., Sumlu, E., Aslan, E., Koca, H.B., Pektas, M.B., Sadi, G., Akar, F. (2019). High-fructose in drinking water initiates activation of inflammatory cytokines and testicular degeneration in rat. *Toxicology Mechanisms and Methods*, *29*(3), 224–232. https://doi.org/10.1080/15376516.2018.1543745
48. Zafar, M.I., Frese, M., Mills, K.E. (2021). Chronic fructose substitution for glucose or sucrose in food or beverages and metabolic outcomes: An updated systematic review and meta-analysis. *Frontiers in Nutrition*, *8*, art. no. 647600. https://doi.org/10.3389/fnut.2021.647600
49. Zaki, S.M., Fattah, S.A., Hassan, D.S. (2019). The differential effects of high-fat and high-fructose diets on the liver of male albino rat and the proposed underlying mechanisms. *Folia Morphologica*, *78*(1), 124–136. https://doi.org/10.5603/FM.a2018.0063
50. Zhang, H.-J., Chen, C., Ding, L., Shi, H.-H., Wang, C.-C., Xue, C.-H., Zhang, T.-T., Wang, Y.-M. (2020). Sea cucumbers-derived sterol sulfate alleviates insulin resistance and inflammation in high-fat-high-fructose diet-induced obese mice. *Pharmacological Research*, *160*, art. no. 105191. https://doi.org/10.1016/j.phrs.2020.105191
51. Zubiría, M.G., Gambaro, S.E., Rey, M.A., Carasi, P., Serradell, M.Á., Giovambattista, A. (2017). Deleterious metabolic effects of high fructose intake: The preventive effect of *Lactobacillus kefiri* administration. *Nutrients*, *9*(5), art. no. 470. https://doi.org/10.3390/nu9050470

ORIGINAL ARTICLE
http://journal.pan.olsztyn.pl

Polish Journal of Food and Nutrition Sciences
2023, Vol. 73, No. 2, 130–138
DOI: 10.31883/pjfns/162874
ISSN 1230-0322, e-ISSN 2083-6007

Microbiological Quality and Physicochemical Characteristics of Pork Livers Supplied by an Industrial Slaughterhouse

Narcís Feliu-Alsina, Elena Saguer*

Institute for Food and Agricultural Technology (INTEA), University of Girona, Escola Politècnica Superior (EPS-1), C/Maria Aurèlia Capmany 61, 17003 Girona, Spain

Pork liver is a by-product generated daily in large quantities due to the high number of pigs slaughtered and its relatively high weight in relation to the carcass weight. However, it is not widely accepted by consumers for direct consumption due to its organoleptic properties. The present work aims to provide information of interest that may be useful for obtaining protein extracts from pork liver with potential as techno-functional ingredients. Specifically, the obtained results indicate that pork liver has a high protein content, with collagen representing only a small protein fraction and being poor in non-protein nitrogenous compounds. In addition, from the solubility profile obtained in the pH range from 4.8 to 8.5, high extraction yields can be expected at alkaline pH. However, and despite the high microbiological quality of pork livers properly collected and processed, their pH, water content and nutritional richness make them highly susceptible to microbiological spoilage.

Key words: meat by-products, valorisation, pork liver, thermal properties, solubility, chemical composition

INTRODUCTION

The recovery of food by-products is a strategy fully framed in the context of the circular economy, an alternative economic system to the linear model applied up to now, whose aim is to improve the efficiency of resources. This is particularly important in the case of animal production, given the high demand for natural resources and the generation of greenhouse gases. This impact on the environment is becoming a matter of great concern due to the increase in both the world population and the number of inhabitants with enough purchasing power to be able to include products of animal origin in their diet [FAO, 2022].

The edible internal organs obtained during the slaughter of animals are known as offal. Offal is present in many traditional regional cuisine dishes around the world, both for its nutritional value and for its organoleptic characteristics (flavour and texture). However, its consumption in Western countries has drastically declined in recent decades due to changes in consumer preferences. Increasing offal consumption has been suggested as a realistic strategy to reduce the contribution of meat production to environmental impacts, since fewer animals would need to be slaughtered. Therefore, the valorisation of non-meat edible parts obtained during the slaughter of animals with a lower value than meat but with good nutritional and/or techno-functional properties should cease to be an option and become an obligation due to the increase in demand for animal protein that is expected to happen soon [da Costa *et al.*, 2019].

In the case of the pig, the offal yield is around 17% by live weight, among which the liver stands out; its nutritional value is equivalent to that of meat, but with a higher content of vitamins and minerals. This makes liver to be considered a first-grade meat by-product due to its richness in proteins, vitamins, and mineral elements [Kakimov *et al.*, 2018]. However, a slight metallic taste together with a bitter taste which could be related to the presence of iron/blood and bile production, respectively, along with

***Corresponding Author:**
tel.: +34 972 41 84 54; e-mail: elena.saguer@udg.edu (E. Saguer)

Submitted: 10 February 2023
Accepted: 31 March 2023
Published on-line: 5 May 2023

its less tender texture make pork liver less appetising. In addition, off-flavours can become intense during liver processing/storage due to iron-catalysed oxidation of unsaturated fatty acids [Im *et al.*, 2004].

Currently, proteins of plant origin are increasingly attractive compared to those of animal origin both because of the lower environmental impact in obtaining them and for ethical issues. However, we must not forget that the human species is essentially omnivorous. While reducing meat consumption at the individual level must be a reality to address the environmental challenges we face, large-scale meat production is unlikely to slow down in the face of projected population growth and taking into account the higher requirements of rich-protein foods that will come associated. For this reason, betting on an efficient use of the raw material must also be a priority in the meat industry. The great mismatch between the daily production of pork livers in slaughterhouses and the low demand from consumers forces us to seek alternatives for their use and recovery. An interesting way of valorising pork liver could be through obtaining protein fractions to use them as food ingredients, not only as meat extenders but also as techno-functional constituents. This work aims to deepen some characteristics of the livers supplied by an industrial slaughterhouse and, in particular, of their protein fraction, in order to obtain useful information for further studies focused on obtaining ingredients for food formulation. Therefore, the microbiological quality and the colour of livers, the solubility and the thermal properties of proteins, as well as the chemical composition of liver homogenates were determined in this study.

MATERIAL AND METHODS

Material handling

Every sampling day (six days in total), three fresh pork livers from healthy adult animals (Large White × Landrace × Pietrain × Duroc commercial crossbred; live weight of approximately 100 kg and 6 months old), regardless of sex, were supplied by a local abattoir (NORFRISA SA, Riudellots de la Selva, Spain), once their gallbladder was separated. At the slaughterhouse, each liver was placed separately in a sterile bag. Livers were transported and kept under refrigerated conditions for approximately half an hour, until they were processed upon arrival at the laboratory. First, each liver was visually inspected and weighed under sterile conditions (precision of 0.1 g). Next, 10 g of liver were placed in a sterile stomacher bag by taking a sample from each of the lobes in order to determine the microbiological contamination as described below. After that, pH was measured in quadruplicate using a Crison GLP 22 pH-meter (Hach Langue SLU, Ames, IA, USA) coupled to an insert-type electrode (2-Pore F, XS Instruments, Capri, Italy). The colour of some livers was measured as indicated below. Finally, the remaining blood vessels and the most evident connective tissue were completely removed from all livers.

Determination of total mesophilic aerobic bacterial counts

Counts of total mesophilic aerobic bacteria (MAB) were determined on 10 g-samples from each liver (n=18) weighed into a sterile stomacher bag under sterile conditions in a Telstar BV-100 laminar flow chamber (Telstar, Terrassa, Spain). Next, 90 mL of 10 g/L tryptone water (L42, Oxoid Ltd, Basingstoke, UK) with 5 g/L NaCl were added. After that, each sample was serially diluted in sterile tryptone water and plated on plate count agar (PCA, Oxoid Ltd) by the pour-plate method. The plates were then incubated at 30°C for 72 h. The results were expressed as log colony-forming unit (cfu) per g.

Instrumental colour analysis

Surface and inner colour of six different fresh livers was measured in quadruplicate in the CIELab colour space using a Minolta CR-400 colorimeter (Minolta Co., Ltd, Osaka, Japan) with an optical geometry d:0° (diffuse illumination/0° viewing angle) and equipped with a CIE D_{65} illuminant and a CIE 2° standard observer. The L^* coordinate corresponded to lightness, while hue angle ($h°$) and chroma (C^*) were calculated from the chromaticity coordinates a^* [(–)greenness/(+)redness] and b^* [(–)blueness/(+)yellowness] from Equations (1) and (2), respectively.

$$h° = \arctan(b^*/a^*) \quad (1)$$

$$C^* = (a^{*2}+b^{*2})^{(1/2)} \quad (2)$$

Determination of thermal properties by differential scanning calorimetry (DSC)

Samples from six different livers were individually analysed to determine their thermal properties using a Q2000 V24.4 Build 116 differential scanning calorimeter (TA Instruments, New Castle, DE, USA). Samples were accurately weighed (15–20 mg) into Tzero aluminium pans (40 µL), using a precision balance (±0.01 mg, Analytical Plus, Mettler-Toledo S.A.E., Cornellà de Llobregat, Spain), and sealed hermetically. Then, they were heated from 30°C to 100°C at a scan rate of 3°C/min. An empty aluminium Tzero pan served as a reference. The transition temperatures (°C) and the transition enthalpy (ΔH, J/g) were determined from the thermogram obtained using the Universal Analytics Program, version 4.7 (TA Instruments).

Protein solubility determination

Samples coming from three different livers were used to determine the protein solubility in the pH range from 4.5 to 8.5, taking measurements at each pH unit. For each liver, pieces of the different lobes were taken and ground with a household electric mixer to obtain a homogeneous sample. Then, 10% (*w/v*) protein dispersions were prepared at the required pH using different solutions: citric acid-Na_2HPO_4 (pH 4.5); KH_2PO_4-Na_2HPO_4 (pH 5.5–7.5); and Tris-HCl (pH 8.5). The dispersions were first homogenised using a Polytron PT 30 laboratory homogeniser (Kinematica AG, Malters, Switzerland) at 7,000 rpm for 3 min, then shaken for 30 min at 3,000 rpm at room temperature and finally centrifuged at 2,500×g for 15 min in a SORVALL RC 5C Plus centrifuge (Dupont, Newtown, MA, USA). Soluble protein content in the supernatant was determined by the Kjeldahl method [ISO, 1978]. Protein solubility was presented as g of soluble protein

per kg of the total protein content of pork liver. Both soluble protein and total protein were determined in duplicate.

Physicochemical characterisation of pork liver homogenates

On each sampling day, after removing the connective tissue, each liver was cut into small pieces and a pork liver homogenate (PLH) was prepared by mixing and grinding equal amounts of the three livers (500 g final weight) at 2,100 rpm for 1 min with a Cutter Sammic CKE-5 food processor-emulsifier (Sammic S.L., Azkoitia, Spain). Moisture, fat, crude protein, and ash contents of all liver homogenates were determined according to the methods recommended by the American Oil Chemists' Society [AOCS, 2009]. A specific factor of 6.25 was applied to convert total Kjeldahl nitrogen to crude protein content according to ISO 937:1978 procedure [ISO, 1978]. Elemental analysis was performed after acid hydrolysis of the ash using a SpectrAA Varian 50B atomic emission/absorption spectrophotometer (Varian Inc., Palo Alto, CA, USA) at a specific wavelength for each mineral (Na, 589.0 nm; K, 766.5 nm; Ca, 422.7 nm; Mg, 285.2 nm; Fe, 248.3 nm; Zn, 213.9 nm; Cu, 324.7 nm; and Mn, 279.5 nm). Non-protein nitrogen (NPN) and collagen contents were also analysed in liver homogenates from three of the sampling days. NPN was determined by Kjeldahl method as the fraction soluble in 12.5% (*w/v*) trichloroacetic acid (TCA). Total collagen was calculated by multiplying the hydroxyproline (Hyp) content by 8. Hyp content was determined using the Nordic Committee on Food Analysis–Association of Official Agricultural Chemists (NMKL–AOAC) colorimetric method described by Kolar [1990].

Statistical analysis

Mean and standard deviation (SD) were calculated for all the parameters analysed as statistical descriptors. For solubility data, sampling days were considered as blocks in a randomised complete block design in which pH was the main factor. This statistical analysis was carried out using IBM SPSS Statistics 28 (IBM Corporation International, Armonk, NY, USA). Data were submitted to the analysis of variance (ANOVA) using the general linear model procedure (PROC GLM). A polynomial contrast was applied when a significant effect was obtained. The significance level applied was α=0.05.

RESULTS AND DISCUSSION

Characterisation of fresh pork liver

The morphology of all livers used in this study completely matches that described in the scientific literature, without any anomalies. They were multilobar, with four main lobes (2 lateral and 2 medial, one right and the other left in each case) and adopting a typical trefoil shape. The caudate lobe, which is smaller and attached to the right lateral lobe was also observed in the visceral face of all livers. Some authors have described a sixth lobe known as the square lobe only visible on the visceral face; it is the smallest one [Ntonas *et al.*, 2020]. In the present study, only the main lobes have been considered.

Pork livers weighed 1.72±0.18 kg as supplied by the industrial slaughterhouse, thus showing a variation coefficient ~10%. Liver weight depends on many factors including age and diet [Cliplef & McKay, 1993]; it also varies markedly among animals of similar weight due to differences in fasting time before slaughter or in the level of post-sacrifice bleeding of this organ [Loeffel & Koch, 1970]. In spite of that, our results are fully consistent with those found in the literature for healthy pigs intended for meat production, *i.e.* 6 months of age and weighing around 100 kg [Cliplef & McKay, 1993]. Accordingly, liver weight would represent ~1.7% of animal weight, a percentage that matches that reported for omnivores by Elefson *et al.* [2021]. At slaughter weight of pigs (100 kg), the liver is by far the heaviest organ of the red viscera group and being only exceeded by the small intestine when all viscera are considered together.

According to our results and as observed by other authors [Steen *et al.*, 2016], the pH of pork liver was slightly acidic (6.38±0.16). Similar values have been obtained in the case of livers from other animal species also intended for human consumption such as cattle, buffaloes, and lambs [Devatkal *et al.*, 2004]. However, some authors have also reported lower values for pork livers [Tomović *et al.*, 2016]. Relatively low pH values are usually obtained in animals that have not been fasted or when measurements were not made shortly after the animal sacrifice.

Total mesophilic aerobic bacteria counts

The pork liver is thinner and smaller in volume compared to the liver of other animals, making its specific surface area relatively large, which can have implications from the point of view of their microbiological contamination. Mesophilic aerobic bacteria (MAB) are often tested for food safety. The livers analysed in this study showed MAB counts of 3.52±0.66 log cfu/g. In the European Union, there is no specific legislation for microbiological quality of offal. However, taking as reference the European Commission (EC) Regulation No 1441/2007 [European Commission, 2007] relative to the microbiological criteria applicable to food products and, specifically, for minced meat, the livers may be deemed suitable for human consumption. In spite of that, a rapid liver cooling and maintenance of the cold chain until their use are key aspects to minimise microbiological risks.

Colour

The colour of pork livers was low in lightness, with a predominance of the $+a^*$ component over the $+b^*$ component (Table 1). Our data also showed a significantly ($p<0.05$) yellower colour inside the livers relative to the surface, which translates into significant ($p<0.05$) changes in the value of $h°$ and C^* parameters, both higher at the inner region. The obtained values fully match the reddish-brown or light brown attribute that is frequently used to describe the colour of fresh and healthy pork livers. Conversely, the colour coordinates of pork liver are very different from those of duck liver, a product with a much higher commercial value, which is lighter, less red, more yellow and with a predominance of the $+b^*$ component over the $+a^*$ component [Fernandez *et al.*, 2010].

Table 1. Pork livers surface and internal colour parameters.

Colour parameter	Surface	Inner
L^*	31.63±0.26	31.41±1.78
a^*	16.87±1.9	17.43±0.75
b^*	6.07±1.07[a]	8.74±0.34[b]
$h°$	19.36±3.27[a]	26.41±1.90[b]
C^*	17.25±2.00[a]	19.40±0.83[b]

L^*, lightness; a^*, (–)greenness/(+)redness; b^*, (–)blueness/(+)yellowness), $h°$, hue angle, C^*, chroma. Results are shown as mean±standard deviation (n=6). Different lowercase letters in the same row mean significant differences (p<0.05).

Thermal properties

Knowing the transition temperatures and the enthalpies of phase transitions associated to liver proteins can be useful to determine the effects of different processes on their native conformation as well as the potential of using them as techno-functional ingredients due to the effects of heating on their rheological properties. In this study, the thermal properties of pork liver proteins were estimated from the DSC thermograms, which showed a complex thermal behaviour (Figure 1). At temperatures <40°C, an endothermic thermal transition was observed in all the thermograms with the minimum of the peak at 32.5±0.05°C (not shown), which could correspond to the fat melting [Sasaki *et al.*, 2006]. At higher temperatures, two other endothermic peaks together with two shoulders (T_1–T_4) were also observed, which could be related to the protein denaturation. These thermal transitions occurred in the temperature range from 48°C to 96–97°C, with the most important one taking place around ~67°C. The specific temperature for each transition is indicated in Figure 1. The thermal transitions associated with the denaturation of rat liver proteins occur in a temperature range similar to that of pork liver; moreover, the range for liver samples was also wider than that obtained for muscle tissue samples [Ritchie *et al.*, 1994].

The liver is one of the most metabolically active organs, involved in many physiological functions. This makes its proteome very complex. Bovo *et al.* [2018] identified approximately 500 different proteins in pork liver. Blood is also found in liver with hepatic blood volume accounting for 10% to 15% of the total volume [Lautt, 1977]. This means that haemoglobin can be also present in a relatively high percentage. In addition, transitions linked to other macromolecules or supramolecular structures present in cells or liver tissue could also contribute to the thermal transitions observed in the DSC profile in this range of temperatures [Ritchie *et al.*, 1994].

For all liver samples, the last endothermic transition reached a minimum peak value close to 90°C, which shows that some of the liver molecules were highly thermally stable. Haemoglobin in the liver samples could contribute to this thermal transition; the DSC thermograms of this protein present two endothermic peaks with a bigger one around 78–79°C and the other at 90°C. In addition, the deoxyribonucleic acid (DNA) unfolding could also contribute to this transition; normally, it is considered to take place around 85°C [Yan & Iwasaki, 2004]. In this sense, it should be considered that liver consists of several cell types, with hepatocytes constituting 70–80% of the total liver cell population and representing around 80% of the total liver volume [Racanelli & Rehermann, 2006; Vekemans & Braet, 2005].

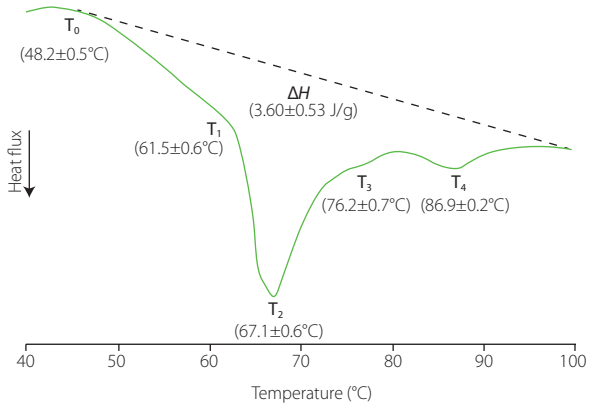

Figure 1. Differential scanning calorimetry profile of pork liver samples from 30 to 100°C. ΔH, transition enthalpy; T_0, onset temperature; T_{1-4}, transition temperatures related to protein denaturation. Values are shown as mean and standard deviation (n=6).

Protein solubility as a function of pH

A high protein solubility is desirable both for the economic viability of the recovery process and for the use of the extracted proteins as techno-functional ingredients. In the present study, protein solubility was determined at pH values ranging from pH 4.5 to pH 8.5, *i.e.*, a range that does not include overly aggressive conditions. As it was shown in Figure 2, protein solubility of about 400 g/kg was obtained at the lowest pH tested (pH 4.5), while at the highest pH (pH 8.5) approximately 900 g/kg of the proteins were solubilised. A high protein solubility at alkali conditions has been also observed for other offal [Gault & Lawrie, 1980]. In addition, the protein solubility increased successively along with pH increase, following a linear trend, as indicated by the results obtained by applying a polynomial contrast (p<0.05). An asymmetrical parabolic shape in the solubility profile of proteins from both animal and vegetal sources has been often reported, with the minimum solubility occurring near to the isoelectric point (p*I*) due to the prevalence of protein-protein interactions [Hrynets *et al.*, 2011; Khalid *et al.*, 2003]. Isoelectric points in the range from 4.5 to 6.8 have been described

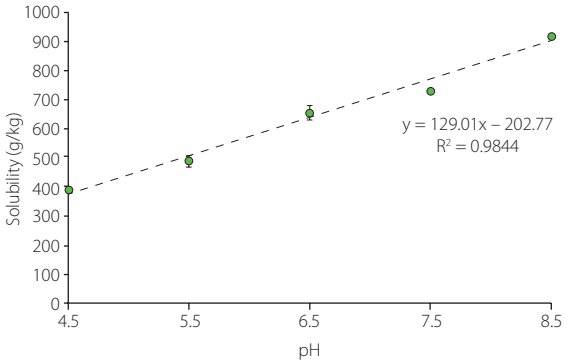

Figure 2. Solubility of pork liver proteins as affected by pH. Values are shown as mean and standard deviation (n=3).

for different pork liver proteins [Canduri *et al.*, 1988; Yamada *et al.*, 1981]. Therefore, the low solubility at pH 4.5 could be not surprising. In addition, although protein solubility increases both below and above the p*I*, normally the increase at pH values below the p*I* is more abrupt than at higher pHs. The successive increase observed in this study would be consistent with this behaviour. In addition, it would be in agreement with the results obtained by da Costa *et al.* [2019] also for pork liver proteins.

Acidic or negatively charged amino acids contribute more favourably to protein solubility than basic or positively charged, polar neutral and non-polar amino acids, in this order respectively [Trevino *et al.*, 2007]. Seong *et al.* [2014] showed that basic and non-polar amino acids accounted for 17 and 42% of the total amino acids, respectively, while acidic and polar amino acids together represented 41% in pork liver. Because aspartic acid/asparagine and glutamic acid/glutamine were non differentiated, it was not possible to quantify these last ones separately. According to Kramer *et al.* [2012], negative surface charge positively correlates with protein solubility, probably due to strong binding of water by the acidic amino acids. Average pK_a values of 3.5±1.2 and 4.2±0.9 for Asp and Glu, respectively, have been reported by Grimsley *et al.* [2009]; the dispersion in these values is due to the effect of the local environment on the pK_a of the ionisable groups in folded proteins. Therefore, they are mostly negatively charged in the tested pH range. However, pK_a values of basic amino acids are found mostly outside the tested range (Lys, 10.4; Arg, >12); only in the case of histidine does it fall within the range (His, 6.6±1.0). This means that many of the basic groups will be positively charged at the tested pHs. The number of acidic and basic groups charged in the protein molecules will therefore be a determinant factor of their solubility.

Chemical composition of pork liver homogenates

The chemical composition of the pork liver homogenates (PLH) is shown in Table 2. Moisture, fat, protein, and ash contents accounted all together for ~98% of the total composition. The rest would correspond to carbohydrates. Although water is the most abundant component, its content was relatively low compared to most offal, including the small intestine, lung, spleen, stomach, and heart [Alfaia *et al.*, 2020]. As expected, PLHs were rich in crude protein (180–190 g/kg). These results completely agree with those obtained by other authors [Saguer *et al.*, 2019; Steen *et al.*, 2016; Venegas Fornias, 1996], but higher (210–250 g/kg) and lower (~140 g/kg) contents have also been reported [Babicz *et al.*, 2019; Nuckles *et al.*, 1990; Seong *et al.*, 2014]. Variation in liver protein content may be related to breed, age, and nutrition pattern. Importantly, the protein content of pork liver obtained in this study was very similar to that reported for fresh pork lean meat [Jiménez Torres *et al.*, 2013]. Liver recovery is particularly attractive considering that it does not only contain all the essential amino acids, but also that they meet the requirements of the Food and Agriculture Organization (FAO) [FAO, 2013; Zou *et al.*, 2018]. Essential amino acids in pork liver proteins are close to 50%, according to Venegas Fornias [1996]. Seong *et al.* [2014] found that both pork liver and pancreas proteins were richer in essential amino acids compared to other edible offal such as spleen and heart. In addition, liver is low in fat, with levels comparable to the lean parts of pork [Alfaia *et al.*, 2020; Jiménez Torres *et al.*, 2013; Saguer *et al.*, 2019; USDA, 1992]. Phospholipids are the most abundant lipid class in pork liver; specifically, they represent more than 75% of total lipids, and phosphatidylcholine accounts for about 60% of total phospholipids [Hunter *et al.*, 1973]. In fact, pork liver is one of the richest foods in phospholipids, surpassed only by egg yolk and beef brain [Zheng *et al.*, 2018]. Phospholipids are the main components of biological membranes, but are also found in bile, exclusively as phosphatidylcholine in pork liver [Alvaro *et al.*, 1986].

Carbohydrate content is usually calculated by difference. Saguer *et al.* [2019] estimated a content of ~15 g/kg, while a value of ~25 g/kg was indicated in the United States Department of Agriculture (USDA) report [USDA, 1992]. These differences may be partially due to the specific protocols applied to animals before slaughter and may have some implications from a food safety point of view; livers from slaughtered animals with lower glycogen content have a higher pH [Warriss & Bevis, 1987]. Liver cells store large deposits of glucose in the form of glycogen. However, glycogen is consumed during fasting time [Warriss & Bevis, 1987].

As measured, crude protein represents the nitrogen-containing fraction, so it can include NPN-containing molecules. A low non-protein nitrogen (NPN) content was obtained for PLH (Table 2), which represented 5.2±0.1% of the total nitrogen. In land animals, NPN compounds usually make up no more than 10%. However, their content could gradually increase during storage under refrigeration conditions due to endogenous and exogenous proteolytic enzyme activity [Custódio *et al.*, 2016; Silva *et al.*, 2020]. Pork liver is particularly rich in nucleic acid nitrogen and exhibits a high purine content [Kaneko *et al.*, 2014]. This could be important because purines have effects on liver taste. It is well-accepted that high-purine foods are umami foods [Johnson *et al.*, 2013]. This savoury taste enhances flavour properties and is

Table 2. Chemical composition of pork liver homogenates.

Compound		Content
Moisture (g/kg)		745±9
Fat (g/kg)		35±4
Crude protein (g/kg)		189±4
Collagen (g/kg)		7.0±0.8
Non-protein nitrogen (g/kg)		1.6±0.1
Ash (g/kg)		13±1
Macroelements (mg/kg)	Na	1,269±22
	K	1,415±264
	Ca	73±10
	Mg	203±39
Microelements (mg/kg)	Fe	211±30
	Zn	59±20
	Cu	14±4
	Mn	3±1

Results are shown as mean±standard deviation (n=6, except for collagen and non-protein nitrogen contents, for which n=3).

also able of supressing bitterness and heightening saltiness. In addition, umami has also been shown to improve appetite but also satiety [Masic & Yeomans, 2014].

The collagen content of PLH is shown in Table 2. It was low, particularly if the content was expressed in relation to total protein content (3.7%). Babicz *et al.* [2019] reported a similar percentage, while Nuckles *et al.* [1990] determined even lower values (3.4 g/kg that represented 1.5% of total protein). This can be considered an important difference in relation to other viscera. Connective tissue in pork lungs, stomach, small and large intestines represents approximately 20% of total protein [Gault & Lawrie, 1980]. However, this tough connective tissue means that the consumption of pork liver is not as popular as that of other species (beef, calf, or chicken). In the pork liver – unlike the liver of other animals intended for human consumption – the connective tissue is visible because it is surrounding its lobules, forming a fibrous envelope that interconnects the adjacent portal areas. In addition, it can also be found within lobules, both adjacent to the sinusoids and around the central veins [Mik *et al.*, 2018].

The liver, together with the pancreas and spleen, are the pork offal with the highest ash content [Alfaia *et al.*, 2020]. In the present work, an average content of 13 g/kg has been determined (Table 2), which agrees with those most frequently cited in the literature [Alfaia *et al.*, 2020; Seong *et al.*, 2014], although Steen *et al.* [2016] recorded a slightly higher content (19.7 g/kg). Its contribution to the nutritional richness associated with liver consumption is due to the abundance of some essential trace elements. It is widely accepted that mineral elements tend to accumulate in some offal such as liver and kidney. Liver is a rich source of iron, zinc, copper, and manganese [Babicz *et al.*, 2019; Mulvihill, 2014; Stasiak *et al.*, 2017; Tomović *et al.*, 2019]. In addition, it is very rich in some macroelements, such as calcium, sodium, and potassium. As it was shown in Table 2, the liver content of iron far exceeds zinc. With some exceptions [Stasiak *et al.*, 2017], this agrees with what is mostly reported in the literature [Alfaia *et al.*, 2020; Tomović *et al.*, 2011]. Opposite is true for meat [Tomović *et al.*, 2011]. Both iron and zinc in meat and meat products are considered highly bioavailable while their absorption from plant foods is quite limited, probably due to the presence of phytates that act as antinutritional agents blocking mineral absorption [Mulvihill, 2014]. Iron deficiency is the most common nutritional disorder in the world, in both developed and developing countries [Mulvihill, 2014]. Globally, anemia prevalence was 22.8% in 2019, but being the highest among children under five years [Gardner & Kassebaum, 2020]; adolescent girls and pregnant women are also at high risk of deficiency. The actual tend to shift to a plant-based diet from the animal protein diet could have some health implications.

Iron and zinc are the two most abundant trace minerals in the human body. Iron plays a key role as part of haemoproteins, but it is also present in some important proteins related to oxidative phosphorylation and iron storage. It is stored primarily in hepatocytes as ferritin, a cytosolic protein that stores non-heme iron in the form of ferrihydrite phosphate ($[FeOOH]_8[FeOPO_3H_2]$) to protect cells from its accumulation in the free form [Knovich *et al.*, 2009; Wong, 2017]. Excess iron could cause toxicity problems due to its ability to act as a prooxidant agent, by generating reactive species that can damage DNA and proteins [Knovich *et al.*, 2009]. Excessive dietary iron intake has been identified as a risk factor of colorectal cancer through population and animal studies [Chua *et al.*, 2010]. Liver is an especially rich source of non-heme iron, although it also contains a percentage of heme iron. In pork liver, only 20-25% of the iron present is found as heme iron, while in pork loin it accounts for ~66% [Kongkachuichai *et al.*, 2002]. However, in absolute values, the heme-iron content of liver can be considerably higher than that of meat [Kongkachuichai *et al.*, 2002]. This is important because the human body absorbs heme iron more easily than non-heme one. In particular, the intestines absorb about 20-30% of heme iron while only 7% of non-heme [Mulvihill, 2014; Santé-Lhoutellier, 2014]. However, it should be taken into account that calcium inhibits the mucosal absorption of heme iron [Roughead *et al.*, 2005].

Zn is an essential micronutrient required in many enzymes that participates in a multitude of basic biochemical and physiological processes in the cells of the human body [Grüngreiff *et al.*, 2016; Tapiero *et al.*, 2003]. Liver is the main organ involved in Zn metabolism, but it is mainly found in muscle and bone (~85% of body's stores), while the liver accounts for ~5% [Grüngreiff *et al.*, 2016]. Despite that, pork liver is by far one of the richest foods in Zn, even compared to livers from other animal species [Aoyagi *et al.*, 1995; Stasiak *et al.*, 2017].

Cu is also an essential micronutrient that acts as an important catalytic cofactor in redox reactions involved in fundamental biological functions of the human body [Tapiero *et al.*, 2003]. Its main function is as a component of enzymes involved in iron metabolism [Tomović *et al.*, 2019]. Pork liver acts as a Cu reservoir, which makes it a very rich source of this element [Keller, 2019; Tomović *et al.*, 2019]. However, as happened with other monogastric mammalian livers, pork liver Cu has very low bioavailability [Aoyagi *et al.*, 1995]; on the contrary, bioavailability of Cu is relatively high in avian and ruminant livers [Aoyagi *et al.*, 1993]. It has been hypothesised that Zn may inhibit Cu utilisation, although the results are inconclusive [Aoyagi *et al.*, 1995]. In addition, high intakes of Cu or Zn are known to interfere with the tissue utilisation and storage of Fe [Tapiero *et al.*, 2003].

Pork liver is also a major source of Mn in the human diet. This element is responsible for the proper functioning of the nervous system, and is a component of the enzymes involved in the digestion and absorption of carbohydrates, lipids, and proteins. The results obtained in the present study regarding Mn content in pork liver (Table 2) are in good agreement with those reported by Stasiak *et al.* [2017]. According to these authors, pork liver is richer in Mn than muscle tissue, where it was completely missing.

CONCLUSIONS

The pork livers derived from the animal's slaughter have a good microbiological quality, which makes them suitable for their valorisation within the food industry itself. The DSC thermograms partially reflect the chemical complexity of the liver

and the thermostability of some of its components. The solubility profile of its protein fraction as a function of pH in the tested range (4.5 to 8.5) allows speculating that relatively high extraction yields can be obtained under basic conditions. This, along with the high protein content of the liver and the fact that only a small fraction of it corresponds to collagen suggests that obtaining protein extracts would be a good alternative for the valorisation of pork liver, especially if it is shown that they present interesting techno-functional properties. However, liver pH, water content and nutritional richness make it particularly susceptible to microbiological spoilage. A rapid processing at low temperatures and in the most hygienic conditions possible or, alternatively, its rapid freezing until the moment of use would be the most recommended in terms of food safety. These guidelines would also minimise oxidation phenomena, both of the lipid fraction and of some mineral elements, particularly iron due to its abundance and its effects on colour. While this would probably not have too much effect on the liver due to its own colour properties, it could strongly affect the colour of the extracts obtained.

ACKNOWLEDGEMENTS

We acknowledge NORFRISA (Girona, Spain) for kindly donation of pork livers.

RESEARCH FUNDING

This work was financially supported by the Government of Spain (project ref. RTA2017-00024-C04-02).

CONFLICT OF INTERESTS

Authors declare no conflict of interests.

ORCID IDs

N. Feliu-Alsina https://orcid.org/0000-0002-5041-3984
E. Saguer https://orcid.org/0000-0003-2126-5991

REFERENCES

1. Alfaia, C.M., Madeira, M.S., Pestana, J., Coelho, D., Lopes, P.A., Toldrá, F., Prates, J.A.M. (2020). Pork Byproducts. In B.K. Simpson, A.N.A. Aryee, F. Toldrá (Eds.), *Byproducts from Agriculture and Fisheries: Adding Value for Food, Feed, Pharma, and Fuels*, John Wiley & Sons Ltd, Chichester, UK, pp. 19–41. https://doi.org/10.1002/9781119383956.ch2
2. Alvaro, D., Cantafora, A., Attili, A.F., Ginanni Corradini, S., De Luca, C., Minervini, G., Di Blase, A., Angelico, M. (1986). Relationships between bile salts hydrophilicity and phospholipid composition in bile of various animal species. *Comparative Biochemistry and Physiology Part B: Comparative Biochemistry*, *83*(3), 551–554. https://doi.org/10.1016/0305-0491(86)90295-6
3. AOCS (2009). *Official Methods and Recommended Practices of the AOCS*. 6th ed., American Oil Chemists' Society, Urbana, IL, USA.
4. Aoyagi, S., Baker, D.H., Wedekind, K.J. (1993). Estimates of copper bioavailability from liver of different animal species and from feed ingredients derived from plants and animals. *Poultry Science*, *72*(9), 1746–1755. https://doi.org/10.3382/ps.0721746
5. Aoyagi, S., Hiney, K.M., Baker, D.H. (1995). Estimates of zinc and iron bioavailability in pork liver and the effect of sex of pig on the bioavailability of copper in pork liver fed to male and female chicks. *Journal of Animal Science*, *73*(3), 793–798. https://doi.org/10.2527/1995.733793x
6. Babicz, M., Kasprzyk, A., Kropiwiec-Domańska, K. (2019). Influence of the sex and type of tissue on the basic chemical composition and the content of minerals in the sirloin and offal of fattener pigs. *Canadian Journal of Animal Science*, *99*(2), 343–348. https://doi.org/10.1139/cjas-2018-0085
7. Bovo, S., Di Luca, A., Galimberti, G., Dall'Olio, S., Fontanesi, L. (2018). A comparative analysis of label-free liquid chromatography-mass spectrometry liver proteomic profiles highlights metabolic differences between pig breeds. *PLoS ONE*, *13*(9), art. no. e0199649. https://doi.org/10.1371/journal.pone.0199649
8. Canduri, F., Ward, R.J., de Azevedo Jr., W.F., Gomes, R.A.S., Arni, R.K. (1998). Purification and partial characterization of cathepsin D from porcine (*Sus scrofa*) liver using affinity chromatography. *Biochemistry and Molecular Biology International*, *45*(4), 797–803. https://doi.org/10.1080/15216549800203222
9. Chua, A.C.G., Klopcic, B., Lawrance, I.C., Olynyk, J.K., Trinder, D. (2010). Iron: An emerging factor in colorectal carcinogenesis. *World Journal of Gastroenterology*, *16*(6), 663–672. https://doi.org/10.3748/wjg.v16.i6.663
10. Cliplef, R.L., McKay, R.M. (1993). Visceral organ weights of swine selected for reduced backfat thickness and increased growth rate. *Canadian Journal of Animal Science, 73*(1), 201–206. https://doi.org/10.4141/cjas93-020
11. Custódio, F.B., Theodoro, K.H., Gloria, M.B.A. (2016). Bioactive amines in fresh beef liver and influence of refrigerated storage and pan-roasting. *Food Control*, *60*, 151–157. https://doi.org/10.1016/j.foodcont.2015.07.037
12. da Costa, C.G.C, Paula, M.M.O., Massingue, A.A., Filho, R.A.T., Ramos, E.M., Carneiro, J.D.S. (2019). Protein concentrates obtained from pig by-products using pH-shifting technique: a preliminary study. *Ciência Rural*, *49*(6), art. no. e20181048. https://doi.org/10.1590/0103-8478cr20181048
13. Devatkal, S., Mendiratta, S.K., Kondaiah, N., Sharma, M.C., Anjaneyulu, A.S.R. (2004). Physicochemical, functional and microbiological quality of buffalo liver. *Meat Science*, *68*(1), 79–86. https://doi.org/10.1016/j.meatsci.2004.02.006
14. Elefson, S.K., Lu, N., Chevalier, T., Dierking, S., Wang, S., Monegue, H.J., Matthews, J.C., Jang, Y.D., Chen, J., Rentfrow, G.K., Adedokun, S.A., Lindemann, M.D. (2021). Assessment of visceral organ growth in pigs from birth through 150 kg. *Journal of Animal Science*, *99*(9), art. no. skab249. https://doi.org/10.1093/jas/skab249
15. European Commission (2007). Commission Regulation (EC) No 1441/2007 of 5 December 2007 amending Regulation (EC) No 2073/2005 on microbiological criteria for foodstuffs. *Official Journal of the European Union*, *L 322*, 12–29.
16. FAO (2013). *FAO Food and Nutrition Paper 92: Dietary protein quality evaluation in human nutrition. Report of an FAO Expert Consultation, 31 March-2 April 2011, Auckland, New Zealand*. Food and Agriculture Organization of the United Nations, Rome, Italy.
17. FAO (2022). *Meat Market Review. Overview of global market and policy developments 2021*. Food and Agriculture Organization of the United Nations, Rome, Italy.
18. Fernandez, X., Lahirigoyen, E., Bouillier-Oudot, M., Vitezica, Z., Auvergne, A. (2010). The effects of stunning methods on product qualities in force-fed ducks and geese. 2. Fatty liver quality. *Animal*, *4*(1), 139–146. https://doi.org/10.1017/S1751731109990863
19. Gardner, W., Kassebaum, N. (2020). Global, regional, and national prevalence of anemia and its causes in 204 countries and territories, 1990–2019. *Current Developments in Nutrition*, *4*(Suppl. 2), art. no. nzaa053_035. https://doi.org/10.1093/cdn/nzaa053_035
20. Gault, N.F.S., Lawrie, R.A. (1980). Efficiency of protein extraction and recovery from meat industry by-products. *Meat Science*, *4*(3), 167–190. https://doi.org/10.1016/0309-1740(80)90047-9
21. Grimsley, G.R., Scholtz, J.M., Pace, C.N. (2009). A summary of the measured p*K* values of the ionizable groups in folded proteins. *Protein Science*, *18*(1), 247–251. https://doi.org/10.1002/pro.19
22. Grüngreiff, K., Reinhold, D., Wedemeyer, H. (2016). The role of zinc in liver cirrhosis. *Annals of Hepatology*, *15*(1), 7–16. https://doi.org/10.5604/16652681.1184191
23. Hrynets, Y., Omana, D.A., Xu, Y., Betti, M. (2011). Comparative study on the effect of acid- and alkaline-aided extractions on mechanically separated turkey meat (MSTM): Chemical characteristics of recovered proteins. *Process Biochemistry*, *46*(1), 335–343. https://doi.org/10.1016/j.procbio.2010.09.006
24. Hunter, M.L., Christie, W.W., Moore, J.H. (1973). The structures of the principal glycerolipids of pig liver. *Lipids*, *8*(2), 65–70. https://doi.org/10.1007/BF02534331
25. Im, S., Hayakawa, F., Kurata, T. (2004). Identification and sensory evaluation of volatile compounds in oxidized porcine liver. *Journal of Agricultural and Food Chemistry*, *52*(2), 300–305. https://doi.org/10.1021/jf030337v

26. ISO (1978). *Meat and meat products — Determination of nitrogen content (Reference method)* (ISO Standard No. 937:1978). International Organization for Standardization, Geneva, Switzerland.
27. Jiménez Torres, R., Medina Domenzáin, R., Ruiz Castañeda, G., Gutiérrez Vargas, M.E. (2013). Quality of pork meat and its nutritional value. *Veterinaria Digital*. Accessed: 12 January 2023. Available at: https://www.veterinariadigital.com/en/articulos/quality-of-pork-meat-and-its-nutritional-value/
28. Johnson, R.J., Nakagawa, T., Sánchez-Lozada, L.G., Lanaspa, M.A., Tamura, Y., Tanabe, K., Ishimoto, T., Thomas, J., Inaba, S., Kitagawa, W., Rivard, C.J. (2013). Umami: the taste that drives purine intake. *The Journal of Rheumatology*, *40*(11), 1794–1796. https://doi.org/10.3899/jrheum.130531
29. Kakimov, A., Suychinov, A., Tsoy, A., Mustambayev, N., Ibragimov, N., Kuderinova, N., Mirasheva, G., Yessimbekov, Z. (2018). Nutritive and biological value of liver and blood of various slaughtered animals. *Journal of Pharmaceutical Research International*, *22*(3), 1–5. https://doi.org/10.9734/JPRI/2018/41448
30. Kaneko, K., Aoyagi, Y., Fukuuchi, T., Inazawa, K., Yamaoka, N. (2014). Total purine and purine base content of common foodstuffs for facilitating nutritional therapy for gout and hyperuricemia. *Biological and Pharmaceutical Bulletin*, *37*(5), 709-721. https://doi.org/10.1248/bpb.b13-00967
31. Keller, S. (2019). The copper recycling pathway through bile. *Pig Progress*. Accessed: 22 December 2022. Available at: https://www.pigprogress.net/health-nutrition/the-copper-recycling-pathway-through-bile/
32. Khalid, E.K., Babiker, E.E., El Tinay, A.H. (2003). Solubility and functional properties of sesame seed proteins as influenced by pH and/or salt concentration. *Food Chemistry*, *82*(3), 361–366. https://doi.org/10.1016/S0308-8146(02)00555-1
33. Knovich, M.A., Storey, J.A., Coffman, L.G., Torti, S.V., Torti, F.M. (2009). Ferritin for the clinician. *Blood Reviews*, *23*(3), 95–104. https://doi.org/10.1016/j.blre.2008.08.001
34. Kolar, K. (1990). Colorimetric determination of hydroxyproline as measure of collagen content in meat and meat products: NMKL collaborative study. *Journal of Association of Official Analytical Chemists*, *73*(1), 54–57. https://doi.org/10.1093/jaoac/73.1.54
35. Kongkachuichai, R., Napatthalung, P., Charoensiri, R. (2002). Heme and non-heme iron content of animal products commonly consumed in Thailand. *Journal of Food Composition and Analysis*, *15*(4), 389–398. https://doi.org/10.1006/jfca.2002.1080
36. Kramer, R.M., Shende, V.R., Motl, N., Pace, C.N., Scholtz, J.M. (2012). Toward a molecular understanding of protein solubility: Increased negative surface charge correlates with increased solubility. *Biophysical Journal*, *102*(8), 1907–1915. https://doi.org/10.1016/j.bpj.2012.01.060
37. Lautt, W.W. (1977). Hepatic vasculature: A conceptual review. *Gastroenterology*, *73*(5), 1163–1169. https://doi.org/10.1016/S0016-5085(19)31879-7
38. Loeffel, W.J., Koch, R.M. (1970). Growth in weight of selected organs, tissues and systems in the pig. *Historical Research Bulletins of the Nebraska Agricultural Experiment Station (1913-1993)*, *235*, 2–18.
39. Masic, U., Yeomans, M.R. (2014). Umami flavor enhances appetite but also increases satiety. *The American Journal of Clinical Nutrition*, *100*(2), 532–538. https://doi.org/10.3945/ajcn.113.080929
40. Mik, P., Tonar, Z., Malečková, A., Eberlová, L., Liška, V., Pálek, R., Rosendorf, J., Jirık, M., Mırka, H., Králíckova, M., Witter, K. (2018). Distribution of connective tissue in the male and female porcine liver: histological mapping and recommendations for sampling. *Journal of Comparative Pathology*, *162*, 1–13. https://doi.org/10.1016/j.jcpa.2018.05.004
41. Mulvihill, B. (2014). Micronutrients in Meat. In C. Devine, M. Dikeman (Eds.), *Encyclopedia of Meat Sciences*, 2nd edition, Academic Press, Cambridge, MA, USA, pp. 124–129. https://doi.org/10.1016/B978-0-12-384731-7.00174-4
42. Ntonas, A., Katsourakis, A., Galanis, N., Filo, E., Noussios, G. (2020). Comparative anatomical study between the human and swine liver and its importance in xenotransplantation. *Cureus*, *12*(7), art. no. e9411. https://doi.org/10.7759/cureus.9411
43. Nuckles, R.O., Smith, D.M., Merkel, R.A. (1990). Meat by-product protein composition and functional properties in model systems. *Journal of Food Science*, *55*(3), 640–643. https://doi.org/10.1111/j.1365-2621.1990.tb05196.x
44. Racanelli, V., Rehermann, B. (2006). The liver as an immunological organ. *Hepatology*, *43*(S1), S54–S62. https://doi.org/10.1002/hep.21060
45. Ritchie, K.P., Keller, B.M., Syed, K.M., Lepock, J.R. (1994). Hyperthermia (heat shock)-induced protein denaturation in liver, muscle and lens tissue as determined by differential scanning calorimetry. *International Journal of Hyperthermia*, *10*(5), 605–618. https://doi.org/10.3109/02656739409022441
46. Roughead, Z.K., Zito, C.A., Hunt, J.R. (2005). Inhibitory effects of dietary calcium on the initial uptake and subsequent retention of heme and nonheme iron in humans: comparisons using an intestinal lavage method. *The American Journal of Clinical Nutrition*, *82*(3), 589–597. https://doi.org/10.1093/ajcn/82.3.589
47. Saguer, E., Carretero, C., Toldrà, M., Parés, D. (2019). Obtención de proteínas tecnofuncionales a partir de hígados de cerdo. In J.M. Rodríguez Calleja, J.Á. Santos Buelga, T.M. López Díaz (Eds.), *Impulsando la investigación y la innovación, X Congreso Nacional CyTA/CESIA, León, 15-17 de mayo de 2019*, Universidad de León, León, Spain, p. 256 (in Spanish).
48. Santé-Lhoutellier, V. (2014). Meat and Human Diet: Facts and Myths. In C. Devine, M. Dikeman (Eds.), *Encyclopedia of Meat Sciences*, 2nd edition, Academic Press, Cambridge, MA, USA, pp. 118–123. https://doi.org/10.1016/B978-0-12-384731-7.00178-1
49. Sasaki, K., Mitsumoto, M., Nishioka, T., Irie, M. (2006). Differential scanning calorimetry of porcine adipose tissues. *Meat Science*, *72*(4), 789–792. https://doi.org/10.1016/j.meatsci.2005.09.020
50. Seong, P.N., Park, K.M., Cho, S.H., Kang, S.M., Kang, G.H., Park, B.Y., Moon, S.S., Ba, H.V. (2014). Characterization of edible pork by-products by means of yield and nutritional composition. *Korean Journal of Food Science of Animal*, *34*(3), 297–306. https://doi.org/10.5851/kosfa.2014.34.3.297
51. Silva, R.O., Rouxinol, M.I.F.C., Patarata, L.A.S.C. (2020). Pork liver freshness evaluated through spoilage microbiota and a consumer test in shelf life extension experiment. *Journal of Food Quality*, *2020*, art. no. 1092865. https://doi.org/10.1155/2020/1092865
52. Stasiak, K., Roślewska, A., Stanek, M., Cygan-Szczegielniak, D., Janicki, B. (2017). The content of selected minerals determined in the liver, kidney and meat of pigs. *Journal of Elementology*, *22*(4), 1475–1483. https://doi.org/10.5601/jelem.2017.22.1.1314
53. Steen, L., Glorieux, S., Goemaere, O., Brijs, K., Paelinck, H., Foubert, I., Fraeye, I. (2016). Functional properties of pork liver protein fractions. *Food and Bioprocess Technology*, *9*(6), 970–980. https://doi.org/10.1007/s11947-016-1685-2
54. Tapiero, H., Townsend, D.M., Tew, K.D. (2003). Trace elements in human physiology and pathology. Copper. *Biomedicine and Pharmacotherapy*, *57*(9), 386–398. https://doi.org/10.1016/S0753-3322(03)00012-X
55. Tomović, V.M., Petrović, L.S., Tomović, M.S., Kevrešan, Ž.S., Džinić, N.R. (2011). Determination of mineral contents of *semimembranosus* muscle and liver from pure and crossbred pigs in Vojvodina (northern Serbia). *Food Chemistry*, *124*(1), 342–348. https://doi.org/10.1016/j.foodchem.2010.06.043
56. Tomović, V., Šojić, B., Jokanović, M., Škaljac, S., Ivić, M., Tomović, M., Tomašević, I., Stajić, S., Martinović, A. (2019). Mineral contents in pork and edible offal from indigenous pigs. *Journal of Engineering and Processing Management*, *11*(1), 66–72. https://doi.org/10.7251/JEPM1901066T
57. Tomović, V., Žlender, B., Jokanović, M., Tomović, M., Šojić, B., Škaljac, S., Kevrešan, Ž., Tasić, T., Ikonić, P., Okanović, Đ. (2016). Physical and chemical characteristics of edible offal from free-range reared Swallow-Belly Mangalica pigs. *Acta Alimentaria*, *45*(2), 190–197. https://doi.org/10.1556/AAlim.2015.0007
58. Trevino, S.R., Scholtz, J.M., Pace, C.N. (2007). Amino acid contribution to protein solubility: Asp, Glu, and Ser contribute more favorably than the other hydrophilic amino acids in RNase Sa. *Journal of Molecular Biology*, *366*(2), 449–460. https://doi.org/10.1016/j.jmb.2006.10.026
59. USDA (1992). Food Data Central: Pork, fresh, variety meats and by-products, liver, raw. Accessed: 15 January 2023. Available at: https://fdc.nal.usda.gov/fdc-app.html#/food-details/167862/nutrients
60. Vekemans, K., Braet, F. (2005). Structural and functional aspects of the liver and liver sinusoidal cells in relation to colon carcinoma metastasis. *World Journal of Gastroenterology*, *11*(33), 5095–5102. https://doi.org/10.3748/wjg.v11.i33.5095
61. Venegas Fornias, O. (1996). *FAO Animal Production and Health Paper 123: Edible by-products of slaughter animals.* Food and Agriculture Organization of the United Nations, Rome, Italy.
62. Warriss P.D., Bevis, E.A. (1987). Liver glycogen in slaughtered pigs and estimated time of fasting before slaughter. *British Veterinary Journal*, *143*(4), 354–360. https://doi.org/10.1016/0007-1935(87)90070-4
63. Wong, C. (2017). Iron deficiency anaemia. *Paediatrics and Child Health*, *27*(11), 527–529. https://doi.org/10.1016/j.paed.2017.08.004
64. Yamada, K., Sasaki, T., Sakagami, T. (1981). Phosphatidylcholine and phosphatidylinositol exchange proteins in pig liver. *The Tohoku Journal of Experimental Medicine*, *135*(1), 23–36. https://doi.org/10.1620/tjem.135.23

65. Yan, L., Iwasaki, H. (2004). Fractal aggregation of DNA after thermal denaturation. *Chaos, Solitons and Fractals*, *20*(4), 877–881. https://doi.org/10.1016/j.chaos.2003.09.019
66. Zheng, M., Huang, Y., Ji, J., Xiao, S., Ma, J., Huang, L. (2018). Effects of breeds, tissues and genders on purine contents in pork and the relationships between purine content and other meat quality traits. *Meat Science*, *143*, 81–86. https://doi.org/10.1016/j.meatsci.2018.04.022
67. Zou, Y., Bian, H., Li, P., Sun, Z., Sun, C., Zhang, M., Geng, Z., Xu, W., Wang, D. (2018). Optimization and physicochemical properties of nutritional protein isolate from pork liver with ultrasound-assisted alkaline extraction. *Animal Science Journal*, *89*(2), 456–466. https://doi.org/10.1111/asj.12930

ORIGINAL ARTICLE
http://journal.pan.olsztyn.pl

Polish Journal of Food and Nutrition Sciences
2023, Vol. 73, No. 2, 139–150
DOI: 10.31883/pjfns/163061
ISSN 1230-0322, e-ISSN 2083-6007

Microplastics in a Traditional Turkish Dairy Product: Ayran

Serkan K. Buyukunal[1], Sanae Rbaibi Zipak[2], Karlo Muratoglu[1,*]

[1]Department of Food Hygiene and Technology, Istanbul University-Cerrahpaşa, Istanbul, Turkey
[2]Graduate Education Institute, Istanbul University-Cerrahpaşa, Turkey

Ingestion of microplastic particles (MP) through food has been associated with a multitude of health problems in humans. Although ayran is a traditional and nutritious Turkish beverage, the impact of microplastic pollution is unknown. This study examined the incidence of microplastic pollution on ayran by collecting samples throughout the production processes and the ingredients used to make ayran, including water, salt, cream, starting culture, cups, and lastly, the ayran. Optical and scanning electron microscope was applied for MP visualisation and measurement, and Fourier-transform infrared spectroscopy (FTIR) for polymer identification. Microplastics were detected in all examined filters except for the starter culture samples. The samples with the highest MP number were salty water (43 MP number/100 mL), salt (33 MP number/100 g), and milk samples taken from homogenization and pasteurization phases (26 MP number/100 mL). Additionally, 18 MP number/100 mL contamination was detected in the last product ayran. MP with a size range of 1–150 µm prevailed (37.38%). Ethylene propylene was the most frequently identified polymer in samples (39.30%). The findings of this study can help provide an overview of microplastic contamination in dairy production facilities and the potential human health risks associated with this microplastic exposure.

Key words: fermented milk product, production process, food pollution, microplastic particle

INTRODUCTION

Plastics, which are used in the food industry at the points where there is a possibility of direct or indirect contact with food, have begun to be defined as a potential food safety risk today. Plastics threaten sustainable environmental and public health targets with their uncontrolled waste and residues during their production, use and post-use stages [Chang *et al.*, 2020; Frias & Nash, 2019; Pérez-Guevara *et al.*, 2022].

Microplastic particles (MP) are small particles of plastic waste from 1 µm to 5 mm in size [Chang *et al.*, 2020; Fournier *et al.*, 2021]. Primary MP are industrially used microbeads in different sizes and are released into the environment during production and transportation stages. Microplastics released into the air, soil and seas due to the decomposition of plastic materials and garbage under environmental conditions are defined as secondary microplastics. They are the primary source of microplastics. Microplastics emitted by the friction of tools and equipment used in food production and microplastics emitted from clothes containing polymers are other secondary sources of food contamination [Andrady, 2017; Da Costa Filho *et al.*, 2021; Song *et al.*, 2021].

Many harmful effects of microplastics on living organisms have been revealed. Research on many health concerns is still ongoing. In addition to being a risk that causes trauma to organs and tissues, they can also contain chemical and biological hazards [Allan *et al.*, 2021; Toussaint *et al.*, 2019]. MP from waste may harbour environmental pollutants such as heavy metals, antibiotics, hormones, pesticides, drugs, detergents, disinfectants,

***Corresponding Author:**
tel.: +90 532 625 00 60; e-mail: karlomrt@iuc.edu.tr (K. Muratoglu)

Submitted: 26 October 2022
Accepted: 5 April 2023
Published on-line: 5 May 2023

and microorganisms. They can also act as a carrier for toxic chemicals known as plastic additives [Chen *et al.*, 2020; Ragusa *et al.*, 2021; Yong *et al.*, 2020]. MP may pose four risks: gastrointestinal toxicity, liver toxicity, neurotoxicity, and reproductive toxicity [Chang *et al.*, 2020]. MP are also the medium for biofilm formation and allow pathogenic microorganisms, a significant potential threat, to enter the body [Qiang *et al.*, 2021]. MP have been demonstrated to pass through the placental barrier, which is known to be permeable to a wide range of toxic substances [Ragusa *et al.*, 2021].

MP are frequently taken orally as well as inhaled. Food and water are considered essential carriers at this point [Yong *et al.*, 2020]. They have been reported in many food products, including marine invertebrates, crustaceans, fish [Street & Bernasconi, 2021; Waring *et al.*, 2018], table salt [Gündoğdu, 2018; Kosuth *et al.*, 2018], sugar [Liebezeit & Liebezeit, 2013], beer [Kosuth *et al.*, 2018], water [Kosuth *et al.*, 2018; Mason *et al.*, 2018; Pérez-Guevara *et al.*, 2022; Schymanski *et al.*, 2018; Wiesheu *et al.*, 2016], soft drinks [Shruti *et al.*, 2020], honey [Liebezeit & Liebezeit, 2013, 2015], and broilers [Huang *et al.*, 2020; Kedzierski *et al.*, 2020].

Our research has been focused on the ayran processing steps in a dairy factory with an average daily production of 50,000 L. This traditional and industrially produced Turkish product is encouraged for consumption by people of all ages [TNG, 2015]. Ayran is defined as "a fermented milk product produced by adding drinkable water and salt when necessary, or by adding drinkable water to milk, yogurt bacteria, and if necessary, adding salt after fermentation, by its technique" [TSI, 2013]. The assessment of microplastic contamination in the industrial production process is very important. It was discovered that there is a need for food production process-oriented research when previous studies were examined. In addition to the lack of research on ayran, evaluation of the production process has never been emphasized in a food-related study.

This study aims to investigate the presence of microplastic particles in the industrial production of ayran and to identify the potential sources of contamination at various stages of production.

MATERIAL AND METHODS

Sample collection

The samples for the study were collected from the ayran production line at a Turkish dairy plant in Istanbul with an average daily production of 50,000 L. The process steps were monitored and recorded on-site. Control points were noted in the workflow chart according to the food safety management system applied in the enterprise. The study was repeated on five different days, and parallel sampling was done every sampling day. A total of 180 samples were collected throughout the production process from all process steps, inputs, outputs, and materials that may have been contaminated with microplastic. The scheme of process steps and sampling locations are shown in Figure 1.

Prior to the acceptance of raw milk into the facility, the walls of the stainless-steel raw milk tank (Z) were rinsed with microplastic-free ultrapure water, and a 1,000 mL sample was taken. The samples (1,000 mL or 1,000 g) were collected during raw milk acceptance (RM), filtration (F), clarification (C), water addition (WA), homogenization (H), pasteurization (P), holder (Q), starter culture addition (SCA), salty water addition (SWA), and filtration before filling (FB). In addition, samples of water (tap water, W),

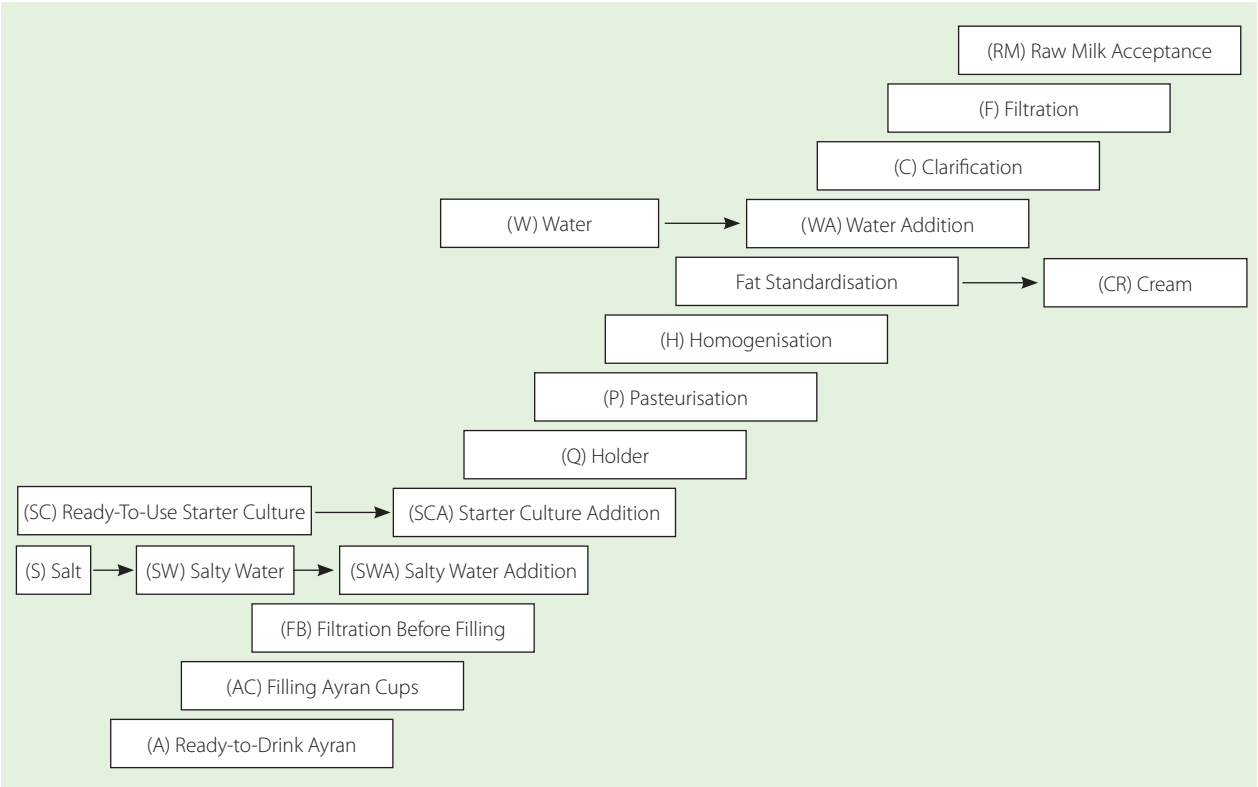

Figure 1. Process steps/sampling locations of ayran production.

separated cream (CR), ready-to-use starter culture (SC), salt (S), salty water (SW), filling ayran cups (AC), and the ready-to-drink ayran (A) were collected. A 1,000 mL sample of ready-to-use starter culture and a 500 g sample of the salt were taken. Microplastic-free ultrapure water was added to the salt to make it up to 10 L and dissolved. A collected sample of 1,000 mL of the solution was filtered. The empty ayran cups were refilled with 1,000 mL of microplastic-free ultrapure water and sealed before being transported to the laboratory with all samples.

Digestion of organic matter of the samples

The method for digestion of organic matter of the samples proposed by Da Costa Filho *et al*. [2021] was followed. Each milk, separated cream, ready-to-use starter culture and ready-to-drink final product (ayran) sample was transferred to an Erlenmeyer flask cleaned with microplastic-free ultrapure water before analysis. Ayran, cream and ready-to-use starter culture were challenging to filter through due to their density. Therefore, these samples were homogenised by vigorously shaking with twice the volume of ultrapure water in an Erlenmeyer flask. This step was not necessary for the milk samples. Next, 25 mL of the samples were mixed with 20 mL of microplastic-free ultrapure water. An aliquot of 2 mL of multi-enzymatic detergent containing protease, amylase, lipase, and cellulase (Deconex® Prozyme Active, Boer Chemie, Zuchwil, Switzerland) was added. The samples were stirred for 2 min at 40°C. Then, 10 mL of ethylenediaminetetraacetic acid (EDTA, Thermo Fisher Scientific, Waltham, MA, USA) was added and stirred at 40°C for 3 min. Finally, 2 mL of tetramethylammonium hydrate (Merck, Darmstadt, Germany) was mixed into the mixture. Samples were incubated at 80°C for 1 min and filtered immediately. The direct filtering stage was started for water, salt, and salty water samples.

Sample filtration

Before and after each sample filtration, all filtration equipment was thoroughly cleaned with microplastic-free ultrapure water. Filtration was carried out at a pressure of approximately 0.5–0.6 bar using glass microfiber filters with a pore size of 1 µm (Whatman grade GF/B glass microfiber filters, diameter 47 mm, Cytiva Marlborough, MA, USA) and a vacuum pump [Kosuth *et al.*, 2018; Liebezeit & Liebezeit, 2015; Schymanski *et al.*, 2018]. At least two replicates of the same samples (each of 100 mL) were processed. Using metal tweezers, the filters were transferred carefully into glass Petri dishes. They were then stored for analysis after being air-dried at room temperature.

Optical microscopy analysis

After filtrations, the glass microfiber filters were viewed under the Olympus CX31 optical microscope (Olympus, Tokyo, Japan) with Canon A640 camera (Canon, Tokyo, Japan) using 4× magnification. The number of microplastic particles *per* volume or weight of sample (MP number/100 mL or MP number/100 g, respectively) was adopted as the unit of quantification. Using Kameram software 1.3.0.8 (Mikrosistem, Istanbul, Turkey), microparticles were captured on film. Using IC Measure software 2.0.0.286 (The Imaging Source, Bremen, Germany), the particles' longest side was measured and classified by colour, shape, and size.

Scanning electron microscopy and Fourier-transform infrared spectroscopy analyses

The morphology of randomly selected microplastics was analysed by scanning electron microscopy (SEM). The images were taken using high-resolution SEM microscope (JSM-7001F, Jeol, Tokyo, Japan) in high vacuum pressure mode operating at 10.00 kV acceleration voltage, in secondary electron and backscattering modes and different magnifications. The filter parts containing the microplastic particles were marked with an architectural drawing pen under the optical microscope, cut with scissors, and carefully transferred with metal tweezers onto double-sided carbon adhesive tape mounted on aluminium SEM pin stubs.

The chemical composition of microplastics was identified using Fourier-transform infrared spectroscopy (FTIR) analysis. Agilent Cary 630 spectrometer (Agilent, Santa Clara, CA, USA) within the 400–4000 cm^{-1} range, 8 scans, and 4 cm^{-1} resolutions was used. The results were evaluated using Agilent Polymer Handheld ATR, Agilent Elastomer Oring and Seal Handheld ATR and Agilent ATR General Libraries.

Procedures adopted to ensure the accuracy of the experiments

Several precautions proposed by Wang *et al.* [2017] were taken in the experiments, from field sampling to laboratory analysis, to ensure the accuracy of results. Cotton lab coats and nitrile gloves were worn to prevent contamination of the samples by airborne polymer particles and fibres. All consumables used were made from glass and stainless steel to avoid plastic contamination. The surfaces were cleaned with microplastic-free ultrapure water and acetone, and the contamination was tried to be reduced to a negligible level or zero. Before filtration, each filter paper package was opened and eventually microplastic contamination of filters was evaluated under the optical microscope. No microplastic contamination was detected in any of them.

Experimental blanks were conducted in all selected sampling locations. At each location, 1,000 mL of MP-free ultrapure water was blank sample [Chae *et al.*, 2015; Dubaish & Liebezeit, 2013; Nuelle *et al.*, 2014]. Each analysis was carried out in five replications. Analyses for blank samples were conducted according to the same procedure as that for water samples. Finally, under the microscope, an average of 0.05±0.04 MP number/L were detected in blank samples.

Samples were analysed in a laminar cabinet, therefore potential MP in the air were examined with Petri dishes with filters placed next to the samples in a laminar flow cabinet and left open for 1 h, which allowed obtaining data about the level of contamination. On average, 0.13±0.06 MP number/h were found under the microscope.

Multi-enzymatic detergent, EDTA and tetramethylammonium hydrate were controlled for microplastics. Before use, empty sample bottles were rinsed with microplastic-free ultrapure water

(1,000 mL), and this water was analysed to investigate the glass bottles' microplastic particle presence. The results of these tests confirmed the absence of contamination. Microplastic-free ultrapure water was included in the analysis protocol as a blank control.

Positive control analysis

Polypropylene (PP), polystyrene (PS), polyethylene (PE), polyvinyl chloride (PVC), linear low-density polyethylene (LLDPE), and thermoplastic elastomers (TPE) were used as positive controls. The sources of these materials were described in Table S1. All positive samples' chemical composition was identified using FTIR. Plastic materials were ground first with an oscillating mill (Retsch MM 400, Haan, Germany) and then with ultraturrax (IKA T 25, Staufen im Breisgau, Germany). Each crushed plastic material (1 mg) was mixed with 1,000 mL of microplastic-free ultrapure water in a microplastic-free glass bottle. After standing overnight, the mixture was subjected to filtration. At least ten replicates of the same samples were processed. Before positive control sample filtration, all safety precautions were taken, as described in the section "Procedures adopted to ensure the accuracy of the experiments". Filtration and optical microscopy analysis were done as described above. Each filter was rinsed with 1,000 mL of microplastic-free ultrapure water in a microplastic-free glass bottle and left overnight.

Calculation of microplastic particle ingestion by humans

The risk assessment was based on the total amount of microplastic particles ingested orally. It has been presumed that drinking ayran provides the entire amount of dairy products recommended for daily diet consumption. This evaluation did not took into account any toxicokinetic components. According to the recommendations of the Turkey Nutrition Guide [TNG, 2015], it was assumed that the daily amount of ayran for adult is three servings (1 serving = 240 mL). Children, adolescents, pregnant-breastfeeding women, and postmenopausal women should consume two to four servings, *i.e.*, 720 mL and 480–960 mL of ayran, respectively, *per* day. Daily intake of MPs with ayran was calculated using Equation (1):

$$EDI = \frac{W \times C}{100} \quad (1)$$

where: EDI, estimated daily intake of MPs with ayran (MP number/day); W, recommended amount of ayran (mL/day); C, microplastic content (MP number/100 mL).

RESULTS AND DISCUSSION

Our study investigated the risk of microplastic contamination in the industrial production processes of ayran, a traditional Turkish beverage. Ayran production processes had been evaluated step by step, and the sources of the hazard had been determined. The microplastic load, type, size, colour, and shape were assessed at each production stage. According to our literature search, although there are studies in different scopes and scales on microplastic contamination of various foods such as honey, salt, sugar, soft drinks, beer, alcohol, meat, broilers, especially seafood and water [Cox *et al.*, 2019; Kedzierski *et al.*, 2020; Toussaint *et al.*, 2019], this is the first study to investigate microplastics' existence in a food production line.

Before and during the study, experimental blank tests were conducted at all selected sampling sites, laboratory areas, ultrapure water, chemicals, instruments and equipment. Experimental blank tests and ultrapure water filtration results to ensure safe analysis conditions revealed that background contamination was minimal and negligible. The filtration and optical microscopy analysis results of the positive control samples' colour, shape, and size distribution are given in Table S2. As a result of the study conducted to evaluate the method performance, the recovery rates of PP, PS, PE, PVC, LLDPE, and TPE were 98±2%, 96±4%, 95±4%, 87±7%, 89±6%, and 91±9%, respectively. These results indicated the method's reliability.

As understandable in the results of this study, microplastic contamination is probable in the ayran production process steps. Microplastic particles were detected in all examined samples except the ready-to-use starter culture. However, the quantities of microplastic particles varied significantly between processing steps (Table 1). The samples with the highest microplastic count were found to be salty water (43 MP number/100 mL), salt (33 MP number/ 100 g), and milk samples from homogenization and pasteurization steps (26 MP number/100 mL). There were total of 313 microplastic particles on the filters of 17 process steps/sampling locations. Microplastics were abundant between 3 and 43 MP number per 100 mL or per 100 g. An average of 19 MP number/100 mL of raw milk on five different production days was determined. This contamination of the raw material was a determinant of the quality of the last product (ayran).

Examining the production and logistics of milk and dairy products revealed several potential microplastic contamination risk points. Plastic pipes, valves and fittings used to pour milk into tankers and transport it to the dairy plants can be a significant source of contamination for microplastic. Tankers carrying milk from milk collection points to dairy production facilities can be considered a risk factor. The water, detergents, disinfectants used for clean in place (CIP), hoses for water transfer, and rubber pipes may pose a risk to the microplastic load [Britz & Robinson, 2008; Walstra *et al.*, 2005]. The other contamination locations are refrigerated storage tanks at farms, stainless steel containers, buckets, and rubber rings of automatic milking units. In addition to cloths, brushes, gloves, and other plastic cleaning equipment, detergents, disinfectants, and water may also be a source of contamination [Caramia & Guerriero, 2010; Lopes & Stamford, 1997]. Due to the expiration of their useful life, poor quality of the polymer used, or unanticipated external factors, a variety of polymers used in the equipment of the food industry may be a source of microplastic contamination in foods [Nady, 2016; Pouliot, 2008; Tan & Rodrigue, 2019]. All seals and filtration units that are not maintained periodically are another important source of contamination. The enlargement of the filter pores by the microplastics, organic materials, mineral substances,

Table 1. Abundance of microplastic particles (MP) and their size in samples collected during ayran production at different process steps/sampling locations.

Process step/sampling location	Microplastic abundance (MP number/100 mL or MP number/100 g)	Microplastic particle size (µm)		
		Range	Mean±SD	Median
Z	3	89–1,613	562±686	150
RM	19	9–4,906	953±1,193	215
F	17	22–4,930	785±1,264	125
C	16	20–4,262	779±1,018	289
W	19	25–1,057	214±266	117
WA	13	50–2,503	628±679	378
CR	9	103–956	314±243	239
H	26	37–4,220	1,001±1,212	367
P	26	50–2,503	641±695	378
Q	9	30–1,259	538±577	266
SC	0	-		-
SCA	12	22–2,425	495±597	219
S	33	18–3,200	413±542	176
SW	43	17–2,070	295±387	155
SWA	16	23–2,070	533±602	179
FB	21	19–2,814	896±766	785
AC	13	22–1,748	586±497	413
A	18	17–965	265±238	190

Z, bulk tank; RM, raw milk acceptance; F, filtration; C, clarification; W, water; WA, water addition; CR, cream; H, homogenization; P, pasteurization; Q, holder; SC, ready-to-use starter culture; SCA, starter culture addition; S, salt; SW, salty water; SWA, salty water addition; FB, filtration before filling; AC, filling ayran cups; A, ready-to-drink ayran; SD, standard deviation.

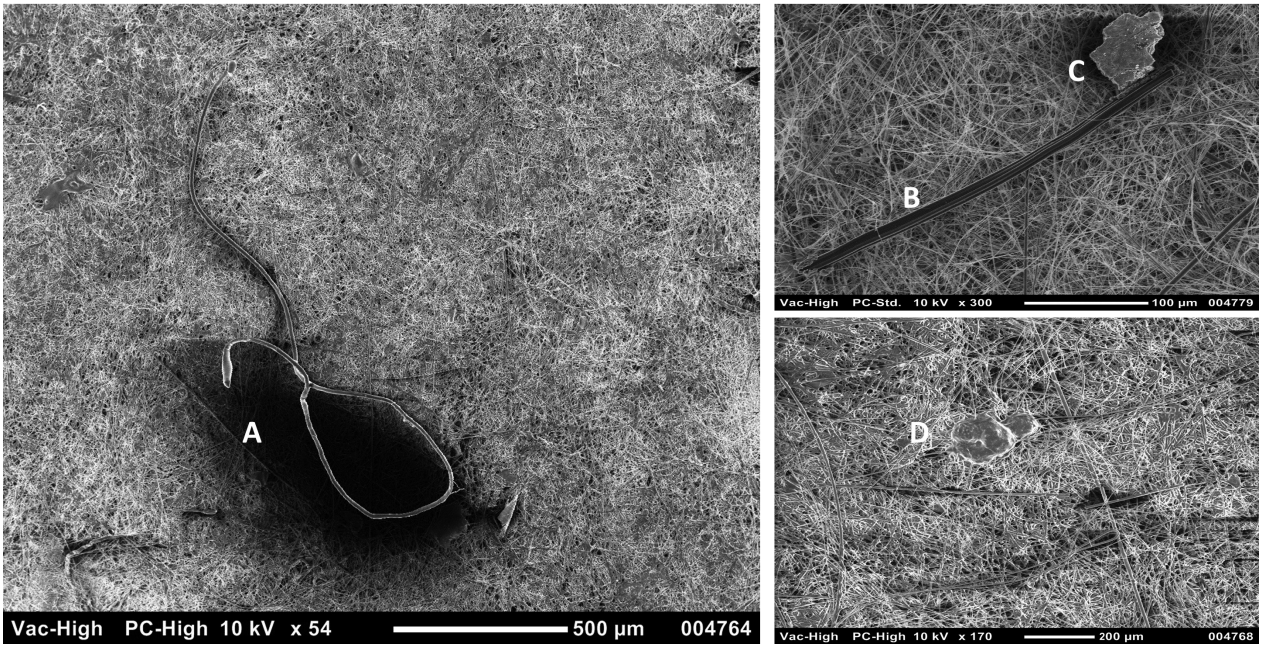

Figure 2. Scanning electron microscopy (SEM) image of microplastic particles: A, ethylene propylene (raw milk); B, ethylene propylene (water); C, polytetrafluoroethylene (water); D, polytetrafluoroethylene (ready-to-drink ayran).

and colloids trapped in the filters during the pressurised liquid flow can increase the risk of contamination of the milk with microplastics [Kumar *et al.*, 2013; Tomasula & Bonnaillie, 2015].

The surface morphology of two representative microplastics observed using SEM is given in Figure 2. SEM is a microscopic technique that can provide information about

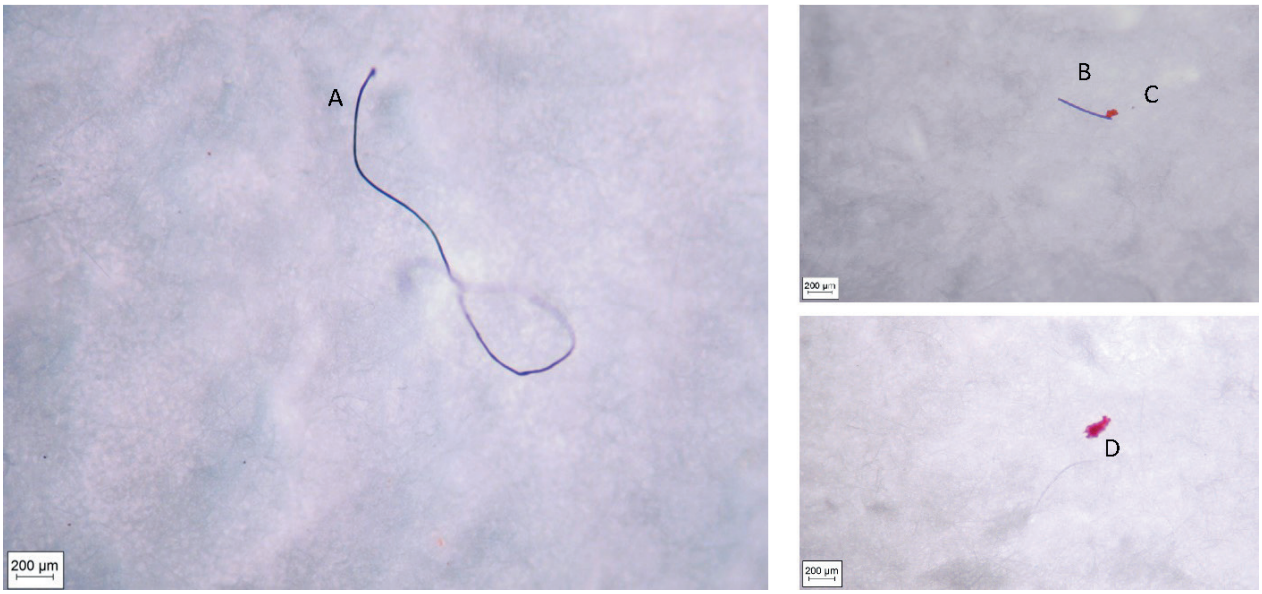

Figure 3. Optical microscopy images of microplastic particles in samples collected during ayran production. A, 3679.22 µm, ethylene propylene (raw milk); B, 468.42 µm, ethylene propylene (water); C, 98.02 µm, polytetrafluoroethylene (water); and D, 215 µm polytetrafluoroethylene (ready-to-drink ayran).

the morphological surface structure of MP, producing high-resolution images of the surface state. It can also provide data on the chemical composition of samples, as it can be equipped with energy dispersive X-ray spectroscopy (EDS) detectors. In our study, an overview of the structures of the particles present was provided by SEM imaging of randomly selected filter surfaces after optical microscopy analysis. However, SEM imaging did not provide enough discriminatory evidence to confirm that the analysed microparticle was an MP or organic residue. Mineral-based particles can be identified through EDS analysis [Mariano *et al.*, 2021]. However, in the trial studies, it was determined that the fibers, organic residues and MP showed similar spectra for C, O and N elements. Therefore, as some researchers have noted, SEM-EDS can be used as a tool to support FTIR, but it has not been shown to be sufficient alone for the identification of MP [Da Costa Filho *et al.*, 2021; Mariano *et al.*, 2021].

Selected optical microscopy images of microplastic particles detected at various stages of ayran production are shown in Figure 3. The particles varied in size and shape. The distribution of microplastic particle size in samples was summarised in Table 2. Microplastic particles with a size range of 1–150 µm (37.38%) prevailed. In addition, 36.42% of the microplastic particles had between 151 and 1,000 µm in size, while size of 26.20% of the particles ranged from 1,001 to 5,000 µm. Microplastic particle size is an essential parameter for translocation in living organisms. This parameter determines the microplastic absorption efficiency through the gastrointestinal, alveolar, and dermal epithelium. After oral ingestion, microplastics and nanoplastics can be dispersed into the blood and lymphatic system, and subsequently the liver, *via* absorption from the gastrointestinal tract. The gastrointestinal epithelium is permeable to particles of 150 µm, >90% of those larger than 150 µm are excreted in the faeces [Dick Vethaak & Leslie, 2016; Kannan & Vimalkumar, 2021]. It has been reported that intestinal absorption of MP smaller than 1.5 µm is possible, and MP smaller than 2.5 µm can enter the systemic circulation *via* endocytosis and phagocytosis [Dris *et al.*, 2016; EFSA, 2016; Hwang *et al.*, 2020; Kannan & Vimalkumar, 2021; Millburn *et al.*, 1967; Yang *et al.*, 2009]. However, particles of 0.1 µm and smaller can cross the blood-brain barrier and placenta [Prietl *et al.*, 2014]. In our study, microparticles smaller than 10 µm were detected only in the raw milk acceptance sample and they accounted for 5.26% of all particles. The filter pore diameter used in filtration does not allow the detection of smaller particles. When discussing the dangers posed by microplastics in food, focus is more on their physical effects and the effects of the endocrine-disrupting ingredients they contain, such as bisphenol A, phthalates, and certain brominated flame retardants. Due to these factors, microplastics can cause serious health problems [Dick Vethaak & Leslie, 2016]. Studies demonstrate that microplastic causes intestinal microbiota changes in mice and gastric adenocarcinoma in humans [Chang *et al.*, 2020]. It has been shown that the consumption of microplastic reduces key gene expressions related to lipogenesis and triglyceride synthesis in the liver, which can lead to mouse hepatic lipid disorder [Lu *et al.*, 2018].

Microplastic particles were visualised using optical microscope in black, blue, brown, dark blue, grey, green, orange, pink, purple, red, transparent, and yellow. The visualization showed that 19.81% of the microplastic particles were recorded as blue, 17.89% as red, 15.02% as transparent, and 11.18% as black (Figure 4). The microplastic particles varied also in shape. Fibre form dominated (49.84%), followed by film (23.32%), fragments (14.70%), and spheres (12.4%) (Table 3). According to Rodriguez-Seijo & Pereira [2017], colours are crucial for visually distinguishing the chemical composition of microplastics. The chemical composition of microplastics can provide clues in predicting the type of polymer from which the food contact or likely to

Table 2. Number of microplastic particles (MP) with different size in samples collected during ayran production at different process steps/sampling locations (MP number/100 mL or MP number/100 g).

Process step/ sampling location	1–10 µm	11–50 µm	51–150 µm	151–500 µm	501–1,000 µm	1,001–5,000 µm
Z	-	-	1 (33.33%)*	1 (33.33%)	-	1 (33.33%)
RM	1 (5.26%)	1 (5.26%)	6 (31.58%)	2 (10.53%)	1 (5.26%)	8 (42.11%)
F	-	4 (23.53%)	5 (29.41%)	2 (11.76%)	2 (11.76%)	4 (23.53%)
C	-	2 (12.50%)	4 (25.00%)	4 (25.00%)	2 (12.50%)	4 (25.00%)
W	-	4 (21.05%)	7 (36.84%)	6 (31.58%)	1 (5.26%)	1 (5.26%)
WA	-	1 (7.69%)	4 (30.77%)	3 (23.08%)	2 (15.38%)	3 (23.08%)
CR	-	-	1 (11.11%)	7 (77.78%)	1 (11.11%)	-
H	-	2 (7.69%)	9 (34.62%)	3 (11.54%)	3 (11.54%)	9 (34.62%)
P	-	1 (3.85%)	8 (30.77%)	6 (23.08%)	4 (15.38%)	7 (26.92%)
Q	-	2 (22.22%)	2 (22.22%)	2 (22.22%)	1 (11.11%)	2 (22.22%)
SC	-	-	-	-	-	-
SCA	-	1 (8.33%)	3 (25.00%)	4 (33.33%)	3 (25.00%)	1 (8.33%)
S	-	4 (12.12%)	10 (30.30%)	11 (33.33%)	4 (12.12%)	4 (12.12%)
SW	-	3 (6.98%)	8 (18.60%)	7 (16.28%)	2 (4.65%)	23 (53.49%)
SWA	-	3 (18.75%)	4 (25.00%)	3 (18.75%)	2 (12.50%)	4 (25.00%)
FB	-	2 (9.52%)	4 (19.04%)	3 (14.29%)	3 (14.29%)	9 (42.86%)
AC	-	1 (7.69%)	1 (7.69%)	5 (38.46%)	4 (30.77%)	2 (15.38%)
A	-	2 (11.11%)	6 (33.33%)	7 (38.89%)	3 (16.67%)	-

*Percentage of the number of microplastic particles in the sample is given in brackets Z, bulk tank; RM, raw milk acceptance; F, filtration; C, clarification; W, water; WA, water addition; CR, cream; H, homogenization; P, pasteurization; Q, holder; SC, ready-to-use starter culture; SCA, starter culture addition; S, salt; SW, salty water; SWA, salty water addition; FB, filtration before filling; AC, filling ayran cups; A, ready-to-drink ayran.

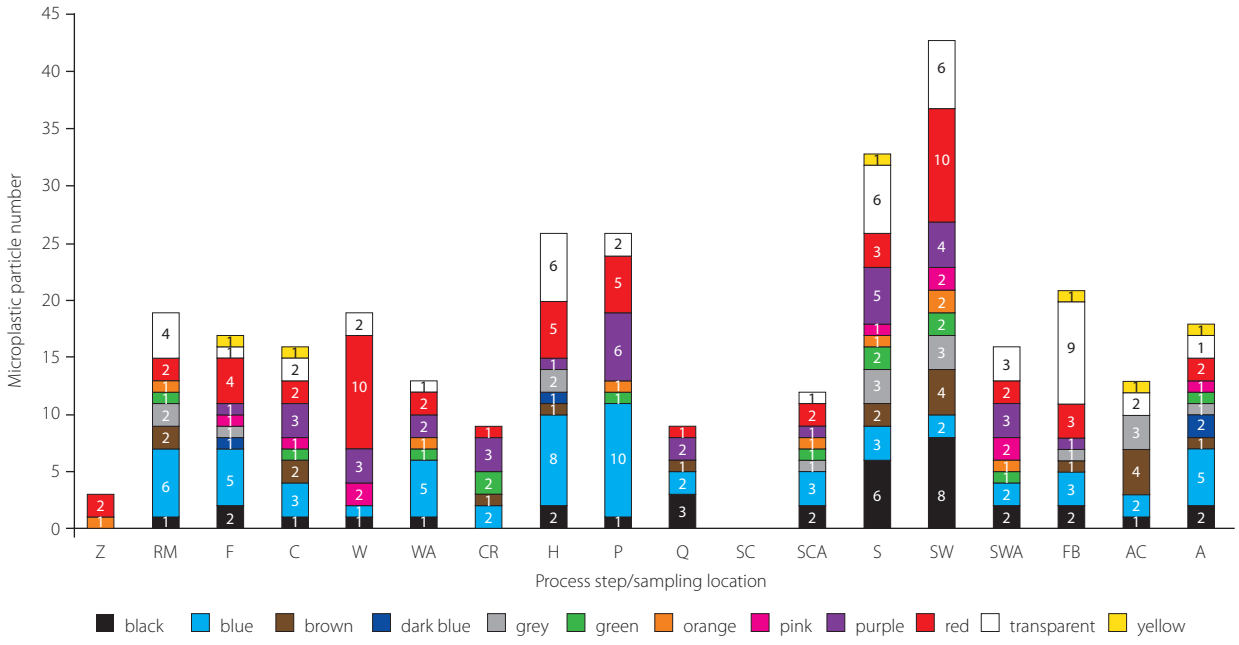

Figure 4. Number of microplastic particles with different colour in samples collected during ayran production at different process steps/sampling locations: Z, bulk tank; RM, raw milk acceptance; F, filtration; C, clarification; W, water; WA, water addition; CR, cream; H, homogenization; P, pasteurization; Q, holder; SC, ready-to-use starter culture; SCA, starter culture addition; S, salt; SW, salty water; SWA, salty water addition; FB, filtration before filling; AC, filling ayran cups; A, ready-to-drink ayran.

Table 3. Number of microplastic particles (MP) with different shapes and microplastic polymer type in samples collected during ayran production at different process steps/sampling locations (MP number/100 mL or MP number/100 g).

Polymer type	Polymer shape	Z	RM	F	C	W	WA	CR	H	P	Q	SC	SCA	S	SW	SWA	FB	AC	A
EP (39.30%)*	Fibre	1	7	6	5	5	8	8	6	16	1	0	2	8	8	4	10	2	5
	Film	–	1	–	1	–	–	–	1	–	–	–	–	–	1	1	–	1	–
	Fragment	–	1	–	–	–	–	1	6	1	1	–	–	1	–	–	–	1	2
	Sphere	–	–	–	–	–	–	–	–	–	–	–	–	–	–	–	1	–	–
NP (10.22%)	Fibre	–	1	–	–	–	–	–	–	–	–	–	–	–	–	–	–	–	–
	Film	–	2	–	–	–	1	–	1	1	1	–	1	–	–	1	1	1	3
	Fragment	–	–	–	–	1	–	–	–	–	1	–	–	–	1	–	–	1	2
	Sphere	–	1	1	–	–	–	–	–	–	1	–	–	3	4	1	1	–	–
PA (3.19%)	Fibre	–	–	–	–	–	–	–	–	1	1	–	1	1	–	–	2	–	1
	Film	–	–	–	–	1	–	–	–	–	–	–	–	1	–	–	–	–	–
	Fragment	–	–	–	–	–	–	–	–	–	–	–	–	–	–	–	–	–	–
	Sphere	–	–	–	1	–	–	–	–	–	–	–	–	–	–	–	–	–	–
PAM (11.18%)	Fibre	–	1	1	1	–	–	–	2	–	1	–	2	3	4	2	1	2	1
	Film	–	–	–	–	–	–	–	2	–	–	–	1	3	4	1	1	2	–
	Fragment	–	–	–	–	–	–	–	–	–	–	–	–	–	–	–	–	–	–
	Sphere	–	–	–	–	–	–	–	–	–	–	–	–	–	–	–	–	–	–
PE (2.88%)	Fibre	–	–	–	–	–	–	–	–	–	–	–	–	–	–	–	–	–	–
	Film	–	–	–	–	–	–	–	1	–	–	–	–	–	–	–	–	–	–
	Fragment	–	–	–	–	–	–	–	–	–	–	–	–	–	–	–	–	–	–
	Sphere	–	1	1	–	–	–	–	1	–	–	–	1	2	1	1	–	–	–
PP (7.35%)	Fibre	–	–	2	1	1	1	–	3	3	1	–	1	2	2	1	1	1	–
	Film	–	–	–	–	–	–	–	–	–	–	–	–	–	3	–	–	–	–
	Fragment	–	–	–	–	–	–	–	–	–	–	–	–	–	–	–	–	–	–
	Sphere	–	–	–	–	–	–	–	–	–	–	–	–	–	–	–	–	–	–
PTFE (25.88%)	Fibre	–	–	–	5	–	–	–	–	–	–	–	–	–	–	–	–	–	–
	Film	–	2	3	1	5	1	–	1	2	1	–	1	4	7	2	1	1	2
	Fragment	2	–	3	1	5	1	–	1	1	–	–	2	2	4	1	1	1	1
	Sphere	–	2	–	–	1	1	–	1	1	–	–	–	3	4	1	1	–	1

*Percentage of the number of microplastic particles in the sample is given in brackets; EP, ethylene propylene; NP, neoprene; PA, polyamide; PAM, polyacrylamide; PE, polyethylene; PP, polypropylene; PTFE, polytetrafluoroethylene; Z, bulk tank; RM, raw milk acceptance; F, filtration; C, clarification; W, water; WA, water addition; CR, cream; H, homogenization; P, pasteurization; Q, holder; SC, ready-to-use starter culture; SCA, starter culture addition; S, salt; SW, salty water; SWA, salty water addition; FB, filtration before filling; AC, filling ayran cups; A, ready-to-drink ayran.

come into contact with tools, equipment, materials, packaging materials. This data is valuable to identify the source of food contamination [Nady, 2016; Pouliot, 2008; Tan & Rodrigue, 2019]. In our study, the FTIR data of microplastics (discussed below) revealed that colour would not be a sufficient clue for chemical characterisation. The colour detected under a microscope may depend on the colour pigments and additives used in producing plastic materials; it cannot be associated with the type of polymer [Oßmann *et al.,* 2018].

The FTIR technique used to identify microplastic particles through microscopic imaging detects the FTIR absorption spectrum, reveals the structural fingerprints, and reflects the optical responses of the surface functional groups. In this method, the spectra formed by the absorbance values of the displayed microplastic particles were compared to the spectra of reference polymers in the polymer library [Fan *et al.*, 2021]. The examples of FTIR spectra of MP of samples and reference polymers are given in Figure 5. Seven types

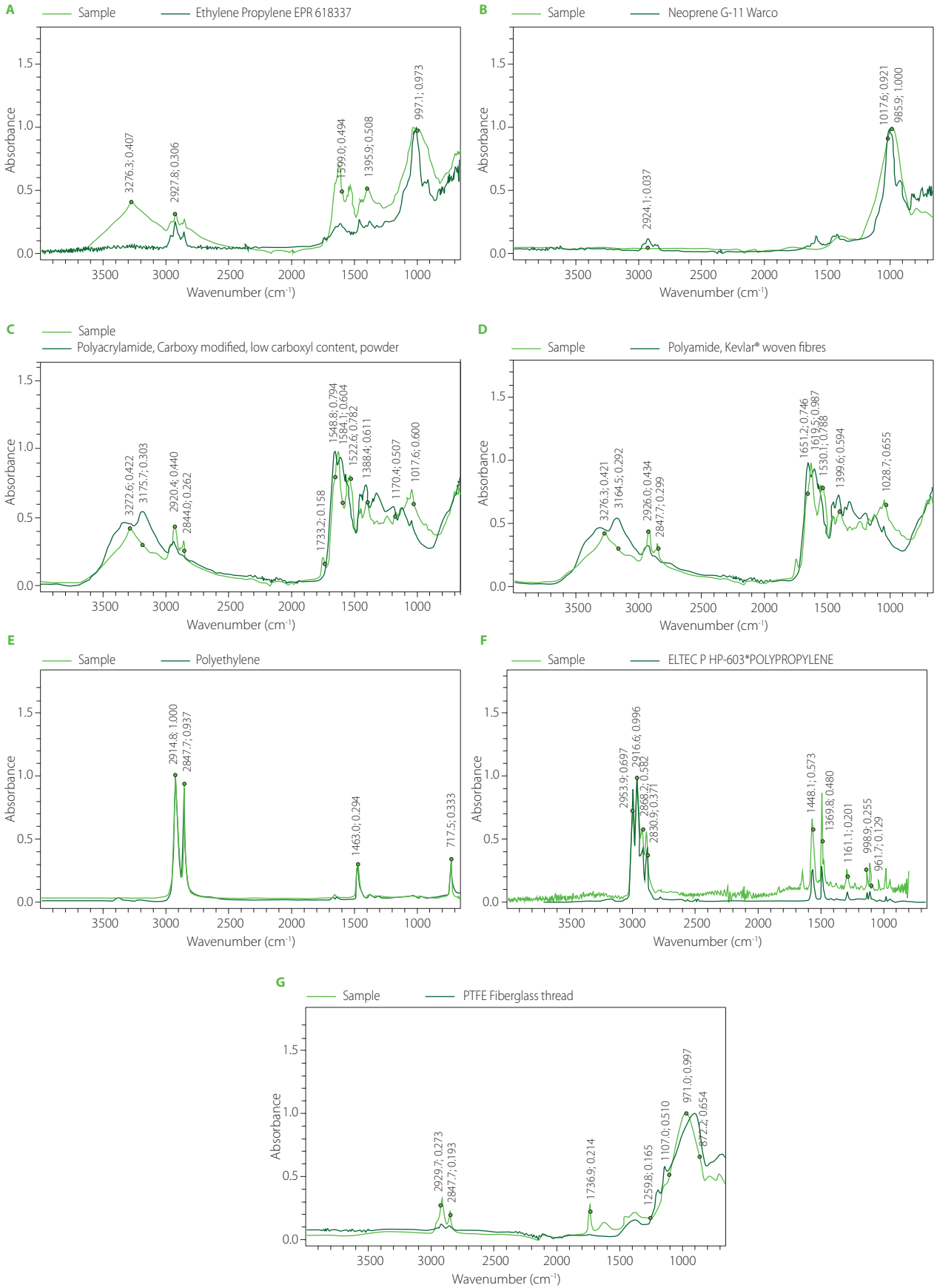

Figure 5. Fourier-transform infrared spectroscopy (FTIR) spectra of microplastic particles of samples collected during ayran production and reference polymers: (**A**) ethylene propylene, (**B**) neoprene, (**C**) polyacrylamide, (**D**) polyamide, (**E**) polyethylene, (**F**) polypropylene, and (**G**) polytetrafluoroethylene.

of microplastics were identified by FTIR in the samples: ethylene propylene (EP) (39.30%), polytetrafluoroethylene (PTFE) (25.88%), polyamide (PA) (11.18%), neoprene (NP) (10.22%), polypropylene (PP) (7.35%), polyacrylamide (PAM) (3.19%), and polyethylene (PE) (2.88%). FTIR analysis revealed that black microplastics were neoprene, polyamide, and polyacrylamide; blues were EP and PE; browns were PTFE, PP and PAM; dark blues were NP, EP, and PE; greys were NP, PA, and PAM; greens were EP; oranges were PTFE; pinks were PTFE and PP; pink and red ones were PTFE and PP; purples were EP, PAM, PA, PP, and PTFE; transparent were EP, NP, PAM, and PA; yellows were PAM and PTFE. The EP, which was identified in the samples of our study, is used as an air and water-sealing gasket; neoprene is used as an oil-sealing gasket in dairy facilities. PAM finds use in agricultural lands for erosion control and improving the physical properties of the soil. Very small amounts of PAM in irrigation water were reported to flow over the soil in irrigation troughs, virtually eliminating the separation and transport of soil particles [Sojka *et al.*, 2007]. PTFE, which is very common in the environment, is seen in milk as a sign of environmental contamination. A series of macro-, micro- and ultrafiltration processes using polymeric membranes, from the milking process to the packaging of the products, can be considered a source of PTFE [Diaz-Basantes *et al.*, 2020; Kutralam-Muniasamy *et al.*, 2020]. PAs replace metal parts in engine components as tough, corrosion-resistant, lighter, and more cost-effective intake manifolds. They are also used as an alternative insulation material for electrical cables. Reinforcing polyamides with typically 30% glass fibres makes them so resilient that they can be used as a metal substitute. In this form, they can be used as building elements. Additionally, they can also be preferred as packaging materials. In wastewater treatment plants, PE is used to produce tanks, equipment, pumps, valves, diaphragms, bellows, and cylinders. Additionally, moving machine parts, toothed wheel rollers, sliding equipment, and conveyor equipment construction are its other uses in the food industry. PP is used in producing beverage containers and bottles in various shapes and capacities. Also, it is a polymer used to preserve cleaning agents, disinfectants and chemical reagents [Pouzada, 2021].

The EDI, which shows the number of microplastics that can be daily swallowed with ayran, was calculated according to the Turkish Nutrition Guide [TNG, 2015]. It was estimated that adults could consume 259±2 MP number/day, and children, adolescents, pregnant-breastfeeding women, and postmenopausal women from 173±14 to 346±7 MP number/day. The risk assessment reveals the total amount of microplastics ingested and the physical distribution of microplastics in the human body. It excludes toxicological hazards associated with the composition of polymers, bacterial film formation on the surface of microplastics, and possible microbiological considerations such as the presence of viruses. It does not indicate ingested microplastic's faecal excretion rate and the intestinal epithelium translocation rate. In a meta-analysis study based on 402 data points from 26 articles representing more than 3,600 processed food samples, Cox *et al.* [2019] calculated total annual microplastic ingestion by age and body weight to range between 39,000 and 52,000 particles. When inhalation exposure was included, this number has been estimated to range between 74,000 and 121,000. Additionally, they had estimated that people who consume only bottled water are exposed to 90,000 microplastics, compared to 4,000 microplastics for those who consume the recommended amount of water by drinking tap water. Pérez-Guevara *et al.* [2022] estimated that Mexico City residents accidentally ingested 42 MP/L through drinking water, with annual exposures of approximately 1.47×10^4 MP *per* adult and 6.73×10^3 MP *per* child. In another study examining the potential exposure of infants to PP microplastics through the consumption of formulas prepared in infant feeding bottles, the exposure ranged from 14,600 to 4,550,000 (mean 1,580,000) microplastics/day *per* baby, depending on the sampling geographic location. Scenario studies revealed that sterilization and exposure to high temperature water of PP infant bottles significantly increased the release of microplastics. Considering that adults were estimated to consume 600 microplastics *per* day through water, food, and air, they have determined that infants were exposed to approximately 2,600 times more microplastics *per* day than adults [Li *et al.*, 2020].

CONCLUSIONS

Studies have revealed the risk of microplastic contamination in the production line of ayran of a medium-sized production facility. Microplastic particles have been detected at each step of production, in raw materials, auxiliary materials, semi-finished materials, and final product. The microplastic particles in the samples collected at different process steps/sampling locations varied in size, colour, shape, and polymer type. Contamination of ayran cups, water, and salt with microplastics was quite severe. Water and salt in food production should be pre-treated with special pore-sized filters against microplastics. Before the filling process, some precaution measures against contamination of cups and bottles with microplastics, like pre-washing with microplastic-free ultrapure water, should be taken. Further studies are needed to detect microplastic contamination sources before the raw milk acceptance step. It is necessary to investigate the content of microplastics in other dairy products, and additional data need to be collected on raw milk contamination with plastic residues.

SUPPLEMENTARY MATERIALS

The following are available online at http://journal.pan.olsztyn.pl/Microplastics-in-a-Traditional-Turkish-Dairy-Product-Ayran,163061,0,2.html; Table S1. The source of positive control materials. Table S2. Colour, shape, and size distribution of positive control samples.

RESEARCH FUNDING

This study was funded by the Scientific Research Projects Coordination Unit of İstanbul University-Cerrahpaşa. Project number: TDK-2021-35711.

CONFLICT OF INTERESTS

The authors declare that there is no conflict of interest.

ORCID IDS

S.K. Buyukunal https://orcid.org/0000-0003-3676-2181
K. Muratoglu https://orcid.org/0000-0001-8705-6813
S. Rbaibi Zipak https://orcid.org/0000-0003-1785-630X

REFERENCES

1. Allan, J., Belz, S., Hoeveler, A., Hugas, M., Okuda, H., Patri, A., Rauscher, H., Silva, P., Slikker, W., Sokull-Kluettgen B., Tong, W., Anklam, E. (2021). Regulatory landscape of nanotechnology and nanoplastics from a global perspective. *Regulatory Toxicology and Pharmacology*, *122*, art. no. 104885. https://doi.org/10.1016/j.yrtph.2021.104885
2. Andrady, A.L. (2017). The plastic in microplastics: A review. *Marine Pollution Bulletin*, *119*(1), 12–22. https://doi.org/10.1016/j.marpolbul.2017.01.082
3. Britz, T., Robinson, R.K. (2008). *Advanced Dairy Science and Technology*. 1st edition. Blackwell Publishing Ltd, Oxford, UK. https://doi.org/10.1002/9780470697634
4. Caramia, M., Guerriero, F. (2010). A milk collection problem with incompatibility constraints. *INFORMS Journal on Applied Analytics*, *40*(2), 130–143. https://doi.org/10.1287/inte.1090.0475
5. Chae, D.-H., Kim, I.-S., Kim, S.-K., Song, Y.K., Shim, W.J. (2015). Abundance and distribution characteristics of microplastics in surface seawaters of the Incheon/Kyeonggi coastal region. *Archives of Environmental Contamination and Toxicology*, *69*(3), 269–278. https://doi.org/10.1007/s00244-015-0173-4
6. Chang, X., Xue, Y., Li, J., Zou, L., Tang, M. (2020). Potential health impact of environmental micro- and nanoplastics pollution. *Journal of Applied Toxicology*, *40*(1), 4–15. https://doi.org/10.1002/jat.3915
7. Chen, G., Feng, Q., Wang, J. (2020). Mini-review of microplastics in the atmosphere and their risks to humans. *Science of The Total Environment*, *703*, art. no. 135504. https://doi.org/10.1016/j.scitotenv.2019.135504
8. Cox, K.D., Covernton, G.A., Davies, H.L., Dower, J.F., Juanes, F., Dudas, S.E. (2019). Human consumption of microplastics. *Environmental Science and Technology*, *53*(12), 7068–7074. https://doi.org/10.1021/acs.est.9b01517
9. Da Costa Filho, P.A., Andrey, D., Eriksen, B., Peixoto, R.P., Carreres, B.M., Ambühl, M.E., Descarrega, J.B., Dubascoux, S., Zbinden, P., Panchaud, A., Poitevin, E. (2021). Detection and characterization of small-sized microplastics (≥ 5 µm) in milk products. *Scientific Reports*, *11*(1), art. no. 24046. https://doi.org/10.1038/s41598-021-03458-7
10. Diaz-Basantes, M.F., Conesa, J.A., Fullana, A. (2020). Microplastics in honey, beer, milk and refreshments in Ecuador as emerging contaminants. *Sustainability*, *12*(14), art. no. 5514. https://doi.org/10.3390/su12145514
11. Dick Vethaak, A., Leslie, H.A. (2016). Plastic debris is a human health issue. *Environmental Science and Technology*, *50*(13), 6825–6826. https://doi.org/10.1021/acs.est.6b02569
12. Dris, R., Gasperi, J., Saad, M., Mirande, C., Tassin, B. (2016). Synthetic fibers in atmospheric fallout: A source of microplastics in the environment? *Marine Pollution Bulletin*, *140*(1–2), 290–293. https://doi.org/10.1016/j.marpolbul.2016.01.006
13. Dubaish, F., Liebezeit, G. (2013). Suspended microplastics and black carbon particles in the Jade system, southern North Sea. *Water, Air, and Soil Pollution*, *224*(2), art. no. 1352. https://doi.org/10.1007/s11270-012-1352-9
14. EFSA Panel on Contaminants in the Food Chain (CONTAM) (2016). Presence of microplastics and nanoplastics in food, with particular focus on seafood. *EFSA Journal*, *14*(6), art. no. e04501. https://doi.org/10.2903/j.efsa.2016.4501
15. Fan, C., Huang, Y.-Z., Lin, J.-N., Li, J. (2021). Microplastic constituent identification from admixtures by Fourier-transform infrared (FTIR) spectroscopy: The use of polyethylene terephthalate (PET), polyethylene (PE), polypropylene (PP), polyvinyl chloride (PVC) and nylon (NY) as the model constituents. *Environmental Technology and Innovation*, *23*, art. no. 101798. https://doi.org/10.1016/j.eti.2021.101798
16. Fournier, E., Etienne-Mesmin, L., Grootaert, C., Jelsbak, L., Syberg, K., Blanquet-Diot, S., Mercier-Bonin, M. (2021). Microplastics in the human digestive environment: A focus on the potential and challenges facing *in vitro* gut model development. *Journal of Hazardous Materials*, *415*, art. no. 125632. https://doi.org/10.1016/j.jhazmat.2021.125632
17. Frias, J.P.G.L., Nash, R. (2019). Microplastics: Finding a consensus on the definition. *Marine Pollution Bulletin*, 138, 145–147. https://doi.org/10.1016/j.marpolbul.2018.11.022
18. Gündoğdu, S. (2018). Contamination of table salts from Turkey with microplastics. *Food Additives and Contaminants: Part A*, *35*(5), 1006–1014. https://doi.org/10.1080/19440049.2018.1447694
19. Huang, Y., Chapman, J., Deng, Y., Cozzolino, D. (2020). Rapid measurement of microplastic contamination in chicken meat by mid infrared spectroscopy and chemometrics: A feasibility study. *Food Control*, *113*, art. no. 107187. https://doi.org/10.1016/j.foodcont.2020.107187
20. Hwang, J., Choi, D., Han, S., Jung, S.Y., Choi, J., Hong, J. (2020). Potential toxicity of polystyrene microplastic particles. *Scientific Reports*, *10*(1), art. no. 7391. https://doi.org/10.1038/s41598-020-64464-9
21. Kannan, K., Vimalkumar, K. (2021). A review of human exposure to microplastics and insights into microplastics as obesogens. *Frontiers in Endocrinology*, *12*, art. no. 724989. https://doi.org/10.3389/fendo.2021.724989
22. Kedzierski, M., Lechat, B., Sire, O., Le Maguer, G., Le Tilly, V., Bruzaud, S. (2020). Microplastic contamination of packaged meat: Occurrence and associated risks. *Food Packaging and Shelf Life*, *24*, art. no. 100489. https://doi.org/10.1016/j.fpsl.2020.100489
23. Kosuth, M., Mason, S.A., Wattenberg, E.V. (2018). Anthropogenic contamination of tap water, beer, and sea salt. *PLoS One*, *13*(4), art. no. e0194970. https://doi.org/10.1371/journal.pone.0194970
24. Kumar, P., Sharma, N., Ranjan, R., Kumar, S., Bhat, Z.F., Jeong, D.K. (2013). Perspective of membrane technology in dairy industry: A review. *Asian-Australasian Journal of Animal Sciences*, *26*(9), 1347–1358. https://doi.org/10.5713/ajas.2013.13082
25. Kutralam-Muniasamy, G., Pérez-Guevara, F., Elizalde-Martínez. I., Shruti, V.C. (2020). Branded milks – are they immune from microplastics contamination? *Science of The Total Environment*, *714*, art. no. 136823. https://doi.org/10.1016/j.scitotenv.2020.136823
26. Li, D., Shi, Y., Yang, L., Xiao, L., Kehoe, D.K., Gun'ko, Y.K., Boland, J.J., Wang, J.J. (2020). Microplastic release from the degradation of polypropylene feeding bottles during infant formula preparation. *Nature Food*, *1*, 746–754. https://doi.org/10.1038/s43016-020-00171-y
27. Liebezeit, G., Liebezeit, E. (2013). Non-pollen particulates in honey and sugar. *Food Additives Contaminants: Part A*, *30*(12), 2136–2140. https://doi.org/10.1080/19440049.2013.843025
28. Liebezeit, G., Liebezeit, E. (2015). Origin of synthetic particles in honeys. *Polish Journal of Food and Nutrition Sciences*, *65*(2), 143–147. https://doi.org/10.1515/pjfns-2015-0025
29. Lopes, A.C., Stamford, T.L. (1997). Critical control points in the pasteurized milk processing fluxogram. *Archivos Latinoamericanos de Nutrición*, *47*(4), 367–371 (in Portuguese, English abstract).
30. Lu, L., Wan, Z., Luo, T., Fu, Z., Jin, Y. (2018). Polystyrene microplastics induce gut microbiota dysbiosis and hepatic lipid metabolism disorder in mice. *Science of The Total Environment*, *631–632*, 449–458. https://doi.org/10.1016/j.scitotenv.2018.03.051
31. Mariano, S., Tacconi, S., Fidaleo, M., Rossi, M., Dini, L. (2021). Micro and nanoplastics identification: Classic methods and innovative detection techniques. *Frontiers in Toxicology*, *3*, art. no. 636640. https://doi.org/10.3389/ftox.2021.636640
32. Mason, S.A., Welch, V.G., Neratko, J. (2018). Synthetic polymer contamination in bottled water. *Frontiers in Chemistry*, 6, art. no. 407. https://doi.org/10.3389/fchem.2018.00407
33. Millburn, P., Smith, R.L., Williams, R.T. (1967). Biliary excretion of foreign compounds. Biphenyl, stilboestrol and phenolphthalein in the rat: Molecular weight, polarity and metabolism as factors in biliary excretion. *Biochemical Journal*, *105*(3), 1275–1281. https://doi.org/10.1042/bj1051275
34. Nady, N. (2016). PES surface modification using green chemistry: New generation of antifouling membranes. *Membranes*, *6*(2), art. no. 23. https://doi.org/10.3390/membranes6020023
35. Nuelle, M.-T., Dekiff, J.H., Remy, D., Fries, E. (2014). A new analytical approach for monitoring microplastics in marine sediments. *Environmental Pollution*, *184*, 161–169. https://doi.org/10.1016/j.envpol.2013.07.027
36. Oßmann, B.E., Sarau, G., Holtmannspötter, H., Pischetsrieder, M., Christiansen, S.H., Dicke, W. (2018). Small-sized microplastics and pigmented particles in bottled mineral water. *Water Research*, *141*, 307–316. https://doi.org/10.1016/j.watres.2018.05.027
37. Pérez-Guevara, F., Roy, P.D., Elizalde-Martínez, I., Kutralam-Muniasamy, G., Shruti, V.C. (2022). Human exposure to microplastics from urban decentralized pay-to-fetch drinking-water refill kiosks. *Science of The Total Environment*, *848*, art. no. 157722. https://doi.org/10.1016/j.scitotenv.2022.157722
38. Pouliot, Y. (2008). Membrane processes in dairy technology — From a simple idea to worldwide panacea. *International Dairy Journal*, *18*(7), 735–740. https://doi.org/10.1016/j.idairyj.2008.03.005

39. Pouzada, A.S. (2021). Development of plastic products. In A.S. Pouzada (Ed) *Design and Manufacturing of Plastics Products: Integrating Traditional Methods with Additive Manufacturing*. 1st edition. William Andrew, Elsevier, Massachusetts, USA, pp. 10-45
40. Prietl, B., Meindl, C., Roblegg, E., Pieber, T.R., Lanzer, G., Fröhlich, E. (2014). Nano-sized and micro-sized polystyrene particles affect phagocyte function. *Cell Biology and Toxicology*, *30*(1), 1–16. https://doi.org/10.1007/s10565-013-9265-y
41. Qiang, L., Cheng, J., Mirzoyan, S., Kerkhof, L.J., Häggblom, M.M. (2021). Characterization of microplastic-associated biofilm development along a freshwater-estuarine gradient. *Environmental Science and Technology*, *55*(24), 16402–16412. https://doi.org/10.1021/acs.est.1c04108
42. Ragusa, A., Svelato, A., Santacroce, C., Catalano, P., Notarstefano, V., Carnevali, O., Papa, F., Rongioletti, M.C.A., Baiocco, F., Draghi, S., D'Amore, E., Rinaldo, D., Matta, M., Giorgini, E. (2021). Plasticenta: First evidence of microplastics in human placenta. *Environment International*, *146*, art. no. 106274. https://doi.org/10.1016/j.envint.2020.106274
43. Rodriguez-Seijo A., Pereira R. (2017). In T.A. Rocha-Santos, A.C. Duarte (Eds) *Characterization and Analysis of Microplastics*. 1st edition. Elsevier, Massachusetts, USA, pp. 49-66.
44. Schymanski, D., Goldbeck, C., Humpf, H.-U., Fürst, P. (2018). Analysis of microplastics in water by micro-Raman spectroscopy: Release of plastic particles from different packaging into mineral water. *Water Research*, *129*, 154–162. https://doi.org/10.1016/j.watres.2017.11.011
45. Shruti, V.C., Pérez-Guevara, F., Elizalde-Martínez, I., Kutralam-Muniasamy, G. (2020). First study of its kind on the microplastic contamination of soft drinks, cold tea and energy drinks – Future research and environmental considerations. *Science of The Total Environment*, *726*, art. no. 138580. https://doi.org/10.1016/j.scitotenv.2020.138580
46. Sojka, R.E., Bjorneberg, D.L., Entry, J.A., Lentz, R.D., Orts, W.J. (2007). Polyacrylamide in agriculture and environmental land management. *Advances in Agronomy*, 92, 75–162. https://doi.org/10.1016/S0065-2113(04)92002-0
47. Song, K., Ding, R., Sun, C., Yao, L., Zhang, W. (2021). Microparticles and microplastics released from daily use of plastic feeding and water bottles and plastic injectors: potential risks to infants and children in China. *Environmental Science and Pollution Research*, *28*(42), 59813–59820. https://doi.org/10.1007/s11356-021-14939-7
48. Street, M.E., Bernasconi, S. (2021). Microplastics, environment and child health. *Italian Journal of Pediatrics*, *47*(1), art. no. 75. https://doi.org/10.1186/s13052-021-01034-3
49. Tan, X., Rodrigue, D. (2019). A review on porous polymeric membrane preparation. Part II: Production techniques with polyethylene, polydimethylsiloxane, polypropylene, polyimide, and polytetrafluoroethylene. *Polymers*, *11*(8), art. no. 1310. https://doi.org/10.3390/polym11081310
50. TNG (Turkey Nutrition Guide) (2015). Ministry of Health Public Health Agency of Turkey, Ankara, Turkey ISBN: 978-975-590-608-9.
51. Tomasula, P.M., Bonnaillie, L.M. (2015). Crossflow Microfiltration in the Dairy Industry. In N. Datta, P. Tomasula (Eds.), *Emerging Dairy Processing Technologies*, John Wiley & Sons Ltd, Chichester, UK, pp. 1–32. https://doi.org/10.1002/9781118560471.ch1
52. Toussaint, B., Raffael, B., Angers-Loustau, A., Gilliland, D., Kestens, V., Petrillo, M., Rio-Echevarria, I.M., Van den Eede, G. (2019). Review of micro- and nanoplastic contamination in the food chain. *Food Additives and Contaminants: Part A*, *36*(5), 639–673. https://doi.org/10.1080/19440049.2019.1583381
53. TSI (2013). *TS 6800 Ayran*. Turkish Standards Institution, 5ss, Ankara, Turkey.
54. Walstra, P., Wouters, J.T.M., Geurts, T.J. (2005). Processes. In P. Walstra., J.T.M. Wouters, T.J. Geurts (Eds), *Dairy Science and Technology*. 2nd edition, CRC Press Inc., Boca Raton, Florida, USA, pp. 207-417. https://doi.org/10.1201/9781420028010
55. Waring, R.H., Harris, R.M., Mitchell, S.C. (2018). Plastic contamination of the food chain: A threat to human health? *Maturitas*, *115*, 64–68. https://doi.org/10.1016/j.maturitas.2018.06.010
56. Wang, W., Ndungu, A.W., Li, Z., Wang, J. (2017). Microplastics pollution in inland freshwaters of China: A case study in urban surface waters of Wuhan, China. *Science of The Total Environment*, *575*, 1369–1374. https://doi.org/10.1016/j.scitotenv.2016.09.213
57. Wiesheu, A.C., Anger, P.M., Baumann, T., Niessner, R., Ivleva, N.P. (2016). Raman microspectroscopic analysis of fibers in beverages. *Analytical Methods*, *8*(28), 5722–5725. https://doi.org/10.1039/C6AY01184E
58. Yang, B., Lee, C., Xiang, W., Xie, J., He, J.H., Kotlanka, R.K., Low, S.P., Feng, H. (2009). Electromagnetic energy harvesting from vibrations of multiple frequencies. *Journal of Micromechanics and Microengineering*, *19*(3), art. no. 035001. https://doi.org/10.1088/0960-1317/19/3/035001
59. Yong, C.Q.Y., Valiyaveettil, S., Tang, B.L. (2020). Toxicity of microplastics and nanoplastics in mammalian systems. *International Journal of Environmental Research and Public Health*, *17*(5), art. no. 1509. https://doi.org/10.3390/ijerph17051509

ORIGINAL ARTICLE
http://journal.pan.olsztyn.pl

Polish Journal of Food and Nutrition Sciences
2023, Vol. 73, No. 2, 151–162
DOI: 10.31883/pjfns/163554
ISSN 1230-0322, e-ISSN 2083-6007

Proposed Use of a Polyvinyl Alcohol with Grape Pomace Extract as an Edible Coating for Strawberries

Gülce B. Kaynarca[1], Deniz D.A. Kamer[2], Emel Yücel[2], Tuncay Gümüş[2]*

[1]Department of Food Engineering, Faculty of Engineering, Kirklareli University, 39100 Kirklareli, Turkey
[2]Department of Food Engineering, Faculty of Agriculture, Tekirdag Namik Kemal University, 59030 Tekirdag, Turkey

Strawberries rich nutrition, flavor, and aroma profiles make them popular. Many studies have tried to extend strawberries shelf life. In the current study, grape pomace extract (GPE) was combined with polyvinyl alcohol (PVA) and used to extend the shelf life of strawberries. Ascorbic acid content, total phenolic content, total anthocyanin content, and antioxidant activity determinations showed that PVA/GPE-coated strawberries were superior to the uncoated fruits during storage. Total mesophilic aerobic bacteria (TMAB) and yeast/mold counts in the uncoated strawberries were 2 and 2.68 log cfu/g at the start of storage, respectively, and 9.8 and 14.00 log cfu/g after 16 days of storage, respectively. Strawberries coated with the PVA solution with 2.5% (*w/v*) GPE showed 32% and 25% less TMAB and yeast/mold counts, respectively, at the end of storage. The PVA/GPE-coated strawberries showed significantly higher firmness compared to the control fruit. The PVA/GPE coating improved strawberry shelf life and functional properties.

Key words: strawberry preservation, PVA, grape pomace extract, edible coating, fungal control

ABBREVIATIONS

PVA, polyvinyl alcohol; EMA, European Medicine Agency; FDA, United States Food and Drug Administration; GP, grape pomace; GPE, grape pomace extract; TSS, total soluble solids; TA, titratable acidity; TPC, total phenolic content; ABTS, 2,2′-azino-bis-3-ethylbenzothiazoline-6-sulfonic acid; DPPH•, 1,1-diphenyl--2-picrylhydrazyl radical, PBS, potassium persulphate solution; TEAC, Trolox-equivalent antioxidant capacity; TAC, total anthocyanin content; TMAB, total aerobic mesophilic bacteria; PCA, plate count agar; PDA, potato dextrose agar.

INTRODUCTION

A third of the world's food production is lost every year, and about 22% of this loss consists of remnants from fruits and vegetables [Ueda *et al.*, 2022]. Fruits and vegetables are difficult to keep fresh for both markets and consumers because they are easily perishable. Therefore, protection can be provided with the use of edible coatings or other postharvest technologies, which can prevent respiration and oxidation reactions [Duarte & Picone, 2022]. Berries, such as raspberries, blueberries and strawberries have a short shelf life and require appropriate technology to maintain or extend their shelf life [Jafarzadeh *et al.*, 2021].

Strawberry (*Fragaria×ananassa*) is also called the "queen of fruits" due to its unique taste and flavor and is one of the most consumed fruits worldwide [Riaz *et al.*, 2021]. The worldwide demand for strawberries has increased by more than 80% in recent decades with production exceeding 9 million tons [Kaur & Kumar, 2022]. Strawberries are rich in minerals, dietary fiber, vitamins, flavonoids (including anthocyanins), ellagitannins and proanthocyanidins [Giampieri *et al.*, 2012]; however, their shelf life is limited to 4–5 days under refrigerating conditions [Khodaei *et al.*, 2021]. They feature poor storage potential due to their sensitive

***Corresponding Author:**
tel.: +90 282 250 21 59; e-mail: tgumus@nku.edu.tr (T. Gumus)

Submitted: 31 December 2022
Accepted: 24 April 2023
Published on-line: 25 May 2023

structure that is weak to impact, their high respiratory and transpiration rates, and sensitivity to fungal spoilage, especially *Botrytis cinerea* [Matar *et al.*, 2020]. Freeze-drying and fungicides are widely used to extend the shelf life of strawberries, but these methods are not sustainable because they are costly and cause the formation of residues [Liu *et al.*, 2021].

Edible coatings have been used for food preservation for twelve centuries, and are still of great interest to researchers today due to their protective properties. The term "edible coating" refers to a thin layer of an edible substance that is applied on the surface of food products in the form of a liquid. Its main purpose is to act as a moisture barrier and protect the product from potential harm caused by mechanical damage and chemical reactions [Pavlath & Orts, 2009]. Edible coatings are applied directly on the product surface by spraying, brushing, or dipping to form a modified atmosphere [Armghan Khalid *et al.*, 2022]. Edible coatings are usually biodegradable products that are obtained from various polymers such as proteins, polysaccharides and essential oils and combinations thereof [Riaz *et al.*, 2021]. Active packaging systems with low water vapor and oxygen permeability and the presence of antioxidants and antimicrobials play an important role in minimizing the rate of respiration and maturation, limiting microbial activity and controlling water loss, thereby preserving the freshness of post-harvest crops [Jafarzadeh *et al.*, 2021].

Polyvinyl alcohol (PVA) is a biodegradable, water soluble, edible, non-toxic, film-forming environmentally-friendly polymer with high mechanical properties. Its use in food applications as a packaging and coating material has been approved by the European Medicine Agency (EMA) and the United States Food and Drug Administration (FDA) [Moreira *et al.*, 2020]. It is also relatively inexpensive compared to other synthetic polymers [Ren *et al.*, 2020]. The specific microstructural arrangement of polymeric matrices and the ability to incorporate active ingredients into its structure makes PVA an ideal component for the development of biodegradable active food packaging [Andrade *et al.*, 2021]. Previous studies have reported the use of PVA/chitosan-based coatings to successfully enhance the storage period of strawberries [Ding *et al.*, 2019; Liu *et al.*, 2017]. Moreira *et al.* [2020] reported that PVA/cashew gum-based coatings could extend the shelf life of strawberries by inhibiting fungal growth.

Natural antimicrobial and antioxidant ingredients are frequently employed in active packaging for food preservation [Parin *et al.*, 2021]. Grape pomace constitutes a major by-product of the winemaking industry. Winemaking by-products and other plant-based agricultural wastes have attracted increasing attention as possible sources of bioactive phenolic compounds in recent years [Makris *et al.*, 2007]. Grape pomace's phenolic profile includes a wide range of compounds, including proanthocyanins and flavan-3-ols like catechin and epicatechin. Moreover, flavonols such as quercetin, laricitrin, and syringetin, and anthocyanins such as malvidin, delphinidin, petunidin, and peonidin were found [Peixoto *et al.*, 2018] The effectiveness of antibacterial activity is closely related to the presence of phenolic compounds and has been reported effective against both Gram-negative and Gram-positive bacteria [Peixoto *et al.*, 2018].

Our previous work showed that grape pomace extract (GPE) and PVA interacted well and formed films with high elasticity [Kamer *et al.*, 2022]. We also determined that these films have low water vapor and oxygen permeability and good mechanical properties [Kaynarca *et al.*, 2023]. To our knowledge, the combination of grape pomace, which is a cheap agricultural-industrial waste, with PVA for the preservation of quality parameters of strawberries has not been reported to date. In the current study, we aimed to increase the preservation time of strawberries with edible PVA coatings combined with GPE at different concentrations (1, 2, and 2.5%, *w/v*). First, the grape pomace was extracted and its antifungal properties were investigated. Next, strawberries were coated with PVA/GPE composite using a dipping method. Finally, the quality parameters and microbial loads were examined during strawberry storage.

MATERIAL AND METHODS

Materials

Grape pomace was obtained as Cabernet Sauvignon winemaking waste from a local winery (Vino Desera Winery) in the Kirklareli province of Turkey. Polyvinyl alcohol (PVA) was supplied by Clearity Chemistry Textile Co., Ltd. (Tekirdag, Turkey). Uniformly sized and shaped strawberries (*Fragaria×ananassa*), exhibiting a surface color intensity of 80% or greater, were procured from a local supplier in Tekirdag, Turkey, soon after being harvested. The strawberries were placed in a cool box after picking and delivered to the laboratory within 1 h. *Botrytis cinerea* 12c, a pathogenic fungus, was obtained from the culture collection of the Department of Plant Protection at Tekirdag Namik Kemal University, Turkey.

Extraction of grape pomace

Grape pomace (GP) was first ground to enable easier extraction, and then incubated with a 1:5 (*w/v*) solution of 70% (*v/v*) ethanol in an orbital shaker (INFORS HT Ecotron, Bottmingen-Basel Switzerland) at 25°C for 48 h [Kaynarca *et al.*, 2022]. The liquids were filtered through paper and the solvent was evaporated in a rotary evaporator (RE 100-PRO, SCI LOGEX, Rocky Hill, CT, USA) at 50–55°C. The extracts of grape pomace were dissolved in distilled water and the solutions were stored at –18°C until use. Our previous research [Kaynarca *et al.*, 2022] details the chemical and mineral composition of GPE, including its phenolic compound contents.

Preparation and formulation of PVA/GPE coating solutions

A solution of polyvinyl alcohol (PVA) with a concentration of 5.0% (*w/v*) was prepared through the dissolution of PVA powder in distilled water at 80°C for 2 h while being stirred. The solution was subsequently cooled to a temperature of approximately 50°C. Aqueous solution of GPE was employed to create a more uniform blend. The dry matter content of GPE was determined to be 16.92%. GPE was added to the PVA solution at concentrations of 1%, 2%, and 2.5% of dry weight of the extract by volume of the solution, and the mixture was stirred for 10 min until it

became homogenous. The mixture was allowed to cool to 25°C before being applied to the strawberries. Coating solutions with added GPE were coded as GPV1, GPV2, GPV2.5, and control, based on the varying mass ratios of GPE.

Application of coating to strawberries

The strawberries underwent a washing process for a duration of 3 min using cool, sterile, distilled water, followed by a subsequent 30-min drying period at a temperature of 20°C. Strawberries that were immersed only in distilled water for 3 min and then left to dry served as the control sample. The other groups of strawberries, labeled as GPV1, GPV2, and GPV2.5, were dipped in a PVA/GPE solution containing varying concentrations of GPE (1%, 2%, and 2.5% (*w/v*), respectively) for 2 min. After coating, the strawberry fruits were drained and dried for 2 h. To perform physicochemical properties, bioactive compound contents, and microbiological analyses of strawberries with different coating applications, 5 strawberries were selected for each analysis set. The strawberries were divided into 5 packages, with each package containing 5 strawberries for analysis on days 0, 4, 8, 12, and 16. This process was repeated three times to conduct the three sets of analyses for each coating application. All strawberries were stored in plastic containers measuring 16×9×5 cm and were refrigerated at 4°C throughout the 16-day analysis period.

Determination of physicochemical characteristics of strawberries

Weight loss

Strawberries were weighed on a digital balance (Isolab, Eschau, Germany) on the first day of the experiment after coating and on 4, 8, 12, and 16 day through the storage period. The percentage of weight loss relative to the initial weight was calculated with Equation 1:

$$\% \text{ Weight loss} = \left(\frac{wi - wf}{wi}\right) \times 100 \quad (1)$$

where: w*i* is the weight measured on the initial day and w*f* is the weight measured on different days of storage.

Total soluble solid content, titratable acidity, and pH

Total soluble solid (TSS) content of strawberry fruit juice was determined at 20°C using a digital refractometer (ATAGO, Tokyo, Japan), with results represented in %. The titratable acidity (TA) was calculated by extracting 10 g fruit in 50 mL of distilled water and titrating the solution with 0.1 M sodium hydroxide until it reached a final pH of 8.1. TA was represented as percentage (%) of citric acid. The acidity of the fruit was measured by a pH meter (HANNA HI2002, HANNA Instruments, Woonsocket, RI, USA). For the chemical analysis, 5 randomly chosen fruits (with a total approximate mass of 30 g) were homogenized with a high-speed mixer and each sample was tested three times.

Texture parameters

The hardness of the strawberries was measured with a texture analyzer (TA-HD plus, Stable Micro Systems, Godalming, Surrey, UK) with a P/36R probe and a crosshead speed of 5 mm/min. Two sets of measurements were made for each replicate on opposite sides of the central zone [Ding *et al.*, 2019]. The values were expressed as Newton (N). Five different strawberries were analyzed for each treatment, and results were given as the mean value.

Color parameter analysis

The skin color of strawberries was measured using a CR-400 Chroma Meter (Konica Minolta Inc., Tokyo, Japan). The chromaticity parameters *L**, *a**, and *b** were used to describe the lightness, the greenness/redness, and the blueness/yellowness, respectively.

Determination of bioactive compound contents and antioxidant activity of strawberries

Ascorbic acid

Strawberries were tested at different times during storage for their ascorbic acid content using the 2,6-dichlorophenol-indophenol (0.25 g/L) titrimetric assay [Vahid, 2012]. Each mL of 2,6-dichlorophenol-indophenol solution was equivalent to 0.2 mg ascorbic acid. Results were expressed as mg of L-ascorbic acid per 100 g of strawberries.

Total phenolic content

Total phenolic content (TPC) was evaluated using the Folin-Ciocalteu reaction. Briefly, strawberries were blended at 1:20 (*w/v*) with 80% (*v/v*) methanol and extracted at 25°C for 24 h. Next, 500 µL of Folin-Ciocalteu reagent were added to 100 µL of each sample. After 2 min, 1 mL of 75 g/L Na_2CO_3 was added, followed by 94 mL of distilled water [Pineli *et al.*, 2011]. After 60 min of incubation in the dark, the absorbance was measured at 760 nm with a Shimadzu 02910 spectrophotometer (Shimadzu, Kyoto, Japan). Pure gallic acid was used to generate a standard curve, and the results were calculated as g of gallic acid equivalents (GAE) *per* kg on a fresh weight basis (g GAE/kg).

Antioxidant activity

Antioxidant activity was evaluated using the 2,2'-azino-bis(3-ethylbenzothiazoline-6-sulfonic) acid radical cation ($ABTS^{\bullet+}$) and 1,1-diphenyl-2-picrylhydrazyl radical ($DPPH^{\bullet}$). Antioxidant activities of the uncoated control fruits and the coated fruits were determined on the first day and throughout the storage period. The extracts of the samples obtained as described above were added to 600 µL of a methanolic solution of DPPH radical (1 mM). The mixture was incubated in the dark for 30 min and the absorbance was measured at 517 nm. The radical scavenging activity was expressed as IC_{50} (as the amount of extract that scavenges 50% of the DPPH radicals, mg/L of reaction mixture) [Yıldırım-Yalçın *et al.*, 2022].

The ABTS assay was conducted as described by Re *et al.* [1999] with some modifications. A stock solution was generated with 7 mM of ABTS in phosphate buffer solution (PBS) with 2.45 mM of potassium persulphate solution ($K_2S_2O_8$) and then allowed to stand at 25°C in the dark for 15–16 h. PBS was used to dilute the stock solution to a final absorbance value of 0.700±0.05.

A Trolox calibration curve was used to calculate Trolox-equivalent antioxidant capacity (TEAC) values expressed as µmol Trolox equivalent *per* kg fresh weight (µmol Trolox/kg).

Total anthocyanin content

The total anthocyanin content (TAC) of strawberries was determined by the pH differential method as described previously [Wrolstad, 1993]. To this end, anthocyanins from the strawberries were extracted using 2% HCl in methanol at a fruit to solvent ratio of 1:5 (*w/v*) for 60 min. The supernatant was taken and filtered through a 0.45 µm filter. The residue left behind in the filter was re-extracted until a clear solution was obtained. The pH of the diluted fruit extracts was adjusted to 1.0 and 4.5 using potassium chloride buffer and sodium acetate buffer, respectively. The absorbance of the diluted samples was recorded at 522 (A_{522}) and 700 nm (A_{700}) using a Shimadzu 02910 spectrophotometer and A value was calculated with Equation 2:

$$A = (A_{522} - A_{700})_{pH1.0} - (A_{522} - A_{700})_{pH4.5} \quad (2)$$

The TAC of the strawberries was calculated on the basis of a molar absorptivity (ε) of 22,400 L/(mol×cm) and molecular weight (MW) of 433.2 g/mol of pelargonidin 3-glucoside (Pg3G) using Equation 3:

$$TAC = \frac{A \times MW \times DF \times 1{,}000}{\varepsilon \times L} \quad (3)$$

where: DF, dilution factor; L, pathlength (L=1 cm).

Microbiological analyses

The total aerobic mesophilic bacteria (TMAB) and total yeast and mold contents for each treatment were analyzed after 0, 4, 8, 12, and 16 days of storage using the spread plate method. Strawberries were homogenized using a Stomacher (Interscience, Saint Nom la Brétèche, France) in a Stomacher bag and then diluted in sterile peptone water. TMAB count was determined after 48 h of incubation at 30°C with the surface plate method on plate count agar (PCA, Merck, Darmstadt, Germany). Yeast and mold counts were determined on potato dextrose agar (PDA, Merck) after incubation for 5 days at 25°C. The microbiological counts of strawberries were expressed as log colony forming units (cfu) *per* g of sample. Three replicates were carried out for each treatment and storage duration.

Determination of bioactive compound contents and functional properties of the coating solution

The total anthocyanin content, antioxidant activity, and total phenolic content of coating solutions were evaluated using the methods detailed in the section titled "*Determination of bioactive compound contents and antioxidant activities of strawberries*."

The antifungal activity of coating solutions with 1%, 2% and 2.5% GPE (*w/v*) was determined according to the method of Bouchra *et al.* [2003] with some modifications. To this end, coating solutions were prepared with ethanol to a final concentration of 2,000 mg/L and then mixed with sterile PDA to obtain final concentrations of 0, 20, 80, 100, 120, and 200 mg/L. *B. cinerea* was first cultured on PDA at 25°C. Petri dishes were inoculated with a mycelial plug (6 mm) of 7-day-old culture of *B. cinerea*. Three replicates on individual Petri dishes were carried out for each treatment. Ethanol was used as a negative control. After 48 h of incubation at 22°C, the inhibition zones were measured. Results of antifungal activity were expressed as IC_{50} (concentration that reduced mycelial growth by 50%) determined by regressing the inhibition of radial growth values (percent control) [Mendoza *et al.*, 2013].

Statistical analysis

All data were statistically analyzed using the SPSS, version 18.0 (SPSS Inc., Chicago, IL, USA). Data was subjected to analysis of variance (ANOVA). Tukey's post hoc test was used to compare the differences in data means. Differences at the level of $p<0.05$ were considered as significant. Experiments were carried out in triplicate.

RESULTS AND DISCUSSION

Physicochemical characteristics of strawberries

Weight loss

Strawberries with PVA/GPE coating and the uncoated control samples both showed a successive weight loss during storage (Figure 1A). The processes of respiration, sweating, and oxidation can cause fruits to lose weight while they are being stored [Ayranci & Tunc, 2003]. Notable differences were found between the control and coated fruits throughout the storage period (Figure 1A). A comparison of the three coatings revealed that the GPV2.5 coating provided the best protection with only 8.26% weight loss during storage after 16 days, compared to 15.03% loss in the control fruits. Lower GPE concentrations of the coating solution were less effective at preventing weight loss. The use of coatings is evidently useful in providing a physical barrier against moisture loss, thereby delaying dehydration and shriveling of the fruit [Fawole *et al.*, 2020].

Total soluble solid content, titratable acidity, and pH

The total soluble solids content of GPV1 and GPV2 samples decreased during the first 4 days of storage, but increased afterwards (Figure 1B). This could be an indication of the transition from optimal ripeness. The initial TSS level was 7.4% in the control fruits and ranged from 7.8 to 8.4% in the coated fruits. It is possible that the presence of water-soluble dry matter in the GPE contributed to the higher initial TSS value obtained with coated strawberries compared to the control group. In contrast to the control fruit, which showed a decrease in TSS content from 7.4 to 5.8% from the 4th to 8th day of storage, fruits coated with GPV1, GPV2, and GPV2.5 showed a progressive increase in TSS content from day 4 to 8. The results of this study align with those of Gol *et al.* [2013], who found that the TSS content of control (uncoated) strawberries decreased from 4 to 8 days of storage, while the TSS content of fruits coated with carboxymethyl cellulose and hydroxypropylmethyl cellulose showed a successive increase until 8 days of storage and then decreased. A breakdown of the cell wall and an increase in dry matter as a result of water

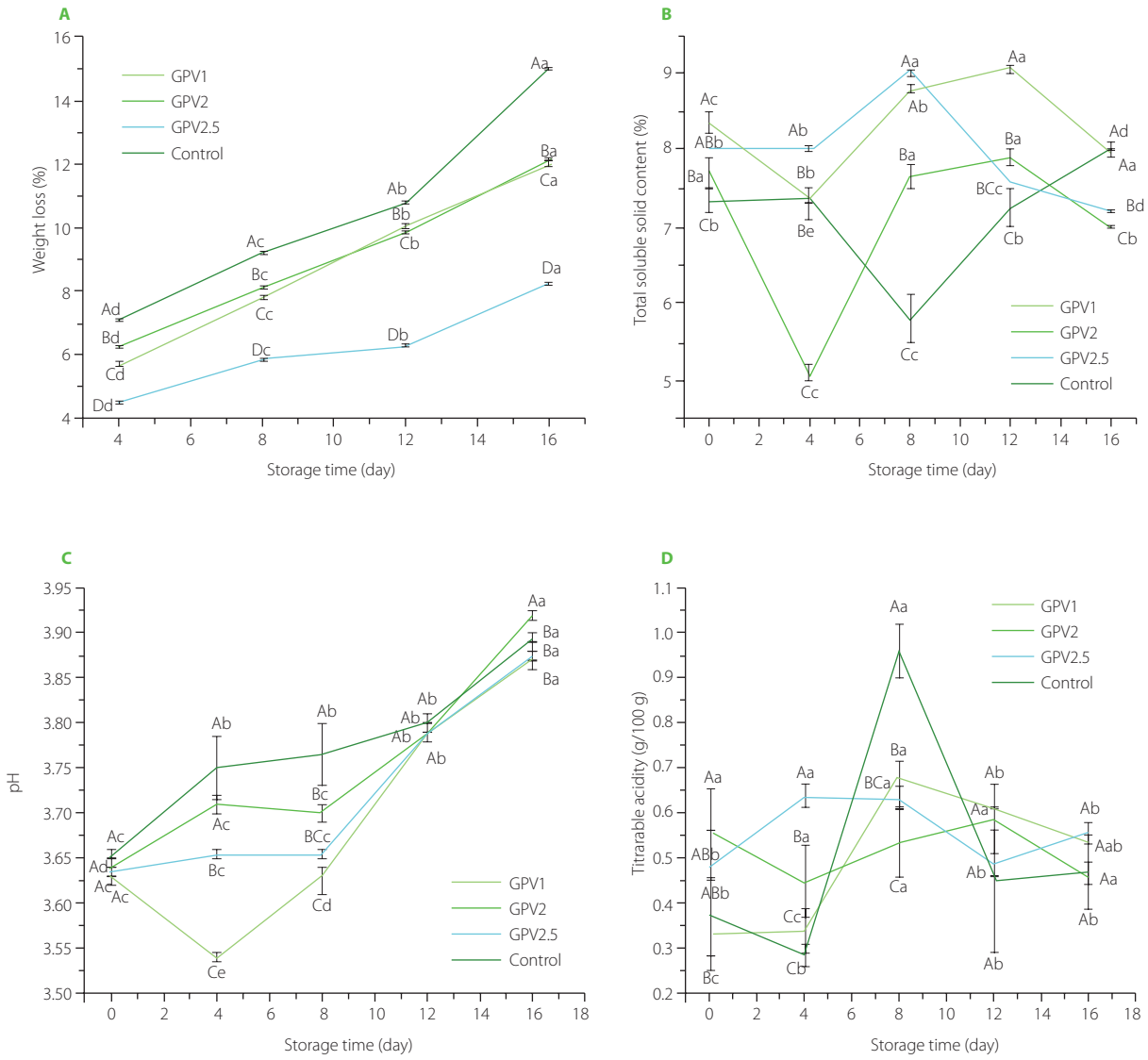

Figure 1. The weight loss, total soluble solid content, pH and titratable acidity of coated by dipping in solution of polyvinyl alcohol with 1%, 2% and 2.5% (*w/v*) grape pomace extract (GPV1, GPV2 and GPV2.5, respectively) and uncoated (control) strawberries during storage at 4°C for 16 days.
Values are given as mean and standard deviation. Different capital letters represent the difference between treatments, different lowercase letters represent the difference between storage times ($p<0.05$).

loss may have increased the TSS level [Cordenunsi *et al.*, 2005]. After the 12th day of storage, the TSS content of coated strawberries was reduced (Figure 1B). It most likely resulted from a total degradation of the fruits. Significant differences in the TSS levels were identified between the three different coatings ($p<0.05$).

The pH values of the coated and uncoated strawberries are shown in Figure1C. The pH of strawberries increased significantly during storage ($p<0.05$). This was expected since organic acids are used for respiration during storage of the fruit [Mohammadi *et al.*, 2021]. No significant differences ($p\geq0.05$) in the pH values were observed on the first day of storage between coated and uncoated fruits; however, significant differences ($p<0.05$) in pH values were observed on the subsequent days of storage with the different coatings.

During the initial 4 days of strawberry storage, a statistically significant reduction ($p<0.05$) in total acidity (TA) was observed in the untreated control group. However, on day 8, all the samples, except GPV2.5, showed an increase in TA levels (Figure 1D). This initial reduction in the TA until day 4 may be attributable to the conversion of acid into sugar due to ongoing respiration in the fruit [Amal *et al.*, 2010]. Significant ($p<0.05$) changes were seen in the TA as a function of duration of storage and between the samples (Figure 1D). The application of GPE coatings minimized the intensity of acidity decrease during storage, possibly due to the lower respiration rates of coated fruit compared to uncoated fruit. Our study results are consistent with the findings of earlier studies [Petriccione *et al.*, 2015; Rasouli *et al.*, 2019].

Texture parameters

The firmness of both coated and uncoated control fruits decreased with storage (Figure 2A). The decrease in the firmness of fruit during storage in the current study was found to be

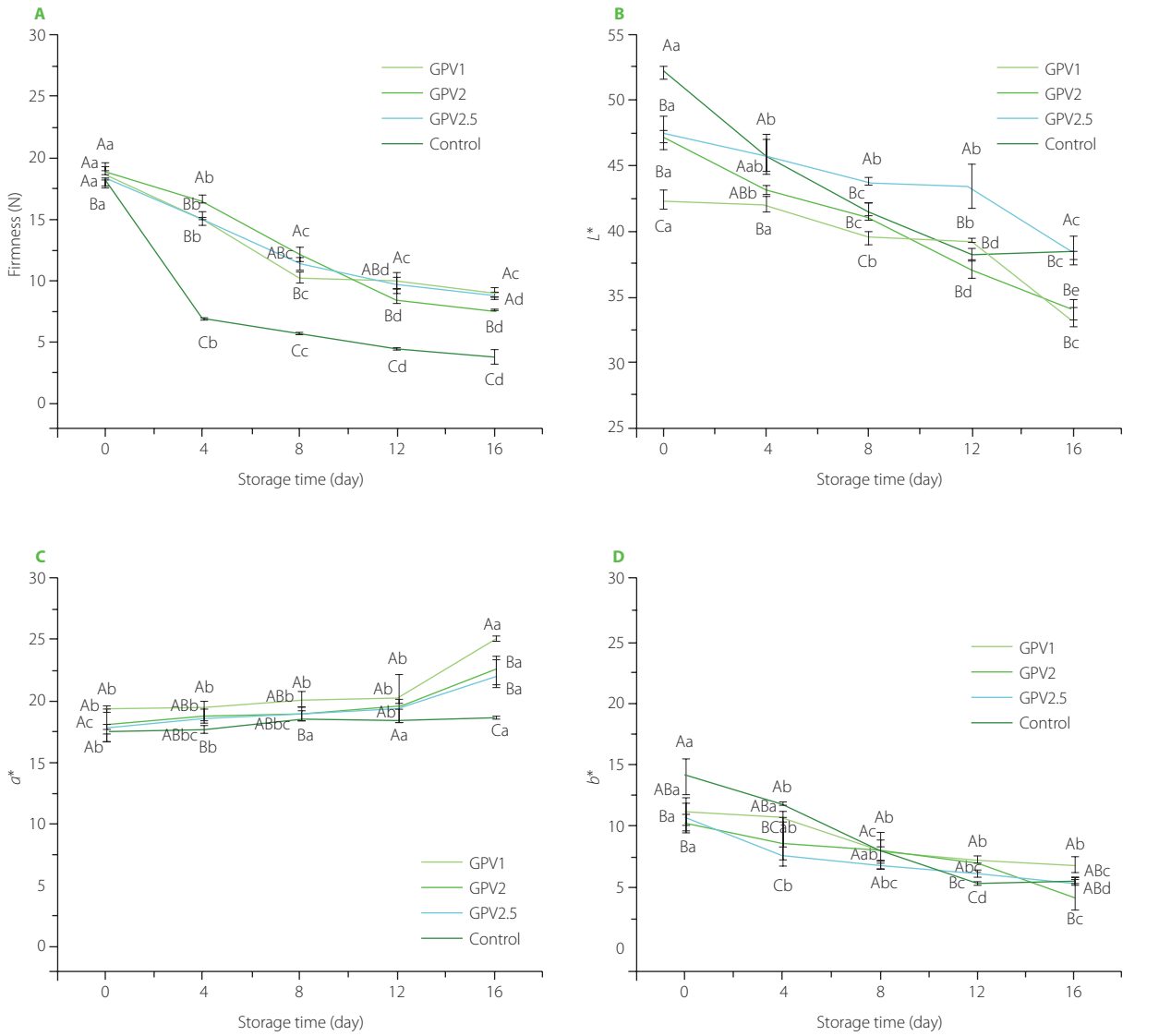

Figure 2. The firmness and color parameters (*L**, *a**, and *b**) of coated by dipping in solution of polyvinyl alcohol with 1%, 2% and 2.5% (*w/v*) grape pomace extract (GPV1, GPV2 and GPV2.5, respectively) and uncoated (control) strawberries during storage at 4°C for 16 days.
Values are given as mean and standard deviation. Different capital letters represent the difference between treatments, different lowercase letters represent the difference between storage times ($p<0.05$).

consistent with the findings reported in available literature on PVA-coated fruits [Ding *et al.*, 2019]. As strawberries ripen, they can lose their firmness significantly over time due to the hydrolysis and depolymerization of pectin contributing to the deterioration of the middle lamella of the cell wall and loss in turgor [Riaz *et al.*, 2021]. Softening of strawberries due to such water loss and deterioration of cell walls can lead to microbial growth [Sayyari *et al.*, 2022]. The PVA/GPE coated fruit showed significantly ($p<0.05$) higher firmness compared to the control fruit (Figure 2A). The firmness of the samples at the beginning of storage was in the range of 18.25–18.93 N. On day 16 of storage, the firmness decreased to 3.81–8.99 N. Nonetheless, the PVA/GPE-coated samples showed a lower reduction in firmness than the uncoated ones. Thus, while a 55% decrease in firmness was observed with the uncoated samples on day 4, a comparable decrease was observed in the GPV1 and GPV2.5 samples on day 16 of storage. The uncoated samples showed a 75% decrease in firmness at the end of the storage period while the GPV2.5 sample showed a 51% decrease in firmness making it the sample with the least decrease.

Color of strawberries

Similarly to firmness, color is an important parameter that defines consumer acceptability of fruits. Photographs showing the color and general appearance of the strawberries taken during their storage are given in Figure 3. Considering the color parameters, in general, the *L** value determined for both coated and uncoated strawberries decreased significantly ($p<0.05$) during storage (Figure 2B). The initial *L** values of 52.15, 42.46, 47.28, and 47.50 in control, GPV1, GPV2, and GPV2.5 samples, respectively, decreased to 38.53, 33.46, 34.04, and 38.20 on day 16, respectively. However, the GPV2.5 samples showed more or less constant *L** values until day 12 of storage. The decrease in *L** value is consistent with a darkening of the fruit during storage, as reported

Figure 3. The appearance of coated by dipping in solution of polyvinyl alcohol with 1%, 2% and 2.5% (*w/v*) grape pomace extract (GPV1, GPV2 and GPV2.5, respectively) and uncoated (control) strawberries during storage for 16 days.

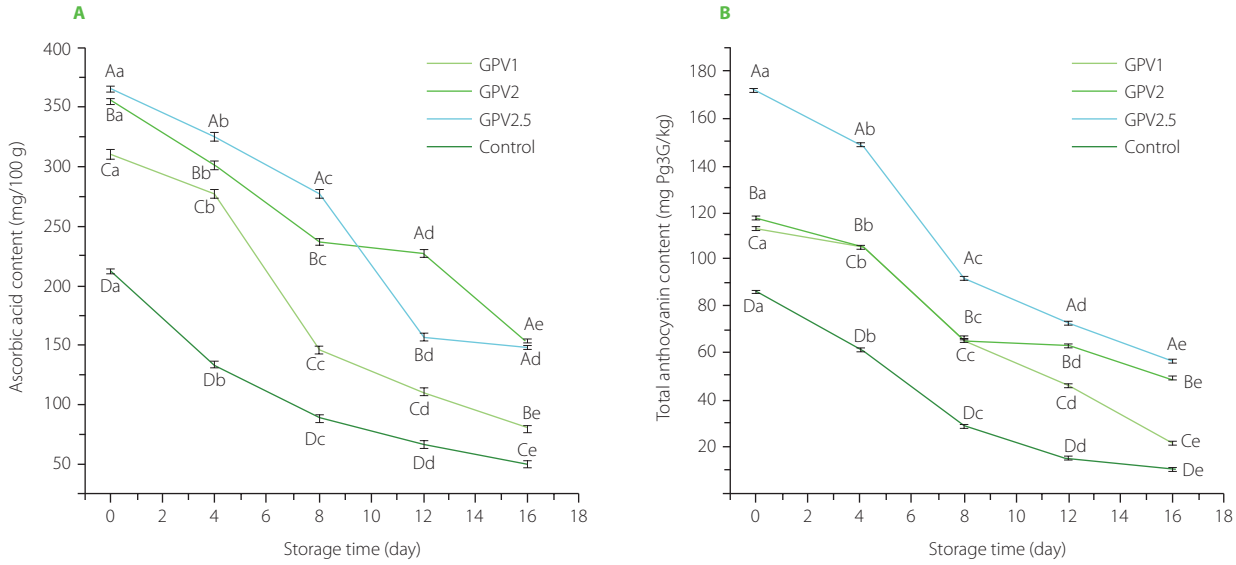

Figure 4. Ascorbic acid and total anthocyanin contents of coated by dipping in solution of polyvinyl alcohol with 1%, 2% and 2.5% (*w/v*) grape pomace extract (GPV1, GPV2 and GPV2.5, respectively) and uncoated (control) strawberries during storage at 4°C for 16 days.
Values are given as mean and standard deviation. Different capital letters represent the difference between treatments, different lowercase letters represent the difference between storage times ($p<0.05$).

previously [Ding *et al.*, 2019; Sayyari *et al.*, 2022]. The redness values of the coated samples remained stable until day 12 and increased afterwards (Figure 2C). There was no change ($p<0.05$) in the a^* values between the coated samples until day 12 of storage. The b^* value showed a significant ($p<0.05$), albeit modest decrease during storage in both coated and uncoated samples (Figure 2D).

Bioactive compound contents and antioxidant activity of strawberries

Ascorbic acid

The initial ascorbic acid content of the PVA/GPE-coated strawberries was significantly ($p<0.05$) higher than that of the control uncoated samples (Figure 4A). Thus, while the initial ascorbic acid content of the control strawberries was 212 mg/100 g, the same for GPV1, GPV2, and GPV2.5 were 311 mg/100 g, 355 mg/100 g, and 365 mg/100 g, respectively. During storage, the ascorbic acid content of both coated and uncoated control fruit showed a decrease. At the end of day 16 of storage, the control group showed a 75.58% decrease in ascorbic acid content, whereas the decreases for coated fruits were 74.39%, 57.10%, and 59.14% in the case of GPV1, GPV2, and GPV2.5 coatings, respectively. Thus, the loss of ascorbic acid was considerably low with the use of both GPV2 and GPV2.5. Such a decrease in strawberries with edible coatings may be attributed to a decrease in respiration, which can delay ascorbic acid

Table 1. The total phenolic content (TPC) and antioxidant activity determined as Trolox equivalent antioxidant capacity (TAEC) in ABTS assay and as IC_{50} of DPPH assay of coated by dipping in solution of polyvinyl alcohol with 1%, 2% and 2.5% (*w/v*) grape pomace extract (GPV1, GPV2 and GPV2.5, respectively) and uncoated (control) strawberries during storage at 4°C.

Parameter	Treatment	Storage time (day)				
		0	4	8	12	16
TPC (g GAE/kg)	Control	190 ± 7^{Da}	145 ± 5^{Db}	141 ± 8^{Cb}	125 ± 4^{Dc}	94 ± 4^{Bd}
	GPV1	234 ± 4^{Ca}	226 ± 1^{Ca}	186 ± 6^{Bb}	151 ± 6^{Cc}	135 ± 4^{Ad}
	GPV2	266 ± 12^{Ba}	236 ± 3^{Bb}	205 ± 3^{Bc}	181 ± 4^{Bd}	143 ± 2^{Ae}
	GPV2.5	358 ± 10^{Aa}	331 ± 9^{Ab}	276 ± 11^{Ac}	202 ± 5^{Ad}	190 ± 4^{Ad}
TEAC (µmol Trolox/kg)	Control	$1{,}820\pm6^{Da}$	$1{,}477\pm9^{Db}$	$1{,}439\pm5^{Dc}$	$1{,}217\pm4^{Dd}$	$1{,}028\pm9^{Ce}$
	GPV1	$1{,}924\pm6^{Ca}$	$1{,}792\pm3^{Cb}$	$1{,}566\pm9^{Cc}$	$1{,}371\pm22^{Cd}$	$1{,}139\pm23^{Be}$
	GPV2	$2{,}233\pm5^{Ba}$	$1{,}993\pm7^{Bb}$	$1{,}938\pm13^{Bc}$	$1{,}866\pm27^{Bd}$	$1{,}272\pm13^{Ae}$
	GPV2.5	$2{,}591\pm13^{Aa}$	$2{,}444\pm9^{Ab}$	$2{,}167\pm45^{Ac}$	$1{,}986\pm13^{Ad}$	$1{,}238\pm22^{Ae}$
IC_{50} (mg/L reaction mixture)	Control	12.81 ± 0.05^{Ae}	15.23 ± 0.09^{Ad}	20.33 ± 0.18^{Ac}	39.77 ± 0.12^{Ab}	30.55 ± 0.09^{Aa}
	GPV1	11.24 ± 0.24^{Bd}	12.28 ± 0.14^{Bc}	16.71 ± 0.13^{Bb}	12.55 ± 0.27^{Bc}	28.35 ± 0.15^{Ba}
	GPV2	8.52 ± 0.32^{Cd}	11.25 ± 0.25^{Cc}	12.11 ± 0.11^{Cb}	11.11 ± 0.09^{Cc}	21.77 ± 0.09^{Ca}
	GPV2.5	4.60 ± 0.22^{De}	9.20 ± 0.20^{Dd}	11.49 ± 0.04^{Db}	10.55 ± 0.27^{Dc}	16.49 ± 0.04^{Da}

Different lowercase letters in the same row indicate storage time differences, whereas capital letters in the same column separately for each parameter represent treatment differences ($p<0.05$). IC_{50}, the amount of extract that scavenges 50% of the DPPH radicals; GAE, gallic acid equivalent.

oxidation [Amal *et al.*, 2010]. These findings are in agreement with Gol *et al.* [2013], who reported that the ascorbic acid content in 1% hydroxypropylmethyl cellulose (HPMC) + 1% chitosan (CH) coated strawberries was significantly higher than in the control samples.

Total phenolic content

Strawberries are an important source of bioactive ingredients, but adverse storage conditions can reduce their quality [Tahir *et al.*, 2018]. The total phenolic content of the strawberries ranged from 94 to 358 g GAE/kg in all samples during storage (Table 1). A statistically significant ($p<0.05$) decrease in the TPC of both coated and uncoated samples was observed during the storage period. On day 4 of storage, the TPC decreased by 24% and 6% in the control and GPV2.5 samples, respectively. Until day 12 of storage, the TPC was the highest in the GPV2.5 sample, followed by the GPV2 and GPV1, respectively. The preservation of the phenolic compounds of the fruit was clearly the greater, the higher was the content of GPE used in the coating material. The control strawberries had the lowest TPC. The decline in TPC observed towards the end of the fruit storage duration could be attributed to the disintegration of cell structure as the fruit undergoes senescence [Macheix *et al.,* 1990]. TPC may have also decreased due to oxidation processes [Ali *et al,* 2019]. The application of PVA/GPE coatings appears to have slowed down the oxidation of phenolic compounds, resulting in their preservation. Yan *et al.* [2019] and Gol *et al.* [2013] have conducted research that yielded comparable findings, demonstrating the beneficial impact of edible coatings enriched with chitosan (CH) and carboxymethyl cellulose (CMC) on TPC in strawberries.

Antioxidant activity

The antioxidant activity of the strawberries was significantly ($p<0.05$) enhanced by coating them with PVA/GPE (Table 1). The GPV2.5 coated samples showed 2,591 µmol Trolox/kg in ABTS assay and IC_{50} of 4.60 mg/L in DPPH assay, giving the highest antioxidant activity among all samples, as expected. This was likely contributed by the high antioxidant activity of grape pomace itself [Rockenbach *et al.*, 2011]. The antioxidant activity of all strawberry samples significantly ($p<0.05$) decreased over time during storage (Table 1). However, the PVA/GPE coating resulted in greater retention of the antioxidant activity over longer periods of time. On day 16 of storage, the antioxidant activity of GPV2.5-coated fruit was 1238 µmol Trolox/kg (ABTS assay) and 16.49 mg/L (IC_{50} of DPPH assay), whereas respective values determined for the control samples were 1,028 µmol Trolox/kg and 30.55 mg/L, respectively. These findings are consistent with a previous study by Petriccione *et al.* [2015] who reported that chitosan-coated strawberries retained higher antioxidant activity after cold storage compared to uncoated strawberries. Due to its functional qualities, the presence of the GPE in the coating not only increased the antioxidant content, but also served as a barrier to oxygen during the coating process, further retaining antioxidant activity.

Total anthocyanin content

Anthocyanins, which are responsible for the red color of strawberries, determine the degree of ripening and the attractiveness of the strawberries [Khodaei & Hamidi-Esfahani, 2019]. A decrease in TAC was observed during the storage of strawberries (Figure 4). This decrease in anthocyanin content could be due

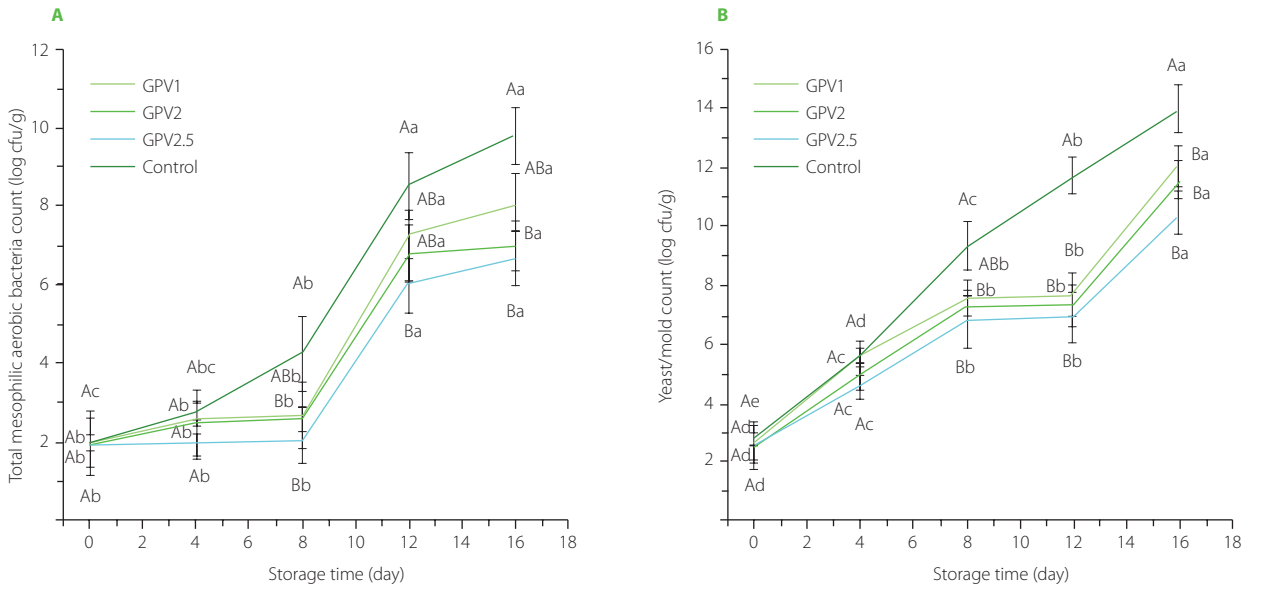

Figure 5. Total mesophilic aerobic bacteria count and yeast/mold count of coated by dipping in solution of polyvinyl alcohol with 1%, 2% and 2.5% (*w/v*) grape pomace extract (GPV1, GPV2 and GPV2.5, respectively) and uncoated (control) strawberries during storage at 4°C for 16 days.
Values are given as means and standard deviation. Different capital letters represent the difference between treatments, different lowercase letters represent the difference between storage times ($p<0.05$).

Table 2. Total phenolic content (TPC), antioxidant activity determined as Trolox equivalent antioxidant capacity (TAEC) in ABTS assay and as IC_{50} of DPPH assay, total anthocyanin content (TAC), and antifungal activity against *Botrytis cinerea* of the coating solutions of polyvinyl alcohol with 1%, 2% and 2.5% (*w/v*) grape pomace extract (GPV1, GPV2 and GPV2.5, respectively).

	GPV1	GPV2	GPV2.5
TPC (g GAE/kg)	263±6^{c}	475±6^{b}	519±15^{a}
TEAC (µmol Trolox/kg)	138±3^{b}	152±9^{ab}	181±1^{a}
DPPH$^{\bullet}$ scavenging activity, IC_{50}* (mg/L)	81.55±1.55^{a}	48.22±0.54^{b}	37.57±1.44^{c}
Antifungal activity, IC_{50}** (mg/L)	48.19±3.43^{a}	38.32±0.40^{b}	26.33±0.65^{c}
TAC (mg Pg3G/kg)	22.00±0.02^{c}	42.00±0.05^{b}	85.00±0.07^{a}

Significant differences ($p<0.05$) are indicated by different letters in the same row. IC_{50}*, the amount of extract that scavenges 50% of the DPPH radicals; IC_{50}**, concentration that reduced mycelial growth by 50%; GAE, gallic acid equivalent; Pg3G, pelargonidin 3-glucoside.

to aging and decay of the fruit [Khodaei & Hamidi-Esfahani, 2019]. Similar outcomes have been reported for strawberries stored in the refrigerator [Khodaei & Hamidi-Esfahani, 2019; Sayyari *et al.*, 2022]. In the current study, the use of edible coatings containing different amounts of GPE was effective in preventing the deterioration of anthocyanins in strawberries during storage. The TAC of the uncoated samples decreased from an initial value of 86.33 mg Pg3G/kg to 11.75 mg Pg3G/kg at the end of storage. GPE is an anthocyanin-rich resource [Rockenbach *et al.*,2011]. Therefore, as expected, the anthocyanin content of the GPV2.5-coated strawberries was approximately two-fold higher than of the control uncoated fruit. The TAC of the GPV2.5-coated fruit decreased from 171.57 mg Pg3G kg to 56.62 mg Pg3G/kg during storage. These values reflect a decrease in the TAC value of 87% in the control sample and 66% in the GPV2.5 sample. The oxygen barrier formed by GPE coating most likely contributed towards the protection of anthocyanin content.

Effect of PVA/GPE coating on microbial growth

The total mesophilic aerobic bacteria (TMAB) and yeast/mold counts of strawberries uncoated and coated with PVA/GPA during the storage period are shown in Figure 5. The initial TMAB count of strawberries was approximately 2 log cfu/g. During storage, the TMAB count increased in all samples, but this increase was seen earlier in the control uncoated samples compared to the coated samples. The uncoated control samples also had significantly ($p<0.05$) higher TMAB counts compared to the coated samples after 8 days of storage. After day 16, the TMAB content of the control, GPV1, GPV2, and GPV2.5 samples was 9.80, 8.01, 7.00, and 6.67 log cfu/g, respectively. The TMAB count of the GPV2.5-coated strawberries remained constant for the first 8 days, which is likely to be due to the antibacterial effect of GPE. The mesophilic bacteria count increased after day 8 in all GPE-coated samples. A statistically significant increase in yeast/mold count was seen in all strawberry samples ($p<0.05$) during storage. The initial yeast/mold count of control,

GPV1, GPV2, and GPV2.5 samples was 2.68, 2.78, 2.60, and 2.56 log cfu/g, which increased to 14.00, 12.06, 11.57, and 10.45 log cfu/g at the end of storage, respectively. The coated samples showed stable yeast/mold counts between 8-12 days of storage, while the TMAB count showed an increase. Grape pomace has a known antimicrobial effect against many bacteria [Hassan *et al.*, 2019]. In addition, extracts with phenolics obtained from mixtures of Cabernet Sauvignon, Carmenere and Syrah grapes have been reported to have a high inhibitory effect against the mycelial growth of the phytopathogenic fungus *B. cinerea* [Mendoza *et al.*, 2013].

Bioactive compound content and functional properties of coating solution

Coating solutions of PVA with 1%, 2%, and 2.5% GPE (*w/v*) were tested for their total phenolic content, antioxidant activity, total anthocyanin content, and antifungal activity against *B. cinerea*. The PVA/GPE solutions demonstrated antioxidant activity, which was positively correlated with the concentration of GPE in solution (Table 2). Thus, GPV2.5 showed the highest TEAC (181 µmol Trolox/kg) compared to GPV2 (152 µmol Trolox/kg) and GPV1 (138 µmol Trolox/kg). The IC_{50} values of DPPH assay ranged from 37.57 mg/mL (GPV2.5) to 81.55 mg/mL (GPV1). The total phenolic content of the coating solutions was increased in direct proportion to the amount of GPE added. TPC was 263, 475, and 519 g GAE/kg for GPV1, GPV2, and GPV2.5, respectively. We have previously reported that GPE is rich in phenolic compounds such as myricetin, gallic acid, quercetin, ellagic acid, syringic acid, epicatechin, chlorogenic acid, catechin and caffeic acid [Kaynarca *et al.*, 2022]. Anthocyanins are remarkable pigments with red, orange, pink and blue colors, and the most common are cyanidin, pelargonidine, delphinidine, petunidine, peonidine, and malvidin [Zhao *et al.*, 2022]. Grape pomace left after wine production is an abundant and inexpensive source of anthocyanins. Grape pomace extracts are primarily composed of malvidin 3-glucoside, followed by peonidine 3-glucoside, along with other components such as petunidin 3-glucoside, delphinidine 3-glucoside, and cyanidin 3-glucoside [Lapornik *et al.*, 2005]. As expected, the highest anthocyanin content was determined in GPV2.5 containing 85.00 mg Pg3G/kg while GPV1 had the lowest anthocyanin content of 22.00 mg Pg3G/kg.

Depending on environmental factors, 80-85% of strawberries perish shortly after harvest due to the presence of gray mold (*B. cinerea*) [Hernandez-Munoz *et al.*, 2008]. Therefore, the antifungal activity of the coating solutions against growth of *B. cinerea* was determined in our study and results are shown in Table 1. The IC_{50} values were found to be 48.19, 38.32, and 26.33 mg/L for GPV1, GPV2, and GPV2.5, respectively. The addition of grape pomace had an obvious antifungal effect, and this effect was more robust at higher concentrations of the pomace ($p<0.05$). Such an antifungal effect of PVA/GPE solutions as well as the findings from other microbiological analyses of stored strawberries suggest that coated with PVA/GPE fruits may be stored for longer periods of time compared to uncoated strawberries.

CONCLUSIONS

PVA/GPE coating solutions, which have high antioxidant activity and phenolic compound content as well as antimicrobial and antifungal properties, could delay the decay of strawberries during storage and prolong their shelf life. The use of coating solutions of PVA with 2.5% (*w/v*) GPA turned out to be the most effective approach to preserve the quality of strawberries as they ensured a significant delay in weight loss and ascorbic acid content and had positive effects on the preservation of higher contents of total phenolics and total anthocyanins. PVA/GPE coating could be used to provide an edible coating with antifungal effects against *B. cinerea*. Overall, the current study shows that extending the shelf life of strawberries by coating them with PVA/GPE solutions may contribute to reducing food loss in the post-harvest chain both during distribution and household storage.

RESEARCH FUNDING

The research received no external funding.

ACKNOWLEDGEMENTS

The authors acknowledge Assoc. Prof. Dr. Nagehan Desen Köycü for sharing a culture of *Botrytis cinerea* 12c.

CONFLICT OF INTERESTS

The Authors declare that there are no conflicts of interest.

ORCID IDS

T. Gümüş https://orcid.org/0000-0001-7635-5519
D.D.A. Kamer https://orcid.org/0000-0002-9119-5979
G.B. Kaynarca https://orcid.org/0000-0001-7896-457X
E. Yücel https://orcid.org/0000-0002-6750-4030

REFERENCES

1. Ali, S., Khan, A.S., Nawaz, A., Anjum, M.A., Naz, S., Ejaz, S., Hussain, S. (2019). *Aloe vera* gel coating delays postharvest browning and maintains quality of harvested litchi fruit. *Postharvest Biology and Technology*, *157*, art. no. 110960. https://doi.org/10.1016/j.postharvbio.2019.110960
2. Amal, S.A., El-Mogy, M., Aboul-Anean, H., Alsanius, B. (2010). Improving strawberry fruit storability by edible coating as a carrier of thymol or calcium chloride. *Journal of Horticultural Science & Ornamental Plants*, *2*(3), 88-97.
3. Andrade, J., González-Martínez, C., Chiralt, A. (2021). Effect of phenolic acids on the properties of films from Poly (vinyl alcohol) of different molecular characteristics. *Food Packaging and Shelf Life*, *29*, art. no. 100711. https://doi.org/10.1016/j.fpsl.2021.100711
4. Armghan Khalid, M., Niaz, B., Saeed, F., Afzaal, M., Islam, F., Hussain, M., Mahwish, Muhammad Salman Khalid, H., Siddeeg, A., Al-Farga, A. (2022). Edible coatings for enhancing safety and quality attributes of fresh produce: A comprehensive review. *International Journal of Food Properties*, *25*(1), 1817-1847. https://doi.org/10.1080/10942912.2022.2107005
5. Ayranci, E., Tunc, S. (2003). A method for the measurement of the oxygen permeability and the development of edible films to reduce the rate of oxidative reactions in fresh foods. *Food Chemistry*, *80*(3), 423-431. https://doi.org/10.1016/S0308-8146(02)00485-5
6. Bouchra, C., Achouri, M., Hassani, L.I., Hmamouchi, M. (2003). Chemical composition and antifungal activity of essential oils of seven Moroccan Labiatae against *Botrytis cinerea* Pers: Fr. *Journal of Ethnopharmacology*, *89*(1), 165-169. https://doi.org/10.1016/S0378-8741(03)00275-7
7. Cordenunsi, B.R., Genovese, M.I., do Nascimento, J.R.O., Hassimotto, N.M.A., dos Santos, R.J., Lajolo, F.M. (2005). Effects of temperature on the chemical composition and antioxidant activity of three strawberry cultivars. *Food Chemistry*, *91*(1), 113-121. https://doi.org/10.1016/j.foodchem.2004.05.054
8. Ding, J., Zhang, R., Ahmed, S., Liu, Y., Qin, W. (2019). Effect of sonication duration in the performance of polyvinyl alcohol/chitosan bilayer films and their effect on strawberry preservation. *Molecules*, *24*(7), art.no. 1408. https://doi.org/10.3390/molecules24071408

9. Duarte, L.G.R., Picone, C.S.F. (2022). Antimicrobial activity of lactoferrin-chitosan-gellan nanoparticles and their influence on strawberry preservation. *Food Research International*, *159*, art. no. 111586. https://doi.org/10.1016/j.foodres.2022.111586
10. Fawole, O.A., Riva, S.C., Opara, U.L. (2020). Efficacy of edible coatings in alleviating shrivel and maintaining quality of Japanese plum (*Prunus salicina Lindl.*) during export and shelf life conditions. *Agronomy*, *10*(7), art. no. 1023. https://doi.org/10.3390/agronomy10071023
11. Giampieri, F., Tulipani, S., Alvarez-Suarez, J.M., Quiles, J.L., Mezzetti, B., Battino, M. (2012). The strawberry: Composition, nutritional quality, and impact on human health. *Nutrition*, *28*(1), 9-19. https://doi.org/10.1016/j.nut.2011.08.009
12. Gol, N.B., Patel, P.R., Rao, T.V.R. (2013). Improvement of quality and shelf-life of strawberries with edible coatings enriched with chitosan. *Postharvest Biology and Technology*, *85*, 185-195. https://doi.org/10.1016/j.postharvbio.2013.06.008
13. Hassan, Y.I., Kosir, V., Yin, X., Ross, K., Diarra, M.S. (2019). Grape pomace as a promising antimicrobial alternative in feed: A critical review. *Journal of Agricultural and Food Chemistry*, *67*(35), 9705-9718. https://doi.org/10.1021/acs.jafc.9b02861
14. Hernandez-Munoz, P., Almenar, E., Del Valle, V., Velez, D., Gavara, R. (2008). Effect of chitosan coating combined with postharvest calcium treatment on strawberry (*Fragaria× ananassa*) quality during refrigerated storage. *Food Chemistry*, *110*(2), 428-435. https://doi.org/10.1016/j.foodchem.2008.02.020
15. Jafarzadeh, S., Nafchi, A.M., Salehabadi, A., Oladzad-Abbasabadi, N., Jafari, S.M. (2021). Application of bio-nanocomposite films and edible coatings for extending the shelf life of fresh fruits and vegetables. *Advances in Colloid and Interface Science*, *291*, art. no. 102405. https://doi.org/10.1016/j.cis.2021.102405
16. Kamer, D.D.A., Kaynarca, G.B., Yücel, E., Gümüş, T. (2022). Development of gelatin/PVA based colorimetric films with a wide pH sensing range winery solid by-product (Vinasse) for monitor shrimp freshness. *International Journal of Biological Macromolecules*, 220, 627-637. https://doi.org/10.1016/j.ijbiomac.2022.08.113
17. Kaur, K., Kumar, A. (2022). Enhancement of strawberry shelf life with coating: A review. *Modern Phytomorphology, 16*(2), 44-48. https://doi.org/10.5281/zenodo.7735668
18. Kaynarca, G.B., Gümüş, T., Kamer, D.D.A. (2022). Rheological properties of fish (*Sparus aurata*) skin gelatin modified by agricultural wastes extracts. *Food Chemistry*, *393*, art. no. 133348. https://doi.org/10.1016/j.foodchem.2022.133348
19. Kaynarca, G.B., Kamer, D.D.A., Gumus, T., Sagdıc, O. (2023). Characterization of poly (vinyl alcohol)/gelatin films made with winery solid by-product (vinasse) extract. *Food Packaging and Shelf Life*, *35*, art. no. 101013. https://doi.org/10.1016/j.fpsl.2022.101013
20. Khodaei, D., Hamidi-Esfahani, Z. (2019). Influence of bioactive edible coatings loaded with *Lactobacillus plantarum* on physicochemical properties of fresh strawberries. *Postharvest Biology and Technology*, *156*, art, no. 110944. https://doi.org/10.1016/j.postharvbio.2019.110944
21. Khodaei, D., Hamidi-Esfahani, Z., Rahmati, E. (2021). Effect of edible coatings on the shelf-life of fresh strawberries: A comparative study using TOPSIS--Shannon entropy method. *NFS Journal*, *23*, 17-23. https://doi.org/10.1016/j.nfs.2021.02.003
22. Lapornik, B., Prošek, M., Wondra, A.G. (2005). Comparison of extracts prepared from plant by-products using different solvents and extraction time. *Journal of Food Engineering*, *71*(2), 214-222. https://doi.org/10.1016/j.jfoodeng.2004.10.036
23. Liu, C., Jin, T., Liu, W., Hao, W., Yan, L., Zheng, L. (2021). Effects of hydroxyethyl cellulose and sodium alginate edible coating containing asparagus waste extract on postharvest quality of strawberry fruit. *LWT – Food Science and Technology*, *148*, art. no. 111770. https://doi.org/10.1016/j.lwt.2021.111770
24. Liu, Y., Wang, S., Lan, W., Qin, W. (2017). Fabrication and testing of PVA/Chitosan bilayer films for strawberry packaging. *Coatings*, *7*(8), art no. 109. https://doi.org/10.3390/coatings7080109
25. Macheix, J.J., Fleuriet, A., Billot, J. (1990). Changes and metabolism of phenolic compounds in fruits. In Macheix, J.J. (Ed.). *Fruit Phenolics*. 1st Edition. CRC Press, Boca Raton, Florida, ABD, pp. 149-239.
26. Makris, D.P., Boskou, G., Andrikopoulos, N.K. (2007). Polyphenolic content and *in vitro* antioxidant characteristics of wine industry and other agri--food solid waste extracts. *Journal of Food Composition and Analysis*, *20*(2), 125-132. https://doi.org/10.1016/j.jfca.2006.04.010
27. Matar, C., Guillard, V., Gauche, K., Costa, S., Gontard, N., Guilbert, S., Gaucel, S. (2020). Consumer behaviour in the prediction of postharvest losses reduction for fresh strawberries packed in modified atmosphere packaging. *Postharvest Biology and Technology*, *163*, art. no. 111119. https://doi.org/10.1016/j.postharvbio.2020.111119
28. Mendoza, L., Yañez, K., Vivanco, M., Melo, R., Cotoras, M. (2013). Characterization of extracts from winery by-products with antifungal activity against *Botrytis cinerea*. *Industrial Crops and Products*, *43*, 360-364. https://doi.org/10.1016/j.indcrop.2012.07.048
29. Mohammadi, L., Ramezanian, A., Tanaka, F., Tanaka, F. (2021). Impact of *Aloe vera* gel coating enriched with basil (*Ocimum basilicum L.*) essential oil on postharvest quality of strawberry fruit. *Journal of Food Measurement and Characterization*, *15*(1), 353-362. https://doi.org/10.1007/s11694-020-00634-7
30. Moreira, B.R., Pereira-Junior, M.A., Fernandes, K.F., Batista, K.A. (2020). An ecofriendly edible coating using cashew gum polysaccharide and polyvinyl alcohol. *Food Bioscience, 37*, art. no. 100722. https://doi.org/10.1016/j.fbio.2020.100722
31. Parin, F.N., Terzioğlu, P., Sicak, Y., Yildirim, K., Öztürk, M. (2021). Pine honey–loaded electrospun poly (vinyl alcohol)/gelatin nanofibers with antioxidant properties. *The Journal of The Textile Institute*, *112*(4), 628-635. https://doi.org/10.1080/00405000.2020.1773199
32. Pavlath, A., Orts, W. (2009). Edible films and coatings: Why, what, and how?. In Embuscado, M.E., Huber, K.C. (Eds.). *Edible Films and Coatings for Food Applications*.Vol. 9, Springer New York, NY, pp.1-23.
33. Peixoto, C.M., Dias, M.I., Alves, M.J., Calhelha, R.C., Barros, L., Pinho, S.P., Ferreira, I.C. (2018). Grape pomace as a source of phenolic compounds and diverse bioactive properties. *Food Chemistry*, *253*, 132-138. https://doi.org/10.1016/j.foodchem.2018.01.163
34. Petriccione, M., Mastrobuoni, F., Pasquariello, M.S., Zampella, L., Nobis, E., Capriolo, G., Scortichini, M. (2015). Effect of chitosan coating on the postharvest quality and antioxidant enzyme system response of strawberry fruit during cold storage. *Foods*, *4*(4), 501-523. https://doi.org/10.3390/foods4040501
35. Pineli, L.D.D., Moretti, C.L., dos Santos, M.S., Campos, A.B., Brasileiro, A.V., Cordova, A.C., Chiarello, M.D. (2011). Antioxidants and other chemical and physical characteristics of two strawberry cultivars at different ripeness stages. *Journal of Food Composition and Analysis*, *24*, 11-16. https://doi.org/10.1016/j.jfca.2010.05.004
36. Rasouli, M., Saba, M.K., Ramezanian, A. (2019). Inhibitory effect of salicylic acid and *Aloe vera* gel edible coating on microbial load and chilling injury of orange fruit. *Scientia Horticulturae*, *247*, 27-34. https://doi.org/10.1016/j.scienta.2018.12.004
37. Re, R., Pellegrini, N., Proteggente, A., Pannala, A., Yang, M., Rice-Evans, C. (1999). Antioxidant activity applying an improved ABTS radical cation decolorization assay. *Free Radical Biology and Medicine*, *26*(9-10), 1231-1237. https://doi.org/10.1016/S0891-5849(98)00315-3
38. Ren, T., Gan, J., Zhou, L., Chen, H. (2020). Physically crosslinked hydrogels based on poly (vinyl alcohol) and fish gelatin for wound dressing application: Fabrication and characterization. *Polymers*, *12*(8), art. no. 1729. https://doi.org/10.3390/polym12081729
39. Riaz, A., Aadil, R.M., Amoussa, A.M.O., Bashari, M., Abid, M., Hashim, M.M. (2021). Application of chitosan-based apple peel polyphenols edible coating on the preservation of strawberry (*Fragaria ananassa* cv Hongyan) fruit. *Journal of Food Processing and Preservation*, *45*(1), art. no. e15018. https://doi.org/10.1111/jfpp.15018
40. Rockenbach, I.I., Rodrigues, E., Gonzaga, L.V., Caliari, V., Genovese, M.I., Gonçalves, A.E.D.S.S., Fett, R. (2011). Phenolic compounds content and antioxidant activity in pomace from selected red grapes (*Vitis vinifera* L. and *Vitis labrusca* L.) widely produced in Brazil. *Food Chemistry*, *127*(1), 174-179. https://doi.org/10.1016/j.foodchem.2010.12.137
41. Sayyari, M., Esna-Ashari, M., Tarighi, T.H. (2022). Impacts of salicylic acid, chitosan, and salicyloyl chitosan on quality preservation and microbial load reduction in strawberry fruits during cold storage. *Journal of Food Processing and Preservation*, *46*(7), art. no. e16710. https://doi.org/10.1111/jfpp.16710
42. Tahir, H.E., Xiaobo, Z., Jiyong, S., Mahunu, G.K., Zhai, X., Mariod, A.A. (2018). Quality and postharvest-shelf life of cold-stored strawberry fruit as affected by gum arabic (*Acacia senegal*) edible coating. *Journal of Food Biochemistry*, *42*(3), art. no. e12527. https://doi.org/10.1111/jfbc.12527
43. Ueda, J.M., Pedrosa, M.C., Heleno, S.A., Carocho, M., Ferreira, I.C.F.R., Barros, L. (2022). Food additives from fruit and vegetable by-products and bio-residues: A comprehensive review focused on sustainability. *Sustainability*, *14*(9), art. no. 5212. https://doi.org/10.3390/su14095212
44. Vahid, B. (2012). Titrimetric determination of ascorbic acid contents in plant samples by 2, 6-dichlorophenolindophenol method. *Journal of the Chemical Society of Pakistan*, *34*(6), 1510-1512. https://doi.org/10.1002/jps.2600720208
45. Wrolstad, R.E. (1993). Color and pigment analyses in fruit products. *Station Bulletin*, 624, 1-17.

46. Yan, J., Luo, Z., Ban, Z., Lu, H., Li, D., Yang, D., Aghdam, M.S., Li, L. (2019). The effect of the layer-by-layer (LBL) edible coating on strawberry quality and metabolites during storage. *Postharvest Biology and Technology*, *147*, 29-38. https://doi.org/10.1016/j.postharvbio.2018.09.002
47. Yıldırım-Yalçın, M., Şeker, M., Sadıkoğlu, H. (2022). Effect of grape derivatives and cross-linked maize starch coatings on the storage life of strawberry fruit. *Progress in Organic Coatings, 167*, art. no. 106850. https://doi.org/10.1016/j.porgcoat.2022.106850
48. Zhao, L., Liu, Y., Zhao, L., Wang, Y. (2022). Anthocyanin-based pH-sensitive smart packaging films for monitoring food freshness. *Journal of Agriculture and Food Research*, *9*, art, no. 100340. https://doi.org/10.1016/j.jafr.2022.100340

ORIGINAL ARTICLE
http://journal.pan.olsztyn.pl

Polish Journal of Food and Nutrition Sciences
2023, Vol. 73, No. 2, 163–174
DOI: 10.31883/pjfns/163612
ISSN 1230-0322, e-ISSN 2083-6007

Effects of *Tremella fuciformis*-Derived Polysaccharides with Different Molecular Weight on D-Galactose-Induced Aging of Mice

Donghui Luo[1], Xiaofei Liu[1], Jingjing Guan[1], Guili Jiang[1], Yanglin Hua[1], Xinfei Zhang[2], Xiaofei Xu[1]*

[1]College of Food Science and Engineering, Guangdong Ocean University, Yangjiang 529500, PR China
[2]College of Food Science and Engineering, South China University of Technology, Guangzhou 510640, PR China

The structure-bioactivity relationship of *Tremella fuciformis* polysaccharides (TFPs) in anti-aging *in vivo* is rarely reported. In the present study, a purified TFP, named HM, mainly composed of mannose, fucose, xylose, and glucose in a molar ratio of 4.14:0.98:0.81:0.62, was obtained from the fruiting body of *T. fuciformis*. Subsequently, two differentially degraded TFPs, named MM and LM, respectively, were prepared by a combined method of ultrasonic irradiation (US) and H_2O_2 treatment. Their structural properties, scavenging activities against free radicals *in vitro*, and anti-aging effects on D-galactose-induced aging of mice were determined. The average molecular weight of HM, MM, and LM was 58.3×10^6, 4.68×10^6, and 3.14×10^5 Da, respectively. All three TFPs were devoid of triple helix conformation and exhibited concentration- and molecular weight--dependent scavenging activity against radicals. The TFPs markedly relieved skin aging, effectively attenuated oxidative stress, and significantly decreased inflammation in D-galactose-induced aging mice. MM exhibited the best anti-aging effect among the TFPs. Additionally, TFPs partially restored the alterations in pH and the total content of short-chain fatty acids (SCFAs) in the colon but exhibited various impacts on the content of the individual SCFAs. These findings would provide rational guidance for a better application of TFPs in anti-aging foods and expand our understanding of the structure-function relationship of mushroom polysaccharides.

Key words: mushroom, polysaccharide purification, anti-oxidant activity, anti-aging activity, structure-function relationship, anti-oxidant enzyme

INTRODUCTION

Mushrooms have been a part of human diet for centuries and have been proven to confer a number of benefits against human diseases, such as cancer, infection, atherosclerosis, diabetes, neurodegenerative conditions, *etc.*, in addition to their nutritional and culinary values [Venturella *et al.*, 2021]. Polysaccharides in mushrooms are considered the main active components responsible for their health-promoting benefits [Huang & Nie, 2015]. Numerous studies have documented the structural properties of polysaccharides, such as monosaccharide composition, molecular weight, and conformation, to be closely associated with their bioactivities [Ferreira *et al.*, 2015]. For example, the anti-tumor activity of β-glucan derived from *Lentinula edodes* strongly depends on its triple-helical conformation [Zhang *et al.*, 2005]. Degraded polysaccharides from *Ganoderma lucidum* with a lower molecular weight (13.6 kDa) have higher hypolipidemic and antioxidant activities in high-fat diet-induced obese mice than the original polysaccharides (3,060 kDa) [Xu *et al.*, 2019]. Thus, exploring the structure-bioactivity relationship of mushroom polysaccharides contributes to a better development and application of polysaccharides for the prevention and/or management of human diseases.

***Corresponding Author:**
tel./fax: +86662-2162166; e-mail: xfxufe@gdou.edu.cn (X. Xu)

Submitted: 15 January 2023
Accepted: 25 April 2023
Published on-line: 25 May 2023

Tremella fuciformis, commonly named snow ear, has been consumed as food and used in traditional Chinese medicine for hundreds of years for its nutritional and health beneficial value [Wu *et al.*, 2019]. *T. fuciformis* polysaccharides (TFPs) exhibit a variety of bioactivities, including anti-tumor and immune modulation, anti-oxidation and anti-aging, hypoglycemic and hypocholesterolemic effects, neuroprotection, *etc*. [Wu *et al.*, 2019; Yang *et al.*, 2019]. TFPs not only reduce the levels of free radicals *in vitro* [Ge *et al.*, 2020; Li *et al.*, 2020], but also show protective effects of antioxidant enzymes in aging animal models *in vivo* [Zhang *et al.*, 2014], indicating their great potential in the management of oxidative stress-induced health problems. To date, many different structures of TFPs have been reported, which vary greatly depending on the sources, extraction methods, and purification processes [Wu *et al.*, 2019]. For instance, the molecular weight of TFPs reported in different studies ranges from 1.08×10^3 to 3.74×10^6 Da [Wu *et al.*, 2019; Yang *et al.*, 2019]. Previous research indicated that TFPs with a low molecular weight showed high anti-oxidant activity *in vitro* [Li *et al.*, 2020]. However, the *in vitro* model cannot simulate the internal conditions within cells [Heinrich *et al.*, 2020]. Considering the great differences in the biochemical circumstances between *in vitro* assays and within cells in an organism, it is necessary to investigate the relationship between the structure and bioactivity of TFPs from the view of mammalian model to promote a better application of TFPs in functional foods and nutraceuticals.

In the present study, to better focus our attention on the effect of *T. fuciformis* polysaccharides with different molecular weights on anti-aging activities *in vivo*, a high-molecular-weight TFP was first obtained from the fruiting body of *T. fuciformis*. Then, two differentially degraded TFPs were prepared from the above TFP using a combined method of ultrasonic irradiation (US) and H_2O_2 treatments. Subsequently, the structural properties of the three TFPs and their anti-oxidant activities against 1,1-diphenyl-2-picrylhydrazyl (DPPH) radical, hydroxyl radical, and superoxide anion radical *in vitro* were examined. Finally, D-galactose-aged mice were used to assess their anti-aging effects *in vivo* by measuring the content of hydroxyproline and hyaluronic acid in the skin; the activity of glutathione peroxidase (GSH-Px) and superoxide dismutase (SOD); the content of malondialdehyde (MDA) in serum, liver, and heart; the level of interleukin 1β (IL-1β) and tumor necrosis factor α (TNF-α) in serum; and the alteration in pH and production of short-chain fatty acids (SCFAs) in the gastrointestinal tract.

MATERIAL AND METHODS

TFPs extraction and purification

Dried *T. fuciformis* fruiting bodies were purchased from a local agricultural market in Gutian, Fujian province, China. They were dried by heat air in an electrically-heated oven under normal pressure. First, the *T. fuciformis* fruiting bodies were crushed and sifted through 40 mesh for use. TFPs were extracted using boiling tap water (1:60, *w/v*) for 6 h. The extract solution was then centrifuged (3,000×*g*, 5 min) and the supernatant was concentrated to a quarter of the original weight under vacuum at 70°C. Subsequently, deproteination was performed by adjusting the solution pH to pH 4.0 with citric acid and kept at 4°C for 4 days to enable the complete precipitation of the proteins by the isoelectric precipitation method [Oliveira *et al.*, 1999]. The supernatant was collected and three equivalent volumes of 95% ethanol were added to precipitate polysaccharides at 4°C overnight. The precipitate was collected by centrifugation (5,000×*g*, 5 min) and re-dissolved in distilled water (0.2 g/100 g). Ultra-filtration of the solution with a 50 nm pore size membrane was performed using an ultrafiltration system LDS-L1 (AITESEN Co., Ltd, Suzhou, China). The retained fluid was collected and dialyzed using a dialysis bag (cut-off of 3,000 Da) against distilled water for 4 days. The dialysis solution was freeze-dried to obtain white TFPs powder. No apparent absorption was observed at 260 and 280 nm by ultraviolet scanning (data not shown), suggesting the absence of protein and nucleic acid in the TFPs.

Preparation of differentially degraded TFPs

Degraded TFPs were prepared by a combined method of US and H_2O_2 treatment [Li *et al.*, 2020] with slight modifications. Briefly, the original TFPs was dissolved in distilled water to obtain a 0.2 g/100 g solution. H_2O_2 solution was added to the TFPs solution with a final concentration of 0.5 g/100 g. The degradation processes were then conducted in an ultrasonic processor (KQ-250DE, Kunshan Ultrasonic Instrument Co., Ltd, Kunshan, China) by setting the amplitude of 50% on the controller panel. The degradation degree of TFPs was determined by measuring the viscosity of the TFPs solution with a viscometer (DV2T, Brookfield, Middleboro, MA, USA) at 25±0.5°C. The viscosity of the original TFPs solution was 106.7 mPa×s. The viscosity of the moderately degraded TFPs solution and the highly degraded TFPs solution was 22.4 and 5.7 mPa×s, respectively. The degraded TFPs were obtained by dialysis (cut-off of 1,000 Da) and lyophilization. The original TFPs with high molecular weight, moderately degraded TFPs, and highly degraded TFPs were named HM, MM, and LM, respectively.

Structure characterization

Carbohydrate content and monosaccharide composition analysis

The carbohydrate content of all samples was detected by phenol sulfuric acid analysis with mannose as a standard [Liu *et al.*, 2019]. The monosaccharide composition of HM was detected according to a previous method [Huang *et al.*, 2011] with slight modifications. In brief, 10 mg HM was dissolved with 4 mL of 2 M trifluoroacetic acid in a glass tube, sealed, and hydrolyzed at 121°C for 4 h. Acetylation was performed with 10 mg hydroxylamine hydrochloride and 0.5 mL pyridine for 30 min at 90°C, and next the mixture was cooled to room temperature. Then, 1 mL of acetic anhydride was added to the solution and reacted at 90°C for 30 min to obtain alditol acetate derivative. The alditol acetate derivative was analyzed using a 6890N Agilent gas chromatograph (Agilent, Santa Clara, CA, USA) with a DB-1701 capillary column (30 m×0.25 mm, Agilent). The chromatography

conditions were as follows: nitrogen flow rate: 1 mL/min; inlet temperature: 250°C; evaporation chamber temperature: 250°C; detector temperature: 300°C; injection volume: 1 μL; split ratio: 20:1. Glucose, fucose, mannose, galactose, arabinose, xylose, glucuronic acid, rhamnose were chosen as standards (Sigma-Aldrich, Saint Louis, MO, USA).

Nuclear magnetic resonance (NMR) and Fourier transform infrared spectroscopy (FT-IR) analysis

Thirty mg of HM sample were dissolved in 1.5 mL 99% D_2O and then lyophilized. This process was repeated two times. The lyophilized HM was dissolved with 0.8 mL of D_2O, and transferred to an NMR tube. ^1H and ^{13}C NMR spectra were obtained on a Bruker AVANCE III HD 600 NMR spectrometer (Bruker, Billerica, MA, USA). FT-IR spectra of the TFPs samples were measured in the range of 4,000–400 cm^{-1} by KBr-disk method using an FT-IR spectrometer (Nicolet IS50-Nicolet Continuum, Thermo Fisher Scientific, Waltham, MA, USA) [Li *et al.*, 2020]. OMNIC software (Thermo Fisher Scientific) was used for spectroscopy analysis.

Molecular weight analysis

The molecular weight distribution was determined by high-performance gel permeation chromatography (HPGPC) analysis [Liu *et al.*, 2019]. In brief, TFPs were dissolved to 2 mg/mL in mobile phase (0.02 M KH_2PO_4 solution, pH 6), then the TFP solutions were filtered through a 0.45 μm membrane filter, followed by injection into an HPGPC system (Ultimate 3000, Thermo Fisher Scientific) equipped with Ultrahydrogel 1000 (7.8×300 mm) and Ultrahydrogel 500 (7.8×300 mm) columns (Thermo Fisher Scientific). The flow rate was 0.8 mL/min. A calibration curve was plotted by measuring a series of dextran standards. Each run was recorded for 35 min. Additionally, the conformational characteristic of TFPs in solution was measured using the Congo red approach reported previously [Lee *et al.*, 2009]. Yeast β-glucan (Tokyo Chemical Industry Co., Ltd, Tokyo, Japan) was chosen as a positive control.

Anti-oxidation activity analysis *in vitro*

Determination of DPPH radical scavenging activity

DPPH radical (DPPH•) scavenging activity of TFPs was determined according to the previous method [Ye *et al.*, 2012] with slight modifications. Briefly, 2.0 mL of the TFP solution (150 and 300 μg/mL, respectively) were mixed with 2.0 mL of DPPH• (Sigma-Aldrich) dissolved in ethanol (0.02 mg/mL). Subsequently, the mixture was kept in a lucifugal cabinet at room temperature for 30 min. The absorbance of supernatant was measured at 517 nm using an ultraviolet-visible (UV-Vis) spectrophotometer (752N, Shanghai Jingke Scientific Instrument Co., Ltd, Shanghai, China) after centrifugation at 5,000×*g* for 10 min. Ascorbic acid (AA) was chosen as a positive control. The absorbance of the mixture was measured in triplicate and the test of DPPH• scavenging activity was repeated three times. The DPPH• scavenging activity was calculated using Equation (1).

$$\text{DPPH}^{\bullet}\text{ scavenging activity (\%)} = \left(1 - \frac{A_1 - A_2}{A_0}\right) \times 100 \quad (1)$$

where: A_1 is the absorbance of the solution containing TFPs and DPPH•; A_2 is the absorbance of the solution containing TFPs and ethanol; and A_0 is the absorbance of the solution containing only deionized water and DPPH•.

Determination of hydroxyl radical scavenging activity

The hydroxyl radical (•OH) scavenging activity was measured by the previously reported method [Liu *et al.*, 2009] with slight modification. Briefly, the hydroxyl radical was produced by mixing 0.4 mL of 0.2 M sodium phosphate buffer (pH 7.4), 0.6 mL of 5 mM 1,10-phenanthroline, 0.6 mL of 5 mM $FeSO_4$, and 0.8 mL of H_2O_2 (0.1 g/100 g). After adding 0.6 mL of the TFPs solution (150 and 300 μg/mL, respectively) or deionized water, the mixture was incubated at 37°C for 60 min. The absorbance was determined at 536 nm using a 752N UV-Vis spectrophotometer (Shanghai Jingke Scientific Instrument Co., Ltd) in triplicate. The •OH scavenging activity was calculated according to Equation (2).

$$\text{•OH scavenging activity (\%)} = \left(\frac{A_{sample} - A_{blank}}{A' - A_{sample}}\right) \times 100 \quad (2)$$

where: A' is the absorbance of the deionized water instead of H_2O_2; A_{sample} is the absorbance of TFPs solution, and A_{blank} is the absorbance of the deionized solution instead of TFPs solution. AA was used as a positive control. Test was repeated three times.

Determination of superoxide anion radical scavenging activity

The superoxide anion radical ($O_2^{\bullet-}$) scavenging activity was determined following the previously described method [Cao *et al.*, 2007] with some modifications. Briefly, 3.0 mL of the TFPs solution (150 and 300 μg/mL, respectively) or deionized water as a blank were added to 3.0 mL of 0.05 M Tris-HCl buffer (pH 8.2). The mixture was shaken thoroughly and incubated at 25°C for 20 min. Then, 100 μL of 5 mM pyrogallol (1,2,3-trihydroxybenzene) were added to the mixture and incubated at 25°C for 5 min. The absorbance was recorded at 325 nm using a 752N UV-Vis spectrophotometer (Shanghai Jingke Scientific Instrument Co., Ltd). Test was repeated three times. AA was chosen as a positive control. The $O_2^{\bullet-}$ scavenging activity was estimated using Equation (3).

$$O_2^{\bullet-}\text{ scavenging activity (\%)} = \left(1 - \frac{A_{sample}}{A_{blank}}\right) \times 100 \quad (3)$$

where: A_{sample} is the absorbance of the TFP solution, and A_{blank} is the absorbance of deionized water.

In vivo experiment

Animal and experiment procedure

Specific-pathogen-free (SPF) grade 4-week-old male Kunming mice (body weight, BW, 18±2 g) were purchased from Guangdong Medical Experimental Animal Center and raised in the Laboratory Animals Center at Guangzhou University of Chinese Medicine, Guangzhou, China. The animals were kept under SPF laboratory conditions: the room temperature was kept at 22±2°C under 60~80% relative humidity with a 12 h light/dark cycle.

Food and water were freely available to mice. Experimental procedures were consistent with the Health Guide for the Care and Use of Laboratory Animals of National Institutes and the China legislation concerning the use and care of laboratory animals and approved by the Ethical Committee of Guangzhou University of Chinese Medicine. After two weeks of adaption to the SPF environment, a total of 40 male mice were randomly assigned to five groups: Normal group, Model group, HM group, MM group, and LM group. Mice in the Normal group were intraperitoneally injected daily with physiological saline, while those in other groups were injected with D-galactose (Macklin Biochemical Co., Shanghai, China) at a dosage of 120 mg/kg of body weight (BW) instead [Zhao *et al.*, 2019]. Mice in the HM, MM, and LM groups were additionally administered orally with HM, MM, and LM, respectively, at a dosage of 100 mg/kg of BW per day. The treatment lasted for eight weeks. During the period of the experiment, trained and skilled animal technicians undertaken monitoring observations at least twice daily to minimize the pain in mice. At the end of the experiment, all mice were fasted for 12 h but had free access to water and then euthanized. Blood samples were collected and centrifuged to obtain serum at 5,000×*g* for 15 min at 4°C. The liver and heart tissues were immediately removed and washed with pre-cooled phosphate buffer saline (PBS) (Gibco, Thermo Fisher Scientific, Grand Island, NY, USA). A 1×1 cm^2 dorsal skin was collected from each mouse after hair removal. The contents of the small intestine and colon were collected separately on ice. All samples were stored at -80°C until further analysis within two months.

Determination of the content of hydroxyproline and hyaluronic acid in the skin

The skin sample was cut into about 2×2 mm^2 pieces and then ground into powder using a mortar under liquid nitrogen. Subsequently, the skin sample was treated with acetone-diethyl ether (1:1, *v/v*) to remove lipids. After drying, a 20 mg tissue sample was collected and then the content of hydroxyproline and hyaluronic acid was determined using a mouse hydroxyproline ELISA kit and a mouse hyaluronic acid ELISA kit, respectively, according to the manufacturer's instructions (Jiangsu Meimian Biotech., Yancheng, China).

Anti-oxidant enzyme activity and MDA content assays

The activities of SOD, GSH-Px, and the level of MDA in serum were determined using a SOD assay kit (WST-1 method), a GSH-PX assay kit (colorimetric method), and an MDA assay kit (thiobarbituric acid method), respectively, according to the manufacturer's instructions (Nanjing Jiancheng Bioengineering Institute, Nanjing, China). Additionally, 10% (*w/v*) liver and heart tissue PBS homogenates were prepared by tissue grinder (TissueLyser LT, QIAGEN, Hilden, Germany), and then supernatants were obtained by centrifugation (5,000×*g* for 15 min at 4°C), respectively. After protein quantification in supernatants by BCA kit (CoWin Biosciences, Beijing, China), the activities of SOD, GSH-Px and the levels of MDA were determined according to the kit manufacturer's instructions (Nanjing Jiancheng Bioengineering Institute).

Cytokine concentration assay in serum

The concentration of IL-1β and TNF-α in serum was measured according to the instructions of mouse IL-1β and TNF-α ELISA kits (Jiangsu Meimian Biotech.).

Measurement of pH and determination of the content of short-chain fatty acids in the gastrointestinal tract

The samples of the contents of the small intestine and colon were thawed and then diluted with pure neutral water in a ratio of 1:1 (*w/v*). The pH of the solution was measured with a pH meter (FE28, Mettler Toledo, Columbus, OH, USA). SCFAs contents in the small intestine and colon contents were determined using gas chromatography mass spectrometry (GC-MS) as previously reported [Zhao *et al.*, 2018] with slight modification. Briefly, 100 mg of intestinal contents were homogenized with 1.5 mL of phosphate buffer (pH 7.4) and centrifuged. One mL of supernatant was acidified by adding 0.5 mL of 50% (*v/v*) sulfuric acid. Then, organic extraction was performed by adding 2 mL of diethyl ether, followed by vortexing and centrifugation at 5,000×*g* for 5 min. The supernatants, after filtering by 0.22 μm membrane, were analyzed using the GC-MS system (GC-2010PLUS, Shimadzu, Kyoto, Japan) with a DB-FATWAX capillary column (30 m×0.25 mm, Agilent). Acetic, propionic, isobutyric, *n*-butyric, isovaleric, and *n*-valeric acids were used as standards (Macklin Biochemical Co., Shanghai, China). GC conditions: initial temperature 120°C maintained for 2 min, then heating up to 140°C at 5°C/min, held for 3 min, finally enhanced to 170°C at 10°C/min, kept for 5 min; the detector temperature was set at 250°C, the split ratio was 25:1, and the flow rate was 1.8 mL/min.

Statistical analysis

Data were expressed as mean ± standard deviation. The statistical differences between the groups of *in vivo* experiment were calculated using one-way analysis of variance (ANOVA) with Tukey's test using SPSS 22.0 (IBM Corp., Armonk, NY, USA). The differences were considered significant at $p<0.05$.

RESULTS AND DISCUSSIONS

Structure analysis

The carbohydrate content of high molecular weight polysaccharide (HM) of *T. fuciformis* fruiting body was 92.5 g/100 g dry weight. The degraded HM (MM) and highly degraded HM (LM) contained 93.1 and 93.5 g carbohydrates/100 g dry weight, respectively. The GC chromatogram of HM after its acid hydrolysis is shown in Figure 1A. The monosaccharide composition of HM mainly consisted of mannose, fucose, xylose, and glucose in a molar ratio of 4.14:0.98:0.81:0.62, which was estimated from the peak areas. A small amount of glucuronic acid and arabinose was also found in the HM sample. In the ^{1}H NMR spectrum of HM, the peaks in the range of δ 4.3–5.9 ppm (Figure 1 B) were the chemical shifts of the anomeric hydrogen in the sugar ring [Agrawal, 1992]. The peaks at δ 5.57, 5.41, 5.20, and 5.13 ppm demonstrated α-configuration in the polysaccharide molecules, while the peaks at δ 4.53, 4.51, and 4.40 ppm indicated β-configuration. In the ^{13}C NMR spectrum, multiple peaks

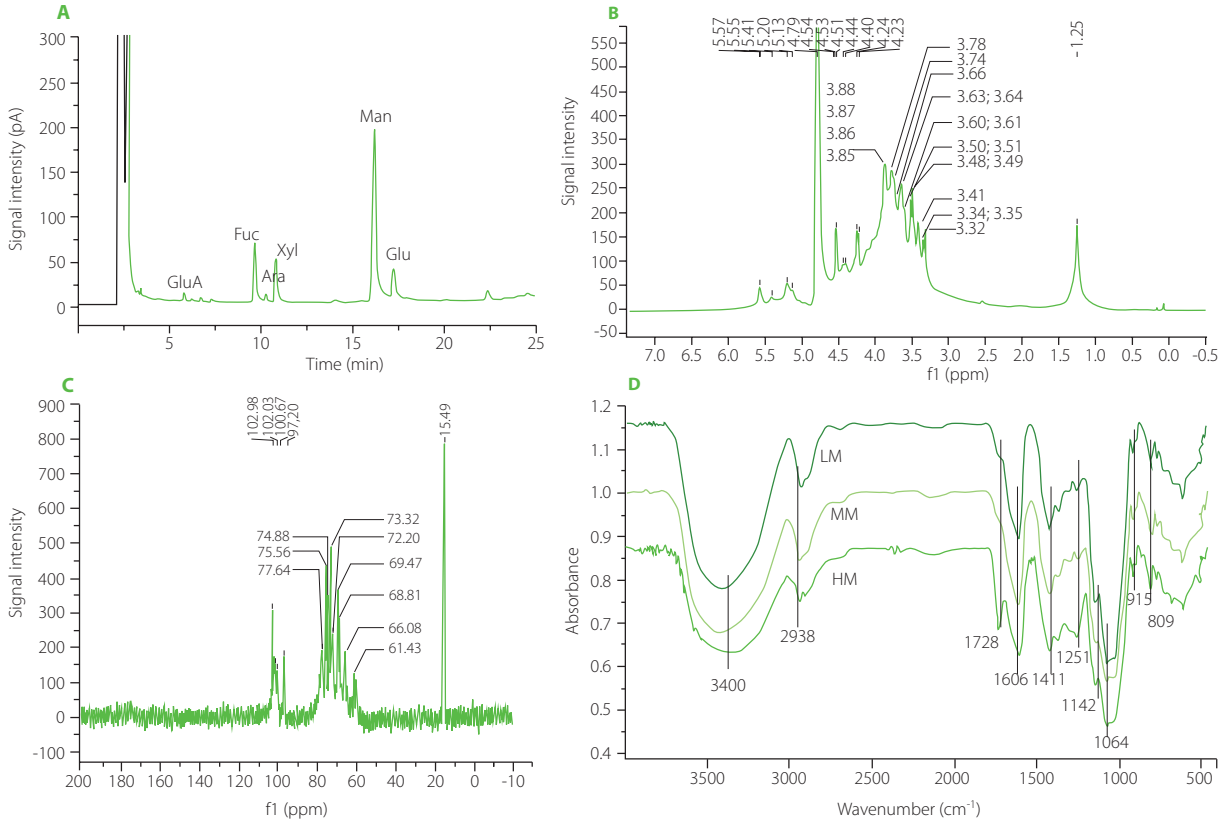

Figure 1. Results of structure analysis of high molecular weight *Tremella fuciformis* polysaccharide (HM), degraded HM (MM) and highly degraded HM (LM). (**A**) Gas chromatography separation of monosaccharides of HM after its hydrolysis; (**B**) ^{1}H NMR spectrum of HM; (**C**) ^{13}C NMR spectrum of HM; (**D**) Fourier-transform infrared spectra of HM, MM, and LM. GluA, glucuronic acid; Rha, rhamnose; Fuc, fucose; Ara, arabinose; Xyl, xylose; Man, mannose; Gal, galactose; Glu, glucose.

in the range of 95.00–110.00 ppm belonged to anomeric carbon signals [Agrawal, 1992], indicating that HM was composed of several monosaccharides (Figure 1C). Specifically, four peaks at δ102.98(C1), 102.03(C1), 100.67(C1), and 97.20(C1) ppm suggested the presence of four types of monosaccharides in the backbone chain of HM [Hu *et al.*, 2016], which was consistent with the results of GC-MS.

The FT-IR spectra of the HM, MM and LM samples showed similar infrared absorption profiles (Figure 1D). Characteristic peaks of the FT-IR spectra were presented at approximately 3,400; 2,938; 1,606; 1,411; 1,142; 1,064; 915, and 809 cm^{-1}. Absorption peaks were observed at 3,400 and 2,938 cm^{-1} due to the stretching vibration of O-H [Chen *et al.*, 2020] and C-H [Jeong *et al.*, 2019], respectively. The peak at 1,606 cm^{-1} is attributed to the bound water in the samples [Velazquez *et al.*, 2003]. Absorption bands in the region of 1,200-1,000 cm^{-1} are typical for polysaccharide molecules due to the stretching vibration of C-O, C-C, and the angular vibration of C-O-H [Barker *et al.*, 1954]. The peak at 915 cm^{-1} indicates the presence of D-glucopyranosyl [Zhang *et al.*, 2013], and the peak at 809 cm^{-1} suggests the presence of α-D-mannopyranose in molecules [Wang *et al.*, 2015; Zhang *et al.*, 2013]. These results indicated that US/H_2O_2 treatment did not affect the major functional groups of TFPs.

In the HPGPC chromatograms of HM, MM and LM (Figure 2A–C), the large peak before the retention time of 20 min belongs to TFPs, and the small peak after 25 min is attributed to the used solvent. HM exhibited a narrow peak, while both MM and LM showed wide peaks, suggesting that US/H_2O_2 treatment reduced the uniformity of polysaccharide molecules. The retention time of the peak for HM, MM, and LM was 13.26, 14.59, and 18.91 min, respectively, corresponding to a molecular weight of 58.3×10^6, 4.68×10^6, and 3.14×10^5 Da, elucidating a gradual approximately 10-fold reduction in the average molecular weight for the three TFPs. Further, the conformation was measured by Congo red method. The maximum absorption wavelength (λ_{max}) of all TFPs solutions gradually declined with increasing NaOH concentration (0–0.5 M), similar to the feature of the Congo red solution (Figure 2D). There was no noticeable shift of λ_{max} in TFPs solutions, demonstrating the absence of triple helix conformation in all TFPs samples. On the contrary, the obvious shift of λ_{max} in yeast β-glucan solution demonstrated that triple helix β-glucan-Congo red complexes formed in the solution.

As a result, HM was found to be novel heteropolysaccharide derived from the fruiting body of *T. fuciformis* based on the monosaccharide composition and the molecular weight distribution, which exhibited a larger molecular weight than previously reported ones [Wu *et al.*, 2019; Yang *et al.*, 2019]. The possible reason for this, besides the resource and purification method, might be the differences in the drying process of the fruiting body of *T. fuciformis* [Lin & Tsai, 2019]. By a combined method of US/H_2O_2 treatment, two TFPs with gradient-decreased molecular weight were prepared successfully. Because US/H2O_2 treatment did not

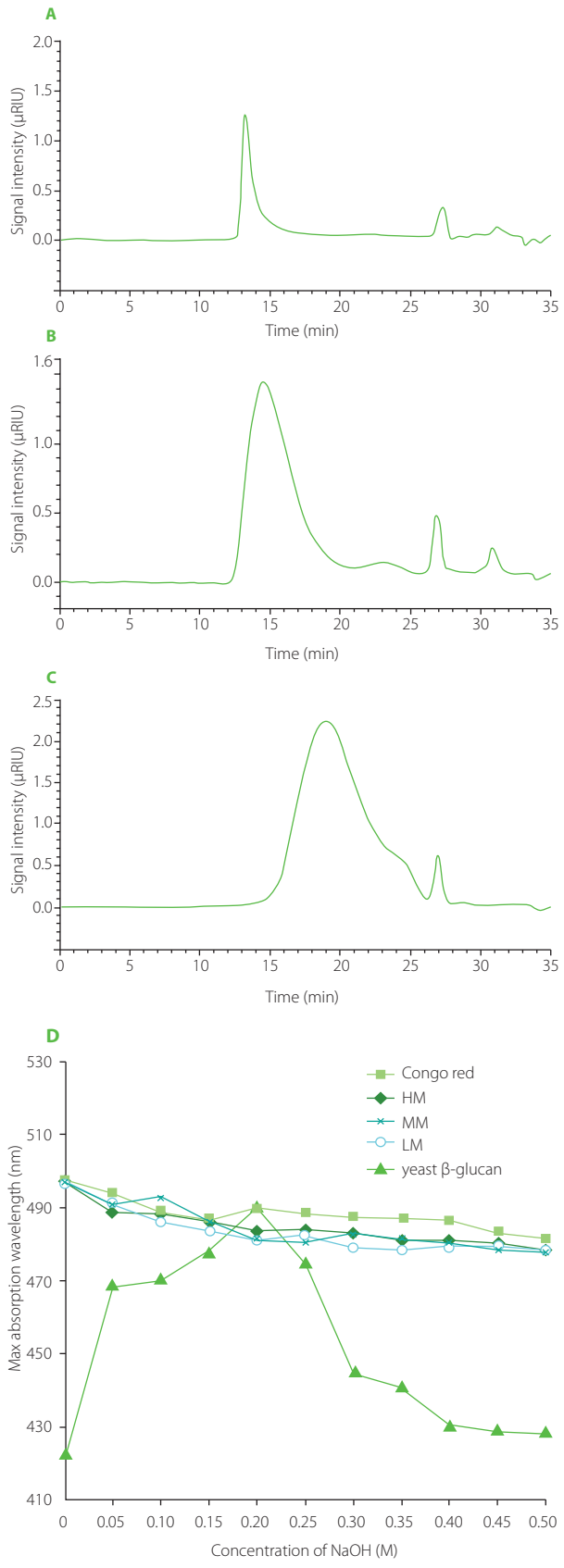

Figure 2. Molecular weight distribution and results of conformation analysis of high molecular weight *Tremella fuciformis* polysaccharide (HM), degraded HM (MM) and highly degraded HM (LM). High-performance gel permeation chromatography (HPGPC) of HM (**A**), MM (**B**), and LM (**C**). (**D**) Maximum absorption wavelength of Congo red solution with polysaccharides and yeast β-glucan at different concentrations of NaOH.

change the primary structures of TFPs, such as monosaccharide composition and glycosidic linkages in the main backbone [Li *et al.*, 2020], therefore, the following anti-oxidant and anti-aging experiments using the three TFPs could mainly focus on the effects of polysaccharides with different molecular weights on bioactivity.

Anti-oxidant activity *in vitro*

As shown in Figure 3, the scavenging activity against DPPH radical, hydroxyl radical, and superoxide anion radical exhibited a concentration-dependent manner and ranged from 5.86 to 14.67% for HM, 2.75 to 11.52% for MM, and 4.75 to 18.95% for LM, respectively, although significantly higher values were determined for AA. Notably, the radical scavenging activity of the three samples also displayed a molecular weight-dependent manner, except for superoxide anion radical when TFPs were applied at a concentration of 150 μg/mL. Specifically, the radical scavenging activity decreased in a sequence of LM, MM, and HM. Unsurprisingly, LM showed the best anti-oxidant activities among the three TFPs. This was consistent with the previous findings that polysaccharides with low molecular weight have higher anti-oxidant activity than those with high molecular weight [Li *et al.*, 2020; Ogutu & Mu, 2017]. Possible reasons might be that polysaccharides with lower molecular weight contained more polysaccharide fractions under the same concentration, which resulted in more hydroxyl groups in molecules being exposed to free radicals in solutions, leading to a higher scavenging activity against radicals [Li *et al.*, 2020; Wu *et al.*, 2018].

Effects of TFPs on D-galactose-induced aging mice

Skin anti-aging activity

During the experimental period, the mice in the Normal group moved flexibly with shiny fur. In contrast, the mice in the Model group were inactive, with fur dull and messy. The behavior and the fur color of the mice improved obviously in the TFPs--treated groups, compared with the Model group. The body weight of the mice in all groups increased gradually and no statistically significant differences were observed between the groups (data not shown). To assess the degree of skin aging, the content of hydroxyproline and hyaluronic acid was evaluated in five groups. As presented in Figure 4, the content of hydroxyproline and hyaluronic acid was extremely lower in the Model group than in the Normal group ($p<0.01$), demonstrating that eight--week treatment with D-galactose substantially accelerated skin aging in mice. Treatments with HM, MM, and LM obviously increased the content of hydroxyproline in the skin by 91.9, 101.4, and 94.6%, respectively, compared with the Model group ($p<0.01$). Similarly, administrations of HM, MM, and LM also greatly improved the content of hyaluronic acid by 34.3, 103.3, and 73.4%, respectively, compared with the Model group ($p<0.01$). These results further confirmed the anti-aging effects of TFPs reported in previous studies [Wen *et al.*, 2016; Zhang *et al.*, 2014]. In particular, MM displayed the best performance in ameliorating the loss of hydroxyproline and hyaluronic acid induced by D-galactose treatment among the three samples.

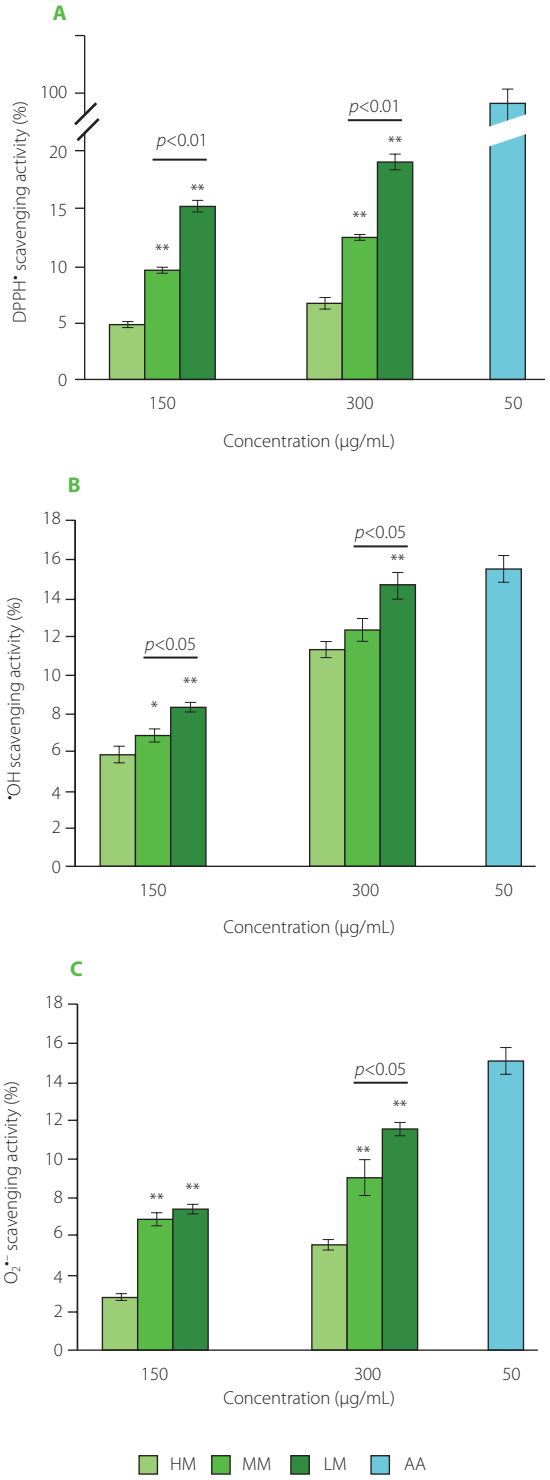

Figure 3. Scavenging activities of high molecular weight *Tremella fuciformis* polysaccharide (HM), degraded HM (MM) and highly degraded HM (LM) against DPPH radical (**A**), hydroxyl radical (**B**), and superoxide anion radical (**C**). AA, ascorbic acid. *, ** represent $p<0.05$, and $p<0.01$, respectively, compared with the HM at the same concentration.

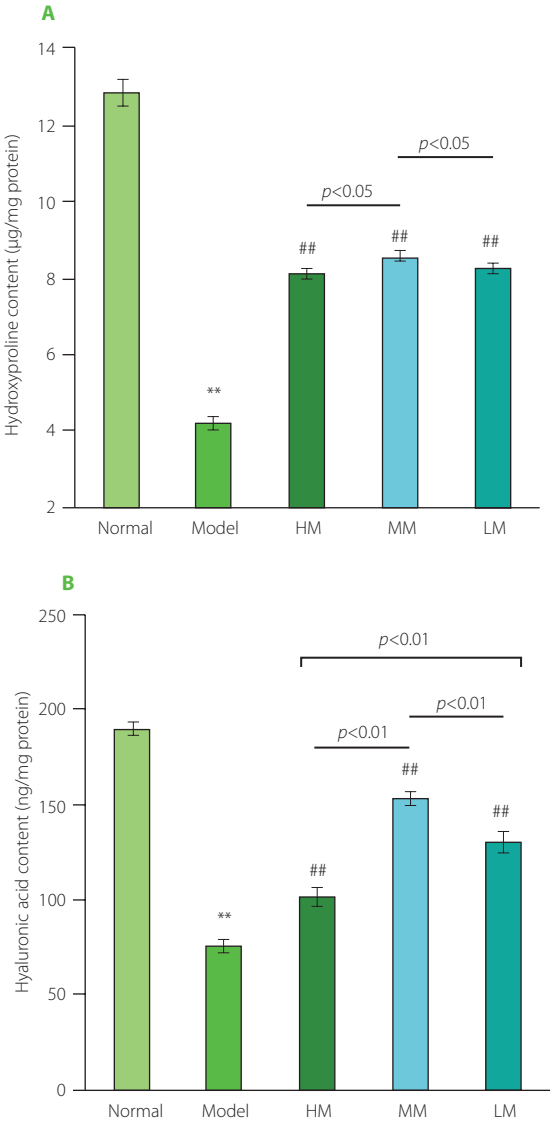

Figure 4. The contents of hydroxyproline (**A**) and hyaluronic acid (**B**) in the skin of D-galactose-induced aging mice treated with high molecular weight *Tremella fuciformis* polysaccharide (HM), degraded HM (MM) and highly degraded HM (LM). *, ** represent $p<0.05$, $p<0.01$, respectively, compared with the Normal group; #, ## represent $p<0.05$, $p<0.01$, respectively, compared with the Model group.

Anti-oxidative stress parameters

In comparison with the Normal group, as shown in Figure 5, treatment with D-galactose substantially decreased the activities of SOD and GSH-Px ($p<0.01$) and dramatically promoted the production of MDA ($p<0.01$) in serum, liver, and heart tissues in mice in the Model group. These results further elucidated that the aging mouse model was established successfully. Notably, three TFPs samples significantly improved the activities of SOD and GSH-Px in serum, liver, and heart tissues in D-galactose-treated mice ($p<0.05$ or $p<0.01$), except for the activity of SOD in heart in the HM group and the activity of GSH-Px in serum in the HM and LM groups. Correspondingly, the level of MDA obviously decreased in serum, liver, and heart tissues in three groups ($p<0.05$ or $p<0.01$) except for liver tissue in the HM group. These results demonstrated that all tested TFPs could mitigate oxidative stress in D-galactose-induced aging mice. Particularly, MM showed the highest efficacy in relieving oxidative stress among the three TFPs.

Notably, the degree of amelioration of skin aging, evidenced by the increased contents of hydroxyproline and hyaluronic acid in the skin, was consistent with the reduction of oxidative stress induced by the three TFPs. This further demonstrated that

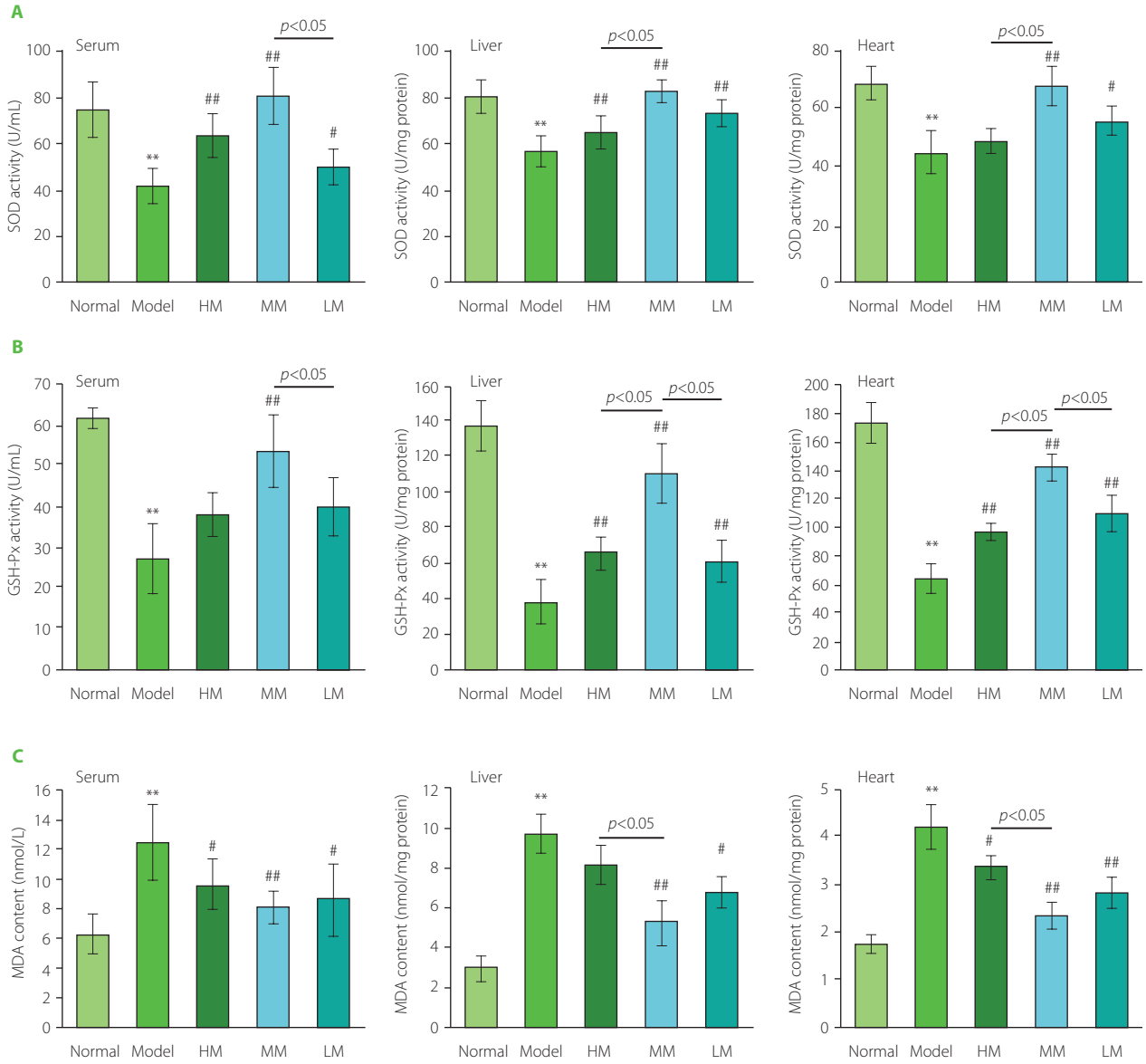

Figure 5. The activities of superoxide dismutase (SOD) (**A**), glutathione peroxidase (GSH-Px) (**B**), and the level of malondialdehyde (MDA) (**C**) in serum, liver, and heart in D-galactose-induced aging mice treated with high molecular weight *Tremella fuciformis* polysaccharide (HM), degraded HM (MM) and highly degraded HM (LM). *, ** represent $p<0.05$, $p<0.01$, respectively, compared with the Normal group; #, ## represent $p<0.05$, $p<0.01$, respectively, compared with the Model group.

the ameliorating effect of TFPs on skin aging could be partially attributed to the improvement in the activity of anti-oxidant enzymes [Wen *et al.*, 2016]. Antioxidants (*e.g.*, polyphenols) provide anti-oxidant protection against oxidative damage *in vivo* by regulating complicated intracellular signals for induction of anti-oxidant enzymes [Forman *et al.*, 2014; Forman & Zhang, 2021]. The nuclear factor erythroid 2-like 2 (Nrf2) is a critical regulator of anti-oxidative responses in intracellular signaling pathways [Vomund *et al.*, 2017]. Nrf2/antioxidant response element (ARE) signaling pathway plays key roles in maintaining intracellular redox homeostasis [Saha *et al.*, 2020]. In a recent study, *Grifola frondose*-derived polysaccharides elevated anti-oxidative capacity in an acute liver injury mouse model by regulating the Nrf2/ARE signaling pathway [Meng *et al.*, 2021]. These results provide new clues for revealing the molecular mechanisms underlying the anti-oxidant activities of TFPs *in vivo*. Further studies are needed to demonstrate the molecular mechanism and the correlation between the molecular weight of polysaccharides and the expression profiles of anti-oxidant genes in the mammalian model.

Anti-inflammatory activity

As shown in Figure 6, the levels of IL-1β and TNF-α substantially increased in the Model group by 2.45 and 3.01 times, respectively, compared with the Normal group, indicating a high level of inflammation in D-galactose-induced aging mice. The levels of IL-1β and TNF-α in all three TFPs-treated groups were lower than those in the Model group ($p<0.01$), demonstrating the excellent anti-inflammatory activity of the samples tested. Specifically, the order of the anti-inflammatory activity of the three TFPs samples was MM, LM, and HM. MM showed the best anti-inflammatory activity among the three TFPs, demonstrating an important role of molecular weight in influencing bioactivity

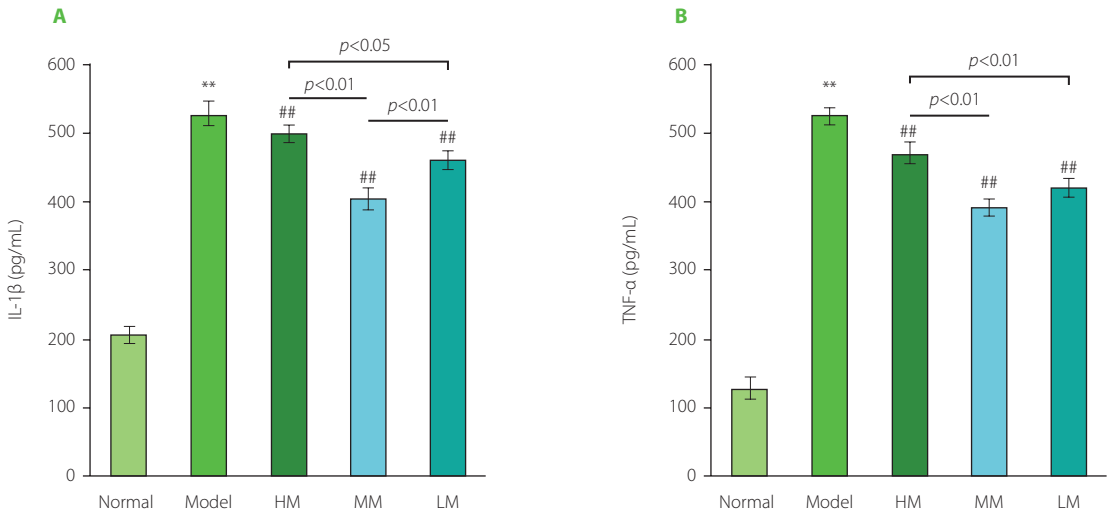

Figure 6. The levels of interleukin 1β (IL-1β) (**A**) and tumor necrosis factor α (TNF-α) (**B**) in serum of D-galactose-induced aging mice treated with high molecular weight *Tremella fuciformis* polysaccharide (HM), degraded HM (MM) and highly degraded HM (LM). ** represent $p<0.01$, compared with the Normal group; ## represent $p<0.01$, compared with the Model group.

for mushroom polysaccharides. Pretreatment with TFPs could attenuate lipopolysaccharide (LPS)-induced oxidative stress and inflammation by inhibiting nuclear factor κB (NF-κB) activation through downregulating miR-155 expression, one of the key small RNAs regulating NF-κB activation, in RAW264.7 macrophages [Ruan *et al.*, 2018]. Numerous studies have documented that mushroom polysaccharides and their metabolites produced by gut microbiota, such as SCFAs, display anti-inflammatory activities through multiple pathways, including modulation of immune cell receptor-involved NF-κB signaling pathway and promotion of the proliferation and differentiation of Foxp3+ regulatory T-cells [Liu *et al.*, 2022]. Given the diverse structures of TFPs [Wu *et al.*, 2019], the low absorption rate of TFPs through oral administration route (only 0.4% in rat) [Gao *et al.*, 2002], and the complexity of gut microbiota in the metabolism of polysaccharides [Song *et al.*, 2021], there remain complex challenges in fully understanding the molecular mechanism of anti-inflammatory activity of TFPs *in vivo*. However, efforts need to be undertaken in future work.

Matrix metalloproteinases (MMPs) can degrade a variety of components of the extracellular matrix (ECM), such as collagen and hyaluronic acid [Chen *et al.*, 2013]. Higher levels of MMPs are observed in aged human skin, and MMPs play an important role in the remodeling of ECM in skin aging [Shin *et al.*, 2019]. Inflammation increases the levels of MMPs in the vascular wall and plasma of obese women [Ozen *et al.*, 2019], suggesting an association between the level of inflammation and the level of MMPs. Mechanically, the activation of activator protein 1 (AP-1) and NF-κB-related intracellular signaling pathways increases the expression of MMPs [Shin *et al.*, 2019], indicating that overproduction of reactive oxygen species (ROS) and a high level of pro-inflammatory cytokines would promote the levels of MMPs. TFPs could inhibit NF-κB activation under inflammatory status in cells [Ruan *et al.*, 2018]. As a theoretical speculation, TFPs might regulate the level of MMPs in aging mice *via* the inactivation of NF-κB-related signaling pathway, leading to a decreased level of MMPs in the skin. In the present study, the degree of amelioration in the loss of hydroxyproline and hyaluronic acid in the aging skin was positively associated with the reduction of inflammatory cytokine levels. This further indicated that the anti-skin aging effect of TFPs, evidenced by amelioration in the loss of hydroxyproline and hyaluronic acid in the skin, might be partially attributed to their anti-inflammatory actions. Further animal experiments should be considered in future studies to elucidate the molecular mechanism of TFPs in modulating MMPs expression.

Alterations in pH and SCFAs production in the gut

To investigate the responses of the gastrointestinal environment to TFPs treatment, the pH and content of SCFAs (acetic acid, propionic acid, *n*-butyric acid, isobutyric acid, *n*-valeric acid, and isovaleric acid) were determined. As shown in Figure 7A and 7B, the pH in the small intestine was weakly alkaline, while the pH in the colon was slightly acidic. There was no statistical difference ($p\geq0.05$) in pH in the small intestinal environment among the five groups. On the contrary, in the colon, the pH in the Model group was lower than that in the Normal group ($p<0.01$), suggesting alterations in microbial metabolites in the colonic environment in D-galactose-treated mice. TFPs treatments differentially reversed the decrease in pH in the colon in D-galactose-treated mice. Interestingly, the pH in the HM group increased significantly (6.50 *vs.* 5.92, $p<0.01$), compared with the Model group. Notably, the pH was higher in the HM group than in the LM group ($p<0.05$), suggesting the differential impacts of the three TFPs on gut microbial metabolism.

Furthermore, almost no SCFAs were detected in the small intestinal contents in all mice. By contrast, acetic acid and propionic acid were the predominant SCFAs in the colon, followed by *n*-butyric acid (Figure 7D). An unexpected increase in the amount of total SCFAs was observed in the Model group ($p<0.01$,

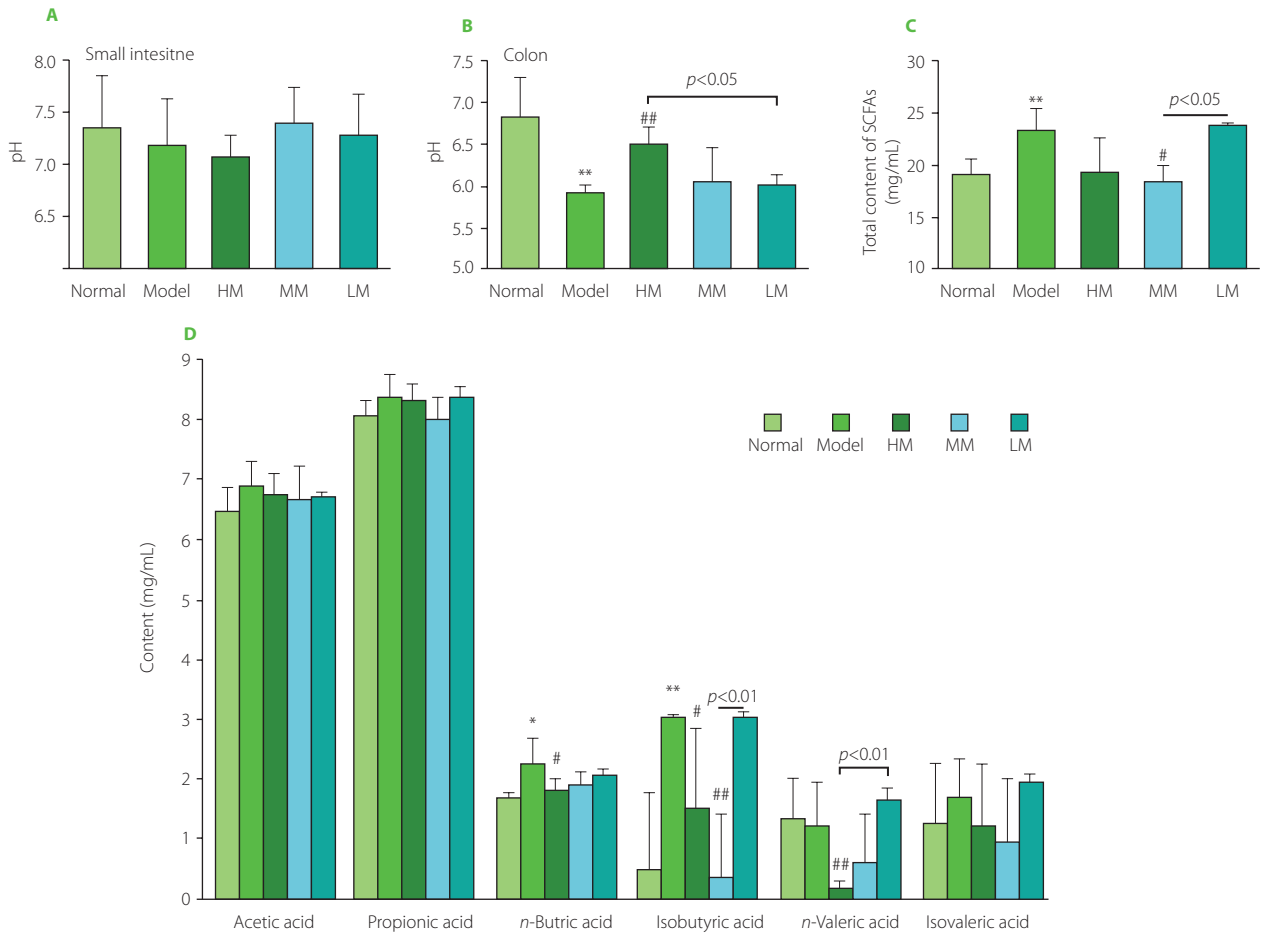

Figure 7. Values of pH in the small intestine (**A**) and colon (**B**), and the total amount of short-chain fatty acids (SCFAs) (**C**) and the production of individual SCFAs in the colon of D-galactose-induced aging mice treated with high molecular weight *Tremella fuciformis* polysaccharide (HM), degraded HM (MM) and highly degraded HM (LM). *, ** represent $p<0.05$, $p<0.01$, respectively, compared with the Normal group; #, ## represent $p<0.05$, $p<0.01$, respectively, compared with the Model group.

Figure 7C). Notably, the amount of total SCFAs in the HM and MM groups decreased, compared with the Model group, whereas the amount of total SCFAs in the LM group was equivalent to that in the Model group. These observations indicated that TFPs with different molecular weights might preferentially be utilized by different SCFAs-producing bacteria and, therefore, exert differential impacts on the colonic microbial metabolism. In previous studies, a decrease in the contents of SCFAs in feces in mice, as well as reduced richness and diversity of the gut microbiota, was induced by D-galactose treatment [Zhang J. *et al.*, 2017; Zhang Z. *et al.*, 2020]. The opposite results of SCFAs production in the current study might be attributed to the differences in housing environments and mouse species, since environmental factors and genetic background strongly influence the composition of gut microbiota [Ericsson *et al.*, 2018]. More investigations are needed to clarify the relationship between the changes in SCFAs production and the progress of aging.

In detail, among the individual SCFAs, the contents of *n*-butyric acid and isobutyric acid in the Model group increased significantly ($p<0.05$ and $p<0.01$), whereas the others did not change obviously, compared with the Normal group (Figure 7D). However, HM and MM treatments markedly reversed the abnormal increases in *n*-butyric acid and isobutyric acid production in D-galactose-treated mice. In particular, the contents of isobutyric acid in the MM group and *n*-valeric acid in the HM group were dramatically decreased compared with those of the Model and LM groups. The inconsistent profiles of the SCFAs in three groups indicated the complicated impacts of TFPs with different structures on microbial metabolism.

Generally, mushroom polysaccharides can modulate gut microbial composition and increase SCFAs-producing bacteria, leading to increased contents of SCFAs in the gut [Li *et al.*, 2021]. Conversely, HM and MM treatments induced a decrease in the amount of total SCFAs. These phenomena suggested that the contents of SCFAs in the gut might vary in a physiological range for a healthy host. For example, an increased total content of SCFAs in the obese subjects was reported compared to the lean ones [Schwiertz *et al.*, 2010]. TFPs might modulate gut microbial community to maintain gut homeostasis through direct and indirect routes. On the one hand, TFPs might reverse the abnormal increase in contents of SCFAs induced by D-galactose treatment through directly modulating the intestinal microbiota due to the prebiotic properties of mushroom polysaccharides [Li *et al.*, 2021]; on the other hand, TFPs could stimulate intestinal mucosal immune responses which, in turn, shape the intestinal microbial composition, resulting in a restoration of the contents of SCFAs. Recent experimental

evidence revealed the bioactive properties of TFPs in the restoration of the gut microbiota in dextran sodium sulfate (DSS)-induced colitis model [Xiao *et al.*, 2021; Xu *et al.*, 2021], as well as the direct anti-inflammatory activity *in vitro* [Ruan *et al.*, 2018; Xiao *et al.*, 2021], suggesting the dual roles of TFPs in modulating gut microbiota. Additionally, oat β-glucan with a lower average molecular weight exhibited a higher production of SCFAs in the *in vitro* gut fermentation model [Dong *et al.*, 2020], partially explaining that LM induced the highest production of SCFAs in the gut among the three TFPs samples. However, well-designed experiments, such as those using a germ-free mouse model and gut microbiota transplantation technology, are urgently needed to reveal whether the alterations in gut microbiota composition and metabolites are a consequence of mushroom polysaccharide interventions or a cause of health benefits of mushroom polysaccharides.

CONCLUSIONS

TFPs with high molecular weight, mainly consisting of mannose, fucose, xylose, and glucose, and two differentially degraded TFPs were obtained from the fruiting body of *T. fuciformis*. Three TFPs with gradient-decreased molecular weight by approximately 10--times, 58.3×10^6, 4.68×10^6, and 3.14×10^5 Da, respectively, showed concentration- and molecular weight-dependent activities in scavenging free radicals *in vitro*. Furthermore, three TFPs effectively relieved aging features in D-galactose-induced aging mice, as evidenced by amelioration of the loss of hydroxyproline and hyaluronic acid in the skin, increased activities of GSH-Px and SOD, and decreased levels of MDA in the serum, liver, and heart tissues, reduced levels of inflammatory cytokines in the serum, and partial restoration of the alterations in pH and SCFAs production in the colon. Particularly, TFPs with the medium molecular weight exhibited the best performance in ameliorating skin aging, reducing oxidative stress, and anti-inflammation. These results not only confirmed the antioxidant activity of TFPs, but more importantly revealed a preliminary relationship between molecular weight and anti-aging activity of TFPs *in vivo*.

RESEARCH FUNDING

This work was supported in part by the program for scientific research start-up funds of Guangdong Ocean University.

ACKNOWLEDGEMENTS

The authors appreciate Prof. Xuewu Zhang and Prof. Xiaolin Wu, College of Food Science and Engineering, South China University of Technology, for help in writing.

CONFLICT OF INTERESTS

The authors declare no conflicts of interest.

ORCID IDS

J. Guan https://orcid.org/0009-0008-6865-4162
Y. Hua https://orcid.org/0009-0008-6466-331X
G. Jiang https://orcid.org/0009-0009-4694-0579
X. Liu https://orcid.org/0009-0005-6249-4194
D. Luo https://orcid.org/0000-0002-8584-7344
X. Xu https://orcid.org/0000-0001-9177-9723
X. Zhang https://orcid.org/0009-0000-7947-138X

REFERENCES

1. Agrawal, P.K. (1992). NMR spectroscopy in the structural elucidation of oligosaccharides and glycosides. *Phytochemistry*, *31*(10), 3307–3330. https://doi.org/10.1016/0031-9422(92)83678-R
2. Barker, S.A., Bourne, E.J., Stacey, M., Whiffen, D.H. (1954). Infra-red spectra of carbohydrates. Part I. Some derivatives of D-glucopyranose. *Journal of the Chemical Society (Resumed)*, 171–176. https://doi.org/10.1039/jr9540000171
3. Cao, S., Zhan, H., Fu, S., Chen, L. (2007). Regulation of superoxide anion radical during the oxygen delignification process. *Chinese Journal of Chemical Engineering*, *15*(1), 132–137. https://doi.org/10.1016/S1004-9541(07)60046-9
4. Chen, Q., Jin, M., Yang, F., Zhu, J., Xiao, Q., Zhang, L. (2013). Matrix metalloproteinases: Inflammatory regulators of cell behaviors in vascular formation and remodeling. *Mediators of Inflammation*, *2013*, art. no. 928315. https://doi.org/10.1155/2013/928315
5. Chen, X., Zhang, R., Li, Y., Li, X., You, L., Kulikouskaya, V., Hileuskaya, K. (2020). Degradation of polysaccharides from *Sargassum fusiforme* using UV/H_2O_2 and its effects on structural characteristics. *Carbohydrate Polymers*, *230*, art. no. 115647. https://doi.org/10.1016/j.carbpol.2019.115647
6. Dong, J.L., Yang, M., Zhu, Y.Y., Shen, R.L., Zhang, K.Y. (2020). Comparative study of thermal processing on the physicochemical properties and prebiotic effects of the oat β-glucan by *in vitro* human fecal microbiota fermentation. *Food Research International*, *138*(Part B), art. no. 109818. https://doi.org/10.1016/j.foodres.2020.109818
7. Ericsson, A.C., Gagliardi, J., Bouhan, D., Spollen, W.G., Givan, S.A., Franklin, C.L. (2018). The influence of caging, bedding, and diet on the composition of the microbiota in different regions of the mouse gut. *Scientific Reports*, *8*(1), art. no. 4065. https://doi.org/10.1038/s41598-018-21986-7
8. Ferreira, S.S., Passos, C.P., Madureira, P., Vilanova, M., Coimbra, M.A. (2015). Structure–function relationships of immunostimulatory polysaccharides: A review. *Carbohydrate Polymers*, *132*, 378–396. https://doi.org/10.1016/j.carbpol.2015.05.079
9. Forman, H.J., Davies, K.J.A., Ursini, F. (2014). How do nutritional antioxidants really work: Nucleophilic tone and para-hormesis *versus* free radical scavenging *in vivo*. *Free Radical Biology and Medicine*, *66*, 24–35. https://doi.org/10.1016/j.freeradbiomed.2013.05.045
10. Forman, H.J., Zhang, H. (2021). Targeting oxidative stress in disease: promise and limitations of antioxidant therapy. *Nature Reviews Drug Discovery*, *20*(9), 689–709. https://doi.org/10.1038/s41573-021-00233-1
11. Gao, Q., Chen, H., Wang, K., Shen, Y. (2002). Studies on the absorption, distribution and clearance of *Tremella* polysaccharide in rats. *Chinese Pharmaceatical Journal*, *37*(3), 205–208.
12. Ge, X., Huang, W., Xu, X., Lei, P., Sun, D., Xu, H., Li, S. (2020). Production, structure, and bioactivity of polysaccharide isolated from *Tremella fuciformis* XY. *International Journal of Biological Macromolecules*, *148*, 173–181. https://doi.org/10.1016/j.ijbiomac.2020.01.021
13. Heinrich, M., Appendino, G., Efferth, T., Fürst, R., Izzo, A.A., Kayser, O., Pezzuto, J.M., Viljoen, A. (2020). Best practice in research – Overcoming common challenges in phytopharmacological research. *Journal of Ethnopharmacology*, *246*, art. no. 112230. https://doi.org/10.1016/j.jep.2019.112230
14. Hu, P., Li, Z., Chen, M., Sun, Z., Ling, Y., Jiang, J., Huang, C. (2016). Structural elucidation and protective role of a polysaccharide from *Sargassum fusiforme* on ameliorating learning and memory deficiencies in mice. *Carbohydrate Polymers*, *139*, 150–158. https://doi.org/10.1016/j.carbpol.2015.12.019
15. Huang, S.Q., Li, J.W., Li, Y.Q., Wang, Z. (2011). Purification and structural characterization of a new water-soluble neutral polysaccharide GLP-F1-1 from *Ganoderma lucidum*. *International Journal of Biological Macromolecules*, *48*(1), 165–169. https://doi.org/10.1016/j.ijbiomac.2010.10.015
16. Huang, X., Nie, S. (2015). The structure of mushroom polysaccharides and their beneficial role in health. *Food Function*, *6*(10), 3205–3217. https://doi.org/10.1039/C5FO00678C
17. Jeong, H.K., Lee, D., Kim, H.P., Baek, S.H. (2019). Structure analysis and antioxidant activities of an amylopectin-type polysaccharide isolated from dried fruits of *Terminalia chebula*. *Carbohydrate Polymers*, *211*, 100–108. https://doi.org/10.1016/j.carbpol.2019.01.097
18. Lee, H.H., Lee, J.S., Cho, J.Y., Kim, Y.E., Hong, E.K. (2009). Structural characteristics of immunostimulating polysaccharides from *Lentinus edodes*. *Journal of Microbiology and Biotechnology*, *19*(5), 455–461. https://doi.org/10.4014/jmb.0809.542
19. Li, M., Ma, F., Li, R., Ren, G., Yan, D., Zhang, H., Zhu, X., Wu, R., Wu, J. (2020). Degradation of *Tremella fuciformis* polysaccharide by a combined ultra-

sound and hydrogen peroxide treatment: Process parameters, structural characteristics, and antioxidant activities. *International Journal of Biological Macromolecules*, *160*, 979–990.
https://doi.org/10.1016/j.ijbiomac.2020.05.216
20. Li, M., Yu, L., Zhao, J., Zhang, H., Chen, W., Zhai, Q., Tian, F. (2021). Role of dietary edible mushrooms in the modulation of gut microbiota. *Journal of Functional Foods*, *83*, art. no. 104538.
https://doi.org/10.1016/j.jff.2021.104538
21. Lin, C.P., Tsai, S.Y. (2019). Differences in the moisture capacity and thermal stability of *Tremella fuciformis* polysaccharides obtained by various drying processes. *Molecules*, *24*(15), art. no. 2856.
https://doi.org/10.3390/molecules24152856
22. Liu, J., Luo, J., Ye, H., Sun, Y., Lu, Z., Zeng, X. (2009). Production, characterization and antioxidant activities *in vitro* of exopolysaccharides from endophytic bacterium *Paenibacillus polymyxa* EJS-3. *Carbohydrate Polymers*, *78*(2), 275–281.
https://doi.org/10.1016/j.carbpol.2009.03.046
23. Liu, X., Luo, D., Guan, J., Chen, J., Xu, X. (2022). Mushroom polysaccharides with potential in anti-diabetes: Biological mechanisms, extraction, and future perspectives: A review. *Frontiers in Nutrition*, *9*, art. no. 1087826.
https://doi.org/10.3389/fnut.2022.1087826
24. Liu, X., Wang, X., Xu, X., Zhang, X. (2019). Purification, antitumor and anti-inflammation activities of an alkali-soluble and carboxymethyl polysaccharide CMP33 from *Poria cocos*. *International Journal of Biological Macromolecules*, *127*, 39–47.
https://doi.org/10.1016/j.ijbiomac.2019.01.029
25. Meng, M., Zhang, R., Han, R., Kong, Y., Wang, R., Hou, L. (2021). The polysaccharides from the *Grifola frondosa* fruiting body prevent lipopolysaccharide/d-galactosamine-induced acute liver injury *via* the miR-122-Nrf2/ARE pathways. *Food and Function*, *12*(5), 1973–1982.
https://doi.org/10.1039/D0FO03327H
26. Ogutu, F.O., Mu, T.H. (2017). Ultrasonic degradation of sweet potato pectin and its antioxidant activity. *Ultrasonics Sonochemistry*, *38*, 726–734.
https://doi.org/10.1016/j.ultsonch.2016.08.014
27. Oliveira, R., Marques, F., Azeredo, J. (1999). Purification of polysaccharides from a biofilm matrix by selective precipitation of proteins. *Biotechnology Techniques*, *13*(6), 391–393.
https://doi.org/10.1023/A:1008954301470
28. Ozen, G., Boumiza, S., Deschildre, C., Topal, G., Longrois, D., Jakobsson, P.J., Michel, J.B., Jacob, M.P., Chahed, K., Norel, X. (2019). Inflammation increases MMP levels via PGE_2 in human vascular wall and plasma of obese women. *International Journal of Obesity*, *43*(9), 1724–1734.
https://doi.org/10.1038/s41366-018-0235-6
29. Ruan, Y., Li, H., Pu, L., Shen, T., Jin, Z. (2018). *Tremella fuciformis* polysaccharides attenuate oxidative stress and inflammation in macrophages through miR-155. *Analytical Cellular Pathology*, *2018*, art. no. 5762371.
https://doi.org/10.1155/2018/5762371
30. Saha, S., Buttari, B., Panieri, E., Profumo, E., Saso, L. (2020). An overview of Nrf2 signaling pathway and its role in inflammation. *Molecules*, *25*(22), art. no. 5474.
https://doi.org/10.3390/molecules25225474
31. Schwiertz, A., Taras, D., Schäfer, K., Beijer, S., Bos, N.A., Donus, C., Hardt, P.D. (2010). Microbiota and SCFA in lean and overweight healthy subjects. *Obesity*, *18*(1), 190–195.
https://doi.org/10.1038/oby.2009.167
32. Shin, J.W., Kwon, S.H., Choi, J.Y., Na, J.I., Huh, C.H., Choi, H.R., Park, K.C. (2019). Molecular mechanisms of dermal aging and antiaging approaches. *International Journal of Molecular Sciences*, *20*(9), art. no. 2126.
https://doi.org/10.3390/ijms20092126
33. Song, Q., Wang, Y., Huang, L., Shen, M., Yu, Y., Yu, Q., Chen, Y., Xie, J. (2021). Review of the relationships among polysaccharides, gut microbiota, and human health. *Food Research International*, *140*, art. no. 109858.
https://doi.org/10.1016/j.foodres.2020.109858
34. Velazquez, G., Herrera-Gómez, A., Martín-Polo, M.O. (2003). Identification of bound water through infrared spectroscopy in methylcellulose. *Journal of Food Engineering*, *59*(1), 79–84.
https://doi.org/10.1016/S0260-8774(02)00428-4
35. Venturella, G., Ferraro, V., Cirlincione, F., Gargano, M.L. (2021). Medicinal mushrooms: Bioactive compounds, use, and clinical trials. *International Journal of Molecular Sciences*, *22*(2), art. no. 634.
https://doi.org/10.3390/ijms22020634
36. Vomund, S., Schäfer, A., Parnham, M.J., Brüne, B., von Knethen, A. (2017). Nrf2, the master regulator of anti-oxidative responses. *International Journal of Molecular Sciences*, *18*(12), art. no. 2772.
https://doi.org/10.3390/ijms18122772
37. Wang, H., Cheng, X., Shi, Y., Le, G. (2015). Preparation and structural characterization of poly-mannose synthesized by phosphoric acid catalyzation under microwave irradiation. *Carbohydrate Polymers*, *121*, 355–361.
https://doi.org/10.1016/j.carbpol.2014.12.046
38. Wen, L., Gao, Q., Ma, C.W., Ge, Y., You, L., Liu, R.H., Fu, X., Liu, D. (2016). Effect of polysaccharides from *Tremella fuciformis* on UV-induced photoaging. *Journal of Functional Foods*, *20*, 400–410.
https://doi.org/10.1016/j.jff.2015.11.014
39. Wu, J., Li, P., Tao, D., Zhao, H., Sun, R., Ma, F., Zhang, B. (2018). Effect of solution plasma process with hydrogen peroxide on the degradation and antioxidant activity of polysaccharide from *Auricularia auricula*. *International Journal of Biological Macromolecules*, *117*, 1299–1304.
https://doi.org/10.1016/j.ijbiomac.2018.05.191
40. Wu, Y.J., Wei, Z.X., Zhang, F.M., Linhardt, R.J., Sun, P.L., Zhang, A.Q. (2019). Structure, bioactivities and applications of the polysaccharides from *Tremella fuciformis* mushroom: A review. *International Journal of Biological Macromolecules*, *121*, 1005–1010.
https://doi.org/10.1016/j.ijbiomac.2018.10.117
41. Xiao, H., Li, H., Wen, Y., Jiang, D., Zhu, S., He, X., Xiong, Q., Gao, J., Hou, S., Huang, S., He, L., Liang, J. (2021). *Tremella fuciformis* polysaccharides ameliorated ulcerative colitis *via* inhibiting inflammation and enhancing intestinal epithelial barrier function. *International Journal of Biological Macromolecules*, *180*, 633–642.
https://doi.org/10.1016/j.ijbiomac.2021.03.083
42. Xu, Y., Xie, L., Zhang, Z., Zhang, W., Tang, J., He, X., Zhou, J., Peng, W. (2021). *Tremella fuciformis* polysaccharides inhibited colonic inflammation in dextran sulfate sodium-treated mice *via* Foxp3+ T cells, gut microbiota, and bacterial metabolites. *Frontiers in Immunology*, *12*, art. no. 648162.
https://doi.org/10.3389/fimmu.2021.648162
43. Xu, Y., Zhang, X., Yan, X.H., Zhang, J.L., Wang, L.Y., Xue, H., Jiang, G.C., Ma, X.T., Liu, X.J. (2019). Characterization, hypolipidemic and antioxidant activities of degraded polysaccharides from *Ganoderma lucidum*. *International Journal of Biological Macromolecules*, *135*, 706–716.
https://doi.org/10.1016/j.ijbiomac.2019.05.166
44. Yang, D., Liu, Y., Zhang, L. (2019). Chapter Sixteen - *Tremella* polysaccharide: The molecular mechanisms of its drug action. In L. Zhang (Ed.) *Progress in Molecular Biology and Translational Science*, Academic Press, pp. 383–421.
https://doi.org/10.1016/bs.pmbts.2019.03.002
45. Ye, S., Liu, F., Wang, J., Wang, H., Zhang, M. (2012). Antioxidant activities of an exopolysaccharide isolated and purified from marine *Pseudomonas* PF-6. *Carbohydrate Polymers*, *87*(1), 764–770.
https://doi.org/10.1016/j.carbpol.2011.08.057
46. Zhang, J., Zhao, X., Jiang, Y., Zhao, W., Guo, T., Cao, Y., Teng, J., Hao, X., Zhao, J., Yang, Z. (2017). Antioxidant status and gut microbiota change in an aging mouse model as influenced by exopolysaccharide produced by *Lactobacillus plantarum* YW11 isolated from Tibetan kefir. *Journal of Dairy Science*, *100*(8), 6025–6041.
https://doi.org/10.3168/jds.2016-12480
47. Zhang, L., Li, X., Xu, X., Zeng, F. (2005). Correlation between antitumor activity, molecular weight, and conformation of lentinan. *Carbohydrate Research*, *340*(8), 1515–1521.
https://doi.org/10.1016/j.carres.2005.02.032
48. Zhang, L., Ye, X., Ding, T., Sun, X., Xu, Y., Liu, D. (2013). Ultrasound effects on the degradation kinetics, structure and rheological properties of apple pectin. *Ultrasonics Sonochemistry*, *20*(1), 222–231.
https://doi.org/10.1016/j.ultsonch.2012.07.021
49. Zhang, Z., He, S., Cao, X., Ye, Y., Yang, L., Wang, J., Liu, H., Sun, H. (2020). Potential prebiotic activities of soybean peptides Maillard reaction products on modulating gut microbiota to alleviate aging-related disorders in D--galactose-induced ICR mice. *Journal of Functional Foods*, *65*, art. no. 103729.
https://doi.org/10.1016/j.jff.2019.103729
50. Zhang, Z., Sun, D., Xu, M., Tian, H., Pan, J. (2014). Study on the antioxidation effect of *Tremella* polysaccharide. *Food Research and Development*, *18*, 10–15.
51. Zhao, L., Zhang, F., Ding, X., Wu, G., Lam, Y.Y., Wang, X., Fu, H., Xue, X., Lu, C., Ma, J., Yu, L., Xu, C., Ren, Z., Xu, Y., Xu, S., Shen, H., Zhu, X., Shi, Y., Shen, Q., Dong, W., Liu, R., Ling, Y., Zeng, Y., Wang, X., Zhang, Q., Wang, J., Wang, L., Wu, Y., Zeng, B., Wei, H., Zhang, M., Peng, Y., Zhang, C. (2018). Gut bacteria selectively promoted by dietary fibers alleviate type 2 diabetes. *Science*, *359*(6380), 1151–1156.
https://doi.org/10.1126/science.aao5774
52. Zhao, X., Yi, R., Zhou, X., Mu, J., Long, X., Pan, Y., Song, J.L., Park, K.Y. (2019). Preventive effect of *Lactobacillus plantarum* KSFY02 isolated from naturally fermented yogurt from Xinjiang, China, on D-galactose–induced oxidative aging in mice. *Journal of Dairy Science*, *102*(7), 5899–5912.
https://doi.org/10.3168/jds.2018-16033

ORIGINAL ARTICLE
http://journal.pan.olsztyn.pl

Polish Journal of Food and Nutrition Sciences
2023, Vol. 73, No. 2, 175–186
DOI: 10.31883/pjfns/163613
ISSN 1230-0322, e-ISSN 2083-6007

Effect of Dry, Vacuum, and Modified Atmosphere Ageing on Physicochemical Properties of Roe Deer Meat

Natalia Kasałka-Czarna[1]*, Róża Biegańska-Marecik[2], Jędrzej Proch[3], Aleksandra Orłowska[3], Magdalena Montowska[1]

[1]Department of Meat Technology, Poznan University of Life Sciences, Wojska Polskiego 31, 60-624 Poznan, Poland
[2]Department of Food Technology of Plant Origin, Poznan University of Life Sciences, Wojska Polskiego 31, 60-624 Poznan, Poland
[3]Department of Analytical Chemistry, Adam Mickiewicz University, Uniwersytetu Poznańskiego 8, 61-614 Poznań, Poland

Consumers around the world are choosing sustainable and unprocessed foods. Roe deer meat, due to the natural origin, is a source of organic and healthy meat. The selection of suitable storage conditions and times plays an important role in a deterioration of the meat's functional and nutritional values. The knowledge about oxidation processes in roe deer meat stored and packed deploying different methods is limited. The main aim of this study was therefore to investigate the effect of storage method on the physicochemical properties of *musculus longissimus thoracis et lumborum* (LTL), *musculus biceps femoris* (BF), and *musculus vastus lateralis* (VL) of roe deer. The muscles were stored either dry (DRY-AGED), vacuum-packed (VAC), or packed under modified atmosphere (MAP) for 21 days. The quality of roe deer meat was assessed based on chemical composition, technological properties, pH values, water activity, colour, and oxidation processes of proteins and lipids. Roe deer meat had high protein (216.5–228.6 g/kg) and low fat content (17.1–25.8 g/kg). Both DRY-AGED and VAC contributed to improving meat tenderness during storage, while the Warner–Bratzler shear force of the MAP muscles increased. The high-oxygen conditions during MAP storage strongly induced the oxidation processes; an average increase of 1,263% for thiobarbituric acid reactive substance (TBARS) level and 155% for protein carbonyl content on day 21. Vacuum packaging and dry-ageing are recommended methods for storing roe deer meat. The high oxygen atmosphere negatively affected the quality of this game species. It carries the risk of increased oxidation of proteins and lipids which may promote the formation of potentially detrimental compounds.

Key words: roe deer, protein oxidation, lipid oxidation, vacuum, modified atmosphere, dry-ageing

INTRODUCTION

Today, despite its many advantages for human nutrition, meat is considered a less sustainable food choice due to growing concerns about health and the environment. Recently, many changes in dietary recommendations have been noticed, focusing much attention on the heavy environmental burden of meat production. In Central and Western Europe, there is a strong tradition of meat consumption, but increased health awareness has led to a demand for alternative, low-fat, and antibiotic-free types of meat [Hoffman & Wiklund, 2006; Niewiadomska *et al.*, 2020]. In addition, consumers are looking for balanced and nutritious meat that can be included in a climate-friendly diet. When estimating the carbon footprint of farmed meat, many relative factors must be considered, ranging from feeding to energy,

***Corresponding Author:**
e-mail: natalia.czarna@up.poznan.pl (N. Kasałka-Czarna)

Submitted: 6 December 2022
Accepted: 25 April 2023
Published on-line: 25 May 2023

transportation, and slaughter. Therefore, the calculations for farmed meat are much higher than those for free-living game meat. For consumers who like meat, a pro-climate choice can be venison. In Poland, the most common species of deer is roe deer. Its meat is characterised by a unique taste and aroma but also by high quality and unique dietary and health-promoting properties. Roe deer meat is high in protein, unsaturated fatty acids, iron, and low in fat and saturated fatty acids [Cygan-Szczegielniak & Janicki, 2012a; Zomborszky *et al.*, 1996]. The high content of polyunsaturated fatty acids (PUFAs) is characteristic of the muscle tissue of game animals and much higher than that of farm animals [Klupsaite *et al.*, 2020; Razmaitė *et al.*, 2015]. Importantly, deer meat is free from antibiotics and growth and development enhancers, and animals are not exposed to the stress of commercial breeding [Cygan-Szczegielniak & Janicki, 2012b; Zomborszky *et al.*, 1996]. Another important aspect is the higher vitamin, folate, and mineral content of venison meat compared to many farmed species [Królikowski & Deptuła, 2020]. Despite its many advantages, the consumption of venison in Poland remains surprisingly low compared to pork, poultry, and beef. It is also significantly lower than in other European countries [Cygan-Szczegielniak & Janicki, 2012b; Królikowski & Deptuła, 2020; Kwiecińska *et al.*, 2018].

Venison meat and meat products obtained in Poland are largely exported to the markets of Western Europe; meanwhile, conditions in Poland could successfully contribute to an increase in the share of venison in the meat industry [Królikowski & Deptuła, 2020]. The high price of game meat and problems in maintaining quality during carcass processing and storage are the main reasons for low consumption [Kwiecińska *et al.*, 2018]. Most of the research carried out on the storage of meat has focused on the meat of farm animals [Daszkiewicz *et al.*, 2008; Vergara *et al.*, 2003]. The selection of suitable storage conditions and time plays an important role from the point of view of both consumer acceptance and the meat industry. However, incorrect storage can directly affect the deterioration of raw material quality [Kwiecińska *et al.*, 2018]. Meat is rich in many nutrients, but these compounds are prone to degradation processes, including oxidative ones especially in the case of proteins and lipids [Domínguez *et al.*, 2019].

Monitoring oxidative processes in food systems is important from the perspective of human nutrition and is therefore crucial for the meat industry [Lund *et al.*, 2011; Soladoye *et al.*, 2015]. Oxidative processes result in the deterioration of meat's functional properties and negatively affect its nutritional value [Estévez 2021; Kasałka-Czarna *et al.*, 2022; Li *et al.*, 2020; Soladoye *et al.*, 2015]. In addition to a reduction in the nutritional quality and bioavailability of oxidised proteins, the consumption of these modified proteins may be associated with an increased risk of certain disease states [Estévez & Xiong, 2019; Lund *et al.*, 2011; Soladoye *et al.*, 2015; Thøgersen *et al.*, 2020]. Soladoye *et al.* [2015] conducted a comprehensive review of the oxidative processes of proteins in processed meat, which highlighted the impact of the consumption of oxidised proteins in ageing and diseases associated with oxidative modifications of proteins and included Alzheimer's disease, kidney failure, and diabetes, among others. Protein oxidation results in the formation of oxidised muscle protein products, but the characteristics of these products are highly dependent on the amino acids involved and mechanisms of oxidation process initiation. The oxidative changes of proteins include modifications of amino acid side chains, fragmentation, aggregation and polymerisation of proteins Oxidative changes in proteins can be monitored by measuring the content of formed carbonyl groups [Estévez, 2011; Soladoye *et al.*, 2015]. Scientific studies have shown that processing and storage influence the development and intensity of oxidation processes in farmed species [Lund *et al.*, 2011]. In the case of game animals, which are characterised by a higher content of iron, myoglobin, and polyunsaturated fatty acids, the susceptibility to oxidation increases [Chaijan, 2008]. Despite this, there is still a scarcity of scientific research on oxidative processes within wild game meat. The main non-microbiological cause of meat deterioration is lipid oxidation, which is one of the main factors affecting meat quality, acceptability, and shelf life [Domínguez *et al.*, 2022]. Oxidative processes begin at slaughter and then intensify during processing, handling, and storage. The formation of lipid oxidation products results in discolouration, unpleasant odour and taste, and changes in texture [Chaijan, 2008]. In addition to reducing the nutritional value of meat, the aldehydes and oxysterols formed upon lipid oxidation exert pro-inflammatory, cytotoxic, and mutagenic effects [Domínguez *et al.*, 2022; Sottero *et al.*, 2019]. As Chaijan [2008] suggested, lipid oxidation leads to the formation of a wide range of aldehyde products that induce the oxidation of oxymyoglobin, resulting in an increase in the peroxidative activity of metmyoglobin. Oxidation processes can be effectively controlled by using appropriate packaging, storage or preservation technologies [Bao & Ertbjerg, 2019; Moczkowska *et al.*, 2017; Wazir *et al.*, 2019].

The objective of this study was to use different storage methods and storage times for venison to preserve its quality (pH, colour, tenderness, water activity, water loss during cooking and storage) and to inhibit protein and lipid oxidation. Identifying differences in biochemical processes and quality of venison may allow improving production and packaging techniques and changing nutritional strategies for this type of meat. These factors have already been evaluated for common slaughter species, whereas studies on roe deer are still lacking.

MATERIALS AND METHODS

Sampling

Samples for the research were obtained from five carcasses of roe deer (*Capreolus capreolus*). Animals were hunted in Hunter District No. 57, OHZ, Sarbia Forest District (Poland). The selection was based on similarity of sex (male) and age (2–4 years), verifying the development of the dentition. Shooting and evisceration were performed under hunting protocol (internal carcass inspection report based on Regulation (EC) No 853/2004). The carcass was then cooled and stored at 0°C for 5 days at the Venison Buying Station (Drzązgowo Forestry, Sarbia Forest District). This procedure is an ageing procedure, which is longer

for game meat than for slaughtered farm animals. Carcasses were assessed after skinning to exclude meat with defects (damaged elements by shooting, inappropriate pH value or improperly cooled meat). From each skinned roe deer carcass, three muscles were excised without bone and meat on the bone, namely *musculus longissimus thoracis et lumborum* (LTL), *musculus biceps femoris* (BF), and *musculus vastus lateralis* (VL). The cuts were vacuum-packed and transported to the Department of Meat Technology, Poznan University of Life Sciences, Poland in a portable car refrigerator with a permanent power supply (18445, Norauto, Warsaw, Poland). The muscles (without bone) were divided into equal, selected parts (approximately 80 g). Muscles (in triplicate) were vacuum-packed (VAC) in barrier bags (MULTIVAC Seep Haggenmüller SE & Co. KG, Wolferschwenden, Germany) and in a modified atmosphere (MAP) (80% O_2, 20% CO_2) (Multivac T200 packaging machine) and sealed with polyethylene terephthalate/polyethylene (PET/PE) film. Samples were stored at 4±1°C for 21 days. Muscles on the bone were stored in a dry-ageing cabinet (DRY-AGED) at 2°C and 80% humidity for 21 days (Dry-Aged Cooler SW-28, Arnsberg, Germany). Samples were analysed immediately after preparation (0 days) and on the day 7 and 21 of storage, for each variant.

Proximate composition analysis

The proximate composition (protein, moisture, fat, and ash contents) was determined in triplicate for each muscle on fresh meat before packing. The composition was evaluated according to ISO standards. The protein content was calculated based on total nitrogen content and the 6.25 conversion factor for meat and dairy products following ISO 937:1978. In turn, respective Polish Standards: PN-ISO 1442:2000, PN-ISO 1444:2000, and PN-ISO 936:2000, were used for the other parameters tested. Samples for analysis were homogenised using a food processor (Moulinex S 643.23, Paris, France).

Analysis of the composition of minerals

Ash of raw meat samples (0.500±0.001 g) was digested with 5.0 mL of 65% HNO_3 (Merck, Darmstadt, Germany) in closed Teflon vessels (55 mL) at 180°C using the Mars 6 microwave digestion system (CEM, Matthews, NC, USA). Digested samples were diluted with high-pure deionized water (≥18 MΩ×cm resistivity) obtained from Milli-Q water purification system (Merck Millipore, Burlington, MA, USA) to a final volume of 10 mL. The procedure was reproduced after Zubaidi *et al.* [2021]. Contents of 13 minerals (K, Na, Mg, Ca, Zn, Fe, Al, Cu, Pb, Cd, Cr, Mn, and Ni) were determined in the samples with the inductively coupled plasma high-resolution optical emission spectrometry (ICP-HROES), using a PlasmaQuant PQ 9000 Elite spectrometer (Analytic Jena, Germany). The settings were as follows: radio frequency (RF) power 1.2 kW, auxiliary gas flow 0.5 L/min, nebulizer gas flow 0.5 L/min, plasma gas flow 12 L/min, and axial plasma view. High-resolution optics were echelle double monochromator and charge-coupled device (HR CCD), which was cooled to −10°C using the Peltier system. The following wavelengths of emission lines were applied: K 769.897 nm, Na 588.995 nm, Mg 285.213 nm, Ca 315.887 nm, Zn 206.200 nm, Fe 238.204 nm, Al 396.152 nm, Cu 324.754 nm, Pb 220.353 nm, Cd 214.441 nm, Cr 267.716 nm, Mn 257.610 nm, and Ni 231.604 nm. Acquisition time was 1 s and signal was measured in 5 replicates. Argon was used as the internal standard (Ar 420.068 nm). Detection limits (DLs) were estimated at the level of 0.03 mg/kg dry weight (DW). ICP commercial analytical standards (Romil, Cambridge, UK) were used for calibration. Standard addition method was used in the quality control with acceptable recovery (80–120%). The uncertainty for the complete analytical process (including sample preparation) was at the level of 20%.

Water activity, pH and colour measurements

The water activity, pH and colour indices were measured on fresh meat before packing and on stored meat for 7 and 21 days under VAC, MAP, and DRY-AGED treatment. The water activity measurement was performed using a LabMaster-a_w neo instrument (Novasina AG, Lachen, Switzerland) at 25±1°C. The meter was calibrated with standard SAL-T 97% tagged with an automatic recognition system (RFID). The pH values were measured at room temperature (22–24°C) with a portable Handylab 2 pH meter equipped with an L68880 pH combination electrode (Schott AG, Mainz, Germany). The pH buffers 4.01 and 7.00 (Testo Ltd., Alton Hampshire, UK) were used for calibration. The colour on the cross-section of freshly cut samples was measured three times by the CIELab colour space using a Dr. Lange LMG161 portable colorimeter (Dr. Bruno Lange GmbH & Co. KG, Berlin, Germany). The values of lightness (L^*), greenness/redness (a^*), and blueness/yellowness (b^*) were measured. The setting parameters were as follows: illuminant D65, aperture size of 5.0 mm, and observer angle of 10°. The instrument was standardised using a white standard (no. 3125).

Purge and cooking losses determination

The purge and cooking losses were expressed as a percentage, by weighing the samples before and after thermal treatment or the storage period. The purge losses were determined after 7 and 21 days of storage for each storage method while cooking losses were also determined for fresh meat. To determine cooking losses, 25 mm slices of meat wrapped in aluminium foil were heated to a core temperature of 72°C in a Rational combi model SCC 61 convection oven (Landsberg am Lech, Germany) at a temperature of 160°C and a 75% humidity in the cooking chamber. Cooking losses were determined on cooled samples at room temperature.

Warner-Bratzler shear force measurement

The samples cooked and cooled according to the procedure for cooking losses determination were cut into cuboids (1×1×3 cm). The Warner-Bratzler shear force (WBSF) for every muscle was tested before packing and after 7 and 21 days of storage (VAC, MAP, DRY-AGED). WBSF was measured by a TA.XT.plus texture analyser (Stable Micro Systems, Godalming, UK) using a Warner-Bratzler add-on device. The shear force expressed as N was measured perpendicularly to the arrangement of muscle fibres at a traverse speed of 100 mm/min.

Protein carbonyl content determination

Protein oxidation was determined by the total carbonyl content using 2,4-dinitrophenyl hydrazine (DNPH) derivatisation method according to Levine *et al.* [1994], with slight modifications. Fresh samples and packed meats (VAC, MAP, DRY-AGED) stored for 7 and 21 days were subjected to the analysis. One gram of meat was homogenised (Ultra Turrax) in 20 mM sodium phosphate buffer containing 6 M NaCl (pH 6.5) for 30 s, and immediately filtered through filter paper. Samples from homogenate (two aliquots of 0.4 mL) were precipitated by cold 10% trichloroacetic acid (TCA) (1.5 mL) and incubated at 20°C for 20 min. After incubation, the samples were centrifuged for 5 min at 4°C at 10,000×*g*. One of the pellets was treated with 1 mL of 2 M HCl (for the protein content measurement), the second with 1 mL of 10 M DNPH in 2 M HCl (for the carbonyl content measurement), and then were incubated for 30 min at 37°C. Afterward, the samples were treated with 1 mL of 10% TCA and centrifuged for 5 min at 4°C and 10,000×*g*. To remove excess DNPH after centrifugation, the precipitates were washed 3×1 mL with a solution of ethanol and ethyl acetate (1:1, *v/v*). The obtained pellets were then dried at room temperature for 1 h. The dried samples were dissolved in 1.5 mL of 20 mM sodium phosphate buffer containing 6 M guanidine hydrochloride (pH 6.5) and incubated for 30 min at 37°C. To remove insoluble fragments, the samples were centrifuged for 5 min at 4°C at 10,000×*g*. The absorbance was measured (Ultrospec 2000, Pharmacia Biotech, Uppsala, Sweden) at 280 nm (A_{280}) and 370 nm (A_{370}) and carbonyl content (nmol mg protein) was calculated using Equation (1) [Levine *et al.*, 1994]:

$$Carbonyl\ content = \frac{A_{370}}{22{,}000 \times (A_{280} - A_{370} \times 0.43)} \times 10^6 \quad (1)$$

Determination of thiobarbituric acid reactive substance content

The thiobarbituric acid reactive substance (TBARS) content of LTL, BF, and VL was assessed according to the method described by Lo Fiego *et al.* [2004], with minor modifications. The analysis was performed for fresh samples and in meat stored (VAC, MAP, DRY-AGED) for 7 and 21 days. Raw meat samples from each muscle (10 g) were homogenised in 20 mL of 20% TCA at 10,000×*g* for 60 s and then centrifuged at 3,502×*g* for 15 min at 4°C. The supernatant was filtered through qualitative filter paper by vacuum filtration. The volume of 5 mL of 20 mM 2-thiobarbituric acid was added to 5 mL of the filtrate. The blank was 5 mL of TCA and 5 mL of 2-thiobarbituric acid solution. Solutions were heated for 20 min in a boiling water bath and afterward cooled to 21°C. Absorbance was measured using an Ultrospec 2000 spectrophotometer (Pharmacia Biotech) at 532 nm. Results were expressed as mg of malonic dialdehyde (MDA) equivalents per kg of meat (mg MDA/kg).

Statistical analysis

Statistical analysis of the results was performed using Statistica 13.1 (StatSoft Inc., Tulsa, OK, USA). The statistics were consistent with the assumption of a normal distribution (verified by the Shapiro-Wilk test). One-way and two-way analysis of variance (ANOVA) was used. Tukey's Honestly Significant Difference (HSD) test was used to assess the significance of differences. The influence of the storage method of LTL, BF, and VL samples, as well as storage period up to 21 days on the quality characteristics, were assessed. The results were considered to be statistically significant at $p<0.05$, and expressed as mean ± standard error of mean (SEM).

RESULTS AND DISCUSSION

The proximate composition, physicochemical properties, and shear force

The proximate composition of the three muscles tested (LTL, BF, VL) is shown in Table 1. Based on ANOVA, it was found that the type of muscle significantly ($p<0.05$) affected the chemical composition (protein and fat content). The protein content of roe meat was 216.5–228.6 g/kg, while the fat content was 17.1–25.8 g/kg. Roe deer meat can therefore be categorised as low-fat meat. The muscle containing the most protein and the least fat was LTL. The protein content of VL and BF muscles was lower, while the fat content was higher than that of LTL. There were no statistically significant differences in moisture and ash contents between the muscles.

According to Ivanović *et al.*, [2020], the protein content of LTL from roe deer was 21.40%, while the fat content was 1.31%. Other authors [Daszkiewicz *et al.*, 2018] showed a similar protein content in this muscle, *i.e.* 229.76 g/kg, to that determined in the present study. As reported by Cygan-Szczegielniak & Janicki [2012a], the age of the animal had a direct effect on the proximate composition of the muscle derived from it. LTL muscle obtained from roe deer aged 2–3 had the highest protein content

Table 1. Proximate composition of roe deer muscles: *longissimus thoracis et lumborum* (LTL), *biceps femoris* (BF), and *vastus lateralis* (VL).

Component (g/kg)	LTL	BF	VL	*p*
Protein	228.6±1.1[a]	217.3±1.3[b]	216.5± 1.7[b]	***
Moisture	738.9±1.6	744.4±2.1	742.6±2.1	NS
Fat	17.1±1.0[b]	22.6±1.0[a]	25.8±0.8[a]	***
Ash	14.1±1.6	15.6±1.7	15.0±2.0	NS

Results are shown as mean ± standard error of mean (SEM). Means with different letters (a,b) in a row indicate significant differences between the muscles ($p<0.05$). *$p<0.05$; **$p<0.01$; NS, non-significant (one-way ANOVA).

(24.02%) compared to the other age groups (4–5 and 6–7 year old), and a low fat content (0.43%). According to other studies, the fat content of roe deer in LTL ranged from 0.36 to 1.76% and depended on the season [Dominik *et al.*, 2012]. Compared to wild boar meat, which is also a representative of game, roe deer meat is richer in protein and has a lower fat content [Kasałka-Czarna *et al.*, 2022]. Nevertheless, the proximate composition of game meat is strongly influenced by diet, season, hunting, habitat, sex, and animal activity [Ivanović *et al.*, 2020].

Table S1 (in Supplementary Materials) shows the content of selected minerals in the LTL, BF, and VL. The highest contents were determined for potassium, sodium, magnesium, zinc and iron. The content of iron ranged from 14.8 to 24.6 mg/kg of meat. No heavy metals, such as cadmium, chromium, manganese, or nickel, were found. Roe deer meat was richer in potassium, magnesium, iron, and phosphorus than that of wild boar [Kasałka-Czarna *et al.*, 2022; Zomborszky *et al.*, 1996].

The physicochemical properties of muscles of roe deer (fresh and stored for 7 and 21 days in VAC, MAP and DRY-AGED variant) are presented in Table 2. Their values indicate a significant effect of storage time and method as well as their interaction on the pH of the tested muscles (Table 3). The pH values of fresh meat ranged from 5.53 to 5.63, depending on muscle type. Of all the roe deer muscles, VL had the highest pH for each storage method. Significantly higher pH values, compared to the other methods, were observed for DRY-AGED muscles on both day 7 and 21 of storage (pH ranged from 5.53 to 5.74 for LTL), while the pH of the muscles stored in MAP on day 7 was similar to the pH of the VAC samples, with exception of VL. On day 21, the highest decrease in pH was noted for BF in MAP (5.44). The VAC muscles featured the greatest fluctuations in pH values. Similar relationships between the effect of storage method and time were shown for the wild boar muscles in a similar experiment, but MAP storage resulted in a significant decrease in pH for each wild boar muscle (compared to 5.23 for BF) [Kasałka-Czarna *et al.*, 2022]. According to Daszkiewicz *et al.* [2018], the pH value measured 48–54 h *post-mortem* in LTL of roe deer was 5.52. However, for the LTL taken 24 h *post-mortem*, the pH was 5.72 [Ivanović *et al.*, 2020]. Other researchers have also shown that the pH of fresh meat from roe deer measured 120 h *post-mortem* ranged from 5.52 to 5.56, depending on the muscle metabolism [Dominik *et al.*, 2012]. A characteristic of game meat is the high content of lactic acid produced by glycolysis, which influences meat acidity. The pH values of venison meat measured up to 96 h *post-mortem* ranged from 5.4 to 5.6. These values also changed according to season, sex, and age [Dominik *et al.*, 2012]. Storage time resulted in differences in meat pH. Vergara *et al.* [2003] studied deer meat stored in a modified atmosphere in three gas mixtures (40% CO_2 + 60% N_2, 80% CO_2 + 20% O_2, and 80% CO_2 + 20% N_2). They noted that storage time affected the increase in pH for each method. In turn, Gill [1990], found that the pH of lamb meat decreased when it was packaged in a CO_2-rich atmosphere. Thus, depending on a given species, meat undergoes different changes with the same gas atmosphere in packaging.

The study demonstrated a significant effect of storage time and method as well as their interaction on the lightness values (L^*) of the BF and VL (Table 3). For VL, there was a weaker interaction between storage method and storage time than for BF. The value of L^* color parameter of meat on day 21 of MAP and VAC storage increased compared to the fresh samples (Table 2). For a^* and b^* values, an interaction was demonstrated between the storage method and time for each muscle (Table 3). Time did not significantly affect a^* values of BF and VL and b^* values of BF. The storage method also had no significant effect on a^* value of LTL. MAP had a negative effect on the a^* parameter (Table 2). Its value increased in DRY-AGED BF, whereas remained unchanged after 21-storage in VAC. On day 21 of the analysis, significantly lower a^* values were determined in the samples stored in MAP compared to the other two methods. This is most likely due to the formation of oxymyoglobin (OxyMb) under aerobic conditions in an atmosphere with a high oxygen concentration [Chaijan, 2008]. The samples stored in VAC and DRY-AGED had significantly lower values of yellowness (b^*) compared to the meat stored in MAP (Table 2). Vergara *et al.* [2003] found that the b^* value in deer meat increased when the O_2 content of the package was higher. The sharp changes in the b^* parameter values suggest that this gas was responsible for the browning of red deer meat. Oxygen is used to enhance fresh meat colour, as it maintains the characteristic red colour of oxymyoglobin, which is the oxidised form of myoglobin. However, at increased concentrations, oxygen can negatively affect meat colour [Świderski & Sadowska, 2011]. The increase in the b^* value observed during meat storage may be due to metmyoglobin formation [Daszkiewicz *et al.*, 2011]. Myoglobin is involved in the storage of oxygen in red muscles. The addition of oxygen can retard its formation, but when oxygen-free packaging is used, intense oxidative changes occur, which can contribute to the formation of its large amounts [Świderski & Sadowska, 2011]. A similar effect can be observed with vacuum packaging when oxygen is removed from the meat surface, which can also result in a change in meat colour towards browning. According to Daszkiewicz *et al.* [2011], no significant differences were found between the average values of the colour indices of roe deer meat after 7 days of storage in the case of using vacuum packaging and MAP (40% CO_2 + 60% N_2; 60% CO_2 + 40% N_2). The results also showed that, after 21 days of storage, the use of MAP with 60% N_2 had the smallest effect on colour changes. Other researchers have noted a similar relationship for deer meat [Vergara *et al.*, 2003]. The pH value also affects L^* values, and a lower pH increases protein denaturation, resulting in higher L^* values [Klupsaite *et al.*, 2020].

A significant effect of storage time and method on water activity (a_w) was shown for all muscles (Table 3). However, no significant interaction between method and storage time was observed for LTL. On day 7 of MAP storage, a_w values for all muscles were lower (0.9675 for LTL, 0.9690 for BF, and 0.9686 for VL) compared to fresh meat and meat stored for 21 days (Table 2). No similar relationship was observed for VAC and DRY-AGED. After 21 days, a significant decrease in a_w was determined in DRY-AGED

Table 2. Physicochemical properties of roe deer muscles: *longissimus thoracis et lumborum* (LTL), *biceps femoris* (BF), and *vastus lateralis* (VL) during storage under modified atmosphere (MAP), dry (DRY-AGED) and vacuum (VAC) ageing.

Parameter	Storage time (day)	LTL				BF				VL			
		MAP	DRY-AGED	VAC	*p*-Method	MAP	DRY-AGED	VAC	*p*-Method	MAP	DRY-AGED	VAC	*p*-Method
pH	0	5.53±0.03^{b}	5.53±0.03^{b}	5.53±0.03	NS	5.54±0.01^{a}	5.54±0.01^{c}	5.54±0.01^{b}	NS	5.63± 0.01^{b}	5.63±0.01^{c}	5.63±0.01^{b}	NS
	7	5.59±0.00^{ay}	5.70±0.02^{ax}	5.58±0.02^{y}	***	5.57±0.01^{ay}	5.68± 0.01^{bx}	5.60±0.01^{ay}	***	5.60± 0.01^{cy}	5.69±0.01^{bx}	5.68±0.02^{ax}	***
	21	5.51±0.01^{by}	5.74±0.02^{ax}	5.54±0.02^{y}	***	5.44±0.03^{bz}	5.78 ± 0.02^{ax}	5.54±0.01^{by}	***	5.67± 0.01^{ay}	5.80±0.02^{ax}	5.64±0.01^{aby}	***
p-Time		**	***	NS		***	***	***		***	***	*	
*L**	0	24.41±0.66^{b}	24.41±0.66	24.41±0.66^{b}	NS	28.3±0.60^{b}	28.33±0.60^{a}	28.33±0.60^{b}	NS	26.13±1.28^{b}	26.13±1.28^{ab}	26.13±1.27	NS
	7	31.01±0.15^{ax}	26.87±0.35^{y}	29.79±0.48^{ax}	***	31.45±0.48^{ax}	28.89±0.51^{ay}	30.20±0.49^{axy}	**	31.30±0.45^{ax}	28.72±0.54^{ay}	28.02±0.48^{y}	***
	21	31.26±0.47^{ax}	24.83±0.56^{y}	28.17±0.70^{axy}	***	30.40±0.38^{ax}	24.55±0.44^{by}	30.54±0.35^{ax}	***	31.85±0.90^{ax}	24.77±0.44^{bz}	27.97±0.30^{y}	***
p-Time		***	NS	***		***	***	**		***	**	NS	
*a**	0	14.23±0.59^{a}	14.23±0.59^{a}	14.23±0.59^{a}	NS	11.25±0.29^{a}	11.25±0.29^{b}	11.25±0.29^{a}	NS	11.67±1.09^{a}	11.67±1.09^{a}	11.67±1.09^{ab}	NS
	7	12.21±0.13^{bx}	12.25±0.34^{bx}	10.21±0.49^{by}	***	11.52±0.14^{ax}	11.53±0.31^{bx}	9.95±0.42^{by}	***	11.54±0.30^{abx}	11.53±0.31^{ax}	9.70±0.34^{by}	***
	21	10.28±0.60^{cy}	11.71±0.28^{bxy}	12.66±0.34^{ax}	***	8.00±0.32^{bz}	13.94±0.55^{ax}	11.05±0.16^{ay}	***	8.92±0.78^{by}	13.96±0.55^{ax}	12.44±0.23^{ax}	***
p-Time		***	***	***		***	***	**		*	*	*	
*b**	0	13.59±0.43^{b}	13.59±0.43^{a}	13.59±0.43^{a}	NS	12.87±0.16^{c}	12.87±0.16	12.87±0.16^{a}	NS	11.89±0.42^{b}	11.89±0.42	11.89±0.42	NS
	7	15.12±0.11^{ax}	12.1±0.23^{by}	11.41±0.40^{by}	***	14.53±0.14^{ax}	12.57±0.30^{y}	11.97±0.25^{by}	***	14.67±0.18^{ax}	12.57±0.30^{y}	11.89±0.39^{y}	***
	21	14.23±0.55^{abx}	10.29±0.23^{cz}	11.77±0.29^{by}	***	14.93±0.40^{ax}	13.05±0.46^{y}	11.71±0.19^{bz}	***	13.66±0.39^{a}	13.28±0.48	12.79±0.35	NS
p-Time		*	***	***		***	NS	***		***	NS	NS	
Water activity (–)	0	0.9754±0.0001^{a}	0.9754±0.0001^{a}	0.9754±0.0001^{a}	NS	0.9727±0.0006^{a}	0.9727±0.0006^{a}	0.9727±0.0006^{a}	NS	0.9733±0.0009^{a}	0.9733±0.0009^{a}	0.9733±0.0009^{a}	NS
	7	0.9675±0.0003^{b}	0.9620±0.0025^{b}	0.9712±0.0005^{b}	NS	0.9690±0.0005^{by}	0.9653±0.0007^{bz}	0.9711±0.0004^{ax}	***	0.9686±0.0009^{by}	0.9660±0.0007^{bz}	0.9706±0.0005^{bx}	***
	21	0.9737±0.005^{ax}	0.9590±0.0036^{cy}	0.9700±0.0007^{bx}	***	0.9716±0.0003^{ax}	0.9644±0.0009^{bz}	0.9686±0.0008^{by}	***	0.9718±0.0004^{ax}	0.9656±0.0009^{bz}	0.9694±0.0006^{by}	***
p-Time		***	***	***		***	***	***		***	***	***	
Cooking loss (%)	0	23.03±0.51^{c}	23.03±0.51^{a}	23.03±0.51	NS	28.52±0.34^{b}	28.52±0.34^{b}	28.52±0.34^{b}	NS	22.45±0.35^{c}	22.45±0.35^{b}	22.45± 0.35^{b}	NS
	7	32.15±0.52^{ax}	21.10±0.26^{bz}	22.59±0.35^{y}	***	34.55±0.34^{ax}	30.00±0.24^{ay}	29.31±0.38^{by}	***	34.76±0.37^{ax}	23.28±0.40^{by}	23.03±0.30^{by}	***
	21	29.42±0.45^{bx}	23.12±0.29^{ay}	22.21±0.55^{y}	***	33.80±0.49^{ax}	27.17±0.42^{cy}	32.14±0.46^{ax}	***	31.85±0.39^{bx}	25.55±0.38^{ay}	31.38±0.39^{ax}	***
p-Time		***	***	NS		***	***	***		***	***	***	

Results are shown as mean ± standard error of mean (SEM). Means with different superscripts a–c in a column for a given parameter differ significantly within storage time ($p<0.05$). Means with different superscripts x–z in a row for a given muscle differ significantly within storage methods ($p<0.05$). *p*-Time, effect of time within method; *p*-Method, effect of method within time; *$p<0.05$; **$p<0.01$; ***$p<0.001$; NS, non-significant (one-way ANOVA). *L**, lightness; *a**, greenness/redness; *b**, blueness/yellowness.

Table 3. Effect of time (0, 7, 21 days) and method of storage (dry, vacuum, and modified atmosphere ageing) and their interaction on selected properties of roe deer muscles: *longissimus thoracis et lumborum* (LTL), *biceps femoris* (BF), and *vastus lateralis* (VL) .

Parameter	Muscle	Storage time	Storage method	Storage time × storage method
pH	LTL	***	***	***
	BF	***	***	***
	VL	***	***	***
*L**	LTL	NS	NS	NS
	BF	***	***	***
	VL	***	***	**
*a**	LTL	***	NS	***
	BF	NS	***	***
	VL	NS	*	***
*b**	LTL	***	***	***
	BF	NS	***	***
	VL	***	***	**
Water activity	LTL	*	*	NS
	BF	***	***	***
	VL	***	***	***
Cooking loss	LTL	**	***	***
	BF	***	***	***
	VL	***	***	***
Purge losses	LTL	***	***	***
	BF	***	***	***
	VL	***	***	**
WBSF	LTL	***	***	***
	BF	***	***	***
	VL	***	***	***
TBARS content	LTL	***	***	***
	BF	***	***	***
	VL	***	***	***
Protein carbonyl content	LTL	***	***	***
	BF	***	***	***
	VL	***	***	***

*p<0.05; **p<0.01; ***p<0.001; NS, non-significant (two-way ANOVA). *L**, lightness; *a**, greenness/redness; *b**, blueness/yellowness; WBSF, Warner–Bratzler shear force; TBARS, thiobarbituric acid reactive substances.

meats, *e.g.*, from 0.9754 to 0.9590 for LTL. This decline corresponds to the highest purge losses (Figure 1). The highest a_w was determined for the samples stored for 21 days in MAP, especially for LTL (0.9737). For vacuum packaging, the decrease in water activity was not significant after longer storage. Meat seasoning had a positive effect on a_w, which was also observed for wild boar meat [Kasałka-Czarna *et al.*, 2022]. The growth of microorganisms and the rate of biochemical processes are strongly dependent on water activity. Additionally, according to Florek *et al.* [2019], DRY-AGED meat has a lower water content than those stored in VAC, which affects, among others, its microbiological safety during storage. According to other reports, for the same storage conditions (MAP, VAC, DRY-AGED), at 7, 14 and 21 days of storage, wild boar meat was microbiologically safe [Kasałka-Czarna *et al.*, 2022].

In terms of cooking losses, the interaction effect of storage time × storage method (Table 3) on LTL, BF and VL was significant (p<0.001). Significant effect of time and storage method was found for BF and VL (p<0.001; p<0.001) and LTL (p<0.01; p<0.001), respectively. Cooking losses in fresh meat were 23.03% in LTL, 28.52% in BF, and 22.45% in VL (Table 2). The lowest percentage of thermal loss after 7 days of storage was noted in the DRY--AGED (21.10% for LTL, 30.00% for BF, and 23.28% for VL) and VAC (22.59% for LTL, 29.31% for BF and 23.03% for VL) muscles. For VAC, cooking losses significantly increased on day 21 of storage relative to the fresh sample for VL and BF. Significant differences were noted at day 7 of MAP storage for LTL and VL compared to both the fresh sample and the sample stored for 21 days. The increase of the thermal losses for MAP stored samples indicates a decrease in water retention in the muscle, which may have a direct effect on its texture. This was not observed for VAC in muscles from wild boar, in which cooking losses decreased during storage [Kasałka-Czarna *et al.*, 2022]. According to Daszkiewicz *et al.* [2011], roe deer meat stored (m. *longissimus dorsi*) under vacuum was characterised by increased cooking losses compared to the modified atmosphere with oxygen exclusion. Despite this, no significant differences were observed in cooking losses between MAP and VAC. Therefore, the composition of the modified atmosphere can have an impact on cooking losses. In the early phase of storage, a characteristic crust develops on the surface of DRY-AGED meat due to water loss [Dashdorj *et al.*, 2016]. The increase in water retention capacity is strongly correlated with an increase in meat pH. As a result of the increase in pH, the protein structure became more open and myofibrillar proteins could bind more water. Despite high storage losses and high water loss, DRY-GED meat with the highest pH is of high quality [Dashdorj *et al.*, 2016]. The same result was obtained from wild boar meat analyses (on day 21 of storage of LTL, pH values were 5.31 (MAP), 5.46 (VAC), 5.72 (DRY-AGED), and cooking losses were 30.82%, 30.92%, 20.94%, respectively) [Kasałka-Czarna *et al.*, 2022].

Significant (p<0.001) effect of storage time and storage method on purge losses was found in the study (Table 3). The interaction effect of storage time × storage method (Table 3) on LTL, BF and VL was significant (p<0.001 for LTL and BF; p<0.01 for VL). Purge losses were highest on day 21 of storage for each muscle and storage method (Figure 1, Table S2). The lowest purge losses were determined for MAP and VAC. For LTL on day 21 of storage, there was an increase of 2.3% for MAP and 1.27% for VAC relative to day 7 of storage. For LTL DRY-AGED, the difference was 15.92% (26.12% on day 7 and 42.04% on day 21).

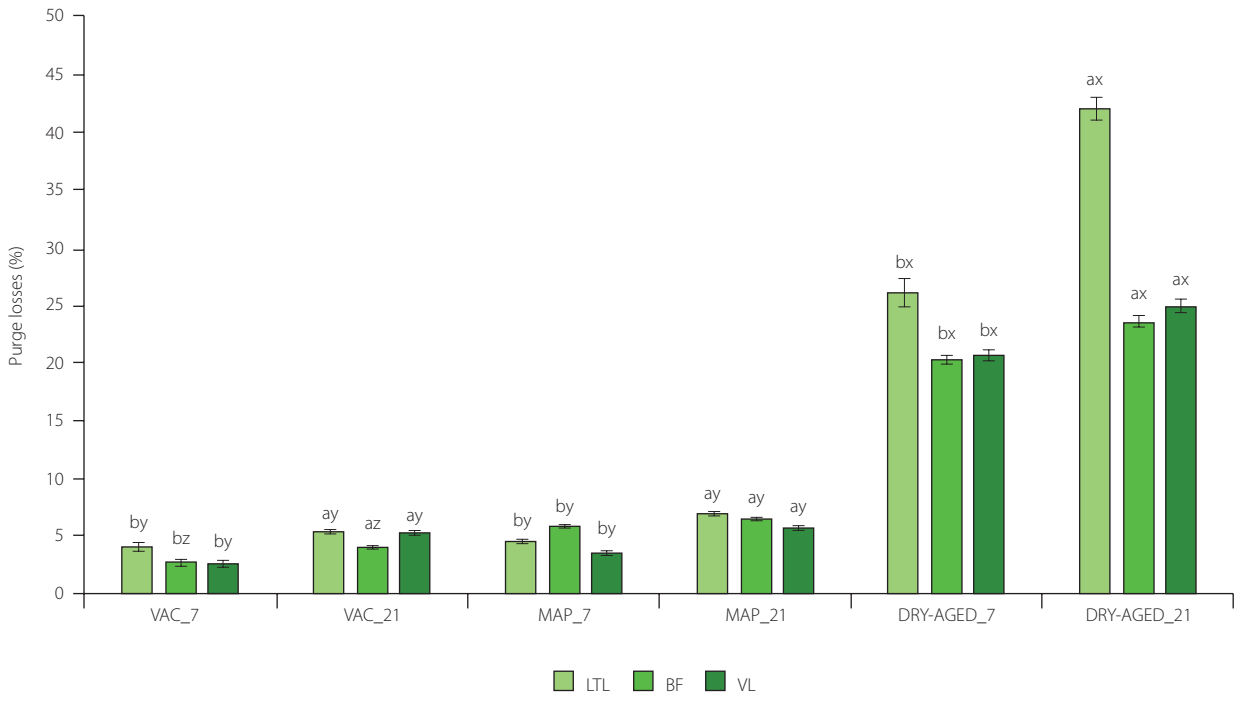

Figure 1. Purge losses in muscles *longissimus thoracis et lumborum* (LTL), *biceps femoris* (BF) and *vastus lateralis* (VL) of roe deer during storage (at day 7 and 21) under modified atmosphere (MAP), dry (DRY-AGED) and vacuum (VAC) ageing. Results are shown as mean and standard error of mean (SEM). Different a and b letters above bars indicate a significant effect of time within the method ($p<0.05$). Different x–z letters above bars indicate a significant effect of the method within time ($p<0.05$).

After 7 and 21 days of storage, the purge losses of DRY-AGED meat due to drying and water loss were significantly four to even seven times higher. Daszkiewicz *et al.* [2008] reported lower losses for roe deer LTL in VAC (1.50% after 7 and 2.17 after 21 days of storage) and observed that the use of modified atmosphere packaging with 60% CO_2 + 40% N_2 resulted in reduced purging. The extent of purge losses can have some economic consequences, as, *e.g.*, DRY-AGED storage of roe deer meat dramatically reduces the overall process efficiency. A higher storage loss was recorded within each method for roe deer compared to wild boar meat [Kasałka-Czarna *et al.*, 2022].

The study demonstrated a significant ($p<0.001$) effect of storage time and method as well as their interaction on the WBSF of the LTL, BF and VL (Table 3). VAC and DRY-AGED had a positive effect on tenderness at day 21 of storage (except for LTL, DRY-AGED and VL), whereas MAP adversely affected this quality attribute during meat storage (Figure 2, Table S2). For LTL muscle stored as DRY-AGED, the lowest values were reached on day 7 of storage (16.91 N). For each of the MAP muscles, WBSF values increased on day 21 relative to the fresh sample. The highest tenderness of BF and VL muscles was reached after 21 days of storage for DRY-AGED (17.83 N and 19.08 N, respectively). For LTL, the lowest values were observed on day 7 of storage for both DRY-AGED and VAC (16.91 N and 16.53 N, respectively). Klupsaite *et al.* [2020] showed that roe deer meat analysed 24 h *post-mortem* had the highest tenderness compared to other game species (wild boar, deer, and beaver), and its tenderness was satisfactory (1.17 kg/cm^2 for m. *glutenus medius*). In another study, cutting force was determined for LTL from roe deer 24 h *post-mortem* at 47.21 N [Dominik *et al.*, 2012]. Therefore, the carcass skin maturation treatment applied in this study for 5 days had a major effect on the tenderness of roe deer meat. The muscles showed satisfactory tenderness on the day the samples were obtained. According to Daszkiewicz *et al.* [2008], in LTL from roe deer, VAC storage for 21 days had a positive effect on tenderness (16.24 N). The researchers used modified atmosphere packaging, but with the elimination of oxygen (40% CO_2 + 60% N_2 and 60% CO_2 + 40% N_2); the analyses showed a positive effect on tenderness development. Other researchers have also reported that high oxygen concentrations may contribute to increased WBSF. This may be due to increased oxidation of proteins and fats, resulting, for example, in the formation of oxygen-induced protein aggregates [Clausen *et al.*, 2009; Moczkowska *et al.*, 2017]. In pork and beef stored in a high-oxygen atmosphere, myosin heavy chains form intermolecular bonds that are not observed without the presence of oxygen. This may contribute to the deterioration of tenderness [Lund *et al.*, 2007]. In addition to the method and time of storage, these differences can also be influenced by different muscle metabolisms. In another study on beef stored in a high-oxygen atmosphere, a reduction in tenderness was confirmed due to cross-linking of myosin through disulphide bond formation [Kim *et al.*, 2010].

Protein and lipid oxidation

Two-way ANOVA showed the significant effect of storage time and method and the effect of storage time × storage method (Table 2) on protein and lipid oxidation in LTL, BF and VL ($p<0.001$). During VAC storage, the content of protein carbonyl

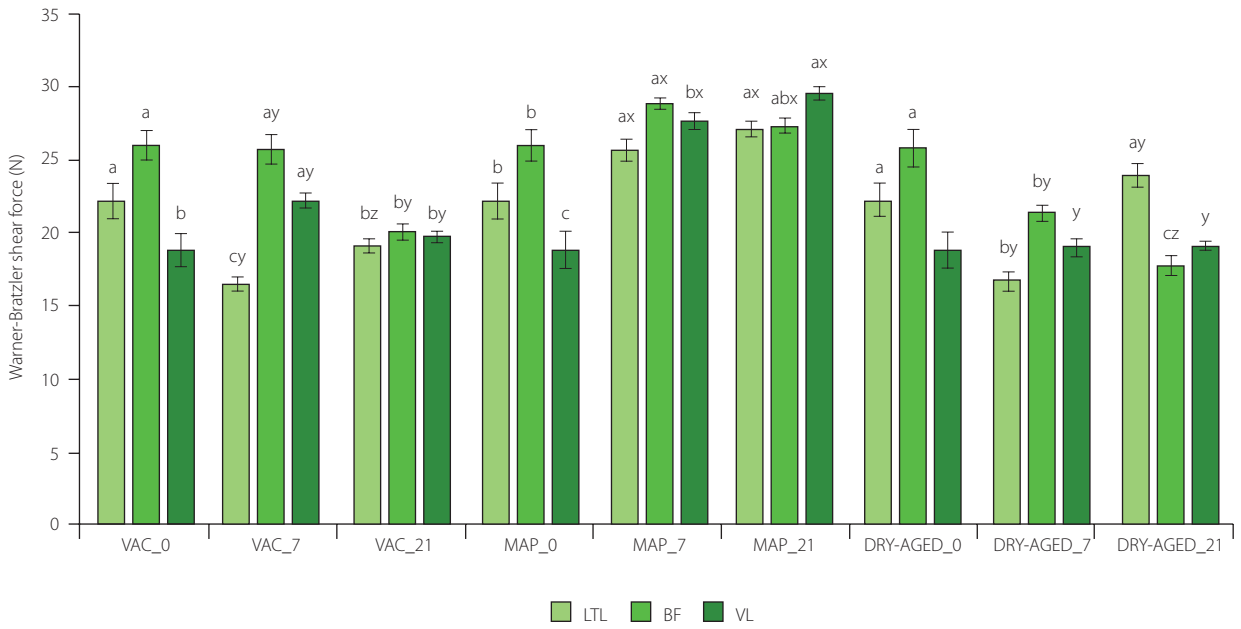

Figure 2. Warner–Bratzler shear force determined for muscles *longissimus thoracis et lumborum* (LTL), *biceps femoris* (BF) and *vastus lateralis* (VL) of roe deer during storage (at day 0 (fresh), 7 and 21) under modified atmosphere (MAP), dry (DRY-AGED) and vacuum (VAC) ageing. Results are shown as mean and standard error of mean (SEM). Different a–c letters above bars indicate a significant effect of time within the method ($p<0.05$); Different x–z letters above bars indicate a significant effect of the method within time ($p<0.05$).

groups decreased in all muscles at both 7 and 21 days of storage compared to the fresh sample (Figure 3, Table S3). On day 21 of VAC storage, the protein carbonyl content ranged from 0.21 to 0.26 nmol/mg protein. On day 7 of storage, the highest levels of carbonyls were determined for all DRY-AGED muscles. They remained stable, and no considerable increase was observed on day 21, except for BF. Oxidative changes in MAP-stored muscles up to day 7 were less intense than in the DRY-AGED muscles. On day 21 of analysis, however, the increase in protein oxidation observed in MAP samples was the highest, *i.e.*, 121.43% for LTL, 141.03% for BF, and 78.26% for VL, compared to the fresh samples.

As a result of protein oxidation, carbonyl group content for all roe deer muscles within each method did not exceed 0.94 nmol/mg protein (21 days MAP, BF). In a similar study on wild boar meat, the carbonyl contents for fresh LTL, BF, and VL muscles were significantly higher (1.26, 1.15, and 0.86 nmol/mg protein, respectively), while MAP storage contributed to protein oxidation products of 2.48–3.29 nmol/mg [Kasałka-Czarna *et al.*, 2022]. As reported by Lindahl *et al.* [2010], greater protein carbonylation in beef muscle was observed with high-oxygen packaging. In other studies, carbonyl levels in pork LTL stored for 7 days in MAP with a high oxygen content (70% O_2 + 30% CO_2) did not change significantly and were slightly higher than for VAC samples. After 14 days, a decrease in carbonyl levels was noted for VAC and a slight increase for MAP samples [Lund *et al.*, 2007]. As reported by Wang *et al.* [2019], 7 days of pork storage in MAP (80% O_2 + 20% CO_2) resulted in enhanced (reaching approximately 2.40 nmol/mg protein) formation of protein carbonyls.

The formation of protein carbonyls may also be promoted by a decrease in pH [Estévez, 2011]. In the current study, it was noted that on day 21 of MAP storage, a significant increase in protein oxidation was consistent with a decrease in pH. A deterioration in tenderness, colour, and odour of MAP-stored roe meat was observed in the present study. There are many hypotheses on the consequences of protein oxidation on meat flavour due to the formation of carbonyl groups [Lund *et al.*, 2011]. According to Ventanas *et al.* [2007] and Fuentes *et al.* [2010], the formation of protein carbonyls can affect the taste and aroma of meat. In contrast, other authors demonstrated the effect of protein oxidation on changes in meat colour [Domínguez *et al.*, 2019; Estévez & Cava, 2004]. This may explain the changes observed in our study for the b^* parameter values of meat during storage in MAP.

The levels of TBARS in fresh roe meat were 0.44, 0.47, and 0.46 mg MDA/kg for LTL, BF, and VL, respectively (Figure 3, Table S3). Daszkiewicz *et al.* [2018] reported 0.92 mg MDA/kg for LTL roe deer, but Klupsaite *et al.* [2020] detected 0.30 mg MDA/kg for m. *gluteus medius*. These values are strongly dependent on muscle metabolism and proximate composition. After 7 days of storage, an increase in lipid oxidation was detected in all samples. Significantly higher TBARS values were noted (after 7 and 21 days of storage) in the samples stored under high oxygen conditions (MAP). The least changes in lipids after 21 days of storage were observed in the samples stored in VAC. In the DRY-AGED muscles, the changes, although significant, occurred more slowly compared with MAP. TBARS values in roe deer meat increased faster than the protein carbonyl content during prolonged storage in MAP (an average increase of 1263% for TBARS and 155% for carbonyls on day 21). In our previous study, we observed that changes within TBARS occurred equally rapidly upon the storage of wild boar meat in a high-oxygen atmosphere [Kasałka-Czarna *et al.*, 2022].

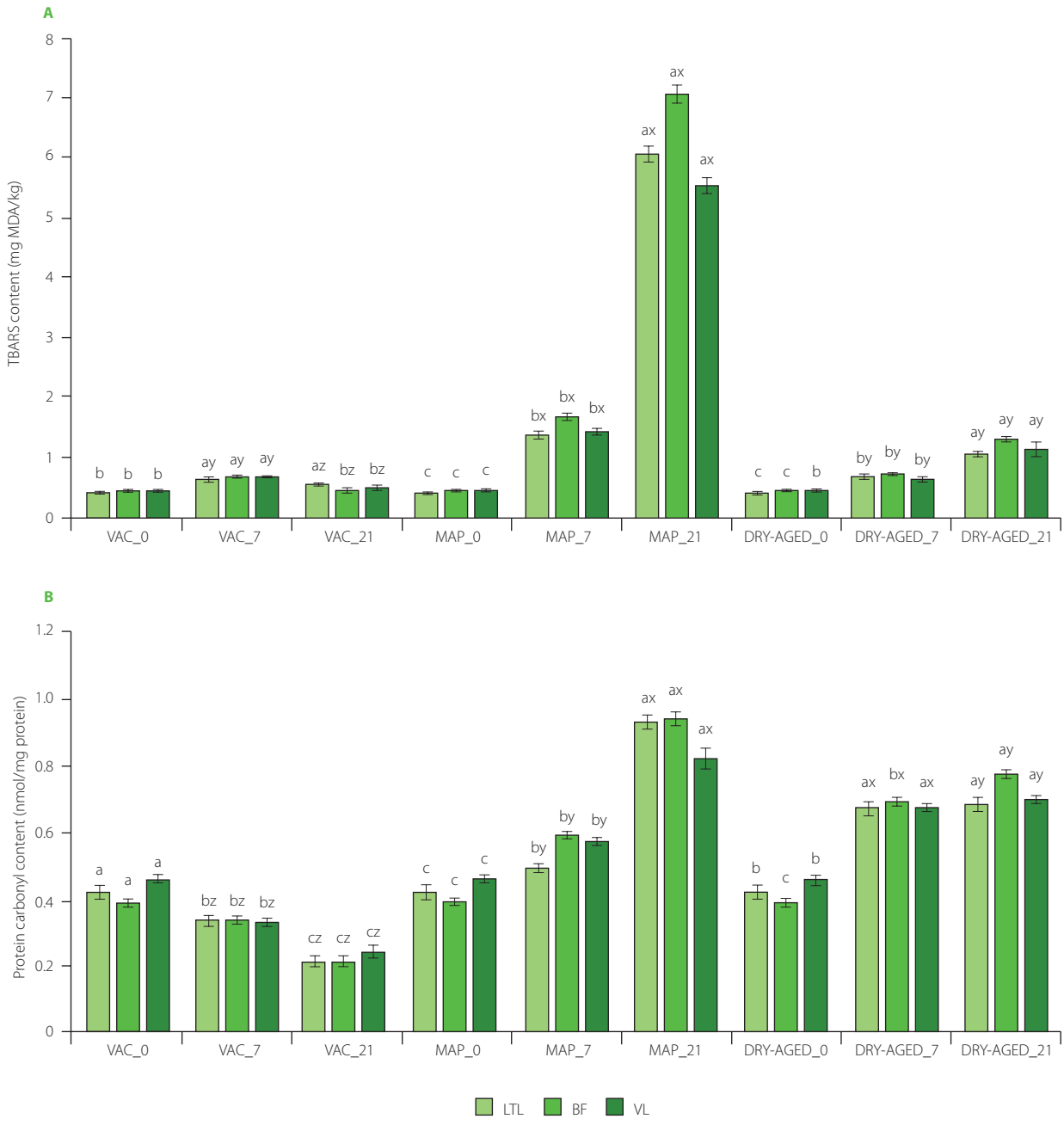

Figure 3. Contents of thiobarbituric acid reactive substances, TBARS (**A**) and protein carbonyls (**B**) in muscles *longissimus thoracis et lumborum* (LTL), *biceps femoris* (BF) and *vastus lateralis* (VL) of roe deer during storage (at day 0 (fresh), 7 and 21) under modified atmosphere (MAP), dry (DRY-AGED) and vacuum (VAC) ageing. Results are shown as mean and standard error of mean (SEM). Different a–c letters above bars for a given parameter indicate a significant effect of time within the method ($p<0.05$). Different x–z letters above bars for a given parameter indicate a significant effect of the method within time ($p<0.05$). MDA, malonic dialdehyde.

Interestingly, TBARS values were not considerably different for roe deer meat compared to wild boar meat. The LTL from wild boar on day 21 of MAP storage contained 6.15 mg MDA/kg, while the LTL from roe deer had 6.07 mg MDA/kg. High TBARS values result in a rancid aroma or noticeable colour change [Domínguez *et al.*, 2019]. The acceptable MDA content for meat products, where no rancid aroma is perceptible, is 2.0–2.5 mg MDA/kg meat [Campo *et al.*, 2006]. Importantly, reducing the oxygen in packaged pork results in the inhibition of both pork protein and lipid oxidation compared with 80% oxygen atmosphere. When the pork was stored in the air, the carbonyl and TBARS contents were lower than in high oxygen MAP [Wang *et al.*, 2019]. Similarly, beef steaks stored in a high oxygen atmosphere (80% O_2 + 20% CO_2) had higher TBARS values compared to the VAC-packed ones [Łopacka *et al.*, 2016].

CONCLUSIONS

In conclusion, a significant effect of storage time and method (dry, vacuum, and modified atmosphere ageing) of muscles of roe deer on pH, water activity, thermal loss, storage loss, WBSF and lipid and protein oxidation was found in the present study. A significant interaction effect of storage time × storage method was also

observed for all traits examined in BF and VL. For LTL, no significant interaction effect was found only for *L** values and water activity. The high-oxygen atmosphere induces the formation of protein carbonyls and lipid oxidation products. The use of MAP also caused negative changes in the technological properties and colour parameters of the muscles during storage. From the point of view of physicochemical analysis and texture properties, muscles stored in the DRY-AGED and VAC system showed no visible signs of deterioration and could be stored in the refrigerator for up to 21 days. The storage time had a positive effect on the tenderness of the meat and the colour of the DRY-AGED samples. The results indicate that the recommended methods for storing roe meat for 21 days are VAC and DRY-AGED. Further research should be carried out using other gas indicators for MAP packaging for this species. Due to its very low fat content and high protein content, roe meat is a valuable component of a balanced diet. Compared to other game species, venison meat is also rich in micro- and macronutrients.

SUPPLEMENTARY MATERIALS

The following are available online at http://journal.pan.olsztyn.pl/Effect-of-Dry-Vacuum-and-Modified-Atmosphere-Ageing-on-Physicochemical-Properties,163613,0,2.html; Table S1. The content (mg/kg) of selected minerals in muscles *longissimus thoracis et lumborum* (LTL), *biceps femoris* (BF) and *vastus lateralis* (VL) of the roe deer. Table S2. Storage loss and Warner-Bratzler shear force (WBSF) for muscles *longissimus thoracis et lumborum* (LTL), *biceps femoris* (BF) and *vastus lateralis* (VL) of roe deer during storage under modified atmosphere (MAP), dry (DRY-AGED) and vacuum (VAC) ageing. Table S3. Contents of thiobarbituric acid reactive substances (TBARS) and protein carbonyls in muscles *longissimus thoracis et lumborum* (LTL), *biceps femoris* (BF) and *vastus lateralis* (VL) of roe deer during storage under modified atmosphere (MAP), dry (DRY-AGED) and vacuum (VAC) ageing.

RESEARCH FUNDING

The study was financed by a grant (number 506.753.03.00) for the development of a young scientist or a doctoral student in the discipline of food technology and nutrition implemented as part of the doctoral dissertation at the Department of Meat Technology, Faculty of Food Science and Nutrition.

CONFLICT OF INTERESTS

The authors declare that they have no financial or commercial conflicts of interest.

ORCID IDS

R. Biegańska-Marecik https://orcid.org/0000-0002-3734-4806
N. Kasałka-Czarna https://orcid.org/0000-0001-9062-0665
M. Montowska https://orcid.org/0000-0002-6331-5726
A. Orłowska https://orcid.org/0000-0003-2941-930X
J. Proch https://orcid.org/0000-0003-0023-044X

REFERENCES

1. Bao, Y., Ertbjerg, P. (2019). Effects of protein oxidation on the texture and water-holding of meat: a review. *Critical Reviews in Food Science and Nutrition*, *59*(22), 3564–3578. https://doi.org/10.1080/10408398.2018.1498444
2. Campo, M.M., Nute, G.R., Hughes, S.I., Enser, M., Wood, J.D., Richardson, R.I. (2006). Flavour perception of oxidation in beef. *Meat Science*, *72*(2), 303–311. https://doi.org/10.1016/j.meatsci.2005.07.015
3. Chaijan, M. (2008). Review: Lipid and myoglobin oxidations in muscle foods. *Songklanakarin Journal of Science and Technology*, *30*(1), 47–53.
4. Clausen, I., Jakobsen, M., Ertbjerg, P., Madsen, N.T. (2009). Modified atmosphere packaging affects lipid oxidation, myofibrillar fragmentation index and eating quality of beef. *Packaging Technology and Science*, *22*(2), 85–96. https://doi.org/10.1002/pts.828
5. Cygan-Szczegielniak, D., Janicki, B. (2012a). Effect of age and sex of roe deer on tenderness and other quality characteristics of *longissimus lumborum* muscle. *ŻYWNOŚĆ. Nauka. Technologia. Jakość*, *6*(85), 127–137 (in Polish, English abstract).
6. Cygan-Szczegielniak, D., Janicki, B. (2012b). Amino acids content and basic chemical composition of roe deer (*Capreolus capreolus* L.) meat. *Polish Journal of Veterinary Sciences*, *15*(4), 645–649. https://doi.org/10.2478/v10181-012-0101-8
7. Dashdorj, D., Tripathi, V.K., Cho, S., Kim, Y., Hwang, I. (2016). Dry aging of beef; Review. *Journal of Animal Science and Technology*, *58*(1), art. no. 20. https://doi.org/10.1186/s40781-016-0101-9
8. Daszkiewicz, T., Janiszewski, P., Kandratowicz, J. (2008). Changes in chemical composition of meat from roe deer (*Capreolus capreolus* L.) bucks during cold storage under vacuum and modified atmosphere. *Polish Journal of Food and Nutrition Sciences*, *58*(3), 331–334.
9. Daszkiewicz, T., Kondratowicz, J., Koba-Kowalczyk, M. (2011). Changes in the quality of meat from roe deer (*Capreolus capreolus* L.) bucks during cold storage under vacuum and modified atmosphere. *Polish Journal of Veterinary Sciences*, *14*(3), 459–466. https://doi.org/10.2478/v10181-011-0068-x
10. Daszkiewicz, T., Kubiak, D., Panfil, A. (2018). The effect of long-term frozen storage on the quality of meat (*Longissimus thoracis et lumborum*) from female roe deer (*Capreolus capreolus* L.). *Journal of Food Quality*, *2018*, art. no. 4691542. https://doi.org/10.1155/2018/4691542
11. Domínguez, R., Pateiro, M., Gagaoua, M., Barba, F.J., Zhang, W., Lorenzo, J.M. (2019). A comprehensive review on lipid oxidation in meat and meat products. *Antioxidants 8*(10), art. no. 429. https://doi.org/10.3390/antiox8100429
12. Domínguez, R., Pateiro, M., Munekata, P.E.S., Zhang, W., Garcia-Oliveira, P., Carpena, M., Prieto, M.A., Bohrer, B., Lorenzo, J.M. (2022). Protein oxidation in muscle foods: A comprehensive review. *Antioxidants*, *11*(1), art. no. 60. https://doi.org/10.3390/antiox11010060
13. Dominik, P., Saláková, A., Buchtová, H., Steinhauser, L. (2012). Quality indicators of roe deer (*Capreolus capreolus* L.) venison in relation to sex. *Polish Journal of Food and Nutrition Sciences*, *62*(3), 185–191. https://doi.org/10.2478/v10222-012-0052-x
14. Estévez, M. (2011). Protein carbonyls in meat systems: A review. *Meat Science*, *89*(3), 259–279. https://doi.org/10.1016/j.meatsci.2011.04.025
15. Estévez, M., Cava, R. (2004). Lipid and protein oxidation, release of iron from heme molecule and colour deterioration during refrigerated storage of liver pâté. *Meat Science*, *68*(4), 551–558. https://doi.org/10.1016/j.meatsci.2004.05.007
16. Estévez, M., Xiong, Y. (2019). Intake of oxidized proteins and amino acids and causative oxidative stress and disease: recent scientific evidences and hypotheses. *Journal of Food Science*, *84*(3), 387–396. https://doi.org/10.1111/1750-3841.14460
17. Florek, M., Domaradzki, P., Żółkiewski, P., Ruda, B., Litwińczuk, Z., Kędzierska-Matysek, M. (2019). Physicochemical properties and indices of shelf life stability of dry aged beef with acid whey. *Medycyna Weterynaryjna*, *75*(8), 487–492 (in Polish, English abstract). https://doi.org/10.21521/mw.6214
18. Fuentes, V., Ventanas, J., Morcuende, D., Estévez, M., Ventanas, S. (2010). Lipid and protein oxidation and sensory properties of vacuum-packaged dry-cured ham subjected to high hydrostatic pressure. *Meat Science*, *85*(3), 506–514. https://doi.org/10.1016/j.meatsci.2010.02.024
19. Gill, C.O. (1990). Controlled atmosphere packaging of chilled meat. *Food Control*, *1*(2), 74–78. https://doi.org/10.1016/0956-7135(90)90088-T
20. Hoffman, L.C., Wiklund, E. (2006). Game and venison – meat for the modern consumer. *Meat Science*, *74*(1), 197–208. https://doi.org/10.1016/j.meatsci.2006.04.005
21. ISO 937:1978. *Meat and meat products — Determination of nitrogen content (Reference method)*. International Organization for Standardization.
22. Ivanović, S., Pisinov, B., Pavlović, M., Pavlović, I. (2020). Quality of meat from female fallow deer (*Dama dama*) and roe deer (*Capreolus capreolus*) hunted in Serbia. *Annals of Animal Science*, *20*(1), 245–262. https://doi.org/10.2478/aoas-2019-0064
23. Kasałka-Czarna, N., Bilska, A., Biegańska-Marecik, R., Montowska, M. (2022). The effect of storage method on selected physicochemical and microbiolog-

ical qualities of wild boar meat. *Journal of the Science of Food and Agriculture*, *102*(12), 5250–5260. https://doi.org/10.1002/jsfa.11878
24. Kim, Y.H., Huff-Lonergan, E., Sebranek, J.G., Lonergan, S.M. (2010). High-oxygen modified atmosphere packaging system induces lipid and myoglobin oxidation and protein polymerization. *Meat Science*, *85*(4), 759–767. https://doi.org/10.1016/j.meatsci.2010.04.001
25. Klupsaite, D., Buckiuniene, V., Sidlauskiene, S., Lele, V., Sakiene, V., Zavistanaviciute, P., Klementaviciute, J., Viskontaite, E., Bartkiene, E. (2020). Comparison studies of the chemical, physical, technological, and microbiological characteristics of the European roe deer, boar, red deer, and beaver hunted wild game meat. *Animal Science Journal*, *91*(1), art. no. e13346. https://doi.org/10.1111/asj.13346
26. Królikowski, T., Deptuła, K. (2020). Game meat in a well-balanced diet as an attractive alternative to livestock meat. *Postępy Techniki Przetwórstwa Spożywczego / Technological Progress in Food Processing*, *2*, 125–130.
27. Kwiecińska, K., Kosicka-Gębska, M., Gębski, J. (2018). Availability of game meat on the Polish market in the context of consumer needs. *Zeszyty Naukowe SGGW - Ekonomika i Organizacja Gospodarki Żywnościowej*, *121*, 83–91 (in Polish, English abstract). https://doi.org/10.22630/EIOGZ.2018.121.6
28. Levine, R.L., Williams, J.A., Stadtman, E.P., Shacter, E. (1994). Carbonyl assays for determination of oxidatively modified proteins. *Methods in Enzymology*, *233*, 346–357. https://doi.org/10.1016/S0076-6879(94)33040-9
29. Li, F., Zhong, Q., Kong, B., Wang, B., Pan, N., Xia, X. (2020). Deterioration in quality of quick-frozen pork patties induced by changes in protein structure and lipid and protein oxidation during frozen storage. *Food Research International*, *133*, art. no. 109142. https://doi.org/10.1016/j.foodres.2020.109142
30. Lindahl, G., Lagerstedt, Å., Ertbjerg, P., Sampels, S., Lundström, K. (2010). Ageing of large cuts of beef loin in vacuum or high oxygen modified atmosphere – Effect on shear force, calpain activity, desmin degradation and protein oxidation. *Meat Science*, *85*(1), 160–166. https://doi.org/10.1016/j.meatsci.2009.12.020
31. Lo Fiego, D.P., Santoro, P., Macchioni, P., Mazzoni, D., Piattoni, F., Tassone, F., De Leonibus, E. (2004). The effect of dietary supplementation of vitamins C and E on the α-tocopherol content of muscles, liver and kidney, on the stability of lipids, and on certain meat quality parameters of the *longissimus dorsi* of rabbits. *Meat Science*, *67*(2), 319–327. https://doi.org/10.1016/j.meatsci.2003.11.004
32. Łopacka, J., Półtorak, A., Wierzbicka, A. (2016). Effect of MAP, vacuum skin-pack and combined packaging methods on physicochemical properties of beef steaks stored up to 12 days. *Meat Science*, *119*, 147–153. https://doi.org/10.1016/j.meatsci.2016.04.034
33. Lund, M.N., Heinonen, M., Baron, C.P., Estévez, M. (2011). Protein oxidation in muscle foods: A review. *Molecular Nutrition and Food Research*, *55*(1), 83–95. https://doi.org/10.1002/mnfr.201000453
34. Lund, M.N., Lametsch, R., Hviid, M.S., Jensen, O.N., Skibsted, L.H. (2007). High-oxygen packaging atmosphere influences protein oxidation and tenderness of porcine *longissimus dorsi* during chill storage. *Meat Science*, *77*(3), 295–303. https://doi.org/10.1016/j.meatsci.2007.03.016
35. Moczkowska, M., Półtorak, A., Montowska, M., Pospiech, E., Wierzbicka, A. (2017). The effect of the packaging system and storage time on myofibrillar protein degradation and oxidation process in relation to beef tenderness. *Meat Science*, *130*, 7–15. https://doi.org/10.1016/j.meatsci.2017.03.008
36. Niewiadomska, K., Kosicka-Gębska, M., Gębski, J., Gutkowska, K., Jeżewska-Zychowicz, M., Sułek, M. (2020). Game meat consumption–conscious choice or just a game? *Foods*, *9*(10), art. no. 1357. https://doi.org/10.3390/foods9101357
37. PN-ISO 1442:2000. *Meat and meat products – determination of moisture content (Reference method)*. Polish Committee for Standardization.
38. PN-ISO 1444:2000. *Meat and meat products – determination of free fat content*. Polish Committee for Standardization.
39. PN-ISO 936:2000. *Meat and meat products – determination of total ash*. Polish Committee for Standardization.
40. Razmaitė, V., Šiukščius, A., Pileckas, V., Švirmickas, G.J. (2015). Effect of different roe deer muscles on fatty acid composition in intramuscular fat. *Annals of Animal Science*, *15*(3), 775–784. https://doi.org/10.1515/aoas-2015-0012
41. Regulation (EC) No 853/2004 of the European Parliament and of the Council of 29 April 2004 laying down specific hygiene rules for food of animal origin (2004), *Official Journal of the European Union*, *L 139*.
42. Soladoye, O.P., Juárez, M.L., Aalhus, J.L., Shand, P., Estévez, M. (2015). Protein oxidation in processed meat: Mechanisms and potential implications on human health. *Comprehensive Reviews in Food Science and Food Safety*, *14*(2), 106–122. https://doi.org/10.1111/1541-4337.12127
43. Sottero, B., Leonarduzzi, G., Testa, G., Gargiulo, S., Poli, G., Biasi, F. (2019). Lipid oxidation derived aldehydes and oxysterols between health and disease. *European Journal of Lipid Science and Technology*, *121*(1), art. no. 1700047. https://doi.org/10.1002/ejlt.201700047
44. Świderski, F., Sadowska, A. (2011). Meat packing in modified atmosphere and vacuum conditions. *Postępy Techniki Przetwórstwa Spożywczego*, *1*, 98–102 (in Polish, English abstract).
45. Thøgersen, R., Gray, N., Kuhnle, G., Van Hecke, T., De Smet, S., Young, J.F., Sundekilde, U.K., Hansen, A.K., Bertram, H.C. (2020). Inulin-fortification of a processed meat product attenuates formation of nitroso compounds in the gut of healthy rats. *Food Chemistry*, *302,* art. no. 125339. https://doi.org/10.1016/j.foodchem.2019.125339
46. Ventanas, S., Ventanas, J., Tovar, J., García, C., Estévez, M. (2007). Extensive feeding versus oleic acid and tocopherol enriched mixed diets for the production of Iberian dry-cured hams: Effect on chemical composition, oxidative status and sensory traits. *Meat Science*, *77*(2), 246–256. https://doi.org/10.1016/j.meatsci.2007.03.010
47. Vergara, H., Gallego, L., García, A., Landete-Castillejos, T. (2003). Conservation of *Cervus elaphus* meat in modified atmospheres. *Meat Science*, *65*(2), 779–783. https://doi.org/10.1016/S0309-1740(02)00282-6
48. Wang, C., Wang, H., Li, X., Zhang, C. (2019). Effects of oxygen concentration in modified atmosphere packaging on water holding capacity of pork steaks. *Meat Science*, *148*, 189–197. https://doi.org/10.1016/j.meatsci.2018.10.001
49. Wazir, H., Chay, S.Y., Zarei, M., Hussin, F.S., Mustapha, N.A., Ibadullah, W.Z.W., Saari, N. (2019). Effects of storage time and temperature on lipid oxidation and protein co-oxidation of low-moisture shredded meat products. *Antioxidants*, *8*(10), art. no. 486. https://doi.org/10.3390/antiox8100486
50. Zomborszky, Z., Szentmihályi, G., Sarudi, I., Horn, P., Szabó, C.S. (1996). Nutrient composition of muscles in deer and boar. *Journal of Food Science*, *61*(3), 625–627. https://doi.org/10.1111/j.1365-2621.1996.tb13172.x
51. Zubaidi, M.A., Proch, J., Konieczny, P., Tomczyk, Ł. (2021). Toxicity testing by the microbial assay for risk assessment (MARA) in relation to trace elements content in King bolete (*Boletus edulis*) collected in several sites of Poland. *Applied Science*, *11*(9), art. no. 4166. https://doi.org/10.3390/app11094166

ORIGINAL ARTICLE
http://journal.pan.olsztyn.pl

Polish Journal of Food and Nutrition Sciences
2023, Vol. 73, No. 2, 187–195
DOI: 10.31883/pjfns/163982
ISSN 1230-0322, e-ISSN 2083-6007

Effect of Maltodextrin on Drying Rate of Avocado (*Persea Americana* Mill.) Pulp by Refractance Window Technique, and on Color and Functional Properties of Powder

Thi-Van-Linh Nguyen[1,*], Thi-Thuy-Dung Nguyen[1], Quoc-Trung Huynh[1], Phuoc-Bao-Duy Nguyen[2, 3]

[1]Faculty of Environmental and Food Engineering, Nguyen Tat Thanh University, 300A Nguyen Tat Thanh Street, District 4, Ho Chi Minh City, Vietnam
[2]Faculty of Electrical and Electronics Engineering, Ho Chi Minh University of Technology (HCMUT), 268 Ly Thuong Kiet Street, District 10, Ho Chi Minh City, Vietnam
[3]Vietnam National University Ho Chi Minh City, Linh Trung Ward, Thu Duc District, Ho Chi Minh City, Vietnam

This study investigated the effects of various maltodextrin contents (0, 6, 7.5, 9, and 10.5 g/100 g of pulp) on the drying rate and powder quality of avocado pulp dried by refractance window technique. Increasing the maltodextrin addition level significantly decreased the drying rate and prolonged the drying time. The maltodextrin considerably affected the drying rate of pulp when its moisture content was higher than 1.0 g/g dry weight. A significant improvement was found in the retention of total contents of phenolics and chlorophylls, antioxidant capacity, and color in avocado powder obtained from pulp with maltodextrin. The addition of 9 g maltodextrin/100 g of pulp allowed to retain 85.60% TPC, 78.78% total chlorophyll content, 83.48% DPPH radical scavenging activity, and 78.89% ferric reducing antioxidant power. However, maltodextrin in the amount of 10.5 g/100 g of pulp had a negative impact on moisture removal and deteriorated the quality of the dried avocado. These findings may have practical application for the production of dried avocado and other fruits.

Key words: antioxidant activity, chlorophyll, drying curve, total phenolics, color parameters

INTRODUCTION

Hydrocolloids were widely applied in food processing as thickeners, gelling agents, structure stabilizers, and emulsifiers [Williams & Phillips, 2000]. During the drying process, particularly for fruit puree or juice, hydrocolloids were added to improve both product quality and drying efficiency. Previous studies applied hydrocolloids to fruit pulp before processing to prevent the stickiness and caking phenomena [Bhandari *et al.*, 1993; Gómez-Pérez *et al.*, 2020; Singh Gujral & Singh Brar, 2003]. After mixing hydrocolloids into the pulp, the glass transition temperature of fruit pulp increased, leading to the drying process being implemented easily and obtaining high-quality products [Bhandari *et al.*, 1993]. It was reported that the increase of maltodextrin (MD) could improve the sensory quality of mango leather [Singh Gujral & Singh Brar, 2003] as well as the lamina and texture properties of murta (*Ugni molinae Turcz*) berry leather [Gómez-Pérez *et al.*, 2020], and enhance the quality of dried fruit powder from tomato pulp [Goula & Adamopoulos, 2008], blackberry [Ferrari *et al.*, 2012], *etc.* Among hydrocolloids, MD was the most popular carrier used in food production [Williams & Phillips, 2000].

Drying technology continues to play an important role in food preservation and processing. The commercial and utilitarian worth of food items was increased as a result of the removal of moisture from their constituents. Among the fruit forms that

***Corresponding Author:**
e-mail: ntvlinh@ntt.edu.vn (T.V.L. Nguyen)

Submitted: 6 February 2023
Accepted: 26 April 2023
Published on-line: 1 June 2023

can be dried, fruit juice and puree get the most attention when it comes to making fruit powder, which is simple to utilise or formulate commercial food goods [Ramaswamy & Marcotte, 2005]. In the research, spray-, drum-, and freeze-drying were the most common methods for producing fruit powder. There were, however, disadvantages to each drying procedure. In spray drying, the powder quality was diminished as a result of the addition of 40 to 60% of carriers [Brennan *et al.*, 1971; Can Karaca *et al.*, 2016; Sobulska & Zbicinski, 2021]. In turn, drum drying at temperatures ranging from 120 to 170°C caused substantial harm to the quality of dried materials [Nindo & Tang, 2007]. Finally, the freeze-drying exclusively produced fruit powder of the highest grade [Ratti, 2013], but the adoption and maintenance of this process were costly.

Recent advancements in drying technology would increase the likelihood of discovering viable drying methods to address pre-existing issues. Recently, refractance window (RW™) drying has received increased interest in the dehydration of fruit purees or slices [Vega-Mercado *et al.*, 2001]. In the RW™ drying technique, moisture diffusion and evaporation occur rapidly due to heat conduction, convection, and radiation at the hot-water interface and air-film interface [Raghavi *et al.*, 2018]. Therefore, the drying process could be finished quickly and preserve the quality of the dried product efficiently. Compared to the above-mentioned drying processes, RW™ drying was addressed in fewer publications; however, the RW™ drying results were substantially more outstanding. In the literature, the RW™ drying was reported to produce good nutritional and sensory quality of dried fruits and vegetables such as carrots, strawberries [Nindo & Tang, 2007], tomatoes [Abul-Fadl & Ghanem, 2011], mango pulp [Caparino *et al.*, 2012], pomegranate leather [Tontul & Topuz, 2017], cornelian cherry pulp [Tontul *et al.*, 2018], low-fat avocado paste [Da Silva & Da Silva, 2018], apple slices [Rajoriya *et al.*, 2019], goldenberry pulp [Puente *et al.*, 2020], *etc*. Besides, the RW™ drying was more thermally efficient than convective and freeze-drying [Nindo & Tang, 2007]. Thus, RW™ drying was anticipated to be an effective method for drying fruits and vegetables. However, additional evidence is required to confirm this notion.

Avocado fruits are nutrient- and phytochemical-dense superfoods [Comerford *et al.*, 2016]. Specifically, bioactive substances with varied medicinal capabilities in avocado have been shown to be associated with consumer health advantages [Lye *et al.*, 2020]. As a result of its climacteric fruit qualities and significant processing constraints, avocado's economic and utilitarian worth decreased.

In this situation, applying the drying process to avocado would be one of the appropriate alternatives. The avocado's shelf life might be prolonged and new avocado-based products could be developed after drying. In previous studies, avocado was reported to be dried by heat-pump [Ceylan *et al.*, 2007], freeze-drying [Castañeda-Saucedo *et al.*, 2014; Rafidah *et al.*, 2014; Souza *et al.*, 2015], hot-air drying [Temu, 2013], and superheated-steam drying [Rafidah *et al.*, 2014]. However, these drying methods took a long operating time (varying from 3 to more than 20 h). A recent report indicated that the RW™ drying temperature greatly affected drying kinetics and avocado pulp quality [Nguyen, *et al.*, 2022b]. The high RW™ drying temperature of 90°C could preserve over 80% of total phenolics and antioxidant activity [Nguyen, *et al.*, 2022b]. It appeared that the RW had a good potential for the manufacturing of avocado fruit powder. While the effect of drying temperature has been well explored, the influence of maltodextrin content has not yet been investigated. Therefore, this study sought to determine the effects of MD content on the drying rate and quality of powder (including total contents of phenolics and chlorophylls, antioxidant capacity, and color parameters) made of avocado pulp dried with the RW™ technique.

MATERIALS AND METHODS

Materials and chemicals

Fresh avocado (*Persea americana* Mill. cv. 'Maluma') fruits were obtained from a local farm in DakLak, Vietnam; only ripe avocados with a green exterior were selected.

Gallic acid, 2,4,6-tripyridyl-*s*-triazine (TPTZ), 2,2-diphenyl--1-picrylhydrazyl (DPPH) radical, and 6-hydroxy-2,5,7,8 tetramethylchromane-2-carboxylic acid (Trolox) were purchased from Sigma-Aldrich (Merck PTE Ltd, Ascent Building, Singapore). The solid sodium tungstate, sodium molybdate, and lithium sulphate were constituents of the Folin-Ciocalteu (2 N) reagent. Maltodextrin (dextrose equivalent in the range of 16.5–19.5, Sigma-Aldrich) was acquired from a local vendor. As well as other chemicals, acetic acid, sodium acetate, chloroform, sodium carbonate, methanol, acetone, diethyl ether, and ferric chloride hexahydrate were of analytical quality.

Avocado pulp preparations

After receiving, the avocado fruits were washed, peeled, devoid of seed, and sliced into slices with 3.00±0.03 mm thickness. Then, the slices were soaked in a sodium bicarbonate solution (0.05%) for 30 min and subjected to steam blanching for 3 min to inactivate the browning enzymes and inhibit other enzymes in materials. Subsequently, the blanched samples were cooled promptly with cold water at 5.0±0.5°C and ground to collect avocado pulp using a commercial blender (BJY-CB2L60-A, Berjaya Steel Product Sdn Bhd, Kuala Lumpur, Malaysia). To prepare the material for drying, the pulp was mixed with MD using a laboratory mixing overhead stirrer (SH-II-6C, Hebei, China). The mix was analyzed for total phenolic content (TPC), total chlorophyll content, antioxidant capacity, and color parameters before drying.

Drying conditions and drying rate determination

This study designed experiments with three replications using the one-factor-at-a-time approach. The samples were prepared using a block design that was randomly generated. Each sample containing 100 g of pulp was mixed with different amounts of MD, *i.e.* 0, 6, 7.5, 9, and 10.5 g. In this investigation, a custom-built refractance window (RW™) drying apparatus comprised of a hot water reservoir (0.42×0.28×0.10 m) and a thermostatically-controlled

water bath was operated in a batch laboratory-scale configuration (Model DH.WB000106, Daihan-Scientific, Wonju-si, South Korea). A polyester film (Mylar™, Jiangsu, China) with a thickness of 0.25 mm was utilized to transfer heat from hot water to fruit pulp placed in 2 mm-thick layers atop the Mylar films. Our earlier research determined that the RW™ drying temperature had a substantial effect on the quality of dried avocado powder, with the highest quality powder being produced at 90°C [Nguyen, *et al.*, 2022b]. Therefore, each sample was dried at 90°C using RW™ drying.

The moisture content of samples was measured using the moisture analyzer (MB23, Ohaus, Parsippany, NJ, USA) in 5-min intervals. The drying process was stopped when the moisture content reached approximately 0.04 g/g dry weight (DW) because this moisture content assured that dried avocado could be ground to powder. The drying rate (g/g DW) was computed from Equation (1).

$$\text{Drying rate (g/g DW/min)} = \frac{M_t - M_{t+\Delta t}}{\Delta t} \quad (1)$$

where: M_t, and $M_{t+\Delta t}$ were the moisture content at drying time t (min), and t+Δt (min), respectively.

Then, the avocado powder was used to analyze TPC, total chlorophyll content, antioxidant capacity, and color parameters.

Preparation of avocado extracts for chemical analysis

The extracts were obtained according to the procedure reported in the literature [Wang *et al.*, 2010]. The fresh pulps as well as dried and powdered avocado pulps with and without MD (0.2 g) were extracted using 10 mL of solvent (7 mL acetone + 0.03 mL glacial acetic acid + 2.97 mL water). Then, the extracts were diluted to 25 mL and analyzed for their TPC and antioxidant capacity.

Total phenolic content determination

The method with Folin-Ciocalteu reagent, as established in ISO 14502-1:2005, was deployed to measure the TPC with distilled water serving as a blank [ISO, 2005]. The UV-9000 spectrophotometer (Metash, Shanghai, China) was used for absorbance measurement. The gallic acid calibration curve was used to calculate the total phenolic content, which was given as mg of gallic acid equivalent per g of dry weight (mg GAE/g DW). The retention percentage of TPC was determined according to Equation (2).

$$\text{Retention of TPC (\%)} = \frac{C_{\text{TPC, after drying}}}{C_{\text{TPC, before drying}}} \times 100\% \quad (2)$$

where: $C_{\text{TPC, before drying}}$ and $C_{\text{TPC, after drying}}$ were the TPC in the sample before drying and after drying, respectively.

DPPH radical scavenging assay (DPPH)

The DPPH radical scavenging activity of the extract was determined according to the procedure described previously [Nguyen *et al.*, 2022b] using a UV-9000 spectrophotometer (Metash). DPPH radical scavenging activity was analyzed using the standard curve for Trolox plotted as the percent of scavenged DPPH radicals *vs.* concentration. Results were expressed as mg Trolox equivalent *per* g of sample dry weight (mg TE/g DW). The retention percentage of DPPH radical scavenging activity was calculated from Equation (3).

$$\text{Retention of DPPH radical scavenging activity (\%)} = \frac{C_{\text{DPPH, after drying}}}{C_{\text{DPPH, before drying}}} \times 100\% \quad (3)$$

where: $C_{\text{DPPH, before drying}}$ and $C_{\text{DPPH, after drying}}$ were the DPPH radical scavenging activity of the sample before drying and after drying, respectively.

Ferric reducing antioxidant power determination

The ferric reducing antioxidant power (FRAP) assay was conducted in accordance with a modified version of the method described in the literature [Benzie & Strain, 1996]. The acetate buffer (0.3 M, pH 3.6), TPTZ (10 mM in 40 mM HCl), and $FeCl_3 \times 6H_2O$ (20 mM) were mixed in a 10:1:1 (*v/v/v*) ratio to make the reagent. In order to measure the FRAP, 2.85 mL of FRAP reagent was applied to 0.15 mL of diluted sample. The reaction mixture was incubated in the dark for 30 min, after which the absorbance was measured at 593 nm with a UV-9000 spectrophotometer (Metash) using distilled water as the blank. Based on the Trolox calibration curve, the ferric reducing antioxidant power was computed and reported as mg Trolox equivalent *per* g of sample dry weight (mg TE/g DW).

The retention percentage of FRAP was calculated from Equation (4).

$$\text{Retention of FRAP (\%)} = \frac{C_{\text{FRAP, after drying}}}{C_{\text{FRAP, before drying}}} \times 100\% \quad (4)$$

where: $C_{\text{FRAP, before drying}}$ and $C_{\text{FRAP, after drying}}$ were the FRAP of the sample before drying and after drying, respectively.

Determination of total chlorophyll content

In order to initiate the extraction process, 0.2 g of avocado pulps or powders was combined with 5 mL of the solvent (chloroform and methanol, 2:1, *v/v*) and vortexed for 30 s at 2,000 rpm. After sonication (40 KHz, 240 W, 5 min), the sample was vortexed again for 10 s and cooled at 4°C for 20 min. After cooling the sample, it was centrifuged at 2,095×*g* for 10 min, and the supernatant was collected. The solvent in the supernatant was evaporated in a Petri dish using an LO-FS100 forced convection oven (LK Lab, Namyangju, Korea) at 50°C for 30 min, and residue was redissolved in 10 mL of pure diethyl ether for analysis of total chlorophyll content as described in the literature [Lichtenthaler & Buschmann, 2001]. Results were calculated according to Equation (5).

$$\text{Total chlorophyll content (μg/g DW)} = \frac{7.62 \times A_{661} + 15.39 \times A_{642}}{m_{\text{sample (DW)}}} \times 10 \quad (5)$$

where: A_{661} and A_{642} corresponded to absorbances measured at 661 and 642 nm using a UV-9000 spectrophotometer (Metash), $m_{\text{sample (DW)}}$ was the dry weight of sample.

The retention percentage of total chlorophyll content was calculated from Equation (6).

$$\text{Retention of total chlorophyll content (\%)} = \frac{C_{\text{Chlorophyll, after drying}}}{C_{\text{Chlorophyll, before drying}}} \times 100\% \quad (6)$$

where: $C_{\text{Chlorophyll, before drying}}$ and $C_{\text{Chlorophyll, after drying}}$ were the total chlorophyll content in the sample before drying and after drying, respectively.

Determination of color parameters

Color of avocado pulps and powders was assessed using the NR110 precision colorimeter (Shenzhen ThreeNH Technology Co. Ltd, Shenzhen, China) in the CIELab color scale. The L^*, a^*, and b^* values were measured. L^* symbolizes lightness on a scale ranging from 0 (black) to 100 (white). Positives and negatives of a^* represent red and green, whereas positives and negatives of b^* represent yellow and blue. Besides, the total color difference (ΔE) was calculated according Equation (7) to evaluate the difference in total color between the tested samples.

$$\Delta E = \sqrt{(L^* - L_0^*)^2 + (a^* - a_0^*)^2 + (b^* - b_0^*)^2} \quad (7)$$

Statistical analysis

Experimental data were evaluated utilizing the SPSS 15 programme (SPSS Inc., Chicago, IL, USA). The significant differences in mean values between the samples were determined using one-way analysis of variance (ANOVA) with Tukey's multiple range test at the 5% significance level for all experiments, which were carried out in triplicate.

RESULTS AND DISCUSSION

Effect of maltodextrin addition on the drying rate

The curves of moisture content *versus* drying time of avocado pulp at different maltodextrin (MD) contents are presented in Figure 1. In addition, the drying curves are shown in Figure 2. The pulps with a higher content of MD had a lower drying rate and a longer drying time. The control sample (0 g MD/100 g of pulp) had the highest drying rate and the shortest drying time. The MD with a moisture content of 3.62±0.04 g/100 g (wet basis) was added to the avocado pulp. Therefore, the increased addition of MD would rise significantly dry matter content of the pulp before drying. According to Rodosta & Schierbaum's [1990] findings, the presence of MD in avocado pulp would create hydrogen bonds with free water molecules. This could cause internal and external diffusion resistance, leading to limited moisture removal from the pulp in the drying process [Goula & Adamopoulos, 2008]. Consequently, the initial drying rate was slower at higher MD content. Some previous studies on the MD effect on drying kinetics of sugar, acid-rich foods [Adhikari *et al.*, 2004], pineapple, and mango leather [Gujral *et al.*, 2013] showed similar findings.

Figure 2 further revealed that moisture removal only occurred during the falling-rate period for all samples. It is likely that during the RW™ drying process with a thin layer of avocado pulp, moisture evaporated rapidly, causing the drying process to occur during the falling-rate period without a constant drying rate period. This finding was consistent with literature data on RW™ drying [Abul-Fadl & Ghanem, 2011; Gómez-Pérez *et al.*, 2020; Nguyen, *et al.*, 2022b; Nindo & Tang, 2007; Ochoa-Martínez *et al.*, 2012].

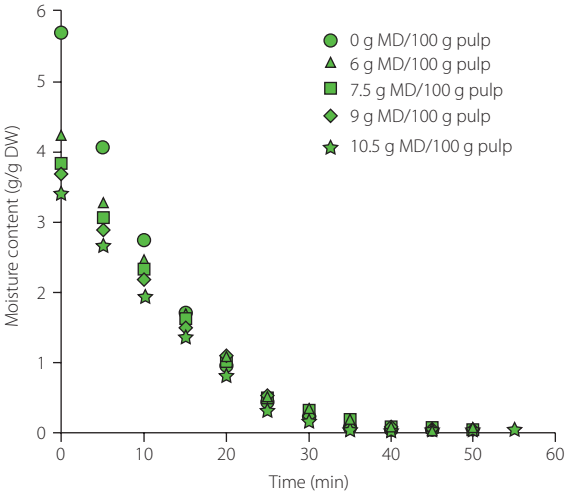

Figure 1. The curves of moisture content *versus* drying time of avocado pulp without (0 g/100 g pulp) and with the addition of 6, 7.5, 9, and 10.5 g maltodextrin (MD/100 g of pulp) dried by refractance window technique. DW, dry weight.

Drying curves of avocado pulps without and with different contents of MD show that the behavior of moisture removal was significantly different between samples at the moisture content higher than 1.0 g/g DW (Figure 2). When the moisture content of the drying material was above this value, the moisture diffusion was directly related to the elimination of free water. When the moisture content was below 1.0 g/g DW, the moisture removal predominantly eliminated bound water. Therefore, when MD was mixed with avocado pulp, the MD predominantly interacted with the free water. Consequently, the MD had a substantial impact on the drying rate curves of avocado pulp with a moisture content greater than 1.0 g/g DW.

Effect of maltodextrin addition on total contents of phenolics and chlorophylls

The TPC and total chlorophyll content of the avocado pulps without and with different MD contents and powders obtained by RW™ drying of pulps are shown in Figure 3. The addition of MD to fresh pulp significantly ($p<0.05$) decreased its TPC and total chlorophyll content and these decreases were dependent on the MD content. The results of phytochemical content analysis were expressed based on dry weight of pulp or powder. Therefore, an increase in MD content would increase the dry matter content of the pulp, resulting in a decrease in the avocado pulp's TPC and total chlorophyll content prior to drying.

The TPC and total chlorophyll content in the samples before drying were significantly ($p<0.05$) higher than in powders after drying (Figure 3), thus the total content of both phenolics and chlorophylls deteriorated during the RW™ drying of the avocado pulp with MD content increasing from 0 to 9 g MD/100 g of pulp; however, phytochemical retentions during the RW™ drying increased (Table 1). The highest retentions (85.60% for TPC, and 78.78% for chlorophylls) were found with

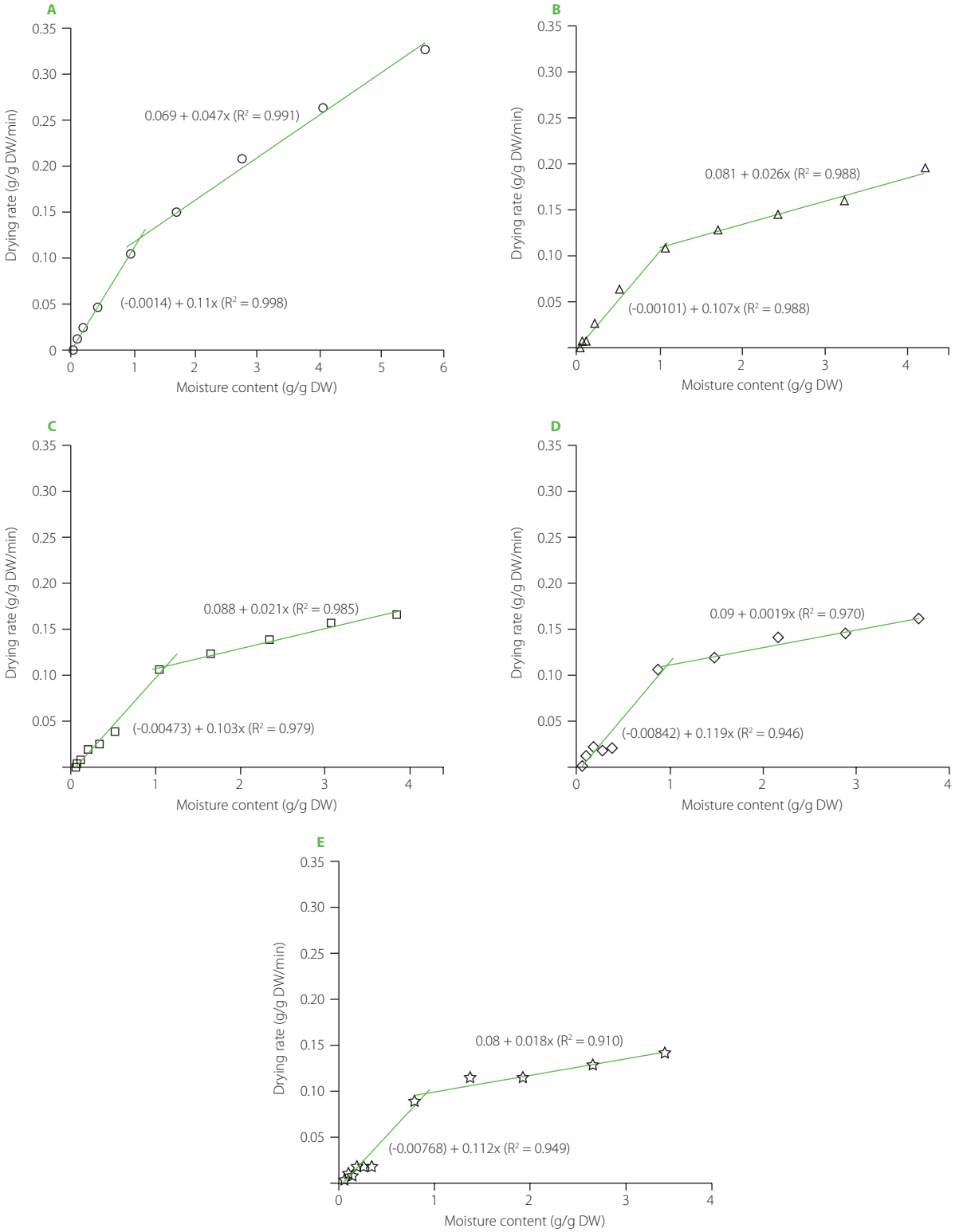

Figure 2. Drying rate curves of avocado pulp without (**A**) and with the addition of 6 g (**B**), 7.5 g (**C**), 9 g (**D**) and 10.5 g (**E**) maltodextrin per 100 g of pulp dried by refractance window technique. DW, dry weight.

the addition of 9 g MD/100 g of pulp, although the TPC retention for the pulp with 7.5 g MD/100 g was not significantly ($p \geq 0.05$) different. When the highest level of MD additive was used (10.5 g MD/100 g of pulp), the retentions of TPC and total chlorophyll content decreased significantly ($p < 0.05$). The enhanced retentions of TPC and chlorophylls by increasing the pulp's MD content may be because MD acted as the coating substance that produces a physical barrier [Osorio *et al.*, 2011], restricting the contact of phytochemicals with external factors like oxygen. Therefore, the rate of phytochemical degradation was slowed, and their retention was increased. As stated previously, MD in pulp increased the dry weight and formed bonds with free water [Radosta &

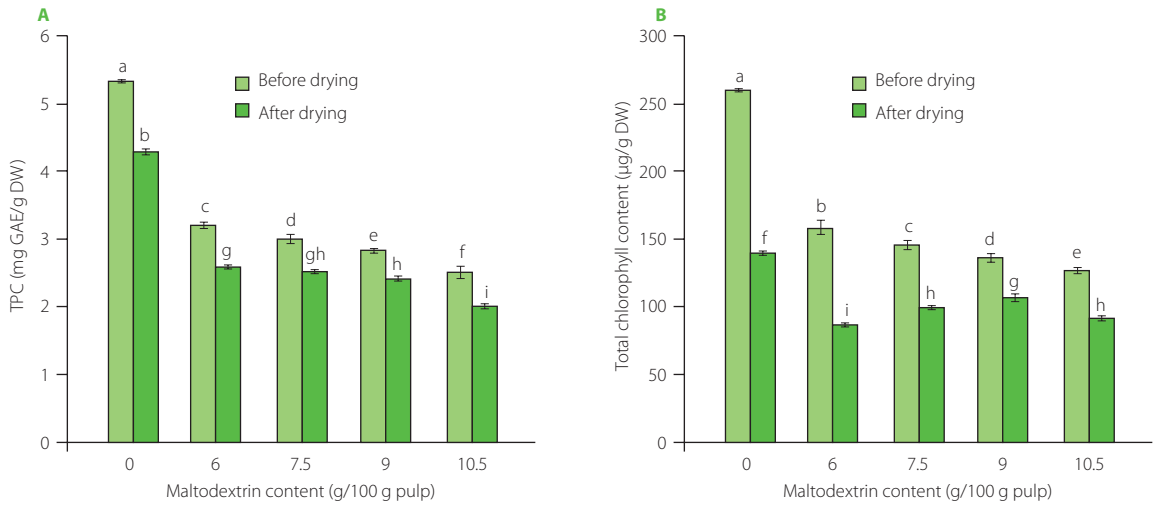

Figure 3. Total phenolic content, TPC (**A**) and total chlorophyll content (**B**) in avocado pulps without and with the addition of maltodextrin, as well as in their powders obtained by refractance window drying. Values with the same letters are not significantly different ($p \geq 0.05$). GAE, gallic acid equivalent; DW, dry weight.

Table 1. The retention of total phenolic content (TPC), total chlorophyll content, and antioxidant capacity in avocado powder obtained from pulp without and with the addition of maltodextrin (MD) by refractance window drying.

Addition of MD (g/100 g pulp)	Retention of TPC (%)	Retention of total chlorophyll content (%)	Retention of DPPH radical scavenging activity (%)	Retention of FRAP (%)
0	80.44±0.98^{b}	53.54±0.75^{d}	61.13±1.24^{c}	75.85±1.75^{b}
6	81.14±0.46^{b}	55.12±1.04^{d}	62.15±1.10^{c}	78.89±0.56^{a}
7.5	84.15±0.75^{a}	68.14±0.95^{c}	77.95±0.25^{b}	77.56±1.06^{a}
9	85.60±1.49^{a}	78.78±1.80^{a}	83.48±1.37^{a}	78.89±0.70^{a}
10.5	80.12±1.10^{b}	72.25±0.95^{b}	79.53±0.58^{b}	74.43±0.83^{c}

Data are expressed as mean ± standard deviation and values within a column with the same letter are not significantly different ($p \geq 0.05$). FRAP, ferric reducing antioxidant power.

Schierbaum, 1990]. Consequently, a larger content of MD would diminish water activity, resulting in decreased enzyme activity that contributes to the retention of phenolics and chlorophylls. Studies on the impact of MD on the drying of pulp/puree have recently mostly concentrated on the assessment of the drying rate and physical characteristics of dried samples. Regarding to the effect of MD on the quality of the dried material, Ahmed *et al.* [2009] observed that after hot-air drying, MD was positively linked with the phenolic content in purple sweet potato flour. Furthermore, compared to the avocado pulp without MD, the addition of MD allowed to retain higher TPC after infrared radiation drying [Nguyen *et al.*, 2021].

However, when 10.5 g MD/100 g of pulp was utilized, the preservation of phenolics and chlorophylls in pulp decreased. In the drying process, the operating time was also the reaction time [Nguyen *et al.*, 2020]. Therefore, RW^{TM} drying of avocado pulp with 10.5 g MD required the longest drying time, resulting in greater phytohemcial loss.

■ Effect of maltodextrin addition on antioxidant capacity

The antioxidant capacity of avocado pulps without and with MD and powders after RW^{TM} drying was determined as DPPH radical scavenging activity and as FRAP. Results are reported in Figure 4. Additionally, the results of antioxidant capacity retention after drying are shown in Table 1. Similarly to the total content of phenolics and chlorophylls, the antioxidant capacity tended to decrease as increasing amounts of MD were added to fresh pulp. Significantly ($p<0.05$) lower values for powders compared to pulps before drying were also noted. Moreover, the effect of MD addition level to pulp on retention of DPPH radical scavenging activity after RW^{TM} drying was similar as on retention of phytochemical contents. The content of 9 g MD/100 g of pulp allowed to retain the highest DPPH radical scavenging activity after drying. In the case of FRAP, when MD content was in the range of 6 to 9 g/100 g of pulp, the differences in retention were insignificant ($p \geq 0.05$). Furthermore, the samples with MD additions ranging from 6 to 9 g/100 g of pulp retained more FRAP than those without MD or with 10.5 g MD/100 g of pulp ($p<0.05$).

According to a previous report, the phenolics and chlorophylls identified in avocados are responsible for their antioxidant potential, but the contribution of the former is definitely greater than the latter [Wang *et al.*, 2010]. In addition, avocado pulp may contain other antioxidants, such as ascorbic acid and carotenoids [Lye *et al.*, 2020]. In our study, the trend of DPPH radical

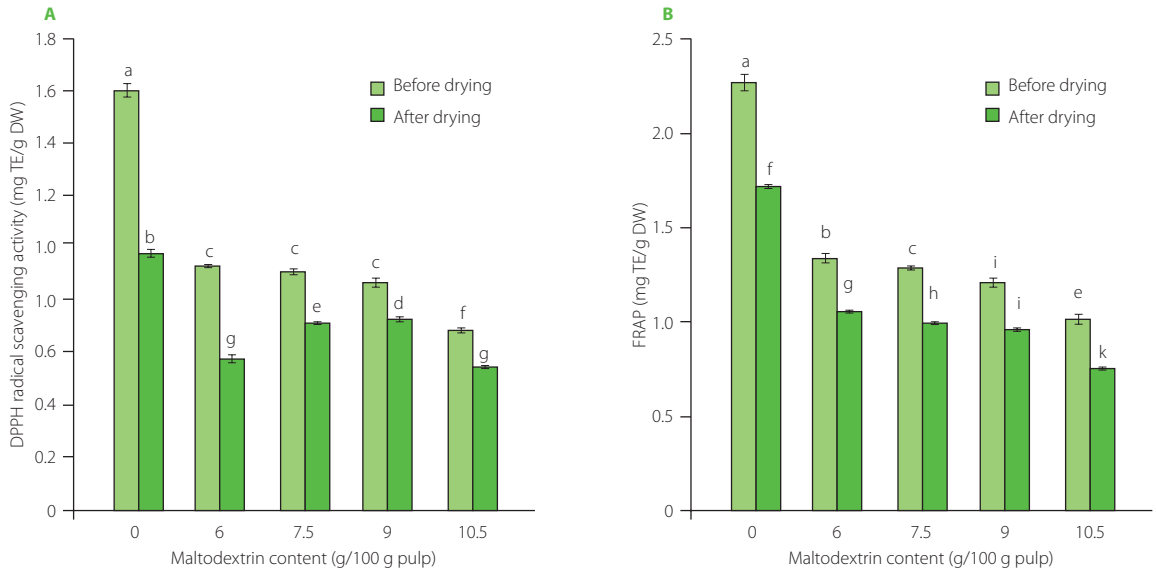

Figure 4. DPPH radical scavenging activity (**A**) and ferric reducing antioxidant power, FRAP (**B**) of avocado pulps without and with the addition of maltodextrin, as well as in their powders obtained by refractance window drying. Values with the same letters are not significantly different ($p \geq 0.05$). TE, Trolox equivalent; DW, dry weight.

scavenging activity differentiation between samples was comparable to the variations of TPC and total chlorophyll content. According to the evidence, both phenolics and chlorophylls may have contributed to DPPH radical scavenging activity of pulps and powders. However, TPC, chlorophylls, and other antioxidants in avocado may affect FRAP.

Effect of maltodextrin addition on color parameters

The color of avocado pulp changed significantly after RW^{TM} drying (Table 2). Specifically, the L^* and b^* values of the color of the powders decreased, whereas the a^* value increased compared to the color of the fresh pulp. The results indicated that the samples became darker, more yellow, and less green. When MD content changed from 0 to 7.5 g/100 g of pulp, the L^* value in dried samples gradually increased, while the a^* and b^* values did not change significantly ($p \geq 0.05$). The color of powder obtained from pulp with 9 g MD/100 g of pulp had the greatest greenness, as well as the lowest total color difference value. The highest addition of MD to the pulp caused the greatest color change with a ΔE value of 12.38.

The color played a key role in the customer's buying choice; therefore, this criterion retains its important significance. In processing and preservation, color was also used to assess processing efficiency because it correlates with the quality change of items. Pigment loss, oxidation, enzymatic or non-enzymatic browning, *etc.*, accounted for the majority of the color change during the drying process [Bahloul *et al.*, 2009]. In our study, the decrease of L^* may have been due to browning reactions occurring during drying. With regard to a^* values, a rise in a^* indicated that the dried samples were less green. For green-pigmented foods like avocado, the biotransformation of chlorophylls to pheophytins, with the replacement of magnesium with hydrogen, was primarily responsible for the loss of greenness [Rudra *et al.*, 2008]. In addition, according to the literature, MD could decrease the browning index value [Caliskan & Dirim, 2016] and increase the L^* value of dried product [Nguyen *et al.*, 2022a].

Table 2. Color parameters of avocado pulp and powders obtained from pulp without and with the addition of maltodextrin (MD) by refractance window drying.

Material	Addition of MD (g/100 g pulp)	L^*	a^*	b^*	ΔE
Pulp	0	61.05±1.02^{a}	–23.77±1.17^{b}	55.05±1.09^{a}	–
Powder	0	51.91±1.34^{c}	–20.54±0.87^{a}	51.49±1.45^{b}	10.33±0.32^{b}
	6	52.57±1.28^{bc}	–18.89±0.95^{a}	50.52±2.05^{bc}	10.78±0.51^{b}
	7.5	53.15±0.75^{b}	–20.15±1.01^{a}	50.14±0.55^{bc}	9.98±0.54^{b}
	9	54.64±1.17^{b}	–23.04±0.45^{b}	50.25±0.77^{bc}	8.04±0.14^{c}
	10.5	51.10±1.02^{c}	–19.21±0.43^{a}	49.25±0.65^{c}	12.38±0.48^{a}

Data are expressed as mean ± standard deviation and values within a column with the same letter are not significantly different ($p \geq 0.05$). L^*, lightness; a^*, redness-greenness; b^*, yellowness-blueness; ΔE, total color difference.

CONCLUSIONS

The addition of MD dramatically altered the behavior of moisture removal and the quality of avocado pulp and powder obtained by RW™ drying. The increase in MD content decreased the drying rate and the initial TPC, total chlorophyll content and antioxidant capacity of pulp but had a beneficial effect on the retention of these phytochemicals, bioactivity and color of the powders. The most effective in protecting functional properties and bioactive compounds of powders was the addition of 9 g MD/100 g of pulp. Although a higher MD content in pulp could increase the quality of drying products, too much MD led to a slower drying rate, which resulted in a longer drying time and greater product damage. Overall, this study demonstrated the RW™ drying technique had great potential for the production of avocado powder with high-quality retention if the appropriate amount of MD was added prior to drying. These findings could be implemented for the manufacturing of fruit powder. To produce the highest quality fruit powder, additional research should concentrate on identifying optimal drying conditions or assessing alternative creative drying procedures.

RESEARCH FUNDING

The study was supported by The Youth Incubator for Science and Technology Program, managed by Youth Development Science and Technology Center - Ho Chi Minh Communist Youth Union and Department of Science and Technology of Ho Chi Minh City, the contract number is "07/2020/HĐ-KHCNT-VU".

ACKNOWLEDGEMENTS

The authors would like to thank Nguyen Tat Thanh University for permission and for providing facilities, Ho Chi Minh City University of Technology (HCMUT), VNU-HCM for supporting this study and DAKADO GROUP for supplying avocado fruits during the research period.

CONFLICT OF INTERESTS

The authors declare no conflict of interest.

ORCID IDS

Q.T. Huynh https://orcid.org/0009-0000-9129-6035
P.B.D. Nguyen https://orcid.org/0000-0001-6827-919X
T.T.D. Nguyen https://orcid.org/0000-0002-1701-0729
T.V.L. Nguyen https://orcid.org/0000-0003-1471-6352

REFERENCES

1. Abul-Fadl, M., Ghanem, T. (2011). Effect of refractance-window (RW) drying method on quality criteria of produced tomato powder as compared to the convection drying method. *World Applied Sciences Journal*, *15*(7), 953–965.
2. Adhikari, B., Howes, T., Bhandari, B.R., Troung, V. (2004). Effect of addition of maltodextrin on drying kinetics and stickiness of sugar and acid-rich foods during convective drying: Experiments and modelling. *Journal of Food Engineering*, *62*(1), 53–68. https://doi.org/10.1016/S0260-8774(03)00171-7
3. Ahmed, M., Akter, M.S., Chin, K.-B., Eun, J.-B. (2009). Effect of maltodextrin concentration and drying temperature on quality properties of purple sweet potato flour. *Food Science and Biotechnology*, *18*(6), 1487–1494.
4. Bahloul, N., Boudhrioua, N., Kouhila, M., Kechaou, N. (2009). Effect of convective solar drying on colour, total phenols and radical scavenging activity of olive leaves (*Olea europaea* L.). *International Journal of Food Science & Technology*, *44*(12), 2561–2567. https://doi.org/10.1111/j.1365-2621.2009.02084.x
5. Benzie, I.F., Strain, J.J. (1996). The ferric reducing ability of plasma (FRAP) as a measure of "antioxidant power": The FRAP assay. *Analytical Biochemistry*, *239*(1), 70–76. https://doi.org/10.1006/abio.1996.0292
6. Bhandari, B., Senoussi, A., Dumoulin, E., Lebert, A. (1993). Spray drying of concentrated fruit juices. *Drying Technology*, *11*(5), 1081–1092. https://doi.org/10.1080/07373939308916884
7. Brennan, J.G., Herrera, J., Jowitt, R. (1971). A study of some of the factors affecting the spray drying of concentrated orange juice, on a laboratory scale. *International Journal of Food Science & Technology*, *6*(3), 295–307. https://doi.org/10.1111/j.1365-2621.1971.tb01618.x
8. Caliskan, G., Dirim, S.N. (2016). The effect of different drying processes and the amounts of maltodextrin addition on the powder properties of sumac extract powders. *Powder Technology*, *287*, 308–314. https://doi.org/10.1016/j.powtec.2015.10.019
9. Can Karaca, A., Guzel, O., Ak, M.M. (2016). Effects of processing conditions and formulation on spray drying of sour cherry juice concentrate. *Journal of the Science of Food and Agriculture*, *96*(2), 449–455. https://doi.org/10.1002/jsfa.7110
10. Caparino, O.A., Tang, J., Nindo, C.I., Sablani, S.S., Powers, J.R., Fellman, J.K. (2012). Effect of drying methods on the physical properties and microstructures of mango (Philippine 'Carabao' var.) powder. *Journal of Food Engineering*, *111*(1), 135–148. https://doi.org/10.1016/j.jfoodeng.2012.01.010
11. Castañeda-Saucedo, M.C., Valdés-Miramontes, E.H., Tapia-Campos, E., Delgado-Alvarado, A., Bernardino-García, A.C., Rodríguez-Ramírez, M.R., del Pilar Ramirez-Anaya, J. (2014). Effect of freeze-drying and production process on the chemical composition and fatty acids profile of avocado pulp. *Revista Chilena de Nutrición*, *41*(4), 404–411. https://doi.org/10.4067/S0717-75182014000400009
12. Ceylan, İ., Aktaş, M., Doğan, H. (2007). Mathematical modeling of drying characteristics of tropical fruits. *Applied Thermal Engineering*, *27*(11–12), 1931–1936. https://doi.org/10.1016/j.applthermaleng.2006.12.020
13. Comerford, K.B., Ayoob, K.T., Murray, R.D., Atkinson, S.A. (2016). The role of avocados in complementary and transitional feeding. *Nutrients*, *8*(5), art. no. 316. https://doi.org/10.3390/nu8050316
14. Da Silva, C., Da Silva, C. (2018). *U.S. Patent No. 9,894,908*. Washington, DC: U.S. Patent and Trademark Office.
15. Ferrari, C.C., Germer, S.P.M., Alvim, I.D., Vissotto, F.Z., de Aguirre, J.M. (2012). Influence of carrier agents on the physicochemical properties of blackberry powder produced by spray drying: Spray drying of blackberry pulp. *International Journal of Food Science & Technology*, *47*(6), 1237–1245. https://doi.org/10.1111/j.1365-2621.2012.02964.x
16. Gómez-Pérez, L.S., Navarrete, C., Moraga, N., Rodríguez, A., Vega-Gálvez, A. (2020). Evaluation of different hydrocolloids and drying temperatures in the drying kinetics, modeling, color, and texture profile of murta (*Ugni molinae* Turcz) berry leather. *Journal of Food Process Engineering*, *43*(2), art. no. e13316. https://doi.org/10.1111/jfpe.13316
17. Goula, A.M., Adamopoulos, K.G. (2008). Effect of maltodextrin addition during spray drying of tomato pulp in dehumidified air: II. Powder properties. *Drying Technology*, *26*(6), 726–737. https://doi.org/10.1080/07373930802046377
18. Gujral, H.S., Oberoi, D.P.S., Singh, R., Gera, M. (2013). Moisture diffusivity during drying of pineapple and mango leather as affected by sucrose, pectin, and maltodextrin. *International Journal of Food Properties*, *16*(2), 359–368. https://doi.org/10.1080/10942912.2011.552016
19. ISO (2005). ISO 14502-1: 2005. Determination of substances characteristic of green and black tea—Part 1: Content of total polyphenols in tea-colorimetric method using Folin-Ciocalteu reagent. International Organization for Standardization Switzerland.
20. Lichtenthaler, H.K., Buschmann, C. (2001). Chlorophylls and carotenoids: Measurement and characterization by UV-VIS spectroscopy. *Current Protocols in Food Analytical Chemistry*, *1*(1), F4-3. https://doi.org/10.1002/0471142913.faf0403s01
21. Lye, H.S., Ong, M.K., Teh, L.K., Chang, C.C., Wei, L.K. (2020). Chapter 4 – Avocado. In C.M. Galanakis (Ed.), *Valorization of Fruit Processing By-products,* Academic Press, pp. 67–93. https://doi.org/10.1016/B978-0-12-817106-6.00004-6
22. Nguyen, T.-V.-L., Ngo, P.-T., Huynh, T.-T.-N., Vo, P.-N.-T., Hoang, T.-N.-A., Nguyen, P.-B.-D. (2022a). Refractance window drying of mango pulp (*Mangifera indica*): Impact of hydrocolloids on drying characteristics and color parameters. *AIP Conference Proceedings*, *2610*(1), art. no. 060022. https://doi.org/10.1063/5.0100826
23. Nguyen, T.-V.-L., Nguyen, Q.-D., Nguyen, P.-B.-D. (2022b). Drying kinetics and changes of total phenolic content, antioxidant activity and color parameters of mango and avocado pulp in refractance window drying. *Polish Journal of Food and Nutrition Sciences*, *72*(1), 27–38. https://doi.org/10.31883/pjfns/144835

24. Nguyen, T.-V.-L., Nguyen, Q.-D., Nguyen, P.-B.-D., Tran, B.-L., Huynh, P.T. (2020). Effects of drying conditions in low-temperature microwave-assisted drying on bioactive compounds and antioxidant activity of dehydrated bitter melon (*Momordica charantia* L.). *Food Science & Nutrition*, *8*(7), 3826–3834. https://doi.org/10.1002/fsn3.1676
25. Nguyen, T.-V.-L., Nguyen, Q.-D., Nguyen, T.-T.-D., Nguyen, P.-B.-D. (2021). Effects of infrared drying conditions and maltodextrin addition on some physicochemical characteristics of avocado (*Persea americana*) pulp powder. *Applied Sciences*, *11*(24), art. no. 11803. https://doi.org/10.3390/app112411803
26. Nindo, C., Tang, J. (2007). Refractance window dehydration technology: A novel contact drying method. *Drying Technology*, *25*(1), 37–48. https://doi.org/10.1080/07373930601152673
27. Ochoa-Martínez, C., Quintero, P., Ayala, A., Ortiz, M. (2012). Drying characteristics of mango slices using the Refractance Window™ technique. *Journal of Food Engineering*, *109*(1), 69–75. https://doi.org/10.1016/j.jfoodeng.2011.09.032
28. Osorio, C., Forero, D.P., Carriazo, J.G. (2011). Characterisation and performance assessment of guava (*Psidium guajava* L.) microencapsulates obtained by spray-drying. *Food Research International*, *44*(5), 1174–1181. https://doi.org/10.1016/j.foodres.2010.09.007
29. Williams, P.A., Phillips, G.O. (2000). Chapter 1 – Introduction to food hydrocolloids. In G.O. Phillips and P.A. Williams (Ed.), *Handbook of Hydrocolloids*. CRC Press Boca Raton, FL, pp. 1–22.
30. Puente, L., Vega-Gálvez, A., Ah-Hen, K.S., Rodríguez, A., Pasten, A., Poblete, J., Pardo-Orellana, C., Muñoz, M. (2020). Refractance Window drying of goldenberry (*Physalis peruviana* L.) pulp: A comparison of quality characteristics with respect to other drying techniques. *LWT – Food Science and Technology*, *131*, art. no. 109772. https://doi.org/10.1016/j.lwt.2020.109772
31. Radosta, S., Schierbaum, F. (1990). Polymer-water interaction of maltodextrins. Part III: Non-freezable water in maltodextrin solutions and gels. *Starch-Stärke*, *42*(4), 142–147. https://doi.org/10.1002/star.19900420405
32. Rafidah, H., Ando, Y., Amin, I., Shirai, Y., Mohd Ali, H. (2014). Enhanced polyphenol content and antioxidant capacity in the edible portion of avocado dried with superheated-steam. *International Journal of Advanced Research*, *8*, 241–248.
33. Raghavi, L., Moses, J., Anandharamakrishnan, C. (2018). Refractance window drying of foods: A review. *Journal of Food Engineering*, *222*, 267–275. https://doi.org/10.1016/j.jfoodeng.2017.11.032
34. Rajoriya, D., Shewale, S.R., Hebbar, H.U. (2019). Refractance window drying of apple slices: Mass transfer phenomena and quality parameters. *Food and Bioprocess Technology*, *12*, 1646–1658. https://doi.org/10.1007/s11947-019-02334-7
35. Ramaswamy, H.S., Marcotte, M. (2005). Chapter 5 – Food dehydration. In *Food Processing: Principles and Applications*. CRC Press, Boca Raton, FL, pp. 233-316. https://doi.org/10.1201/9780203485248
36. Ratti, C. (2013). Chapter 3 – Freeze drying for food powder production. In B. Bhandari, N. Bansal, M. Zhang, P. Schuck (Eds.). *Handbook of Food Powders*. Woodhead Publishing Series in Food Science, Technology and Nutrition, pp. 57–84. https://doi.org/10.1533/9780857098672.1.57
37. Rudra, S.G., Singh, H., Basu, S., Shivhare, U.S. (2008). Enthalpy entropy compensation during thermal degradation of chlorophyll in mint and coriander puree. *Journal of Food Engineering*, *86*(3), 379–387. https://doi.org/10.1016/j.jfoodeng.2007.10.020
38. Singh Gujral, H., Singh Brar, S. (2003). Effect of hydrocolloids on the dehydration kinetics, color, and texture of mango leather. *International Journal of Food Properties*, *6*(2), 269–279. https://doi.org/10.1081/JFP-120017846
39. Sobulska, M., Zbicinski, I. (2021). Advances in spray drying of sugar-rich products. *Drying Technology*, *39*(12), 1774–1799. https://doi.org/10.1080/07373937.2020.1832513
40. Souza, D.S., Marques, L.G., Gomes, E. de B., Narain, N. (2015). Lyophilization of avocado (*Persea americana* Mill.): Effect of freezing and lyophilization pressure on antioxidant activity, texture, and browning of pulp. *Drying Technology*, *33*(2), 194–204. https://doi.org/10.1080/07373937.2014.943766
41. Temu, A. (2013). Effect of temperature and slice size on avocado pulp drying rate and oil yield. *Tanzania Journal of Engineering and Technology*, *34*(2), 116–124. https://doi.org/10.52339/tjet.v34i2.464
42. Tontul, I., Eroğlu, E., Topuz, A. (2018). Convective and refractance window drying of cornelian cherry pulp: Effect on physicochemical properties. *Journal of Food Process Engineering*, *41*(8), art. no. e12917. https://doi.org/10.1111/jfpe.12917
43. Tontul, I., Topuz, A. (2017). Effects of different drying methods on the physicochemical properties of pomegranate leather (pestil). *LWT – Food Science and Technology*, *80*, 294–303. https://doi.org/10.1016/j.lwt.2017.02.035
44. Vega-Mercado, H., Góngora-Nieto, M.M., Barbosa-Cánovas, G.V. (2001). Advances in dehydration of foods. *Journal of Food Engineering*, *49*(4), 271–289. https://doi.org/10.1016/S0260-8774(00)00224-7
45. Wang, W., Bostic, T.R., Gu, L. (2010). Antioxidant capacities, procyanidins and pigments in avocados of different strains and cultivars. *Food Chemistry*, *122*(4), 1193–1198. https://doi.org/10.1016/j.foodchem.2010.03.114

ORIGINAL ARTICLE
http://journal.pan.olsztyn.pl

Polish Journal of Food and Nutrition Sciences
2023, Vol. 73, No. 2, 196–204
DOI: 10.31883/pjfns/166382
ISSN 1230-0322, e-ISSN 2083-6007

Effect of ι-Carrageenan and Its Hydrolysates on the Stability of Milk Ice Cream Mixes

Anna Kot[1]*, Ewa Jakubczyk[1], Magdalena Buniowska-Olejnik[2], Anna Kamińska-Dwórznicka[1]

[1]Department of Food Engineering and Process Management, Institute of Food Sciences, Warsaw University of Life Sciences (WULS-SGGW), Nowoursynowska 159C, 02-776, Warsaw, Poland
[2]Department of Dairy Technology, Institute of Food Technology and Nutrition, University of Rzeszow, Ćwiklinskiej 2D St., 35601 Rzeszow, Poland

The objective of this research was to determine the influence of ι-carrageenan and its acid and enzymatic hydrolysates on the physical properties of milk ice cream mixes. The main factors considered were the Turbiscan stability index, backscattering profile, particle size distribution and median diameter (D_{50}), the consistency index and the flow behavior index of ice cream mix before and after 24 h of maturation at 4°C. The microstructure of emulsion was also analysed based on confocal laser scanning microscopy (CLSM). The addition of ι-carrageenan resulted in lower stability of emulsion compared to emulsions with its acid and enzymatic hydrolysates. The sedimentation, coalescence and flocculation were observed based on the backscattering profile and CLSM images. The addition of stabilisers contributed to an increase in D_{50} of ice cream mix from 17.56 to 37.05–45.50 µm before maturation and from 34.73 to 46.73 µm after maturation. The ι-carrageenan after commercial lactase treatment improved the stability of milk ice cream mixes by increasing the consistency index to 0.104 and a flow behaviour index to 0.702. Finally, it may be concluded that the stabilisers used – ι-carrageenan and its hydrolysates – significantly influenced the physical properties of milk ice cream mixes and, hence, can be used as beneficial ingredients in the recipe of milk ice cream mixes.

Key words: ice cream mix emulsion, particle size, confocal laser scanning microscopy

INTRODUCTION

The colloidal structure of ice cream has recently been an object of research interest for the global audience. It is known that the final physicochemical structure of ice cream may be regarded as a four-phase system, which includes air bubbles, fat globules, ice crystals and an unfrozen serum phase. In this unfrozen serum phase, there exist the unadsorbed casein micelles in a suspension of sugars, salts, whey proteins and high molecular weight polysaccharides. The structure of ice cream characterizes its complexity as a result of several stages of manufacturing such as pasteurisation, homogenisation, maturation, freezing and hardening. The colloidal aspects of ice cream, such as interactions between protein and emulsifier, the partial coalescence of fat or interactions between protein and partially coalesced fat, allow for a better understanding of this unique system [Gelin *et al*., 1994; Goff, 1997, 2002; Goff & Hartel, 2013; Konstantas *et al*., 2019].

During the manufacturing process, the ice cream mix emulsion is foamed, the dispersed phase of air bubbles is formed, and frozen to obtain another dispersed phase of ice crystals. The ice cream mix contains fat droplets, coated with a protein-emulsifier layer as a dispersed phase. The ice cream mix can also be classified as emulsion-filled gel, in which macromolecular gel contains dispersed fat particles (fillers). Therefore, the structure and rheological properties of the ice cream mix can be affected

***Corresponding Author:**
e-mail anna_kot1@sggw.edu.pl (A. Kot)

Submitted: 1 December 2022
Accepted: 15 May 2023
Published on-line: 2 June 2023

as a result of distinctive interactions of the filler gel matrix [Chen *et al*., 2019; Daw & Hartel, 2015; Goff, 1997; Innocente *et al*., 2009; Voronin *et al*., 2020].

Not only is the formation of the ice phase significant but stability is also equally crucial in the structure of ice cream. Desirable stability includes no changes in the size distribution or spatial arrangement of droplets. Stability plays a crucial role in controlling the shelf-life of ice cream or its texture and mouthfeel during consumption. It may be understood as the ability to resist undesirable changes in physicochemical properties. Loss of stability may occur due to various processes, such as creaming, flocculation, coalescence, partial coalescence, Ostwald ripening or phase inversion [Cheng *et al*., 2015; Dickinson, 1994, 2010; Pal, 2019]. The initial stability of emulsion in the ice cream mix is obtained by simultaneous adsorption of proteins and emulsifiers during the homogenisation process. Subsequently, during the maturation process, changes in the physical state occur in the liquid phase, not only in the emulsified fat but also in the adsorbed layer of mono- and diglycerides. Additionally other changes take place during maturation except for the mentioned process, such as the hydration of milk proteins and stabilisers, the crystallization of fat globules or the rearrangement of the surfactant membrane. They all contribute to a smoother texture and consequently better quality of ice cream [Gelin *et al*., 1994; Goff, 1997; Mendez-Velasco & Goff, 2012; Segall & Goff, 2002b].

Furthermore, the stability of emulsion in the ice cream mix may be considered through the prism of stabiliser addition. Despite the increasing viscosity, one of the main functions of stabilisers is to stabilise the emulsion and prevent separation [Akbari *et al*., 2019; Lomolino *et al*., 2020; Pintor & Totosaus, 2012; Seisun, 2010]. An example of such stabilisers is carrageenan that has been proved effective in preserving quiescent stability/shear instability in the emulsion with a low protein surface concentration [Segall & Goff, 2002a]. This happens as the migration of the milk protein from the solution to the oil-water interface in the emulsion is inhibited by carrageenans. Due to specific interaction with the milk proteins, carrageenans are employed in milk ice cream production. The favourable interactions between carrageenan and milk proteins depend on the number of sulphate groups in carrageenan structure and environmental conditions [Pintor & Totosaus, 2012]. ι-Carrageenan is one of the three forms of carrageenan (next to κ- and λ-carrageenan) that exhibits the specific ability to form a soft elastic gel in the presence of calcium ions, and stands out through other forms owing to the fact that it can form intra-molecular bonds between sulphate groups of anhydro-D-galactose and D-galactose *via* calcium as a divalent cation [Kiran-Yildrim *et al*., 2021; Thrimawithana *et al*., 2010]. Additionally, there are pieces of evidence that hydrolysates of carrageenan have a better ability to stabilize ice cream than native carrageenan. For instance, in the research by Kamińska-Dwórznicka *et al*. [2015] or Kot *et al*. [2022], it was noticed that hydrolysates of κ- and ι-carrageenan had more favourable effect on ice recrystallization inhibition (IRI) then κ-carrageenan in ice cream and ι-carrageenan in model solutions of ice cream, respectively.

This work focused on the influence of ι-carrageenan and its hydrolysates on the physical properties, such as stability, particle size distribution, consistency index and the flow behavior index, of milk ice cream mixes. Knowledge concerning these stabilisers in such products before freezing is lacking. Moreover, our previous research, in which the addition of ι-carrageenan and its acid and enzymatic hydrolysates allowed achieving desired size of crystals in a model milk solution, gave rise to the idea of using such stabilisers in this work [Kot *et al*., 2022]. This research might provide a valuable insight into the interactions between hydrocolloids and milk ice cream mixes.

MATERIALS AND METHODS

Materials

Pure ι-carrageenan powder was obtained from Sigma-Aldrich (St. Louis, MO USA). β-Galactosidase (1,000 U/mg, from *Escherichia coli*) and lactase (min. activity 5,200 NLU/g) for ι-carrageenan hydrolysis were purchased from Sigma-Aldrich and Serowar s.c. (Szczecin, Poland), respectively. The ingredients used to prepare the ice cream mixes were acquired from Mlekovita, Wysokie Mazowieckie, Poland (milk 0.5%, skimmed milk in powder); Orafti BENEO, Tienen, Belgium (inulin); Diamant, Poznań, Poland (white sugar); and Fooding Shanghai, Shanghai, China (emulsifier E471, locust bean gum (LBG), xanthan gum).

The preparation of hydrolysates of ι-carrageenan

The hydrolysis of ι-carrageenan was carried out according to the procedure described in our previous paper [Kot *et al*., 2022]. Briefly, ι-carrageenan was dissolved in distilled water heated up to 40°C to obtain a 0.4 mg/mL solution. The enzymatic hydrolysis was carried out using β-galactosidase for 72 h, at 37°C and a ratio of enzyme to ι-carrageenan solution of 1:1,000 (*v/v*) or using lactase for 24 h, at 5°C and enzyme to substrate ratio of 1:250 (*v/v*). For both hydrolyses, the reaction was stopped by neutralisation at 48°C for 5 min. To perform acid hydrolysis of ι-carrageenan, the substrate was dissolved in 0.1 M hydrochloric acid solution (pH 3). The solution was heated at 60°C for 3 h and then neutralised. All hydrolysates were stored frozen at –18° and thawed just before analysis. To characterise the hydrolysates, their molecular weight was determined by size-exclusion chromatography (SEC) according to the procedure described by Kamińska-Dwórznicka *et al*. [2015] using the Shimadzu high-performance liquid chromatography system consisting of a RID-10A detector, an LC-20 CE pump, a CTO-20A heater (Shimadzu, Kyoto, Japan) and equipped with a PolySep-GFC-P Linear column (300 mm x 7.8 mm, Phenomenex, Torrance, CA, USA). The molecular weight of samples after the hydrolysis by β-galactosidase ranged from 3.20×10^6 to 3.80×10^6 Da; that of hydrolysates obtained by commercial lactase from 3.50×10^6 to 3.60×10^6 Da, and that of acid hydrolysates from 1.48×10^6 to 1.94×10^6 Da.

The preparation of ice cream mixes

The ingredients of the ice cream mixes are presented in Table 1. The control sample (C) was prepared without stabilisers. The ice cream mix with the combination of ι-carrageenan, LBG

Table 1. The composition (%) of ice cream mixes without stabilisers (control, C), with ι-carrageenan (I) and with hydrolysates obtained by acid (A), β-galactosidase (B) and commercial lactase (L) treatment of ι-carrageenan.

Ingredient	C	I	A	B	L
Milk 0.5	76.0	75.49	75.495	75.495	75.495
Inulin	10.0	10.0	10.0	10.0	10.0
Milk powder	7.0	7.0	7.0	7.0	7.0
White sugar	7.0	7.0	7.0	7.0	7.0
Emulsifier E471	0.4	0.4	0.4	0.4	0.4
Locust bean gum	–	0.08	0.08	0.08	0.08
Xanthan gum	–	0.02	0.02	0.02	0.02
ι-Carrageenan	–	0.01	–	–	–
Acid hydrolysate of ι-carrageenan	–	–	0.005	–	–
ι-Carrageenan hydrolysate obtained by β-galactosidase treatment	–	–	–	0.005	–
ι-Carrageenan hydrolysate obtained by lactase treatment	–	–	–	–	0.005

and xanthan gum was coded as I. In turn, samples A, B and L instead of ι-carrageenan contained its acid hydrolysate or hydrolysates obtained using β-galactosidase and commercial lactase, respectively. All components were mixed using a Bosch Maxo -Mixx 750W blender (Bosch, Gerlingen, Germany). The next step involved pasteurization conducted in a Vorwerk thermomixer (Vorwerk, Wuppertal, Germany), at 85°C within 1.5 min. After this process, the mixtures were cooled to 25°C. Finally, the obtained ice cream mixes were matured for 24 h at 4°C in a refrigerator (Whirlpool, Warszawa, Poland). Two liters of ice cream mix were prepared for each experimental variant in duplicate.

Stability analysis of ice cream mixes

The analysis of the stability of ice cream mixes was performed using a Turbiscan Lab Expert device (Formulation SA, Toulouse, France). The Turbisoft 2.0.0.33 software was used to evidence the date of backscattering (BS) and calculate the Turbiscan stability index (TSI). The ice cream mixes were analysed before and after maturation in three replications.

The analysis of particle size distribution of ice cream mixes

The particle size distribution of the ice cream mixes before and after maturation was measured by laser diffraction using a Cilas 1190 analyser (Cilas, Orléans, France). Few drops of emulsion of milk ice cream mixes were suspended in water at an obscuration of 10%. The results were presented as the median diameter (D_{50}) and as diagrams of particle size distribution. Analyses of all samples were performed in three replications.

The rheological analysis of ice cream mixes

The rheological properties of the milk ice cream mixes were examined using the Haake Mars 40 rheometer (Thermo Scientific Inc., Karlsruhe, Germany) in a rotational mode within a shear rate of 0–100 s^{-1} at a constant temperature of 25°C. The analyses were performed in triplicate. The apparent viscosity (η_{app}) curve as a function of shear rate ($\dot{y}$) in the semi-logarithmic scale (the flow curves) was plotted by the RheoWin v.4.86. Job Manager (Thermo Scientific). Based on the obtained results, only Ostwald de Waele model (1) was used to describe the flow curves and to determine the flow behaviour index.

$$\eta_{app} = K\dot{y}^{n-1} \quad (1)$$

where: K is the consistency index (Pa×s^n), $\dot{y}$ is the shear rate (s^{-1}), and n is the flow behavior index (dimensionless).

The adequacy of fitted model was estimated using regression analysis which delivered the correlation coefficient (R).

Characterization of the ice cream mix emulsion using confocal laser scanning microscopy (CLSM)

The microstructure of the emulsion of the ice cream mix (before and after the maturation step) was analysed using a confocal laser scanning microscope FLUOVIEW FV300 (Olympus, Tokyo, Japan), according to the method described by Ahn *et al.* [2022]. The fluorescence dye – Nile red – was used to label lipids in the samples. An aliquot of 200 µL of the emulsion for all ice cream mixes and 3 µL of the Nile red solution (1 µg/mL) were mixed. Then, the samples were stained on glass slides, covered with a coverslip and observed at excitation and emission wavelengths of 630 and 660 nm, respectively. From every sample of ice cream mix, 6 photos were made and only representative ones were chosen for to results.

Statistical analysis

The results were expressed as a mean with standard deviations. The analysis of variance (ANOVA) was performed for the TSI,

the D_{50} and data from rheological properties. The analysis was performed using STATISTICA 13.3 software (Statsoft Polska, Kraków, Poland) with test significance at α=0.05. The differences between homogenous groups were assessed using the Tukey's honestly significant difference (HSD) test.

RESULTS AND DISCUSSION

The stability of ice cream mixes

The stability of milk ice cream mixes was scrutinised with the turbidimetric method, and respective results are presented as the TSI in Table 2 and as backscattering profile in Figure 1 (for control mix and mix with acid hydrolysate of ι-carrageenan) and in Figures S1–S3 in Supplementary Materials (for other ice cream mixes). The addition of stabilisers (ι-carrageenan and its hydrolysates) contributed to changes in the stability of milk ice cream mixes. The TSI ranged from 1.9 to 2.8. The lowest (p<0.05) value was noted for the sample with the addition of acid hydrolysate of ι-carrageenan (A). Moreover, it was noticed that there was no significant difference (p≥0.05) in the TSI of ice cream mixes with enzymatic hydrolysates of ι-carrageenan (B, after β-galactosidase treatment and L, after lactase treatment) and control sample without stabilisers (C). Nonetheless, the most striking observation was that the addition of ι-carrageenan contributed to the highest TSI value, which indicates slightly worse stability of the mix with ι-carrageenan compared to the other samples. Based on TSI, it may be stated that only the addition of acid hydrolysate of ι-carrageenan (A) contributed to significant improvement in the stability of ice cream mixes compared to the control sample. In research by Seo & Oh [2022], the TSI of ice cream mixes stabilized by the κ-carrageenan/milk protein isolate or Maillard conjugate derived from the reaction of the κ-carrageenan/milk protein isolate during 120 h of storage was less than 1.8.

The backscattering profiles (Figure 1, Figures S1–S3) showed that during maturation time, two phenomena occurred in the milk ice cream mixes. Firstly, it was noticed that the same type of destabilization, such as coalescence/flocculation, occurred in the control sample (C) and in the sample with the addition of ι-carrageenan (I) and that the intensity of backscattering

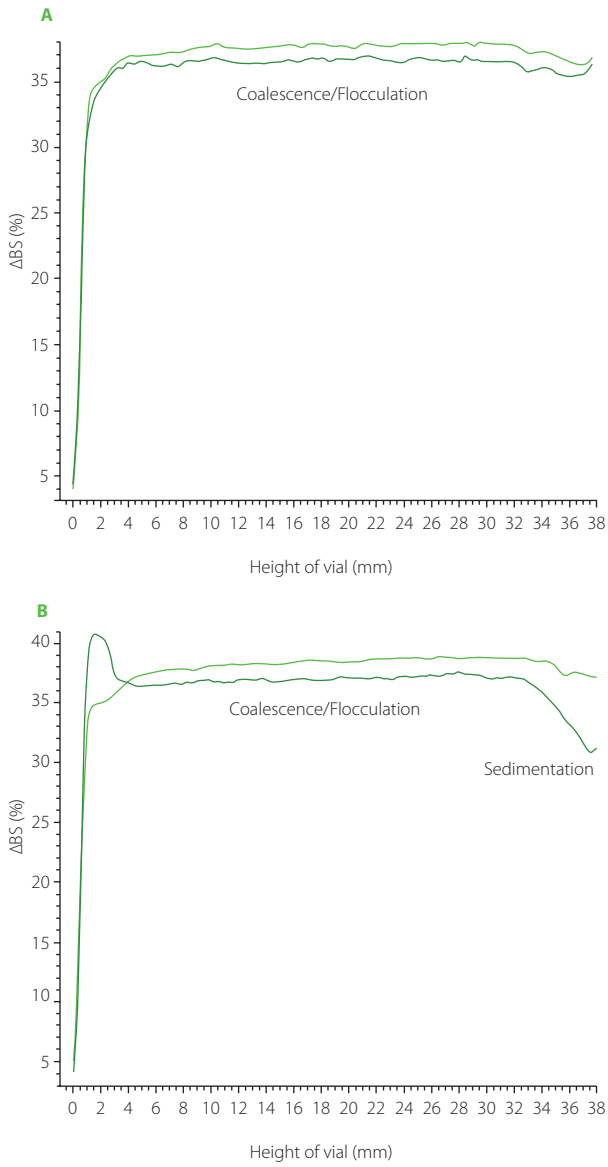

Figure 1. Backscattering (BS) profile of ice cream mixes without stabilisers (control sample) (**A**) and stabilised by the combination of acid hydrolysate of ι-carrageenan, locust bean gum and xanthan gum (**B**) before and after maturation. The dark green line presents measurement before maturation and the light green line presents measurement after maturation.

Table 2. The results of physical properties analysis of milk ice cream mixes with stabilisers before and after maturation.

Ice cream mix	TSI	Before maturation				After maturation			
		D_{50} (μm)	K	n	R	D_{50} (μm)	K	n	R
C	2.2±0.2^{b}	17.56±0.31^{c}	0.009±0.001^{d}	0.900±0.001^{a}	0.99	23.24±2.40^{c}	0.012±0.012^{b}	0.838±0.007^{a}	0.99
I	2.8±0.1^{a}	40.60±2.97^{ab}	0.061±0.005^{b}	0.738±0.022^{c}	0.99	35.57±2.63^{b}	0.059±0.058^{ab}	0.761±0.011^{ab}	0.99
A	1.9±0.1^{c}	45.50±2.37^{a}	0.059±0.005^{bc}	0.765±0.018^{bc}	0.99	46.73±0.19^{a}	0.058±0.057^{ab}	0.771±0.031^{ab}	0.99
B	2.2±0.1^{b}	37.05±2.34^{b}	0.048±0.001^{c}	0.798±0.005^{b}	0.99	34.73±0.90^{b}	0.050±0.049^{b}	0.803±0.016^{ab}	0.99
L	2.2±0.1^{b}	41.08±1.79^{ab}	0.083±0.006^{a}	0.727±0.014^{c}	0.99	35.16±1.23^{b}	0.104±0.103^{a}	0.702±0.083^{b}	0.99

Values are presented as mean ± standard deviations. Different superscript letters in column represent significant differences in the means (p<0.05). C, control ice cream mix (without stabilisers); I, ice cream mix with ι-carrageenan, locust bean gum (LBG) and xanthan gum; A, B and L, ice cream mixes with hydrolysates obtained by acid, β-galactosidase and commercial lactase treatment of ι-carrageenan, respectively, LBG and xanthan gum; TSI, Turbiscan stability index, D_{50}, median diameter, K, consistency index (Pax^{n}), n, flow behaviour index; R, correlation coefficient.

was changing across the whole height of the vial. Additionally, observations of CLSM images of these samples before and after maturation (Figure 2) confirmed destabilisation of fat in mixes, as indicated by agglomerates visible in images Ia, Ib (the sample with the ι-carrageenan) and Ca, Cb (the control sample). Furthermore, except for coalescence/flocculation, also sedimentation occurred in the milk ice cream mixes with the addition of acid hydrolysates of ι-carrageenan (Figure 1); as evidenced by significant changes in the intensity of backscattering on the top and bottom and also slightly in the middle of the vial. These processes of destabilisation may take place simultaneously (droplets coalescing during sedimentation) or one by one (for instance, firstly small droplets grow by coalescence before sedimenting). The separation in ice cream mix with ι-carrageenan hydrolysate (β-galactosidase treatment) before maturation was captured in image Ba (Figure 2). The order of this process may depend on the droplet diameter, dispersed phase concentration or viscosity [Frising *et al.*, 2008]. What should be highlighted here is the fact that after the maturation, the median diameter (D_{50}) for samples with the addition of ι-carrageenan or enzymatic hydrolysates decreased (Table 2). It is common knowledge that coalescence or flocculation occurs when the particle size increases not decreases [Goff *et al.*, 1989]. However, as mentioned above, the agglomerates of fat of ice cream mixes were visible in CLSM images (Figure 2). In the research by Cheng *et al.* [2015], flocculation occurred despite a decrease in the average particle size after the maturation of ice cream mixes with different polysaccharide contents. In our research, despite the content of stabilisers and emulsifiers contributing to a decrease in particle size, the change was not significant enough to inhibit the mentioned type of destabilisation.

It was proven that a certain amount of fat destabilisation is covetable in frozen products, such as ice cream [Berger & White, 1971; Goff *et al.*, 1989; Koxhlot *et al.*, 2001, Liu *et al.*, 2022]. As a result of a combination of sheer forces and ice crystallisation during the freezing process, fat globules are mechanically damaged and agglomeration or coalescence takes place. Consequently, such desirable destabilisation contributes to dry appearance, slow meltdown, good shape retention and finally a firmer texture. Albeit, the excessive coalescence of fat may be associated with poor whipping properties or a buttery texture. Furthermore, it is known that the ice cream mix is not only an example of dairy emulsion but also a foamed dairy emulsion [Stanley *et al.*, 1996]. It means that the stability of such products is connected with the presence of air bubbles. In such cases, preventing air bubbles to grow in size or adjacent to coalescing should be considered in the whole conception of the stability of ice cream mixes. Additionally, Liu *et al.* [2022], proved that the higher the amount of fat aggregates in the serum phase, the greater the possibility of a 3D destabilization network formation in ice cream. In our research, destabilisation occurred in ice cream mixes; thus, it may be concluded that fat destabilisation at this step of production could produce conditions for the formation of more favourable and uniform ice crystal structures while freezing. Finally, in the present study, the ice cream mixes remained stables despite TSI value.

The particle sizes of ice cream mixes

The median diameter (D_{50}) of particles of milk ice cream mixes before and after maturation was presented in Table 2, and the particle size distribution in Figure 3. Before maturation, the D_{50} ranged from 17.56 to 45.50 μm. The lowest

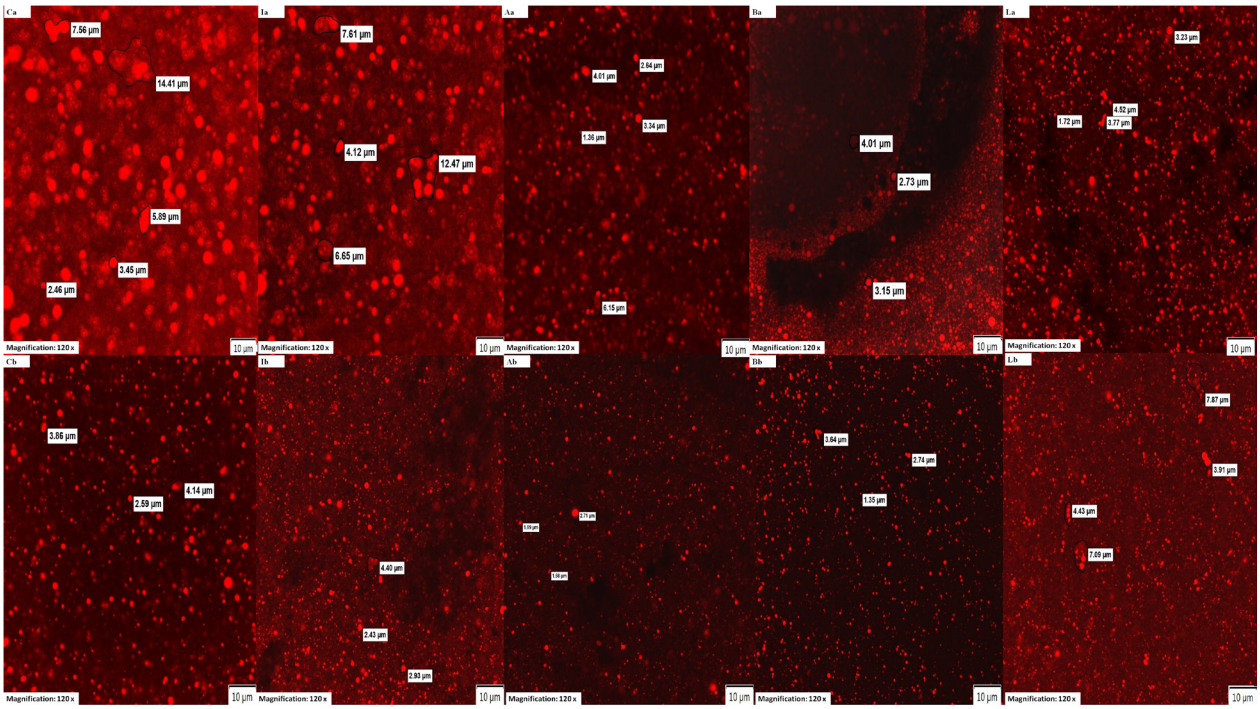

Figure 2. Confocal laser scanning microscopy images of ice cream mixes before (a) and after (b) maturation. C, control ice cream mix (without stabilizers); I, ice cream mix with ι-carrageenan, locust bean gum (LBG) and xanthan gum; A, B and L, ice cream mixes with hydrolysates obtained by acid, β-galactosidase and commercial lactase treatment of ι-carrageenan, respectively, LBG and xanthan gum.

(p<0.05) value of this parameter was noted for the control sample without stabilisers (C), whereas the highest one – for the ice cream mix with the addition of acid hydrolysate of ι-carrageenan (A); however, the values determined for the mixes with ι-carrageenan and with its hydrolysate obtained using lactase did not differ significantly (p≥0.05) from that of sample A. Overall, before the maturation, the addition of stabilisers contributed to the increase in the median diameter of ice cream mix particles. After maturation, the D_{50} ranged from 23.24 to 46.73 µm. The tendency of the variation of this parameter was the same as before maturation. In the control sample (C), the median diameter was at 23.34 µm and in the sample with the addition of acid hydrolysate of ι-carrageenan (A) it reached almost 47 µm. Nonetheless, some changes occurred compared to the values before maturation. The decrease in the size of particles was observed in the ice cream mixes with the addition of enzymatic hydrolysates of ι-carrageenan (B and L) and in the sample with ι-carrageenan (I). On the other hand, a slight increase of D_{50} was noticed in the mix with the acid hydrolysates of ι-carrageenan (A) and the control sample (C). As a result of maturation, the greatest reduction of median diameter (by almost 6 µm) was observed for the sample with the ι-carrageenan hydrolysate obtained using lactase (Table 2). Such changes are desirable to obtain the expected quality of the final product, especially in the context of the formation of ice crystals. In our previous study, vegan ice cream mixes with the same stabilisers were analysed [Kot *et al*., 2021]. Similar results were noticed, *i.e.*, the D_{50} of ice cream mixes decreased as a result of maturation, and only in the control sample was an increase observed. On the other hand, the size of the particles was smaller than in the present paper; the range of median diameter after maturation was from 17.23 to 28.50 µm. Overall, the reason for the large size of particles in ice cream mixes may be the addition of an emulsifier to the recipe. Based on the research by Liu *et al*. [2022], the fat aggregate size and also the fat aggregate percentage increased with the increased amount of the added emulsifier, such as Tweet 80, P4780 and whey protein isolate, to ice cream mixes. In the sample with the addition of 0.25% of emulsifier, the size of fat aggregates was from 1.6 to 66.3 µm. Bolliger *et al*. [2000] also discussed using emulsifiers in ice cream mixes and reported that the increasing amount of emulsifier contributed to the increased fat globule size or aggregate size of fat globules. Furthermore, in the samples without emulsifiers, no stable agglomerates were formed, while the only stable agglomerates were present in ice cream mixes with the addition of this ingredient. Alternatively, Alvarez *et al*. [2005] showed that maturation did not affect the size distribution of fat globules. The authors attributed it to a result of no noticeable destabilisation of emulsions during maturation due to the fact that the changes in the structure of emulsion, such as rearrangement of fat globule membranes, contributed to the lesser stability during maturation.

It is known that the changes in the structure of ice cream mixes, such as the arrangement of fat droplets, affect their texture as well as the melting stability of the final product

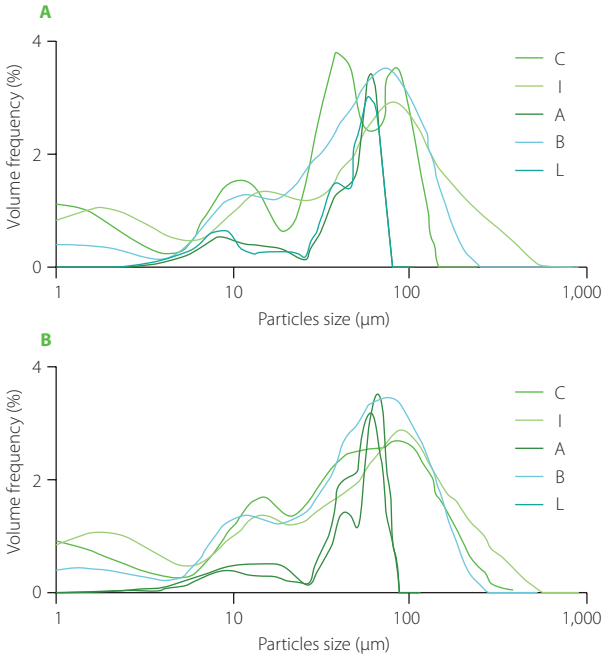

Figure 3. Particle size distribution of ice cream mixes before (**A**) and after (**B**) maturation. C, control ice cream mix (without stabilizers); I, ice cream mix with ι-carrageenan, locust bean gum (LBG) and xanthan gum; A, B and L, ice cream mixes with hydrolysates obtained by acid, β-galactosidase and commercial lactase treatment of ι-carrageenan, respectively, LBG and xanthan gum.

[Mendez-Velasco & Goff, 2012]. The uniform distribution of droplets may be the reason for kinetic instabilities such as creaming or sedimentation [Pal, 2019]. Therefore, the particle size distribution of ice cream mixes was analysed and the results are shown in Figure 2. Considering particle size distribution of the samples before maturation, four peaks were observed for the control sample (with particle size ranges of 0–2, 7–30, 50–80 and 100–120 µm), and the ice cream mix with the addition of hydrolysates obtained using acid and lactase (8–10, 20–40, 60–70, and 80–90 µm). While for the ice cream mixes with the addition of ι-carrageenan and ι-carrageenan after β-galactosidase treatment, three peaks were noted (particle size ranges for I sample: 2–5, 15–30 and 90–110 µm and for L sample: 2–5, 7–15 and 80-110 µm. Moreover, the range and location of peaks were similar for samples C, I, and B. The samples A and L, with the hydrolysates obtained using acid and lactase, respectively, had also similarities in particle size distribution. After maturation, four peaks in particle size distribution were noticed only for the control sample, whereas three-peaks were detected for the other samples (Figure 2). Among the samples with stabilisers, the significant differences in particle size distribution were only visible for the samples with the addition of ι-carrageenan after acid treatment (A) and after lactase treatment (L). In both mixes, particles in the size ranges 10–40, 50–70 and 80–90 µm were dominant. The frequency of particles with diameter less than 5 µm was low. The more frequent particles between 10 to 100 µm could represent fat agglomerates or fat coalescence. The same observation was made for molten ice creams; single fat droplets with a size of 1–1.5 µm and fat

clusters with a diameter of around 10 μm were determined [Liu *et al*., 2022]. Mendez-Velasco & Goff [2012] provided a deep analysis of the influence of the fat structure and properties of ice cream. Unsaturated monoglycerides (from sunflower oil) and saturated monoglycerides (from palm kernel oil) added to ice cream were tested. Based on particle size distribution, it was concluded that ice cream with unsaturated lipids formed larger fat networks with the higher number of droplets as stable particles, while ice cream with saturated lipids destabilized readily with smaller aggregates. The particles with diameters of 0.01–1 and around 100 μm dominated in ice cream with unsaturated lipids, while distribution of particle size was more homogenous in the ice cream with saturated lipids. In our study, the mix of saturated and unsaturated acids (mono- and diglycerides of fatty acids) was used as an emulsifier, which may explain such a wide range of particle sizes in all samples.

The rheological properties of ice cream mixes

The flow behavior and mouthfeel of ice cream are referred to as rheological properties. The rheological behaviour of milk ice cream mixes was described using the Ostwald de Waele model. The accuracy of this model fitting was high, as indicated by high correlation coefficients (Table 2). The rheological parameters of ice cream mixes before and after maturation are shown in Table 2. Data obtained for the samples before maturation shows that consistency index (*K*) ranged from 0.009 to 0.083. The addition of stabilisers contributed to an increase in its values owing to the fact that the lowest value was noted for the control sample. Considering the type of stabilizer used, the highest *K* was determined for the ice cream mix with the addition of ι-carrageenan after lactase treatment (L). In the case of the flow behaviour index of the samples before maturation, the lowest value was determined for L (0.727), but the values achieved for ice cream mix with ι-carrageenan and its acid hydrolysate were similar and did not differ significantly ($p \geq 0.05$) from that determined for L sample. The highest ($p < 0.05$) *n* was determined for the control sample (0.900), which allows concluding that higher *K* was obtained from the lower flow behaviour index. In the research by Atalar *et al*. [2021], flow curves plotted for the hazelnut vegan ice cream mixes were described using the Ostwald de Waele model, and the values of their flow behaviour index ranged from 0.61 to 0.76. Similar *n* values (0.65–0.73) were computed for vanilla ice creams with various contents of milk protein concentrate [Mostafavi *et al*., 2017].

After maturation, the same trend in the variation of *K* and *n* between samples as before maturation was observed. The highest *K* value (0.104) was determined for the ice cream mix with the addition of ι-carrageenan after lactase treatment and the lowest one (0.012) for the control sample. In the case of the flow behaviour index, the lowest value (0.702) was noted for the L sample and the highest one (0.838) for the control sample. Soukoulis *et al*. [2008] showed that the consistency index of the ice cream mixes with the addition of different hydrocolloids and κ-carrageenan ranged from 0.498 to 1.951, which was due to the distinctive ability of κ-carrageenan to form a gel with other hydrocolloids. Thus, the combination of carrageenan with guar gum or carboxymethyl-cellulose should be more favourable than the combination with xanthan gum or sodium alginate, which usually forms weak gel networks. Referring to the views of Alvarez *et al*. [2005], after maturation, an increase in viscosity was observed in milk ice cream mixes. Such a change was understandable due to the hydration of protein and stabilisers during maturation, which results in a change in viscosity.

According to the presented results for all ice cream mixes (before and after maturation), the *n* values were less than 1 (Table 2). It means that the ice cream mixes showed non-Newtonian shear-thinning (pseudoplastic) behaviour [Rao, 2007]. Previous research reported that ice cream mixes exhibited pseudoplastic behaviour due to the aggregated fat globules and polysaccharide stabilisers [Akbari *et al*., 2019]. Consequently, the viscosity decreased with an increasing shear rate.

After maturation, only the samples with the addition of enzymatic hydrolysates of ι-carrageenan (B and L) tended to increase their consistency index (Table 2). It may suggest the same mechanism of rheological behaviour in both ice cream mixes. Our previous study [Kot *et al*., 2022] proved that the mentioned enzymatic hydrolysates of ι-carrageenan were more flexible in comparison to ι-carrageenan or acid hydrolysate of ι-carrageenan in model solutions of ice cream. It may be the reason why the consistency of samples B and L was improved.

Microscopic analysis

The microscopic observation of emulsion may provide pivotal clues to understanding the relationship between microstructure and the stability of the emulsion [Ahn *et al.,* 2022]. The images from the CLSM analysis of the milk ice cream mix before and after maturation are presented in Figure 2. To observe the changes in the stability of samples, Nile red was used to stain the fat droplets. In all samples both before and after maturation, single particles of fat were visible with a size of around 5 μm. This is in agreement with the particle size distribution; the first peak was observed for the particles <10 μm (Figure 3) but larger fat agglomerates were visible in microscopic images as well (Figure 3). Their presence in ice cream mixes was also proven by previous analyses of the TSI and D_{50}. The sizes of agglomerates were around 10 μm or more. Such molecules were visible in the control sample and ice cream mix with the addition of ι-carrageenan before maturation (Figure 3 Ca and Ia, respectively). Additionally, fat droplet deformation was observed in the image of the control sample before maturation. This confirmed flocculation, which was suggested above based on the backscattering profile. Moreover, as can be seen from image Ba, phase separation in the sample with ι-carrageenan after β-galactosidase treatment (before maturation) occurred, which also confirmed the destabilisation of this milk ice cream mix. Frising *et al*. [2008] noticed in the picture of sedimentation of water-in-oil emulsion that droplets which were not evenly distributed tended to gather in more or fewer agglomerates. It means that flocculation may occur in this place later. In

our study, such phenomena could also be observed during maturation (Figure 2). Melted ice cream was also observed by confocal scanning laser microscopy after dynamic freezing [Voronin *et al*., 2020]. Based on the results, the control sample and the sample with the addition of polysorbate 80 (C-P80) were characterized by destabilized fat globules and partial coalescence, especially in the sample with the addition of an emulsifier. The same method was used to observe the protein and fat globules in ice cream mixes with polysaccharides [Cheng *et al*., 2015]. According to the results, flocculation was visible in the examined samples. In our research, the same or similar behaviour of fat destabilisation was observed.

CONCLUSION

The presented study showed that ι-carrageenan and its hydrolysates had a strong influence on the physical properties of milk ice cream mixes. They affected the stability of the emulsion during maturation. The hydrolysates of ι-carrageenan improved the stability of mixes contrary to ι-carrageenan as indicated by TSI. On the other hand, the addition of ι-carrageenan to the mixes affected two different types of destabilisation: coalescence and flocculation, while in the samples with hydrolysates of ι-carrageenan additionally, sedimentation was noted. Before and after maturation, aggregates of fats occurred and particles of distinctive sizes were observed in the ice cream mixes. The used stabilisers contributed to increasing the sizes of particles while maturation decreased it. The addition of the enzymatic hydrolysate of ι-carrageenan after commercial lactase treatment beneficially influenced the rheological properties of the ice cream mix.

It may be concluded that ι-carrageenan and its hydrolysates could serve as effective stabilisers in milk ice cream. However, further investigations are needed to explain the mechanism of their action as stabilisers and the behavior of fat in the presented recipe during maturation. The study ultimately proved that the type of stabilisers, in this case, ι-carrageenan and its hydrolysates, contributed to the destabilisation of ice cream mixes during maturation. Such a conclusion may be useful in planning the ice cream production process or predicting the formation of ice crystal structure.

SUPPLEMENTARY MATERIALS

These are available at http://journal.pan.olsztyn.pl/Effect-of-Iota-Carrageenan-and-Its-Hydrolysates-on-the-Stability-of-Milk-Ice-Cream,166382,0,2.html. Figure S1. Backscattering (BS) profile of ice cream mixes stabilised by the combination of ι-carrageenan, locust bean gum and xanthan gum before and after maturation. Figure S2. Backscattering (BS) profile of ice cream mixes stabilised by the combination of ι-carrageenan hydrolysate obtained using β-galactosidase, locust bean gum and xanthan gum before and after maturation. Figure S3. Backscattering (BS) profile of ice cream mixes stabilised by the combination of ι-carrageenan hydrolysate obtained using commercial lactase, locust bean gum and xanthan gum before and after maturation.

RESEARCH FUNDING

Research equipment was purchased as part of the "Food and Nutrition Centre - modernisation of the WULS campus to create a Food and Nutrition Research and Development Centre (CŻiŻ)" co-financed by the European Union from the European Regional Development Fund under the Regional Operational Programme of the Mazowieckie Voivodeship for 2014-2020 (Project No. RPMA.01.01.00-14-8276/17).

CONFLICT OF INTERESTS

Authors declare no competing interests.

ORCID IDS

M. Buniowska-Olejnik https://orcid.org/0000-0003-3795-4003
E. Jakubczyk https://orcid.org/0000-0002-4080-8851
A. Kamińska-Dwórznicka https://orcid.org/0000-0002-2835-2265
A. Kot https://orcid.org/0000-0003-3850-1743

REFERENCES

1. Ahn, N., Park, J-H., Chai, Ch., Imm, J-Y. (2022). The interaction of milk sphingomyelin and proteins on stability and microstructure of dairy emulsions. *Journal of Dairy Science*, *105*(5), 3832-3845. https://doi.org/10.3168/jds.2021-21253
2. Akbari, M., Eskandari, M.H., Davoudi, Z. (2019). Application and functions of fat replacers in low-fat ice cream: A review. *Trends in Food Science & Technology, 86*, 34-40. https://doi.org/10.1016/j.tifs.2019.02.036
3. Alvarez, V.B., Wolters, C.L., Vodovotz, Y., Ji, T. (2005). Physical properties of ice cream containing milk protein concentrates. *Journal of Dairy Science, 88*(3), 862-871. https://doi.org/10.3168/jds.S0022-0302(05)72752-1
4. Atalar, I., Kurt, A., Gul, O., Yazici, F. (2021). Improved physicochemical, rheological and bioactive properties of ice cream: Enrichment with higher pressure homogenized hazelnut milk. *International Journal of Gastronomy and Food Science*, *24*, art. no. 100358. https://doi.org/10.1016/j.ijgfs.2021.100358
5. Berger, K.G., White, G.W. (1971). An electron microscopical investigation of fat destabilization in ice cream. *International Journal of Food Science and Technology*, *6*(2), 285-294. https://doi.org/10.1111/j.1365-2621.1971.tb01617.x
6. Bolliger, S., Goff, H.D., Tharp, B.W. (2000). Correlation between colloidal properties of ice cream mix and ice cream. *International Dairy Journal, 10*(4), 303-309. https://doi.org/10.1016/S0958-6946(00)00044-3
7. Chen, W., Liang, G., Li, X., He, Z., Zeng, M., Gao, D., Qin, F., Goff, H.D., Chen, J. (2019). Effect of soy proteins and hydrolysates on fat globule coalescence and meltdown properties of ice cream. *Food Hydrocolloids, 94*, 279-286. https://doi.org/10.1016/j.foodhyd.2019.02.045
8. Cheng, J., Ma, Y., Li, X., Yan, T., Cui, J. (2015). Effects of milk protein-polysaccharide interactions on the stability of ice cream model systems. *Food Hydrocolloids, 45*, 327-336. https://doi.org/10.1016/j.foodhyd.2014.11.027
9. Daw, E., Hartel, R.W. (2015). Fat destabilization and melt-down of ice creams with increased protein content. *International Dairy Journal, 43*, 33-41. https://doi.org/10.1016/j.idairyj.2014.12.001
10. Dickinson, E. (1994). Emulsion stability. In K. Nishinari, E. Doi (Eds.). *Food Hydrocolloids: Structures, Properties and Functions*. Springer, Boston, MA, USA, pp. 387-398. https://doi.org/10.1007/978-1-4615-2486-1_61
11. Dickinson, E. (2010). Flocculation of protein-stabilized oil-in-water emulsions. *Colloids and Surfaces B: Biointerfaces*, *81*(1), 130-140. https://doi.org/10.1016/j.colsurfb.2010.06.033
12. Frising, T., Noïk, Ch., Dalmazzone, Ch., Peysson, Y., Palermo, T. (2008). Contribution of the sedimentation and coalescence mechanism to the separation of concentrated water-in-oil emulsions. *Journal of Dispersion Science and Technology*, *29*(6), 827-834. https://doi.org/10.1080/01932690701781501
13. Gelin, J.L., Poyen, L., Courthaudon, J.L., Meste, M.Le., Lorient, D. (1994). Structural changes in oil-water emulsions during the manufacture of ice cream. *Food Hydrocolloids, 8*(3-4), 299-308. https://doi.org/10.1016/S0268-005X(09)80342-1
14. Goff, H.D. (1997). Colloidal aspects of ice cream – A review. *International Dairy Journal*, *7*(6-7), 363-373. https://doi.org/10.1016/S0958-6946(97)00040-X

15. Goff, H.D. (2002). Formation and stabilisation of structure in ice cream and related products. *Current Opinion in Colloid and Interface Science*, *7*(5-6), 432-437. https://doi.org/10.1016/S1359-0294(02)00076-6
16. Goff, H.D., Hartel, R.W. (2013). Composition and Formulations. In H.D. Goff, R.W. Hartel (Eds)., *Ice Cream*, 7th ed.; Springer: New York, pp. 19-44. https://doi.org/10.1007/978-1-4614-6096-1
17. Goff, H.D., Kinsella, J.E., Jordan, W.K. (1989). Influence of various milk protein isolates on ice cream emulsion stability. *Journal of Dairy Science*, *72*(2), 385-397. https://doi.org/10.3168/jds.S0022-0302(89)79120-7
18. Innocente, N., Biasutti, M., Venir, E., Spaziani, M., Marchesini, G. (2009). Effect of high-pressure homogenization on droplet size distribution and rheological properties of ice cream mixes. *Journal of Dairy Science, 92*(5), 1864-1875. https://doi.org/10.3168/jds.2008-1797
19. Kamińska-Dwórznicka, A., Antczak, A., Samborska, K., Lenart, A. (2015). Acid hydrolysis of kappa-carrageenan as a way of gaining new substances for freezing process modification and protection from excessive recrystallization of ice. *International Journal of Food Science and Technology, 50*(8), 1799-1806. https://doi.org/10.1111/ijfs.12820
20. Kiran-Yildrim, B., Hale, J., Wefers, D., Gaukel, V. (2021). Ice recrystallisation inhibition of commercial κ-, ι-, λ-carrageenans. *Journal of Food Engineering, 290*, art. no. 110269. https://doi.org/10.1016/j.jfoodeng.2020.110269
21. Konstantas, A., Stamford L., Azpagic, A. (2019). Environmental impacts of ice cream. *Journal of Cleaner Production, 209*, 259-272. https://doi.org/10.1016/j.jclepro.2018.10.237
22. Kot, A., Kamińska-Dwórznicka, A., Antczak, A., Jakubczyk, E., Matwijczuk, A. (2022). Effect of ι-carrageenan and its acidic and enzymatic hydrolysates on ice crystal structure changes in model sucrose solution. *Colloids and Surfaces A: Physicochemical and Engineering Aspects, 643*, art. no. 128744. https://doi.org/10.1016/j.colsurfa.2022.128744
23. Kot, A., Kamińska-Dwórznicka, A., Galus, S., Jakubczyk, E. (2021). Effects of different ingredients and stabilisers on properties of mixes based on almond drink for vegan ice cream production. *Sustainability, 13*(21), art. no. 12113. https://doi.org/10.3390/su132112113
24. Koxholt, M.M.R., Eisenmann, B., Hinrichs, J. (2001). Effect of the fat globule sizes on the meltdown of ice cream. *Journal of Dairy Sciences*, *84*(1), 31-37. https://doi.org/10.3168/jds.S0022-0302(01)74448-7
25. Liu, X., Sala, G., Scholten, E. (2022). Effect of fat aggregate and percentage of the melting properties of ice cream. *Food Research International,* 160, art. no. 111709. https://doi.org/10.1016/j.foodres.2022.111709
26. Lomolino, G., Zannoni, S., Zabara, A., Da Lio, M., De Iseppi, A. (2020). Ice recrystallisation and melting in ice cream with different proteins levels and subjected to thermal fluctuation. *International Dairy Journal, 100*, art. no. 104557. https://doi.org/10.1016/j.idairyj.2019.104557
27. Mendez-Velasco, C., Goff, H.D. (2012). Fat structures as affected by unsaturated or saturated monoglyceride and their effect on ice cream structure, texture and stability. *International Dairy Journal*, *24*(1), 33-39. https://doi.org/10.1016/j.idairyj.2011.11.009
28. Mostafavi, F.S., Tehrani, M.M., Mohebbi, M. (2017). Rheological and sensory properties of fat reduced vanilla ice creams containing milk protein concentrate (MPC). *Journal of Food Measurement and Characterization, 11*, 567-575. https://doi.org/10.1007/s11694-016-9424-y
29. Pal, R. (2019). Modeling of sedimentation and creaming in suspensions and pickering emulsions. *Fluids*, *4*(4), art. no. 186. https://doi.org/10.3390/fluids4040186
30. Pintor, A., Totosaus, A. (2012). Ice cream properties affected by lambda-carrageenan or iota-carrageenan interactions with locust bean gum/carboxymethylcellulose mixtures. *International Food Research Journal, 19*(4), 1409-1414.
31. Rao, M.A. (2007). Introduction: Food rheology and structure. In M.A. Rao (Ed.) *Rheology of Fluid and Semisolid Foods: Principles and Applications.* Springer Science & Business Media: New York, NY, USA, pp. 1-26. https://doi.org/10.1007/978-0-387-70930-7
32. Segall, K.I., Goff, H.D. (2002a). Secondary adsorption of milk proteins from the continuous phase to the oil-water interface in dairy emulsions. *International Dairy Journal*, *12*(11), 889-897. https://doi.org/10.1016/S0958-6946(02)00116-4
33. Segall, K.I., Goff, H.D. (2002b). A modified ice cream processing routine that promotes fat destabilization in the absence of added emulsifier. *International Dairy Journal*, *12*(12), 1013-1018. https://doi.org/10.1016/S0958-6946(02)00117-6
34. Seisun, D. (2010). Chapter 1 – Introduction. In A. Imeson (Edd.). *Food Stabilisers, Thickeners and Gelling Agents*. Blackwell Publishing Ltd, United Kingdom, pp.1-10. https://doi.org/10.1002/9781444314724.ch1
35. Seo, C.W., Oh, N.S. (2022). Functional application of Maillard conjugate derived from a κ-carrageenan/milk protein isolate mixture as a stabilizer in ice cream. *LWT – Food Science and Technology, 161*, art. no. 113406. https://doi.org/10.1016/j.lwt.2022.113406
36. Soukoulis, Ch., Chandrinos, I., Tzia, C. (2008). Study of the functionality of selected hydrocolloids and their blends with κ-carrageenan on storage quality of vanilla ice cream. *LWT – Food Science and Technology, 41*(10), 1816-1827. https://doi.org/10.1016/j.lwt.2007.12.009
37. Stanley, D.W., Goff, H.D., Smith, A.K. (1996). Texture-structure relationships in foamed dairy emulsions. *Food Research International*, *29*(1), 1-13. https://doi.org/10.1016/0963-9969(95)00063-1
38. Thrimawithana, T.R., Young, S., Dunstan, D.E., Alany, R.G. (2010). Texture and rheological characterization of kappa and iota carrageenan in the presence of counter ions. *Carbohydrate Polymers, 82*(1), 69-77. https://doi.org/10.1016/j.carbpol.2010.04.024
39. Voronin, G.L., Ning, G., Coupland, J.N., Roberts, R., Harte, F.M. (2020). Freezing kinetics and microstructure of ice cream from high-pressure-jet processing of ice cream mix. *Journal of Dairy Sciences*, *104*(3), 2843-2854. https://doi.org/10.3168/jds.2020-19011

REVIEW ARTICLE
http://journal.pan.olsztyn.pl

INSTRUCTIONS FOR AUTHORS

SUBMISSION. Original contributions relevant to food and nutrition sciences are accepted on the understanding that the material has not been, nor is being, considered for publication elsewhere. All papers should be submitted and will be processed electronically via Editorial Manager system (available from PJFNS web site: http://journal.pan.olsztyn.pl). On submission, a corresponding author will be asked to provide: Cover letter; Files with Manuscripts, Tables, Figures/Photos; and Names of two potential reviewers (one from the author's homeland – but outside author's Institution, and the other from abroad). All papers which have been qualified as relevant with the scope of our Journal are reviewed. All contributions, except the invited reviews are charged. Proofs will be sent to the corresponding author and should be returned within one week since receipt. No new material may be inserted in the text at proof stage. It is the author's duty to proofread proofs for errors.

Authors should very carefully consider the preparation of papers to ensure that they communicate efficiently, because it permits the reader to gain the greatest return for the time invested in reading. Thus, we are more likely to accept those that are carefully designed and conform the instruction. Otherwise, papers will be rejected and removed from the online submission system.

SCOPE. The Polish Journal of Food and Nutrition Sciences publishes original, basic and applied papers, and reviews on fundamental and applied food research, preferably these based on a research hypothesis, in the following Sections:

Food Technology:
- Innovative technology of food development including biotechnological and microbiological aspects
- Effects of processing on food composition and nutritional value

Food Chemistry:
- Bioactive constituents of foods
- Chemistry relating to major and minor components of food
- Analytical methods

Food Quality and Functionality:
- Sensory methodologies
- Functional properties of food
- Food physics
- Quality, storage and safety of food

Nutritional Research:
- Nutritional studies relating to major and minor components of food (excluding works related to questionnaire surveys)

"News" section:
- Announcements of congresses
- Miscellanea

OUT OF THE SCOPE OF THE JOURNAL ARE:
- Works which do not have a substantial impact on food and nutrition sciences
- Works which are of only local significance i.e. concern indigenous foods, without wider applicability or exceptional nutritional or health related properties
- Works which comprise merely data collections, based on the use of routine analytical or bacteriological methods (i.e. standard methods, determination of mineral content or proximate analysis)
- Works concerning biological activities of foods but not providing the chemical characteristics of compounds responsible for these properties
- Nutritional questionnaire surveys
- Works related to the characteristics of foods purchased at local markets
- Works related to food law
- Works emphasizing effects of farming / agricultural conditions / weather conditions on the quality of food constituents
- Works which address plants for non-food uses (i.e. plants exhibiting therapeutic and/or medicinal effects)

TYPES OF CONTRIBUTIONS. *Reviews*: (at least: 30 pages and 70 references) these are critical and conclusive accounts on trends in food and nutrition sciences; *Original papers*: (maximally: 30 pages and 40 references) these are reports of substantial research; *Reports on post and forthcoming scientific events, and letters to the Editor* (all up to three pages) are also invited (free of charge).

REVIEW PROCESS. All scientific contributions will be peer-reviewed on the criteria of originality and quality. Submitted manuscripts will be preevaluated by Editor-in-Chief and Statistical Editor (except for review articles), and when meeting PJFNS' scope and formal requirements, they will be sent to a Section Editor who upon positive preevaluation will assign at least two reviewers from Advisory Board Members, reviewers suggested by the author or other experts in the field. Based on the reviews achieved, Section Editor and Editor-in--Chief will make a decision on whether a manuscript will be accepted for publication, sent back to the corresponding author for revision, or rejected. Once a manuscript is sent back to the corresponding author for revision, all points of the reviews should be answered or rebuttal should be provided in the Explanation letter. The revised manuscripts will be checked by Section Editor and by the original reviewers (if necessary), and a final decision will be made on acceptance or rejection by both Section Editor and Editor-in-Chief.

Polish Journal of Food and Nutrition Sciences uses CrossCheck's iThenticate software to detect instances of similarity in submitted manuscripts. In publishing only original research, PJFNS is committed to deterring plagiarism, including self-plagiarism.

COPYRIGHT LICENSE AGREEMENT referring to Authorship Responsibility and Acknowledgement, Conflict of Interest and Financial Disclosure, Copyright Transfer, are required for all authors, i.e. *Authorship Responsibility and Acknowledgement*: Everyone who has made substantial intellectual contributions to the study on which the article is based (for example, to the research question, design, analysis, interpretation, and written description) should be an author. It is dishonest to omit mention of someone who has participated in writing the manuscript ("ghost authorship") and unfair to omit investigator who have had important engagement with other aspects of the work. All contributors who do not meet the criteria for authorship should be listed in an Acknowledgments section. Examples of those who might be acknowledged include a person who provided purely technical help, writing assistance, or a department chairperson who provided only general support. Any financial and material support should also be acknowledged. *Conflict of Interest and Financial Disclosure*: Authors are responsible for disclosing financial support from the industry or other conflicts of interest that might bias the interpretation of results. *Copyright License Agreement*: Authors agree to follow the Creative Commons Attribution-Non--Commercial-NoDerivs 4.0 License.

A manuscript will not be published once the signed form has not been submitted to the Editor with the manuscript revised after positive reviews.

CHANGES TO AUTHORHIP. Authors are expected to consider carefully the list and order of authors before submitting their manuscript and provide the definitive list of authors at the time of the original submission. Any addition, deletion or rearrangement of author names in the authorship list should be made only before the manuscript has been accepted and only if approved by the journal Editor. To request such a change, the Editor must receive the following from the corresponding author: (a) the reason for the change in author list and (b) written confirmation (e-mail, letter) from all authors that they agree with the addition, removal or rearrangement. In the case of addition or removal of authors, this includes confirmation from the author being added or removed.

ETHICAL APPROVAL OF STUDIES AND INFORMED CONSENT. For all manuscripts reporting data from studies involving human participants or animals, formal approval by an appropriate institutional review board or ethics committee is required and should be described in the Methods section. For those investigators who do not have formal approval from ethics review committees, the principles outlined in the Declaration of Helsinki should be followed. For investigations of humans, state in the Methods section the manner in which informed consent was obtained from the study participants (i.e., oral or written). Editors may request that authors provide documentation of the formal review and recommendation from the institutional review board or ethics committee responsible for oversight of the study.

UNAUTHORIZED USE. Unauthorized use of the PJFNS name, logo, or any content for commercial purposes or to promote commercial goods and services (in any format, including print, video, audio, and digital) is not permitted by IAR&FR PAS.

MANUSCRIPTS. A manuscript in English must be singlesided, preferably in Times New Roman (12) with 1.5-point spacing, without numbers of lines. The Editor reserves the right to make literary corrections and to make suggestions to improve brevity. English is the official language. The English version of the paper will be checked by Language Editor. Unclear and unintelligible version will be returned for correction.

Every paper should be divided under the following headings in this order: a **Title** (possibly below 150 spaces); the **Name(s)** of the author(s) in full. In paper with more than one author, the asterisk indicates the name of the author to whom correspondence and inquiries should be addressed, otherwise the first author is considered for the corre-spondence. Current full postal address of the indicated corresponding author or the first author must be given in a footnote on the title page; the **Place(s)** where the work was done including the institution name, city, country if not Poland. In papers originated from several institu-tions the names of the authors should be marked with respective superscripts; the **Key words** (up to 6 words or phrases) for the main topics of the paper; an **Abstract** (up to 250 words for regular papers and reviews) summarizing briefly main results of the paper, no literature references; an **Introduction** giving essential background by saying why the research is important, how it relates to previous works and stating clearly the objectives at the end; **Materials and Methods** with sufficient experimental details permitting to repeat or extend the experiments. Literature references to the methods, sources of material, company names and location (city, country) for specific instruments must be given. Describe how the data were evaluated, including selection criteria used; **Results and Discussion** presented together (in one chapter). Results should be presented concisely and organized to supplement, but not repeat, data in tables and figures. Do not display the data in both tabular and graphic form. Use narrative form to present the data for which tables or figures are unnecessary. Discussion should cover the implications and consequences, not merely recapitulating the results, and it must be accomplished with concise **Conclusions**; **Acknowledgements** should be made to persons who do not fill the authorship criteria (see: Authorship forms); **Research funding** should include financial and material support; **Conflict of Interests**: Authors should reveal any conflicts of interest that might bias the interpretation of results; and **References** as shown below.

REFERENCES each must be listed alphabetically at the end of the paper (each should have an Arabic number in the list) in the form as follows: **Periodicals** – names and initials of all the authors, year of publication, title of the paper, journal title as in Chemical Abstracts, year of publication, volume, issue, inclusive page numbers, or article id.; **Books** – names and initials of all the authors, names of editors, chapter title, year of publication, publishing company, place of publication, inclusive page numbers; **Patents** – the name of the application, the title, the country, patent number or application number, the year of publication.

For papers published in language other than English, manuscript title should be provided in English, whereas a note on the original language and English abstract should be given in parentheses at the end.

The reference list should only include peer-reviewed full-text works that have been published or accepted for publication. Citations of MSc/PhD theses and works unavailable to international Editors, Reviewers, and Readers should be limited as much as possible.

References in the text must be cited by name and year in square parentheses (e.g.: one author – [Tokarz, 1994]; two authors – [Słonimski & Campbell, 1987]; more than two authors – [Amarowicz *et al*., 1994]). If more than one paper is published in the same year by the same author or group of authors use [Tokarz, 1994a, b]. Unpublished work must only be cited where necessary and only in the text by giving the person's name.

Examples:

Article in a journal:

Słonimski, B.A., Campbell, L.D., Batista, E., Howard B. (2008). Gas chromatographic determination of indole glucosinolates. Journal of Science and Food Agriculture, 40(5), 131–143.

Asher, A., Tintle, N.L., Myers, M., Lockshon, L., Bacareza, H., Harris, W.S. (2021). Blood omega-3 fatty acids and death from COVID-19: A pilot study. *Prostaglandins, Leukotrienes and Essential Fatty Acids, 166*, art. no. 102250.

Book:

Weber, W., Ashton, L., Milton, C. (2012). Antioxidants – Friends or Foes? 2nd edition. PBD Publishing, Birmingham, UK. pp. 218–223.

Chapter in a book:

Uden, C., Gambino, A., Lamar, K. (2016). Gas chromatography. In M. Queresi, W. Bolton (Eds.), CRC Handbook of Chromatography, CRC Press Inc., Boca Raton, Florida, USA, pp. 44–46.

ABBREVIATIONS AND UNITS. Abbreviations should only be used when long or unwieldy names occur frequently, and never in the title; they should be given at the first mention of the name. Metric SI units should be used. The capital letter L should be used for liters. Avoid the use of percentages (% g/g,% w/w; Mol%; vol%), ppm, ppb. Instead, the expression such as g/kg, g/L, mg/kg, mg/mL should be used. A space must be left between a number and a symbol (e.g. 50 mL not 50mL). A small x must be used as multiplication sign between numeric values (e.g. 5 × 102 g/mL). Statistics and measurements should be given in figures, except when the number begins a sentence. Chemical formulae and solutions must specify the form used. Chemical abbreviations, unless they are internationally known, Greek symbols and unusual symbols for the first time should be defined by name. Common species names should be followed by the Latin at the first mention, with contracting it to a single letter or word for subsequent use.

FIGURES should be submitted in separate files. Each must have an Arabic number and a caption. Captions of all Figures should be provided on a separate page "Figure Captions". Figures should be comprehensible without reference to the text. Self-explanatory legend to all figures should be provided under the heading "Legends to figures"; all abbreviations appearing on figures should be explained in figure footnotes. Three-dimensional graphs should only be used to illustrate real 3D relationships. Start the scale of axes and bars or columns at zero, do not interrupt them or omit missing data on them. Figures must be cited in Arabic numbers in the text.

TABLES should be submitted in separate files. They should be as few in number and as simple as possible (like figures, they are expensive and space consuming), and include only essential data with appropriate statistical values. Each must have an Arabic number and a caption. Captions of all Tables should be provided on a separate page "Table Captions". Tables should be self-explanatory; all abbreviations appearing in tables should be explained in table footnotes. Tables must be cited in Arabic numbers in the text.

PAGE CHARGES. A standard publication fee has been established at the rate of 450 EUR + tax (if applicable, e.g. for private persons) irrespective of the number of pages and tables/figures. For Polish Authors an equivalent fee was set at 1950 PLN + VAT. Payment instructions will be sent to Authors via e-mail with acceptance letter.

Information on publishing and subscription is available from:

Ms. Joanna Molga
Editorial Office of Pol. J. Food Nutr. Sci.
Institute of Animal Reproduction and Food Research Tuwima 10 Str., 10–748 Olsztyn 5, Poland
phone (48 89) 523–46–70, fax (48 89) 523–46–70;
e-mail: pjfns@pan.olsztyn.pl; http://journal.pan.olsztyn.pl

Nutrition